PSL
UNIVERSITÉ PARIS

THÈSE DE DOCTORAT
DE L'UNIVERSITÉ PSL

Préparée à MINES ParisTech

Optimisation des flexibilités des « consommacteurs » dans le contexte des marchés d'électricité

Optimization of prosumers flexibility in electricity markets

Soutenue par

Carlos Adrián CORREA FLÓREZ

Le 17 avril 2019

École doctorale n°621

Ingénierie des Systèmes, Matériaux, Mécanique, Energétique

Spécialité

Energétique et Procédés

Composition du jury :

Nikos HATZIARGYRIOU National Technical University of Athens	*Président*
Philip Charles TAYLOR Newcastle University	*Rapporteur*
Seddik BACHA Grenoble-Alpes University G2Elab	*Rapporteur*
Hrvoje PANDŽIĆ University of Zagreb	*Examinateur*
Ricardo BESSA INESC TEC	*Examinateur*
Sawsan AL ZAHR Télécom ParisTech (ENST) - LTCI	*Examinateur*
Georges KARINIOTAKIS MINES ParisTech, Directeur de thèse	*Examinateur*
Andrea MICHIORRI MINES ParisTech, Maitre de thèse	*Examinateur*

MINES ParisTech | PSL

Acknowledgements

First of all, I would like to thank my supervisors, Georges Kariniotakis and Andrea Michiorri, for their kindness, constant support and timely advice.

I would also like to thank my family for their love and support, even in the distance.

I am very grateful to my colleagues, for all the patience and affection during these three years of PhD experience. I am already missing you all.

I am also very grateful to have participated in the research and innovation project SENSIBLE (Storage ENabledSustaInable energy for BuiLdings and communitiEs (www.projectsensible.eu), which received funding from the European Union under the Horizon 2020 Framework Programme Grant Agreement No 645963.

Contents

1 Introduction **12**
- 1.1 General overview and context . . . 12
- 1.2 Challenges and research opportunities . . . 13
  - 1.2.1 Motivation . . . 13
  - 1.2.2 Literature review . . . 15
  - 1.2.3 Identified research gaps . . . 18
- 1.3 Scientific objectives . . . 18
- 1.4 Main contributions . . . 19
- 1.5 List of publications . . . 20
- 1.6 Layout of the document . . . 21

2 Mathematical modelling of flexibility for residential aggregation **23**
- 2.1 Literature review . . . 24
  - 2.1.1 Effects of cycling aging in the operation of storage devices . . 24
  - 2.1.2 Aggregation of prosumers . . . 27
- 2.2 Mathematical modeling of prosumer's aggregation for participation in the day-ahead energy market . . . 28
  - 2.2.1 Objective function . . . 28
  - 2.2.2 Load balance constraints . . . 30
  - 2.2.3 BESS constraints . . . 30
  - 2.2.4 TES constraints . . . 31
- 2.3 Description of the test case used for simulations . . . 31
  - 2.3.1 Available forecasts used as data input . . . 32
- 2.4 Solution approach 1: Decomposition method to solve model (2.1)-(2.14) 35
  - 2.4.1 Outline of the Decomposition approach . . . 36
  - 2.4.2 Cycling cost subproblem, the storage disaggregation algorithm (SDA) . . . 37
  - 2.4.3 Day-ahead thermal subproblem . . . 39
  - 2.4.4 Competitive Swarm Optimizer . . . 41
  - 2.4.5 Performance of the SDA . . . 42
  - 2.4.6 Results of the decomposition technique . . . 43
- 2.5 Solution approach 2: Explicit modeling of BESS degradation costs to solve (2.1)-(2.14) . . . 47
  - 2.5.1 Results for piecewise linearization approach . . . 49
  - 2.5.2 Results for piecewise linearization: impacts of cycling aging . 50
  - 2.5.3 Comparative remarks of the decomposition and explicit modelling approaches . . . 51

2.6 Conclusions . . . 52

3 Residential flexibility aggregation under uncertainty 55
3.1 Literature review . . . 55
3.1.1 Robust optimization for uncertainty treatment . . . 57
3.1.2 Discussion . . . 59
3.2 Characterization of uncertainty . . . 59
3.3 Quantile-based two-stage stochastic optimization with SDA . . . 61
3.3.1 Creation of scenarios . . . 63
3.3.2 Analysis of a single day . . . 67
3.3.3 Computational performance of the CSO for the 25-household testbed . . . 68
3.3.4 Performance of the CSO for larger test systems . . . 68
3.4 Adjustable robust optimization approach . . . 70
3.4.1 Results for the robust approach . . . 72
3.4.2 Interaction of devices in the deterministic and robust approaches 75
3.4.3 Impacts of battery efficiency on cost . . . 76
3.4.4 Performance assessment of robust solutions . . . 77
3.4.5 Results of the performance analysis . . . 78
3.4.6 Effects of considering cycling aging in the model . . . 80
3.4.7 Remarks about computational time . . . 81
3.5 Comparative analysis of ARO modified models and hybrid formulations 82
3.5.1 Alternatives of the ARO formulation . . . 83
3.5.2 Comparison of ARO alternatives . . . 85
3.6 Conclusions . . . 93

4 Aggregation of flexibility for participation in multiple markets 96
4.1 Literature review . . . 96
4.1.1 Traditional grid scale approach . . . 96
4.1.2 Provision of services in the presence of RES . . . 97
4.1.3 Home/building aggregation for flexibility services . . . 98
4.1.4 Local flexibility of prosumers and decentralized storage . . . 99
4.2 A first hybrid approach: impacts of local flexibility provision in day-ahead scheduling . . . 101
4.2.1 Mathematical model . . . 102
4.2.2 Results for the Hybrid stochastic/robust model with DSO flexibility requirements . . . 104
4.2.3 A first proposal for bidding in the local market . . . 105
4.3 Complete robust framework for local flexibility provision . . . 107
4.3.1 Description of the aggregators' interactions . . . 107
4.3.2 Main steps of the proposed framework . . . 108
4.3.3 Mathematical model for local provision of flexibilities . . . 109
4.3.4 Results of robust participation in the wholesale market . . . 116
4.3.5 Robust bidding in the local flexibility market . . . 118
4.3.6 Assessing the performance when facing uncertainties . . . 119
4.3.7 Analysis of the probability of bid acceptance . . . 121
4.4 Conclusions . . . 124

5 Concluding remarks **125**
5.1 General conclusions 125
5.2 Perspectives and future work 128

A SDA correction algorithm **130**

B Generalized SDA for scenario-based stochastic approaches **131**

C Obtention of the robust counterpart **133**

D General outline of "Home Analytics" tool for project SENSIBLE **136**
D.0.1 Flexibility forecast 136
D.0.2 Flexibility dispatch 138

E Extended abstract in French **139**
E.1 Résumé du chapitre: Introduction 139
E.2 Résumé du chapitre: Modélisation mathématique de la flexibilité pour l'agrégation résidentielle 142
E.3 Résumé du chapitre: Agrégation de flexibilité résidentielle sous incertitude 146
E.4 Résumé du chapitre: Agrégation de flexibilité pour la participation à plusieurs marchés 149
E.5 Résumé du chapitre: Conclusions 152

List of Figures

1.1 Vision 2050 of energy systems by ETIP-SNET. Taken from [2] 13
1.2 Graphical outline of the main body of the thesis 22

2.1 Schematic diagram of the proposed HEMS 29
2.2 Composition and location of the proposed 25-household HEMS . . . 32
2.3 Example of normalized electrical load probabilistic forecasts 33
2.4 Example of normalized PV probabilistic forecasts 33
2.5 Example of normalized thermal load probabilistic forecasts 34
2.6 Example of forecasted confidence intervals for spot price uncertainty in a typical day in November 2015 34
2.7 Fitted curve for a real life li-ion battery 36
2.8 Scheme of the decomposition approach 37
2.9 Flowchart of the SDA 40
2.10 Flowchart of the CSO algorithm used 42
2.11 Convergence evolution the disaggregation algorithm under 100 random cases 43
2.12 Cost evolution evolution of the disaggregation algorithm for 100 random initialization values 44
2.13 Evolution of daily cost for the deterministic model under the analyzed cases and for the whole month of November 45
2.14 Aggregated SOC for deterministic cases 1 (—●—), 2 (—■—), 3 (—⟡—) and 4 (—⊟—) 46
2.15 Negative imbalance (I^-) costs for deterministic case when all combined PV and load quantiles are analized 47
2.16 Energy purchased on the energy market for the deterministic (—●—) case 48
2.17 Example of piecewise linearization. Cycling Cost Vs. DoD for a selected li-ion battery 50
2.18 Impact of number of segments on the value of the objective function 50
2.19 Error of the objective function as a function of the number of segments 51
2.20 Accumulated SOC when cycling cost is included (—●—). Accumulated SOC when cycling cost is neglected (-⊖-) 51
2.21 Accumulated SOC when for the explicit modeling of cycling (——). Accumulated SOC for cycling cost modelled with the decomposition approach (——) 53

3.1 Average net load intervals calculated with equation (3.1) 60

3.2 Net load interval for two days. November 5th (——) and November 27th (——) . . . 60
3.3 Flowchart of the SDA to two-stage stochastic approaches . . . 62
3.4 Normalized load and PV curves for each of the quantiles needed for scenario generation . . . 64
3.5 Normalized neat load per scenario . . . 65
3.6 Evolution of daily cost for the deterministic case under the analyzed cases and for the whole month of November. Values in p.u. of mean SS 66
3.7 Power purchase boxplot for each DA timeframe . . . 67
3.8 Imbalance boxplot for each scenario in the stochastic optimization . 67
3.9 Aggregated SOC for each scenario in the stochastic approach . . . 68
3.10 Accumulated SOC when cycling cost is included: Deterministic (—●—), ARO (—■—). Accumulated SOC when cycling cost is neglected: Deterministic (-⊖-), ARO (-⊡-). . . . 73
3.11 Day-ahead energy purchase: deterministic (—◇—), ARO (—□—) . . . 73
3.12 Comparison of imbalance needs for the deterministic and the robust approach when $\Gamma^{DA} = 24$, $\Gamma^{D} = 1$ and $\Gamma^{th} = 1$ . . . 74
3.13 Daily average operation (state of charge) of BESS and EWHs . . . 75
3.14 Sensitivity analysis for variations of charging and discharging efficiency. Average daily cost for November. Deterministic (—◦—) and Robust case (—▫—) . . . 76
3.15 Flowchart of the algorithm to find best trade-off solutions . . . 77
3.16 Average operation cost for two days under different budgets of uncertainty and Pareto front . . . 79
3.17 Performance Cumulative Density Functions for selected Robust Solutions . . . 80
3.18 Cumulative Density Functions for the robust model when cycling is considered and neglected . . . 81
3.19 Solution time for ARO (——), NS (——) and deterministic (——) case 82
3.20 Example of KDE sampling and scenarios obtained after backward reduction technique for energy prices . . . 83
3.21 Error evolution as a function of price scenarios for the stochastic solution for three independent trials. . . . 87
3.22 Performance points (green dots) and Pareto fronts (•) for each alternative 1 to 8. Deterministic solution in blue squares . . . 89
3.23 Performance points for alternative 4 (blue dots) and alternative 8 (red crosses). Deterministic solution in green square. . . . 92
3.24 Comparison of all Pareto points. . . . 92
3.25 Computational time boxplots for each optimization alternative. Each datum corresponds to the optimization time for a given combination of control parameters. . . . 93

4.1 Schematic diagram of the proposed framework . . . 104
4.2 Day-ahead committed energy for $P_t^{PCC_{max}} = 0.03$ MW (——), $P_t^{PCC_{max}} = 0.05$ MW (——), $P_t^{PCC_{max}} = 0.07$ MW (——) when constant $R_t = 0.03$ MW/h . . . 105

4.3 Day-ahead committed energy for $R_t = 0.01$ MW/h (—●—), $R_t = 0.03$ MW/h (—■—), $R_t = 0.06$ MW/h (—●—) when constant $P_t^{PCC_{max}} = 0.05$ MW . . . 106
4.4 Demand bidding curves for t = 14h (green), t = 21h (orange) 106
4.5 flexibility supply bidding curves for t = 14h (green), t = 21h (orange) 107
4.6 Sequence of actions . . . 108
4.7 Real time performance evaluation: action E . . . 115
4.8 Demand bidding curves in the wholesale market for t = 14h and different levels of robustness without local constraint support (Action A = Action B). . . . 116
4.9 Day-ahead committed energy for $R_t = 0.01$ MW/h (—●—), $R_t = 0.03$ MW/h (—■—), $R_t = 0.06$ MW/h (—●—) when constant $P_t^{PCC_{max}} = 0.05$ MW . . . 117
4.10 Local flexibility bidding curves for t = 21h . . . 118
4.11 Boxplots of expected negative and positive imbalances to comply with robust flexibility bids in figure 4.3.5, for t=21h . . . 119
4.12 Average (organge) state of charge and boxplots (blue) of batteries and EWHs for the bidding quantities in t=21h . . . 120
4.13 Performance CDF of different bidding strategies : deterministic, ARO1: $\Gamma^{DA,PV,D} = 12, 0.2, 0.4$, ARO2: $\Gamma^{DA,PV,D} = 18, 0.2, 0.2$ ARO3: $\Gamma^{DA,PV,D} = 12, 0.4, 0.6$, for november 15th and flexibility activated of -10 kW (up regulation). . . . 120
4.14 Average expected costs for different levels of flexibility bid accetpance. Simulation for november 15th and flexibility activated of -10 kW (up regulation). . . . 122
4.15 Comparison of average expected costs for different levels of flexibility bid acceptance. Simulation for november 15th and flexibility activated of -10 kW (up regulation). . . . 122
4.16 Average expected costs for different levels of flexibility bid acceptance. Simulation For november 15th and flexibility activated of -10 kW (up regulation). . . . 123
4.17 Average expected costs for different levels of flexibility bid acceptance. Simulation For november 15th and flexibility activated of -10 kW (up regulation). . . . 123

D.1 Topology of the test system. . . . 137

List of Tables

2.1 Cost of resource management for the deterministic scheme. Average daily costs. *Includes cycling effects in the optimization. **Calculated after the optimization 44
2.2 Computational performance of the CSO for one typical day in November 46
2.3 Cost comparison for the optimal solution obtained with the decomposition and explicit cycling aging approaches 52

3.1 Scenarios included in the stochastic scheme 64
3.2 Computational performance of the CSO and PSO for one typical day in November 69
3.3 Computational Performance for different test systems 69
3.4 Average daily costs of resource management 75
3.5 Details of the Pareto fronts values and improvement with respect to deterministic solution 79
3.6 Daily average computational performance of the ARO, NS and deterministic approaches 82
3.7 Details of the Pareto front values and improvements with respect to the deterministic solution. *Γ^D is valid for the unified approach and Γ^{PV} is valid for the separated approach 90
3.8 Descriptors (Desc.) and assessment of each alternative. 91
3.9 Details of computational time for each alternative. 93

4.1 Operation costs for different values of flexibility requirements 105
4.2 Remuneration π^{dso} for the aggregator for different values of allowed ramping and maximum power 117
4.3 Performance for participation in different markets with different robust bidding strategies. *$R_t = 30kW/h$, $P_t^{PCC_{max}} = 50kW$ 121

Nomenclature

Abbreviations

ARO Adjustable Robust Optimization

BESS Battery Energy Storage Systems

BRP Balancing Responsible Party

DoD Depth of Discharge [kWh]

DR Demand Response

DSO Distribution System Operator

EV Electric Vehicle

EWH Electric Water Heater

HEMS Home Energy Management System

LFM Local Flexibility Market

LMO Local Market Operator

LV Low Voltage

MG Microgrid

MPC Model Predictive Control

MT Micro Turbine

MV Medium Voltage

PCC Point of Common Coupling

PDF Probability Density Function

PV Photovoltaic

RES Renewable Energy Sources

RO Robust Optimization

SO Stochastic Optimization

SOC State of Charge

SRB Smart Residential Building

TES Thermal Energy Storage

Indices

$\hat{}$ Marker to identify central forecasts

e index for scenarios, $e = 1, 2, ..., NS$

h index for household, $h = 1, 2, ..., N$

i index for uncertain quantities, $i = \{c, -, +, pv, d, th\}$

s index for segment of the piece-wise cycling cost function of the battery, $s = 1, 2, ..., S$

t index for time step, $t = 1, 2, ..., T$

Parameters

$\bar{H}_h$ TES device maximum power [kW]

$\bar{P}_h^{\text{ch}}$ Battery's maximum charging power [kW]

$\bar{P}_h^{\text{dch}}$ Battery's maximum discharging power [kW]

$\bar{X}_h$ Battery's maximum SOC [kWh]

$\bar{Y}_h$ TES device maximum SOC [kWh]

η^c Battery's charging efficiency

η^d Battery's discharging efficiency

Γ Robustness parameter

$\mu_t^{-/+}$ Negative/Positive price [EUR/kWh]

π^{dso} Remuneration for providing constraint support at the PCC [EUR]

π^{fl} Remuneration for providing flexibility service [EUR]

π_t Spot price [EUR/kWh]

$\underline{X}_h$ Battery's minimum SOC [kWh]

$\underline{Y}_h$ TES device minimum SOC [kWh]

$a_{h,s}, b_{h,s}$ Parameters of piecewise cost functions

C_h Thermal capacitance of TES device

$D_{t,h}$ Electrical load

$D_{t,h}^{q\%}$ q-th quantile of electrical load

$P_{t,h}^{q\%}$ q-th quantile of PV production

$Q_{t,h}$ EWH load [kW]

$Q_{t,h}^{q\%}$ q-th quantile of thermal load

R_h Thermal resistance of TES device

Variables

$H_{t,h}$ EWH input [kW]

$I_t^{-/+}$ Negative/Positive energy imbalance [kWh]

$l_{t,h,s}$ Binary variable to detect active segment of cycling cost function

$P_{t,h}^{\mathrm{c}}$ Battery charging power [kW]

$P_{t,h}^{\mathrm{d}}$ Battery discharging power [kW]

$P_{t,h}^{pv}$ PV panel production [kW]

$P_t^{\mathrm{pcc}_{\min/\max}}$ Minimum/Maximum allowed power at the PCC [kW]

P_t^g Day-ahead energy commitment in the wholesale market [kWh]

R_t Net ramping rate at the PCC [kW/h]

$u_{t,h}$ Binary variable. Equals "1" if battery is charging, "0" otherwise

$X_{t,h,s}^{Ds}$ Battery DoD at the beginning of a charging cycle in segment s [p.u.]

$X_{t,h}$ Battery SOC [kWh]

$x_{t,h}$ Binary variable to detect beginning of a charging cycle

$X_{t,h}^{D}$ Battery DoD at the beginning of a charging cycle [p.u.]

$Y_{t,h}$ SOC of TES device

$z^{(i)}, q^{(i)}, y^{(i)}$ Dual and auxiliary variables of the robust counterpart

Chapter 1

Introduction

1.1 General overview and context

Energy transition calls for multiple efforts at all levels, involving actions from governments, industry, stakeholders and citizens. A low-carbon society has been part of the public discussion during the last decades, with several historical landmarks, some more mediatized than others, such as the 1992 United Nations Framework Convention on Climate Change (UNFCCC), the Kyoto Protocol in 1997, or the the 21st Conference of the Parties (CoP) to the UNFCCC in 2015, held in Paris.

There seems to be a consensus of the parties on the importance of limiting the temperature rise below 2 degrees Celsius and also on the challenges that this limit imposes at political, technical and economical levels [1]. To face the challenges of energy transition, at European authority-level in particular, the European Commission issued in 2016 the package of measures Clean Energy for All Europeans with ambitious goals in the areas of energy efficiency and renewable energies, but and also accounting for fair deals for consumers [2]. To decrease dependency on carbon, the energy sector must suffer a transformation, in which renewable energy resources (RES), digitalized/decentralized systems and energy efficiency are key role players.

This transformation and its main drivers are compatible (and dynamically interact) with the concept of smart grids, which has been matter of ample discussion during the last years in the energy-related specialized literature. Although multiple definitions for smart grids have been proposed, broadly speaking, it is generally accepted that a smart grid integrates, at least, the following features: the increasing presence of Distributed Energy Resources (DER), advanced metering/automation and multiple-way communication for optimal decision making. The vision of 2050 proposed by The European Technology and Innovation Platform for Smart Networks for the Energy Transition (ETIP-SNET), under the EU Horizon 2020 Programme [3], also points out that smart energy systems should aim for: protecting the environment, creating affordable and market-based energy services; and ensure security, reliability and resilience. In concrete, special attention is drawn towards the importance of participation of citizens as active consumers. These ideas are condensed in figure 1.1 by showing an outline of the transition and the differences with the current state of energy systems.

In order to face these challenges and promote consumers (and their aggregators) as key role players, multiple research opportunities arise. To mention a few, regula-

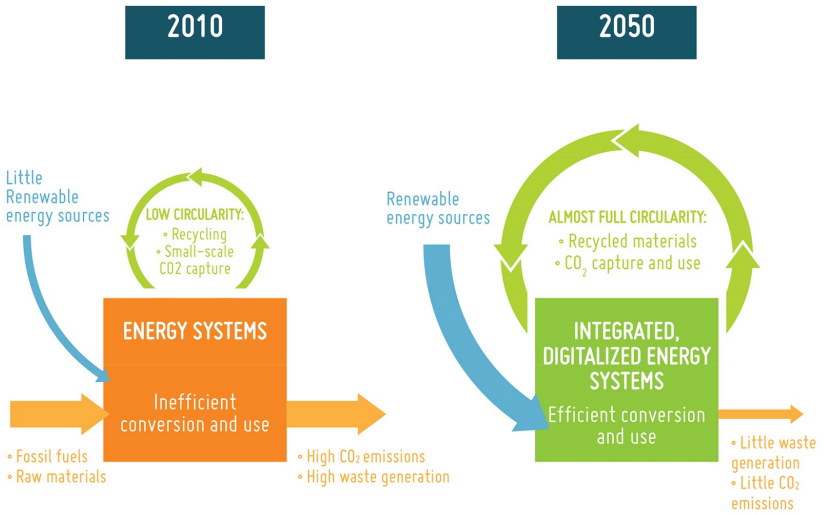


Figure 1.1: Vision 2050 of energy systems by ETIP-SNET. Taken from [2]

tory frameworks and new market designs should be further explored, residential-level multi-energy systems have to be coordinated and managed, new and improved monitoring and automation systems have to be developed to support decision-making, new optimization models have to be proposed to exploit end-users capabilities within these emerging context, forecast and uncertainty models have to be enhanced in order to face decision-making under uncertainty, breakthrough technological advances have to be made to: a) decrease equipment costs, b) improve energy storage devices and capabilities, c) increase data-handling capabilities.

This thesis is circumscribed in the field of optimization models to facilitate aggregator's decision-making processes and scheduling of residential devices for participation in energy markets. Given the multiple sources of uncertainty, the mathematical models presented here emphasize on optimization alternatives that can maintain optimality and feasibility under uncertainty coming from these sources: energy prices, local RES production and consumer's demand.

1.2 Challenges and research opportunities

1.2.1 Motivation

Energy Storage Systems (ESS) and Demand Side Management (DSM) play an important role to support decisions made by the multiple actors present in power systems. In the case of Distributed Energy Resources (DER), management of devices is also important to locally offset variation in load or RES, and also to achieve minimum cost operation. When it comes to Distribution System Operator's (DSO) potential opportunities, we can list many technical and economical advantages such as voltage support, reactive power compensation, congestion management, investment deferral, loss reduction, among others. In addition, the presence of microgrids (MG) in lower layers of the distribution grid in the form of aggregated smart build-

ing/homes or energy communities, makes it possible for active load management and storage devices to support operational decisions and to increase/decrease profit/cost when market rules permit trading flexibility services in the wholesale, reserve or local markets. Different actors can be involved in the ownership and operation of the DER, hence, the models and the potential of the multiple services that these resources can provide need to be explored.

Review [4] points out the lack of a common framework for defining and classifying flexibility in the new contexts of power systems. In addition, a clear distinction of the impacts that reliability and flexibility have on power systems should also be developed accounting also for inclusion of probabilistic flexibility metrics. The latter, considering that intermittent sources and disturbance are ruled by uncertain behaviour, and this uncertainty might lead to technical and economical issues.

The existing limitations are logical, given that markets were designed before the massive penetration of RES and distributed generation. Hence, the redefinition of responsibilities and roles for retailers, aggregators, Virtual Power Plants (VPP), MG, and other actors, must be aligned with the current needs and gaps in the regulation. Moreover, decentralized and coordinated request for flexibility should be possible for DSOs and Transmission System Operators (TSO).

A distinction between technical and market flexibility is carried out in [5] to conclude that flexibility can be used for balancing the system and solving constraints, and on the other hand, available flexibility can be used by different market players for maximizing individual portfolios. Authors argue that this scenario can produce conflict of interests not only among grid owners at different levels, but also among participating actors. In the concrete case of local flexibility trading, authors highlight three main directions: 1) taking advantage of current markets (Day-Ahead, intraday, balancing); 2) creating new and separate markets; and 3) contracting flexibility as a system reserve. At medium-voltage (MV) and low-voltage (LV) levels, not only ESS are called to play an important role in the flexible grid operation, but also the aggregation of resources at the building and home level must play an important role in portfolio optimization of different actors while providing flexibility [6].

European authorities have highlighted the importance of promoting consumer participation in energy markets by creating the necessary marketplaces or by removing market barriers to enable participation of local energy communities [7]. This stimulation of consumers in order to put them at the center of the energy market can be done from individual participation standpoints or by aggregated mechanisms. In this context, DSOs are also encouraged to manage challenges imposed by renewable generation by using local strategies, which is also in line with promoting coordination frameworks between consumers and DSO. This change of paradigm allows consumers to increase integration of local generation for self consumption and market participation, so that they become prosumers.

In this thesis, the definition of prosumer is in line with the report of the European Commission, which defines residential prosumers as consumers that can produce their own energy, with a focus on onsite generation by means of small-scale solar PV [8]. It is worth to mention that solar PV is one of the most widespread generation technologies at the residential level [9].

The current recommendations for enabling prosumers as key players in the energy transition process, emphasize on promoting storage technologies, consumers'

engagement with aggregators, empowering them to participate in the electricity market with adequate remuneration of flexibility. In order to contribute in the mentioned directions and established priorities by industry and government, new mathematical models to optimally manage prosumers' resources and exploit flexibility have to be developed. Given that direct participation of prosumers might not be possible, aggregators appear as an option to bridge the gap. However, besides the well-known market barriers depending on the evolution of different regulatory frameworks, uncertainty has to be accounted for in the new mathematical optimization models and also imposes additional complexity to the decision-making process.

In general, the main current challenges can be summarized as follows:

1. Need for development of uncertainty management models in the smart grid context and specifically for prosumer-oriented emerging frameworks.

2. Analysis of regulation approaches and development of business models to define appropriate frameworks for integration of prosumers in flexibility aggregation schemes and allow participation in energy markets, ancillary markets and local flexibility markets.

3. Definition of the devices' mathematical models into these aggregation schemes and inclusion of operational costs into decision-making formulations (i.e. battery energy storage systems) in order to adequately quantify flexibility costs and remuneration.

1.2.2 Literature review

This literature review aims to identify the high-level research gaps addressed in this thesis. A more detailed review of these topics is presented in each chapter.

Several research papers have concluded on and recommended the importance of including uncertainty in a smart grid context [4,10]. For instance, to bid properly in day-ahead energy markets, some knowledge about the next day's prices is required to hedge risk. In addition, uncertainty about both demand and the RES installed at the residential level can lead to sub-optimal scheduling plans for residential aggregators due to the imbalances produced by the actual production and load patterns during the operation day [11, 12]. This risk has to be properly quantified and embedded in the operation and scheduling of flexibility, and remains an open field of research due to the complexity of uncertainty modelling and the algorithms required to solve this type of optimization problems.

One common practice to facilitate these processes is Stochastic Optimization (SO), which typically aims to determine the optimal solution among a number of expected predefined scenarios [13]. However, drawbacks of SO include factors such as the requirements for probabilistic information of uncertain variables, the implementation of specialized scenario generation and afterwards reduction techniques, and the computational burden related to large number of scenarios, as also concluded in [4]. For an adequate modeling of uncertain variables in residential aggregation applications, advanced scenario auto-correlation analysis for RES and load should

be conducted to find a coherent set of scenarios. This leads to increasing the complexity and the burden on the pre-processing of the necessary information to build up the optimization model.

An alternative approach which has gained substantial attention in recent years is Robust Optimization (RO) [14], which is an interval-based optimization method. RO does not require knowledge of the Probability Density Function (PDF) of uncertain variables, but rather requires moderate information, i.e. an uncertainty set for each uncertain variable. RO provides a robust optimal solution that is feasible (immunized) within the confidence interval.

Some research has been recently published to exploit RO capabilities for handling uncertainty in medium-size DER and microgrids. Price uncertainty is modeled in [15, 16], and RES and/or load uncertainty modelling is proposed in [17–22].

Very little work has been published regarding home-level storage management using RO. Robust management for home appliances is presented in [23] to minimize electricity bills in a single house and include uncertainty in comfort variables. Regarding robust aggregation of storage at the residential level, reference [24] proposes a scheme for real-time decision-making considering batteries and price uncertainty. Reference [25] does not include battery aggregation, but instead considers exploitation of thermal storage at the residential level in a 20-household testbed, using RO to account only for thermal demand uncertainty. Although this research does not include price or electrical load uncertainty, or RES integration, is does give an interesting insight into the scalability of the proposed model. Reference [26] presents a community energy management system disregarding batteries, but including PV and wind power. RO is used to include uncertainty in RES and prices.

One common critique of RO is its over-conservative solutions, given that RO in its original formulation takes into account all potential deviations of the uncertain parameters or coefficients. This can be countered by Adjustable Robust Optimization (ARO) [27] through the introduction of robust control parameters. In the case of MV-level MG, limited analysis of control parameters has been proposed. For the case of residential aggregators, and to the author's knowledge, research on the impacts of uncertainty budget is virtually inexistent.

The specialized literature has presented some models for residential aggregation with RES and storage technologies, in which different objectives are pursued, such as energy and reserve market participation [28], and definition of billing systems and incentive mechanisms [29]. Uncertainty was included by means of SO and chance-constrained method in [28], and Model Predictive Control (MPC) in [29].

Different storage technologies and their coordination can also help provide flexibility and counter uncertainty in scheduling tasks. However, aggregation models that analyse interactions of thermal and electrochemical storage at the residential level are not commonly present in the literature. The model proposed in [30] combines thermal and electrical storage for a residential microgrid with the purpose of shaving demand peak and enhancing the system's self-sufficiency. The day-ahead stochastic model in [31] does not include Battery Energy Storage Systems (BESS), but features electro-thermal storage from a retailer's perspective. Moreover, sizing and operation of storage devices in smart buildings is presented in [32], including electrical and thermal storage. These two types of storage were also modelled in [33] to analyse cooperative schemes among smart residential buildings. The approach

in [34] presents a methodology for intraday management of PV and Electric Water Heaters (EWH) in an LV network, with the EWH acting as a flexible load in order to achieve minimum operation costs.

From the analysis of the current published research, and up to the author's knowledge, optimization models that integrate uncertainty of multiple sources with residential-based storage, have received little attention in the literature.

When including electrochemical storage, unconstrained cycling patterns can lead to faster degradation of BESS and loss of life. The aging process of storage devices is complex, and depends on the degradation of active materials due to cycling and aging of non-active components [35, 36]. Among the aggregation schemes currently published, few present details of storage cycling characteristics for inclusion of equivalent degradation costs, in spite of their importance in energy bidding and scheduling-related problems [37, 38].

Although some previous MG management referenced papers include at least one battery in their respective test systems, none includes the non-linear relation of DoD to account for impacts on degradation and cycling aging. At most, a simplified linear cost (function of power charge and discharge) is included in [15, 18, 19]. The proposed models are simplified and neglect DoD vs cycles characteristic, which presents highly non-linear behaviour and depends on internal chemical reactions with electrode interfaces. The linear costs in [15, 18, 19] assume that degradation is proportional to power charge and discharge, but no further identification of cycles and the respective DoD is proposed. This can lead to suboptimal bidding strategies and device schedules. Moreover, references [17, 20, 21] neglect cycling aging impacts.

Another potential of residential aggregation with storage devices and RES, is the provision of local flexibility services. Local markets are still an emerging topic and subject of conceptual discussion. However, aggregators have to be capable of adjusting device scheduling and energy bids in order to provide these local services to DSOs or to other third parties requesting flexibility, when price signals are convenient. Research that articulates local flexibility and prosumers has emerged in recent years. One common practice is to directly include local flexibility scheduling in distribution power flow calculations to solve voltage and congestion issues [39–43] assuming that the DSO and aggregator form a unique entity, which is able to perform grid analysis.

Separate local market schemes or services have been proposed to provide upward or downward regulation [44], transactive models among energy communities [45], and ramping products [46]. Other studies have also addressed the importance of managing ramping at the distribution level by smoothing net exchanges [17, 47]. In the case of [17], ramping capabilities are not traded locally but in traditional wholesale and ancillary markets.

Reference [48] proposes a local energy system in which an aggregator acts as an intermediate between multi-energy resources and the wholesale market. Although the aggregation is local, the market interaction takes place with the wholesale market only, and assumes that local flexibility is traded in this centralized environment. Similarly [15, 49] propose bidding schemes in traditional wholesale markets.

1.2.3 Identified research gaps

From the previous literature review, the following research gaps are identified:

1. Degradation effects and equivalent cycling aging of BESS can be included in energy market participation to capture batteries' aging costs. Most studies present simplified models of cycling equivalent costs and efforts are mainly dedicated to the field of electric vehicles.

2. There is a lack of optimization models that holistically integrate the following features from the aggregator standpoint:

   (a) Residential aggregation models to participate in day-ahead markets that include uncertainty of prices, RES production and demand in a unique model, are still very scarce in the literature.

   (b) Among the published research, few works have studied storage aggregation along with impacts of uncertainty. The closest studies usually pursue different objectives, such as frequency response services or congestion management from the DSO's perspective.

   (c) Thermal and electrical storage coordination/aggregation models that consider uncertainty, not only in thermal demand, need to be proposed. When thermal demand uncertainty is considered, other sources of uncertainty such as prices, electrical demand and RES production, are usually neglected of partially covered.

3. Exploitation of residential flexibility through aggregation can be used to provide local flexibility services. Strategic and robust schemes for bidding in both energy and local emerging markets are still open research interests.

In line with the philosophy of the previous ideas, in this thesis we carried out research that intends to contribute in areas of interest not only for the academic community regarding mathematical models and research gaps but also aligned with recommendations made by European authorities and taking into account current industry interests.

1.3 Scientific objectives

The objective of this research is to evaluate the benefits and limitations of mathematical models under uncertainty for aggregators of prosumer's flexibility participating in day-ahead energy market and local flexibility markets. The aggregator manages residential storage devices and RES as sources of flexibility to minimize operational costs. From the previous general objective, three specific objectives are detailed:

- To include storage-based flexibility at the residential level from the perspective of an aggregator, taking into account aging and degradation models for electrochemical storage. Residential storage is composed by thermal and electrochemical storage capabilities installed at the home-level.

- To include uncertainty from different sources (prices, RES generation, load) into the mathematical formulation in order to test the solutions performance for the adequate participation in energy markets.
- To determine the optimal day-ahead schedules that result in cost minimization for the flexibility aggregator, including traditional energy market and new schemes for local flexibility provision.

1.4 Main contributions

The main contributions of this thesis are listed below:

1. Two alternatives for including battery's cycling aging cost are presented. First, an approach called Storage Disaggregation Algorithm (SDA) based on Lagrangian relaxation and the Rainflow Counting Algorithm (RCA) is presented. This approach allows decomposing the battery cycling problem solved by the SDA and the day-ahead scheduling of resources. This problem separation logic for scheduling resources of an aggregator has never been used by any previous research in order to solve the resulting scheduling problem including cycling aging of BESS. Second, explicit modeling of battery cycling cost is presented by means of special ordered sets. This degradation modeling allows to capture the non-linear relation between DoD and total life cycling to bid adequate quantities in the day-ahead markets. This contribution is in line with challenge 3 and research gap 1, and has lead to support the publications [CF-1,CF-2,CF-6] detailed in subsection 1.5.
2. A model for optimal operation and coordinated aggregated management of prosumers' resources is proposed, which takes into account the following sources of uncertainty: electrical and thermal demand, PV production and energy prices. These uncertainties are included in the mathematical model by means of ARO theory and a methodology is proposed to detect the best robust solutions for day-ahead participation in energy markets based on Pareto-optimality theory. This approach allows to analyze the performance of multiple robust day-ahead decisions and select the Pareto front offering solutions with the best trade-off between cost and risk. In this case, the risk is measured by the standard deviation after running Monte Carlo simulation for multiple uncertainty realizations. This contribution is in line with challenges 1,3 and research gap 2, and has lead to support the publications [CF-2,CF-4,CF-5,CF-7,CF-8].
3. A new local flexibility management strategy is proposed, which is based on two products: 1) flexibility bids in a local market; and 2) local constraint support for the DSO in the form of maximum allowed net power and net ramping rate. Numerical results demonstrate that the strategic bidding framework is robust enough to enable coordinated participation in three different marketplaces (energy, local flexibility and bilateral trading with DSO) with diverse settlement mechanisms. This contribution is in line with challenge 2 and research gap 3, and has lead to support the publications [CF-3,CF-5,CF-8].

1.5 List of publications

The following publications were developed as a result of this thesis:

Journal Papers

CF-1 **Carlos Adrian Correa-Florez**, Alexis Gerossier, Andrea Michiorri, Georges Kariniotakis, "Stochastic operation of home energy management systems including battery cycling", Applied Energy, Volume 225, 2018, Pages 1205-1218, ISSN 0306-2619, https://doi.org/10.1016/j.apenergy.2018.04.130. Reference [50].

`www.sciencedirect.com/science/article/pii/S0306261918306597`

`https://hal-mines-paristech.archives-ouvertes.fr/hal-01809270`

CF-2 **Carlos Adrian Correa-Florez**, Andrea Michiorri, Georges Kariniotakis, "Robust Optimization for Day-ahead Market Participation of Smart-Home Aggregators". Applied Energy, Volume 229, 2018, Pages 433-445, ISSN 0306-2619, https://doi.org/10.1016/j.apenergy.2018.07.120. Reference [51].

`www.sciencedirect.com/science/article/pii/S0306261918311553`

`https://hal-mines-paristech.archives-ouvertes.fr/hal-01862545`

CF-3 **Carlos Adrian Correa-Florez**, Andrea Michiorri, Georges Kariniotakis, "Optimal Participation of Residential Aggregators in Energy and Local Flexibility Markets", under review in IEEE Transactions on Smart Grid.

CF-4 **Carlos Adrian Correa-Florez**, Andrea Michiorri, Georges Kariniotakis, "Comparative Analysis of Adjustable Robust Optimization Alternatives for the Participation of Aggregated Residential Prosumers in Electricity Markets", in revision in MDPI Energies journal.

CF-5 **Carlos Adrian Correa-Florez**, Alexis Gerossier, Andrea Michiorri, Georges Kariniotakis, "Hybrid stochastic-robust optimization for management of prosumers aggregation considering grid flexibilities", in preparation to be submitted to the International Journal of Electric Power and Energy Systems, after invitation received from Medpower 2018 organizing committee.

Conference proceedings

CF-6 **C. A. Correa**, A. Gerossier, A. Michiorri and G. Kariniotakis, "Optimal scheduling of storage devices in smart buildings including battery cycling", 2017 IEEE Manchester PowerTech, Manchester, 2017, pp. 1-6. doi: 10.1109/PTC.2017.7981199. Reference [52].

`https://ieeexplore.ieee.org/document/7981199`

`https://hal-mines-paristech.archives-ouvertes.fr/hal-01520365`

CF-7 **C. A. Correa-Florez**, A. Gerossier, A. Michiorri, R. Girard and G. Kariniotakis, "Residential electrical and thermal storage optimisation in a market

environment", in CIRED - Open Access Proceedings Journal, vol. 2017, no. 1, pp. 1967-1970, 10 2017. doi: 10.1049/oap-cired.2017.1086. Reference [53].

http://ieeexplore.ieee.org/stamp/stamp.jsp?tp=&arnumber=8316208&isnumber=8315543

https://hal.archives-ouvertes.fr/hal-01518380

CF-8 **Carlos Adrian Correa-Florez**, Alexis Gerossier, Andrea Michiorri, Georges Kariniotakis, "Day-Ahead Management of Smart Homes Considering Uncertainty and Grid Flexibilities", Mediterranean Conference on Power Generation, Transmission, Distribution and Energy Conversion (MedPower 2018). Dubrovnik, Croatia. Reference [54].

https://hal.archives-ouvertes.fr/hal-01948634

This paper was warded as 2nd best paper of the conference MEDPOWER 2018: http://medpower2018.com/best-paper-award/

CF-9 Pedro Castro, Ricardo André, Alexandre Neto, Gisela Mendes, Clara Gouveia, Olli Kilkki, **Carlos Correa**, André Madureira, Andrea Michiorri, "Demand Side Management in a rural area", CIRED Workshop 2018 on Microgrids and Local Energy Communities.

https://hal-mines-paristech.archives-ouvertes.fr/hal-01813262

1.6 Layout of the document

This document is organized as follows:

Chapter 2 presents the details of the mathematical formulation. This chapter shows the modelling of the prosumers' devices and the interaction at the Point of Common Coupling (PCC). The BESS equivalent cycling costs models are described. In concrete, two models are presented, 1) a Lagrangean based algorithm, and 2) explicit modeling by means of special ordered sets. In addition, interactions of both BESS and Thermal Energy Storage (TES) are presented to show the advantages of coordinated operation of storage devices.

Chapter 3 introduces uncertainty into the model presented in chapter 2. The robust counterpart of the deterministic model is presented to model price, demand and PV production uncertainty. A methodology to evaluate performance of the robust solutions is presented and comparison with the deterministic approach is carried out. Moreover, comparisons with hybrid Robust/Stochastic approaches are presented. In this case, stochastic optimization and backward scenario reduction is used as an alternative to model day-ahead price uncertainty.

Chapter 4, extends the day-ahead participation of aggregators under uncertainty towards the inclusion of local flexibility markets. This section presents a robust bidding mechanism in day-ahead energy markets and also for local flexibility service provision. The sequence of actions to create robust bids is described and different situations of bid acceptance by a Local Market Operator are presented to test the methodology.

Finally, chapter 5 outlines the main conclusions of this thesis and the future research opportunities.

The thesis is complemented by four appendices. Appendix A presents additional details of the SDA, regarding a correction algorithm when batteries reach energy boundary values. Appendix B shows the outline of the extension of the SDA for scenario-based optimization models. Afterwards, appendix D shows a specific contribution made during the development of this thesis to the Horizon 2020 project SENSIBLE (Storage ENabled SustaInable energy for BuiLdings and communitiEs - https://www.projectsensible.eu/) in the framework of the use case "Flexibility and demand side management in market participation" [55]. Two algorithms are briefly described, which aim to determine average cost of residential flexibility and to disaggregate flexibility signals to be followed by the devices installed at the residential level. Finally, appendix E presents an extended abstract of the thesis in French language.

A flowchart showing the location of the main models in the present thesis can be seen in figure 1.2.

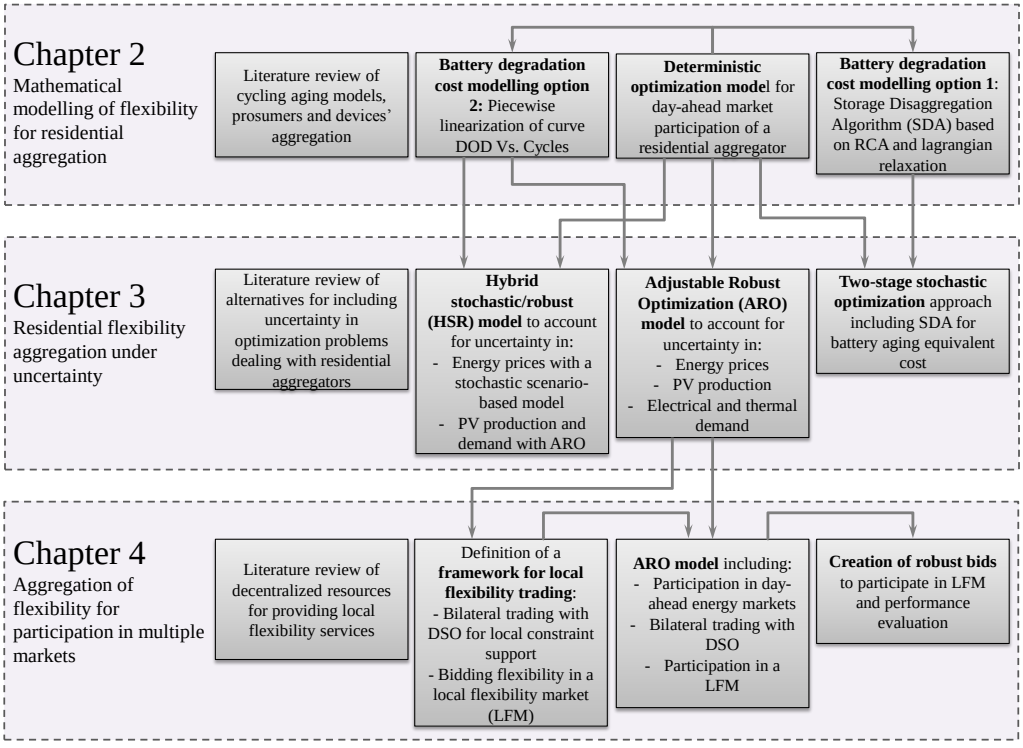


Figure 1.2: Graphical outline of the main body of the thesis

Chapter 2

Mathematical modelling of flexibility for residential aggregation

This chapter presents a discussion and a literature review of flexibility aggregation at building/home levels for participation in energy markets. It also presents the details of the mathematical formulation for the devices present in the test system, a brief overview of the PV and load forecasts used in the model and the description of the test system used in this thesis for validation of the optimization algorithms. In addition, the chapter presents two alternatives for including battery degradation costs in the optimization model for participation of an aggregator in the wholesale energy market.

The models and results presented in this chapter led to publications [CF-1,CF-2,CF-6,CF-7].

Flexibility in power systems covers a wide area of applications such as: peak shaving, demand side management, investment deferral, imbalance reduction, frequency regulation, voltage and reactive power support and reserve markets. In addition, penetration of variable renewable generation such as PV and wind, might jeopardize grid security when high shares of RES supply instantaneous power. In this context, ESS and their fast response characteristics constitute a promising alternative to provide reserves and offset the differences in predicted and actual RES power output to achieve economical and reliable service [56]. In general, BESS act as a key component in the provision of flexibility in power systems in the attempt of mitigating disturbances of any kind present in the system during its operation. Classical definition of flexibility comprises power, ramp and energy as the metrics to assess the operational flexibility resources and requirements [57]. Flexibility provision based on storage devices, has been demonstrated to impact positively in the operation of power systems from the technical and economic standpoint. Technically, some of the advantages of using storage include grid voltage support, grid frequency support, grid angular stability, spinning reserve, power reliability and unbalanced load compensation. Financial benefits resulting in cost reduction or revenue increase are achieved by energy arbitrage, avoiding new generation installation, ancillary services, transmission congestion, reduced demand charges, load

shifting [58, 59].

2.1 Literature review

2.1.1 Effects of cycling aging in the operation of storage devices

Charging and discharging patterns of BESS impact on the battery life. Taking into account this particularity of BESS behaviour, allows to manage the devices in a more realistic way and leads to more accurate definition of capabilities and operation costs.

Battery life in general can be expressed in terms of the actual lifespan of the device (calendar life) or the number of achievable charge and discharge cycles (cycle life). This aging process is complex and depends on the rates of charging/discharging, the consequent chemical reactions with electrode interfaces, and the degradation of active materials due to cycling and aging of non-active components resulting in an accumulated history of voltages, currents and temperatures [35, 60]. In general, this degradation process can be tracked and modelled by determining the cycling patterns, the respective Depth of Discharge (DoD) and the rate at which this process occurs. Although the detailed analysis of this set of interactions is beyond the scope of this thesis, it is important to explore how aging is considered in storage management optimization models for smart grid applications.

To include this process in the operation of decentralized sources, some approaches use predefined limits for the total energy that can be cycled, in the form of equivalent State of Charge (SOC) or DoD values. For example, the work presented in [61] evaluates the impacts of peak shaving when demand response (DR) potential is enhanced through different storage technologies. To include cycling of storage devices, a set of values of the energy that can be cycled are predefined and analysed. Reference [62] presents a model which calculates cycle life depreciation based on a predefined lifespan of 10 years and 3000 cycles for li-ion BESS, and calculating a proportional cost with the net energy input. This calculation method disregards partial cycling of the BESS, and thus can lead to underestimation of actual depreciation cost.

A more detailed [63] electro-thermal battery model is used for determining savings in the secondary reserve market for system operator owned BESS. This model includes variable dispatch cost for batteries by parameter fitting analysis including terminal voltage, currents, temperature and SOC. Although this is a more detailed model of the internal interactions in the BESS, this approach would require parametrization for each analyzed storage unit.

Authors in [64] develop a short-term cost model for the BESS, in order to solve a 24h resource scheduling problem. Number of cycles and the DoD for a given time horizon, are explicitly included in the optimization problem. Given that relation of DoD and life cycles is non-linear, the operation costs of the BESS are based on linearization by segments, and assigning charging cycle variable and constant cost. Similar linearization based modelling is used in [65, 66], for the case of electric vehicles battery degradation.

Following the same logic of the previous work, the research [67] presents an explicit cost function that models battery degradation, which is used to implement

a MPC peak shaving algorithm that includes a 1 MW BESS. The authors achieve the explicit formulation of the degradation costs by detecting transitions between charging/discharging and idle mode by state representation. This way, a quadratic cost function that captures cycling stress in terms of power, DoD and SOC, can be found. One advantage of this approach is the possibility of embedding the aging model into an optimization problem, without adding major complexity in terms of non-linear equations. Another interesting model that considers explicit cycling by counting state transition for the case of EHV is presented in [68].

Quadratic explicit modelling is proposed in [69] to calculate battery degradation costs. This expression does not consider state transitions and is only dependant on the power profile as a sum of a linear and quadratic function. In a different attempt compared to the previous logic, the research in [70] includes detailed behaviour of battery voltages and currents due to operating DoD, with the aim of managing resources in residential microgeneration systems.

Cycling aging is considered in [71] to complement a bidding strategy for DA, spinning reserve and regulation markets. By identifying local adjacent extreme energy points extracted from the SOC curve, and the energy difference between these points is assumed as the DoD at which half cycle occurs. After this, with each DoD, an equivalent cycling is calculated for a complete day.

Another way of taking into account battery aging is by using the rainflow counting algorithm (RCA) [72] originally proposed by Downing in [73] for metal fatigue cycles calculation. This method was recently used in [74] for counting complete and incomplete cycling of batteries that provide fast and slow response to offset wind power variation. The use of the RCA allows assessment of the lifetime depreciation for the provided services. It is important to note that this method is not embedded into an optimization model but is used after a specific SOC is obtained. A similar approach is presented in [75] for battery life estimation adding a step for equivalent life estimation due to incomplete cycles.

Other recent research, attempts to mathematically mirror the state transition identification and counting of the RCA, to find a tractable and convex equivalent model, so as to embed the formulation and solve electricity related problems [37, 38]. These contributions represent an important tool to overcome the difficulty of including the RCA logic in optimization problems in future research. In general, these seem to be a consensus on the accuracy of RCA to include equivalent cycling aging cost as a measure of BESS cycling marginal cost, hence the importance of exploring this one and other options that include transition detection for BESS aggregation studies.

Discussion

For the treatment of cycling aging into battery scheduling problems, three main alternatives are identified:

- First, calculating equivalent cycling offline for a defined time horizon, after a scheduling program has been obtained, i.e. the DoD. Given the non-linear relation between DoD and cycling, this calculation has to be done by means of rainflow methods. Although this appears to be the most accurate way to calculate equivalent aging [38], the disadvantage is the difficulty of accurately

capturing the non-linearities within an optimization problem. A research opportunity that appears in this case, is related to the use of algorithms that allow iterative cycling calculation. If an algorithm, i.e. a metaheuristic, proposes charging/discharging patterns, this information can be used as data for the RCA and for the remaining optimization problem, and then obtaining a total fitness function (i.e. total operation cost). According to the performed literature review no evidence of previous research using this philosophy was found.

- Second, the explicit modelling of this process into an optimization problem as proposed in [67]. The explicit modelling aims to capture, identify and count the state transitions (charging/discharging/idle) and minimize them at the same time, by means of equations containing binary variables. The continuous cycling is penalized in the objective function by assigning an equivalent cost that might come from the actual battery costs. Although this implies a linearization of the DoD-cycling relation, this approach gives the opportunity of keeping tractability on the optimization problem and the possibility of using commercial optimization solvers.

- Third, the inclusion of equations containing relations between DoD, voltages and currents are shown as an option. However, these models are more useful when detailed circuit models of devices are needed, or if voltages and currents are available. For the case of management of flexibilities in market participation of aggregators, voltages and current are not always available or necessary, or could increase the computational effort of an algorithm, which leads to conclude that this might not be a useful for energy market applications.

Cycling life versus calendar life

Besides cycling life to account for battery degradation, another measure is related calendar life. Even if both models (cycle life - calendar life) are interdependent, it is difficult to exactly model all interactions. However, the reasons to opt for cycling life in this thesis instead of calendar life, are threefold:

1. From the perspective of short term electrical markets, such as day-ahead, cycle life is commonly used provided that: a) it allows to calculate an equivalent operation cost of using the batteries to trade energy and include it to the total cost of the system operation for bidding purposes. Multiple research works consider cycling instead of calendar life, such as [64, 65, 71], among many others.

2. This thesis uses the information available in [76], in which the curve of cycles Vs DoD is available. The curve indirectly includes calendar life information, given that 70 % capacity at EOL (End Of Life) is considered to build the curve. This available information from manufacturers allows to explicitly model cycling into the optimization problem as later decribed in sections 2.4 and 2.5.

3. The models presented in this thesis can be used for aggregation applications in order to offer services in ancillary markets and local flexibility markets, in which cycling of batteries is a key factor to consider. This modelling alternative suits the remainder of this thesis and also justifies the use of cycling.

2.1.2 Aggregation of prosumers

New approaches featuring decentralized generation and coordination with demand side flexibility have gained substantial attention in recent years. Some of these new schemes are being developed in the medium and low voltage grid, and most recently at building and home level, leading to the development of concepts such as Smart Residential Buildings (SRB) and Home Energy Management Systems (HEMS) [77]. The control capabilities and IT platforms allow management of the resources present in these home/building levels to maximize profit by offering grid services or by minimizing overall operational costs.

Home/Building optimal management with BESS

Sizing and operation of storage devices in smart buildings is presented in [32], including electrical and thermal storage. This study concludes about the importance of thermal storage for saving energy costs. However, it does not take into account cycling aging and points out that batteries might not be economical due to investment costs and short lifetime. Other approaches have also proposed models for optimal management of resources, in which the same general objective is pursued: minimizing daily energy cost while complying with technical constraints and occupants comfort. For example, in [78] a model to control appliances at the home level is presented, taking into account variable pricing; in [79] a multi-objective model is proposed for finding trade-off solutions with different levels of energy saving and comfort; authors in [80] propose an architecture for real time pricing in order to achieve cost-effective management at the home device level; a day-ahead method for resource scheduling in a HEMS and building energy management system is presented in [81], this scheme presents a three stage optimization process for prediction, supply control and demand control.

Thermal and electric energy storage coordination

Regarding management models for joint thermal and electric storage technologies at the residential level, approaches include the one presented in [30], which proposes a residential microgrid in which thermal and electric storage make it possible to shave the demand peak and enhance the system's self-sufficiency. An intra-day methodology is presented in [34] to manage EWH as a flexible load.

Reference [31] presents an optimization problem for the day-ahead market that minimizes retailer costs represented by imports/exports, and gas costs, along with expected balancing costs in real-time operation. The model does not include BESS, but does include thermal load and electro-thermal storage, which can generate or consume power. An interesting feature of this approach, is the inclusion of thermal discomfort, which is measured and penalized by means of deviation of expected temperature.

A recent paper [33] presents a cooperative scheme of Smart Residential Buildings (SRB) for optimal management of resources, considering batteries, thermal storage and electric vehicles. Although cycling is not taken into account, this study constitutes an interesting benchmark given that different network configurations

are presented, showing the importance of exploiting operational flexibilities when various interactions are analyzed.

A multi-energy microgrid was recently proposed in [40], in which thermal and electrical storage, and heat sources are used to reduce operation costs and alleviate network capacity issues at the PCC. Although it accounts for neither battery cycling nor uncertainties, this paper presents a thorough modeling of different energy sources and their interactions, and is tested on a system comprising 300 households.

From the previous literature review, research opportunities are identified related to prosumers aggregation from the residential perspective, by combining electrical and thermal storage, and also considering cycling aging equivalent costs for BESS into optimization models. The remainder of this chapter introduces the deterministic mathematical model for an aggregator of prosumers that participates in day-ahead energy markets. Details of the devices modelling and the way of including equivalent BESS degradation costs are presented.

2.2 Mathematical modeling of prosumer's aggregation for participation in the day-ahead energy market

The proposed general HEMS to be used for modeling purposes is composed of solar panels, li-ion batteries, EWHs with storage capabilities, a connection to the main grid and a number of households. Each household comprises a total electrical base load to be supplied and a thermal load that has to be met by an EWH, which also stores energy in the form of heat, hence acts as a flexible load. The interaction of all devices allows flexible operation of the system to achieve minimum cost.

In general, EWH input and electrical load during the 24h period can be met by the main grid, the solar panels, and the power injected from the batteries. The idea is to achieve a minimum operation cost by adjusting the setting of the devices in order to optimally manage resources. The diagram of the proposed aggregation of resources is shown in figure 2.1.

One feature of the proposed HEMS is the possibility to independently control the BESS and the EWH when the latter has storage and control capabilities. This means that the LV grid does not directly feed the thermal load ($Q_{t,h}$). In other words, this load is fed by the available stored energy in the TES, and the input for the EWH ($H_{t,h}$) is seen as a load from the LV network. This can be interpreted as a flexible load which responds depending on the price of opportunity captured by the optimization model by storing hot water even if it is not immediately used by the occupants.

The following paragraphs introduce the mathematical optimization model for minimization of operation cost from the standpoint of an aggregator.

2.2.1 Objective function

The present model suposes an aggregator of residential flexibility that participates in the day-ahead energy market by controlling the set-points over a predefined horizon of 24-hour (T) time-steps. The objective function aims to minimize the energy purchases in the wholesale market and the overall operational costs. This model

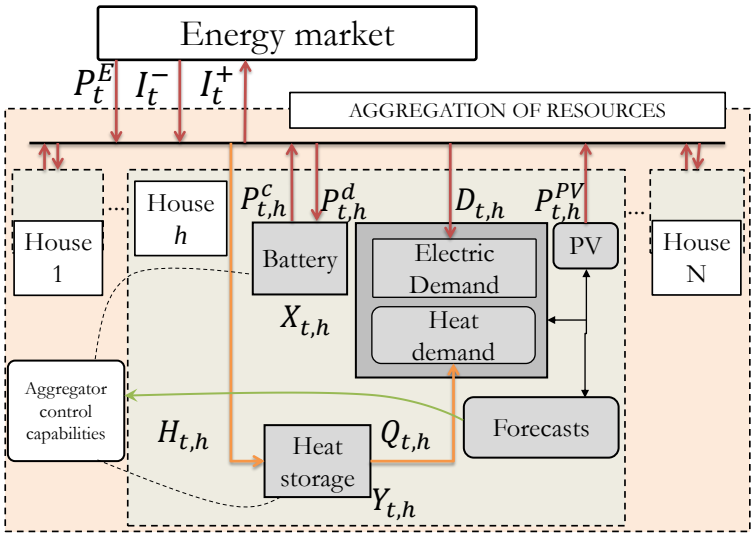


Figure 2.1: Schematic diagram of the proposed HEMS

takes into account day-ahead energy prices (π_t) and the possibility of purchasing or selling energy (P_t^E) at the point of common coupling (PCC). In addition, the aggregator offsets day-ahead purchase deviations with actual generation and demand levels, by participating in the imbalance market, where I_t^- (I_t^+) indicates additional imports (exports) in real time. The present model supposes that energy requirements or surplus at the PCC can be traded in the wholesale market without market or regulation barriers.

As shown in Eq. (2.1), the proposed model minimizes the expected day-ahead operation cost, in which the decision is associated with:

- $\sum_{t=1}^{T} \pi_t P_t^E$: The cost of the day-ahead traded energy in the wholesale market.
- $\sum_{t=1}^{T} \mu_t^- I_{t,s}^- - \mu_t^+ I_{t,s}^+$: The cost of purchasing additional blocks of energy (negative imbalance) and the amount received for selling energy surplus (positive imbalance) due to deviations with respect to the day-ahead committed energy. Imbalance prices suppose an indirect penalization given that they are less attractive than day-ahead settled prices.
- $\sum_{h=1}^{N} f_h^{cyc}(\cdot)$: Cycling or equivalent degradation cost for the batteries installed in each house h, which is a function of the SOC vector ($\mathbf{X}_h = [X_{1,h}, ..., X_{1,T}]'$), i.e. the SOC of each battery during the day-ahead operation time horizon, provided that the SOC represents the cycling pattern.

Subscripts t and h index time step and household, respectively. Parameters π_t, μ_t^-, -μ_t^+, represent respectively, spot price, negative imbalance cost and positive imbalance cost.

$$\text{minimize} \sum_{t=1}^{T}(\pi_t P_t^E + \mu_t^- I_t^- - \mu_t^+ I_t^+) + \sum_{h=1}^{N} f_h^{cyc}(\mathbf{X}_h) \tag{2.1}$$

All of the terms in the objective function are linear, except the one related to the cycling. This term includes the corresponding non-linearities associated with the chemical reactions occurring in the batteries due to temperature changes. This terms creates a complication in the model given the difficulty of accurately expressing this phenomenon in a closed form. Two alternatives for including degradation are presented in this chapter in sections 2.4 and 2.5.

2.2.2 Load balance constraints

Constraint (2.2) represents power balance, in which the exchange with the wholesale market at the PCC should meet the net required power by aggregated prosumers in the portfolio, as also shown in figure 2.1.

$$P_t^g + I_t^- - I_t^+ + \Delta t \sum_{h=1}^{H} P_{t,h}^{net} = 0, \forall t \tag{2.2}$$

$$P_{t,h}^{net} = P_{t,h}^{PV} - P_{t,h}^c + P_{t,h}^d - D_{t,h} - H_{t,h}, \forall t, \forall h \tag{2.3}$$

$$0 \leq P_{t,h}^{PV} \leq P_{t,h}^{PV_{max}}, \forall t, \forall h \tag{2.4}$$

It is important to note that the net power in each house, as per (2.3), considers the battery charging ($P_{t,h}^c$) and discharging ($P_{t,h}^d$), the PV injection ($P_{t,h}^{PV}$), the electrical load ($D_{t,h}$) and the power required by the EWH ($H_{t,h}$). In addition, if a household is not provided with an EWH that has storage capabilities, the variable H becomes the same thermal load.

2.2.3 BESS constraints

Constraints (2.5) - (2.10) describe the energy state for the BESS. Binary variables $u_{t,h,s}$ and $v_{t,h,s}$ are introduced to avoid charging and discharging batteries at the same time. Hence, constraints (2.7)-(2.9) introduce a mixed integer characteristic into the model. Constraint (2.6) ensure the continuity of the operation from one day to another in terms of available stored energy.

$$X_{t,h} = X_{t-1,h} + \eta^c \Delta t P_{t-1,h}^c - \Delta t P_{t-1,h}^d / \eta^d, \forall t, t \neq 1, \forall h, \tag{2.5}$$

$$X_{1,h} = X_{T,h}, \forall h \tag{2.6}$$

$$u_{t,h} + v_{t,h} \leq 1, \forall t, \forall h \tag{2.7}$$

$$0 \leq P_{t,h}^c \leq \bar{P}_h^c \cdot u_{t,h}, \forall t, \forall h \tag{2.8}$$

$$0 \leq P_{t,h}^d \leq \bar{P}_h^d \cdot v_{t,h}, \forall t, \forall h \tag{2.9}$$

$$\underline{X}_h \leq X_{t,h} \leq \bar{X}_h, \forall t, \forall h \tag{2.10}$$

2.2.4 TES constraints

When the EWH present in a house has storage capabilities, then it is denoted as a TES device. In this case, it is assumed that he device can be operated for immediate hot water use or also for storing heat for later use in order to comply with user's expected thermal demand ($Q_{t,h}$). The energy state ($Y_{t,h}$) is represented by the inter-temporal constraint (2.11). Given that TES is capable of heating water for direct consumption (shower, appliances, etc.) or for space heating for upcoming hours, energy losses are present in the model by including R and C (thermal resistance and capacitance, respectively) in equation (2.11), which represent the energy dissipation, in line with [31].

$$Y_{t,h} = Y_{t-1,h} + \Delta t H_{t-1,h} - Y_{t-1,h}/R_h C_h - \Delta t Q_{t-1,h}, \forall t, t \neq 1, \forall h \tag{2.11}$$

$$Y_{1,h} = Y_{T,h}, \forall h \tag{2.12}$$

$$\underline{Y}_{t,h} \leq Y_{t,h} \leq \bar{Y}_{t,h}, \forall t, \forall h \tag{2.13}$$

$$0 \leq H_{t,h} \leq \bar{H}_{t,h}, \forall t, \forall h \tag{2.14}$$

When the EWH has no storage or control capabilities $H_{t,h}$ takes the value of the thermal demand ($Q_{t,h}$) as it can be easily inspected in equation (2.11). In other words, in the absence of TES, the total load to be supplied in each house is given by adding electrical and thermal load.

Equation (2.12) ensures continuity of the thermal storage and equations (2.13) and (2.14) are respectively the boundaries of energy and power of the TES device.

The deterministic Mixed-Integer Linear Programming (MILP) problem presented in equations (2.1)-(2.14) joins flexibilities of three types to be managed by an aggregator: PV production, electrochemical storage and thermal storage. The result of this optimization returns the set-points of all devices and the energy exchanged with the wholesale market in order to achieve minimum operation cost for the portfolio, while complying with electrical and thermal demand in each house.

2.3 Description of the test case used for simulations

The location of the HEMS in the real life distribution network and the resources present in each house are shown in figure 2.2. The 25 houses are located in an LV-rural network in Evora, Portugal, comprising the distribution of resources shown in the figure. In total, there are 25 PV panels, 16 BESS and 15 EWH that can act as TES. The testcase is composed by the HEMS and the control capabilities that an aggregator has on the device settings. The operation and control of the MV and LV distribution networks is carried out by the DSO and are not part of the aggregator's capabilities or responsibilities.

The charging and discharging efficiency of the batteries is assumed to be 95%. 15 batteries are rated 3kW / 3.3 kWh, and the remaining battery is a 10kW / 20 kWh device. All PV panels are rated 1.5 kWp. The cycling behavior is based on the li-ion battery information available on the market for residential applications, and

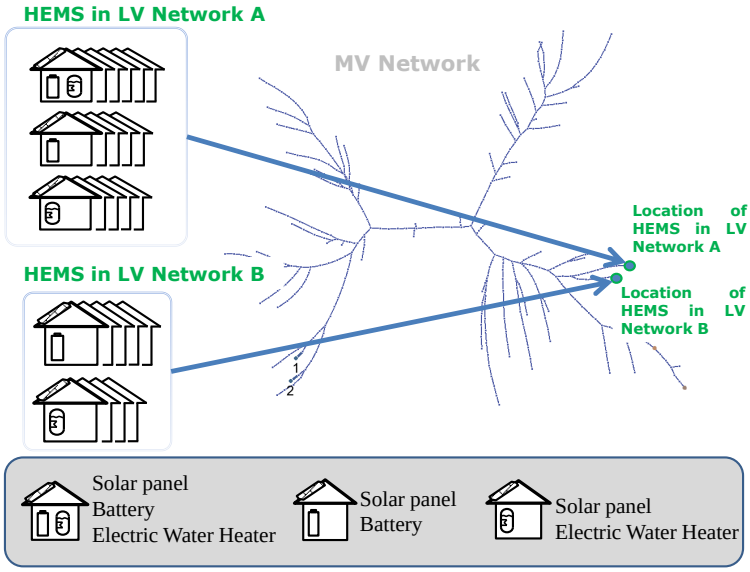


Figure 2.2: Composition and location of the proposed 25-household HEMS

the curve fitting values to obtain the relation of cycle life versus depth of discharge (DoD) are taken from its technical specifications [76].

The battery's initial cost is assumed to be 500 €/kWh, according to the information provided by IRENA on residential storage systems for European countries [82]. The rated power/energy for all EWH is 1.5 kW / 3 kWh according to the information available from the real life demonstrator and typical values from technical specifications, and thermal resistance/capacitance are 568 (°C/kW)/0.3483 (kWh/°C) taken from [31].

2.3.1 Available forecasts used as data input

Electrical load and PV forecasts

To predict the electrical demand of one household for the next day, the model uses the demand during the previous week and the outside temperature predicted for the next day. By means of quantile smoothing spline fitting [83], it is possible to predict day-ahead demand. After quantile regression, a set of forecast quantiles is obtained. Instead of a single-point value, $10\%, 20\%, \ldots, 90\%$ values can be obtained and respectively associated with a $10\%, 20\%, \ldots, 90\%$ chance of measuring a lower actual demand at the instant predicted. For further details readers are advised to review reference [83].

The PV production forecasting model takes into account solar irradiance forecasts. Parameters such as the orientation of the PV panels, shadowing effects and other meteorological factors are estimated depending on the time frame.

Probabilistic forecasts were generated for each time of day covering the entire distribution of PV production. These quantile forecasts are given in steps of the nominal probability, hence obtaining PV forecasts associated with quantiles $10\%, 20\%, \ldots, 90\%$ in a similar fashion to the load forecast. For more details on the

PV forecast method, reference [84] is suggested as complementary reading. The forecasts are generated using the methods described above and based on data collected from smart meters and Numerical Weather Predictions from ECMWF (European Centre for Medium-Range Weather Forecasts).

An example of the forecasts of electrical load and PV used in this thesis are shown in figures 2.3 and 2.4.

To model user's thermal consumption, a normalized thermal load pattern is taken from [34] and scaled with the total forecast demand in each household. This is done given the absence of data for thermal load in the real life demonstrator. An example of the obtained synthetic data is shown in figure 2.5. This data can also be interpreted as the thermal comfort interval of each household in normalized power units. This information is specially useful for defining comfort confidence intervals in robust optimization formulations as shown in chapter 3.

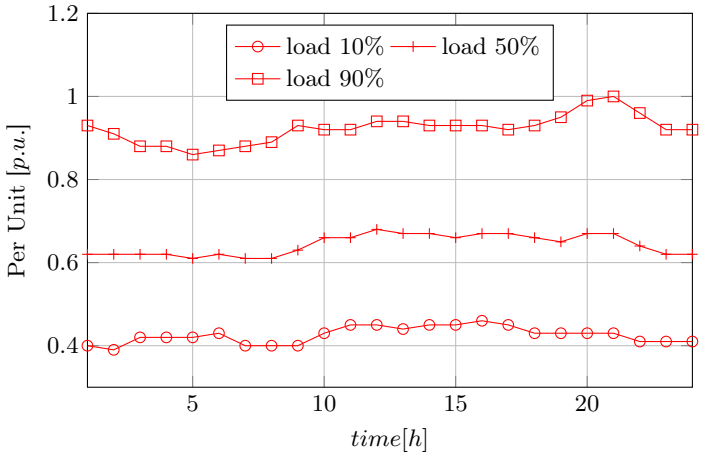


Figure 2.3: Example of normalized electrical load probabilistic forecasts

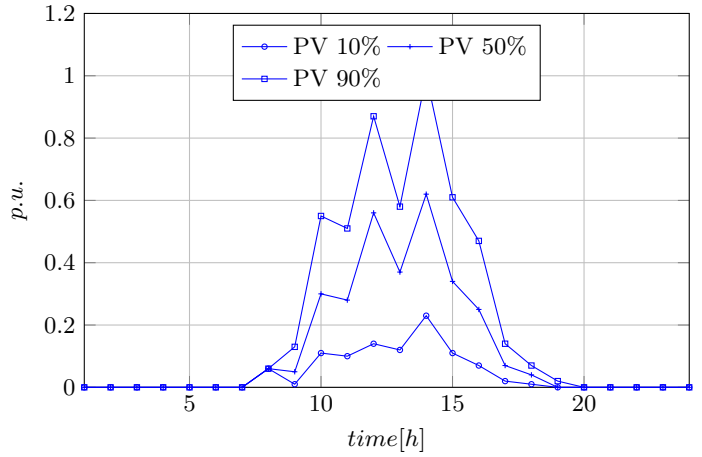


Figure 2.4: Example of normalized PV probabilistic forecasts

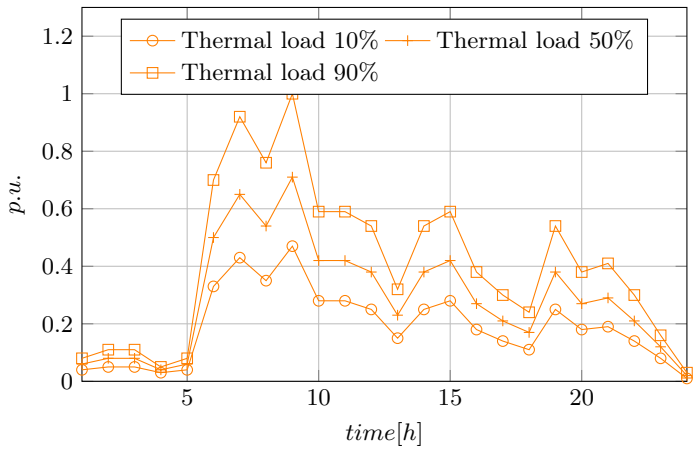


Figure 2.5: Example of normalized thermal load probabilistic forecasts

Energy price forecasts

In this thesis, unless stated otherwise, electricity prices are taken from the ENTSOE database [85], by using data from the last three months prior to the day of dispatch. To form the training set, the data during this period for the same weekday is considered. This is done to consider a realistic case in which an aggregator, when defining day-ahead purchases, does not have the settled prices. Hence, by taking the prices for the same day in the three preceding months, available input data to make decisions is obtained. With this input, the Kernel Density Estimation (KDE) of the Python package "scikit-learn" [86] is used, which also can be used after the model is trained, in order to generate samples of price trajectories.

An example of sampling output coming from the KDE python package with a calculation of percentiles 10% and 90%, is shown in figure 2.6.

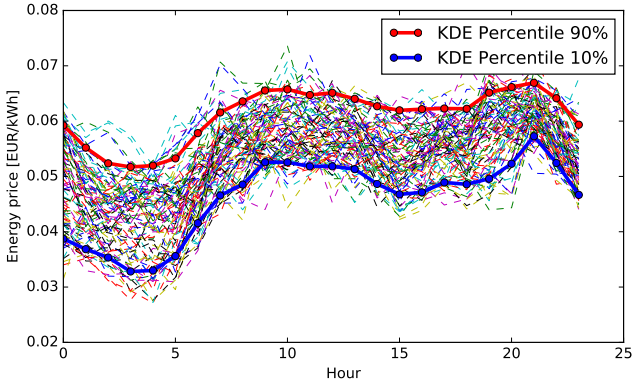


Figure 2.6: Example of forecasted confidence intervals for spot price uncertainty in a typical day in November 2015

Remarks on the size of the test system It is important to consider that the number of households (25) and the rating of their flexible devices is an available

real test case. The use of real measured data is considered a cornerstone of the thesis and a coherent dataset as the one used represents an opportunity to merge optimization algorithms with real life data.

Some European countries have day ahead and intra-day minimum bidding sizes of 0.1 MW [87]. This value can be attained in residential aggregation applications such as the case of this thesis or in commercial buildings applications, which have larger demand and heating and ventilating systems. In any case, the algorithms and approaches described in this thesis remain valid.

Current market rules and regulation remain in many cases still uncertain for demand side participation and vary in each country. This limitation is frequent, considering current market barriers since most energy markets have been designed before the development and expansion of distributed generation and storage. Some recent studies have analyzed this situation and conclude that the market should be flexible enough to allow exploitation of resources at the residential level, by allowing different emerging agents (VPP, aggregators, etc.) to participate in the market and facilitate the inclusion of distributed storage units, demand side management and prosumers participation [5, 88, 89].

One of the motivations of using the 25-household test system configuration comes from the participation in the European Project SENSIBLE [55], specifically in the use case "Flexibility and demand-side management in market participation" that assumes a retailer or other energy service company, which aggregates a number of customers and participates in a market in order to optimize its electricity costs and add value to the flexibilities that customers can offer.

The next sections will be dedicated to tackle the modelling of the cycling aging of the BESS modeled in section 2.2.3 in order to capture its equivalent cost and include it in the objective function described in equation (2.1). Hence, the alternatives for including the non-linear term $\sum_{h=1}^{N} f_h^{cyc}(\mathbf{X}_h)$ and solve the optimization algorithm (2.1)-(2.14) will be described.

2.4 Solution approach 1: Decomposition method to solve model (2.1)-(2.14)

Battery life in general can be expressed in terms of the actual lifespan of the device (calendar life) or the number of achievable charge and discharge cycles (cycle life) [60]. As already mentioned, the aging process is complex and depends on the cycling patterns, rates of charging/discharging, and consequent chemical reactions resulting in an accumulated history of voltages, currents and temperatures [35]. This work considers battery degradation costs as a function of the cycle life intrinsic behaviour and as a function of the DoD. In general, the maximum number of charge/discharge cycles for a battery at a certain value d of DoD, is given by the following expression [71]:

$$n_d = n_{100} d^{-k_p} \tag{2.15}$$

where k_p is a constant that depends on the life cycle - DoD curve given by the manufacturer, and can be extracted from curve fitting. The quantity n_{100} is the

equivalent number of cycles before failure for $d = 100\%$. An example of a fitted curve for a 3 kW / 3.3 kWh battery is shown in figure 2.7.

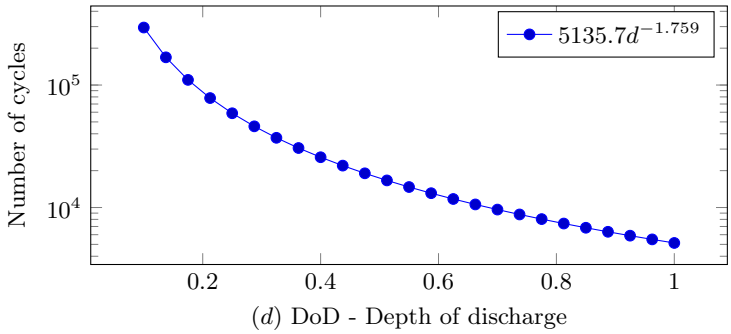


Figure 2.7: Fitted curve for a real life li-ion battery

Cycle counting for a specific DoD is identified from local extreme points based on the SOC curve (vector $\mathbf{X}$), and equivalent half or full cycles are defined. This is carried out following the logic of the Rainflow Counting Algorithm (RCA), which is explained in detail in [72].

Once the cycles counting and their respective DoDs for the 24h period have been calculated, an equivalent cycling cost is obtained according to the following expression:

$$f^{cyc}(\mathbf{X}) = C_{cyc}(d_j) = \sum_{j \in \Omega} L_j \frac{C_{ini}}{n_{100}} d_j^{k_p} \tag{2.16}$$

where Ω is the set of DoDs for the analyzed period, and C_{ini} is the initial cost of the battery. The information of full or half cycles for each d_j is given by L_j, taking values of 1 or 0.5 respectively. The obtained C_{cyc} for a specific SOC is the equivalent cost due to the battery's aging process, and should be added to the total dispatch cost. This is a measure of the battery's operational cost and is useful for bidding more accurate quantities in energy markets.

It should be noted that parameters k_p and n_{100} in equation (2.16) are a direct result of curve fitting, and d_j and L_j are a result of the RCA for a given $\mathbf{X}$.

2.4.1 Outline of the Decomposition approach

Given the difficulty of mathematically embedding the transitions/cycling counting of the RCA that results in (2.16) into the optimization model, the problem formulated in (2.1)-(2.14), can be reformulated in such a way that an algorithm iteratively proposes SOC to be analyzed from two perspectives: 1) the equivalent aging cost that this SOC will produce; and 2) the minimum day-ahead operation attained by the aggregator considering the proposed SOC.

If an algorithm is used to generate SOCs, the RCA can be applied to calculate an equivalent degradation cost by using equation (2.16), which is the equivalent of $\sum_{h=1}^{N} f_h^{cyc}(\cdot)$ in the objective function (2.1), and iteratively achieve a minimum cost solution. In this work, Competitive Swarm Optimizer (CSO) is proposed as the metaheuristic. The specifics of the CSO are detailed in subsection 2.4.4.

The complete optimization problem can be decomposed into two subproblems: one of them analyzes batteries' SOC proposals and calculates the corresponding cycling aging equivalent cost; the second subproblem takes this SOC as a fixed value and calculates the day-ahead cost due to the procurement of energy in the wholesale market and the settings for the remaining HEMS resources. Once the two subproblems are solved, the total cost can be obtained by simply adding both results (day-ahead purchase and cycling cost). The outline is presented in figure 2.8.

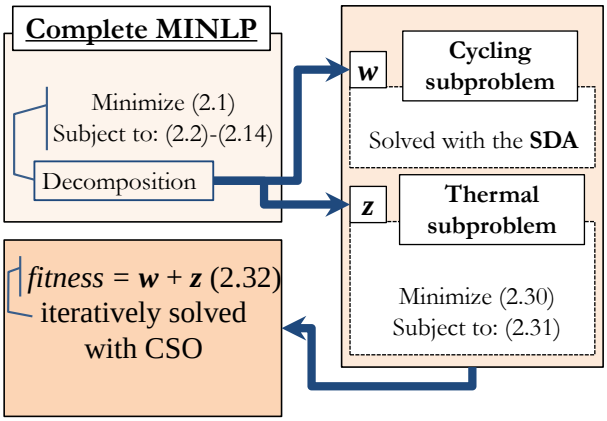


Figure 2.8: Scheme of the decomposition approach

Each solution (also called individual or particle) proposed by the CSO should contain the information of SOC in each time-step and each battery, which would yield a $T \times N$ dimensional search space. Given that a) the aggregation of prosumers usually have several batteries to be exploited; and b) the metaheuristics are sensitive to the size of the search space, it becomes important to reduce the size of the particles to avoid prohibitive computational times.

This thesis proposes a virtual aggregation of the batteries in the system so as to reduce the search space from $T \times N$ to T. With this approach, the dimension will be the same even if the system contains a high number of batteries. Given that an infinite number of possibilities exist to allocate individual SOCs, when an aggregated SOC is proposed, there should be a cost-efficient disaggregation/allocation of charge for each of the batteries, and this is carried out by applying a Storage Disaggregation Algorithm (SDA), as explained in the next section.

2.4.2 Cycling cost subproblem, the storage disaggregation algorithm (SDA)

When a certain aggregated SOC ($\mathbf{X}^{agg}$) is proposed in each iteration by the metaheuristic logic, it has to be optimally allocated/dissagregated in each battery. This depends on each battery's cycling aging characteristics and the associated SOC.

This subproblem can be mathematically formulated as follows:

$$\text{minimize } w = \sum_{h=1}^{N} f_h^{cyc}(\mathbf{X}_h) \tag{2.17}$$

s.t.

$$X_t^{agg} = \sum_h X_{t,h}, \forall t \tag{2.18}$$

The problem is general enough to take into account a different cycling function f_h^{cyc} for each battery installed in each house h. Additionally, $\mathbf{X}_h = [X_{1,h}, ..., X_{T,h}]'$, represents the 24-hour vector of SOC for each battery h. The objective function (2.17) attempts to minimize overall cycling cost for the complete set of batteries in the system and for a given $\mathbf{X}^{agg}$. Note that constraint (2.18) is defined for each time-step. Hence, X_t^{agg} is the aggregated SOC of all batteries in the specific time-frame t.

When applying Lagrangian relaxation to this optimization problem (2.17)-(2.18), one multiplier (λ_t) appears for each time-frame, as shown in the function:

$$\mathcal{L} = \sum_{h=1}^{N} f_h^{cyc}(\mathbf{X}_h) + \sum_{t=1}^{T} \lambda_t (X_t^{agg} - \sum_h X_{t,h}) \tag{2.19}$$

After applying optimality conditions to the langrangian function (2.19) (i.e., derivative with respect to $X_{t,h}$ and λ_t), the obtained equations are:

$$\frac{\partial \mathcal{L}}{\partial X_{t,h}} = \frac{\partial f_h^{cyc}(\mathbf{X}_h)}{\partial X_{t,h}} + \lambda_t = 0, \forall t, \forall h \tag{2.20}$$

$$\frac{\partial \mathcal{L}}{\partial \lambda_t} = X_t^{agg} - \sum_h X_{t,h} = 0, \forall t \tag{2.21}$$

From equation (2.20) it is concluded that the derivative for each time step is battery invariant. This is a very important condition meaning that for a given t, the derivatives of each battery must be the same:

$$\frac{\partial f_1^{cyc}(\mathbf{X}_1)}{\partial X_{t,1}} = \cdots = \frac{\partial f_h^{cyc}(\mathbf{X}_h)}{\partial X_{t,h}} = \cdots$$
$$\cdots = \frac{\partial f_N^{cyc}(\mathbf{X}_N)}{\partial X_{t,N}} = -\lambda_t, \forall t \tag{2.22}$$

To calculate the derivatives in condition (2.20) an additional difficulty arises, given that there is no analytic function to express f_h^{cyc}. To solve this issue, numerical differentiation is used to iteratively find the $X_{t,h}$ that leads to (2.22) while satisfying (2.21):

$$\lambda_t^{(h)} \approx \frac{f_h^{cyc}(\mathbf{X}_h) - f_h^{cyc}(\mathbf{X}_h + \Delta X_{t,h})}{\Delta X_{t,h}} \tag{2.23}$$

Superindex (h) is introduced to denote that a multiplier $\lambda_t^{(h)}$ should be calculated for each battery h, and the iterative process should correct the values $X_{t,h}$ until

the multiplier is the same for all batteries (until $\lambda_t^{(1)} = ... = \lambda_t^{(N)} = \lambda_t$). The evaluation of $f_h^{cyc}(\cdot)$ in (2.23), can be easily performed by using RCA and then applying equation (2.16).

This disaggregation algorithm is initialized by selecting a $X_{t,h}$ in such a way that eq. (2.18) (same as eq. 2.21) is met. After this, $\lambda_t^{(h)}$ are calculated by using (2.23). Given that $X_{t,h}$, in each t, needs to be updated to achieve equal $\lambda_t^{(h)}$ for all batteries, a deviation for each (h) is calculated by:

$$\Delta\lambda_t^{(h)} = \lambda_t^{(h)} - \bar{\lambda}_t \tag{2.24}$$

where,

$$\bar{\lambda}_t = \sum_h \lambda_t^{(h)}/N \tag{2.25}$$

Equation (2.24) measures the deviation of each battery's derivative with respect to the mean, hence, a simple heuristic rule is used to update SOC values according to:

$$X_{t,h}^{new} = X_{t,h}^{old} + \phi \cdot \Delta\lambda_t^{(h)} \tag{2.26}$$

where ϕ is a tuning parameter. Once the SOC is updated for each battery, eq. (2.23) is used again and the process is repeated until all deviations for each t are lower than a tolerance threshold. One very important feature of the presented method is that in this iterative process, optimality condition (2.21) (equivalent to constraint (2.18)) is always automatically ensured, given that $\sum \Delta\lambda_t^{(h)} = 0$. This allows the aggregation of all batteries to equal the aggregated SOC at any time and scenario.

The outline of the proposed disaggregation algorithm is shown in figure 2.9. If any of the $X_{t,h}$ exceeds the boundaries at a certain iteration of the SDA (to ensure constraint 2.10), a correction procedure is applied to maintain the feasible operation of devices, which is explained in annex A. The SDA then returns individual (disaggregated) SOC for each battery h and the total cycling equivalent cost.

2.4.3 Day-ahead thermal subproblem

When a certain SOC is generated with a metaheuristic and then disaggregated by means of the SDA, the problem in equations (2.1)-(2.14) has to be reformulated. This subproblem is called the Thermal Subproblem, given that once an SOC is known, the remaining set points that need to be determined in each household are those associated with the EWH.

Note that after the SDA is applied, the SOC for each battery is found, hence, all batteries' settings can be calculated, and variables $X_{t,h}$, $P_{t,h}^c$ and $P_{t,h}^d$ become known parameters that can be fed into the model. In addition, BESS constraints (2.5)-(2.10) are no longer required.

First, $P_{t,h}^c$ and $P_{t,h}^d$ can be easily determined by using equation (2.5) and solving for $P_{t,h}^c$ and $P_{t,h}^d$. The fact that charging and discharging cannot happen at the same time is conveniently used to apply the following rule:

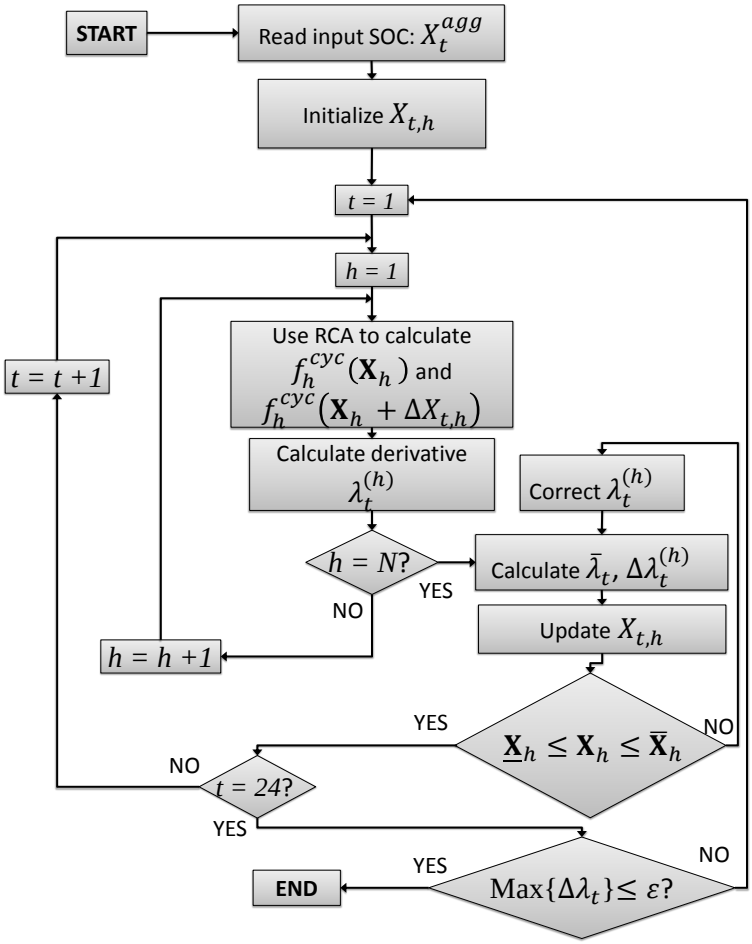


Figure 2.9: Flowchart of the SDA

$$P^c_{t-1,h} = \begin{cases} (X_{t,h} - X_{t-1,h})/(\eta^c \Delta t), & \text{if } X_{t,h} - X_{t-1,h} > 0 \\ 0, & \text{otherwise} \end{cases} \tag{2.27}$$

$$P^d_{t-1,h} = \begin{cases} (X_{t-1,h} - X_{t,h})\eta^d/\Delta t, & \text{if } X_{t-1,h} - X_{t,h} \geq 0 \\ 0, & \text{otherwise} \end{cases} \tag{2.28}$$

It is worth noting that constraint (2.6) implies that both $P^c_{t,h}$ and $P^d_{t,h}$ have to be zero for the last time frame ($t = T$) in order to match the SOC for the first time frame of the following day. Thus, equations (2.27) and (2.28) are valid for $t : \{2, ..., T\}$.

In addition, this simple rule eliminates the Mixed-Integer Non-Linear nature of the complete problem expressed in constraints (2.5)-(2.10), given that equations (2.27)-(2.28) avoid charging and discharging at the same time, which is the reason why binary variables ($u_{t,h}$ and $v_{t,h}$) were necessary in the initial complete formulation.

Once $P^c_{t,h}$ and $P^d_{t,h}$ have been ascertained, a verification of these values is needed to determine if they are higher than the nominal power. If so, the analyzed SOC is infeasible and a penalization of this proposal is required. This penalization is

calculated as follows:

$$Z = \sum_{h=1}^{N} \sum_{t=1}^{T} [(P_{t,h}^{ch} - \bar{P}_h^c) \cdot H(P_{t,h}^c - \bar{P}_h^{ch}) - (P_{t,h}^d - \bar{P}_h^d) \cdot H(P_{t,h}^d - \bar{P}_h^d)] \tag{2.29}$$

where $H(\cdot)$ denotes the Heaviside step function. From (2.29), whenever $P_{t,h}^c$ or $P_{t,h}^d$ are outside the boundaries, Z measures the proportion of the limit violation; and if feasible operation is achieved, then $Z = 0$.

Once the values of $X_{t,h}$, $P_{t,h}^c$, $P_{t,h}^d$ and Z are known, the model (2.1)-(2.14) can be rewritten in the following way as a linear programming problem:

$$\text{minimize } z = \sum_{t=1}^{T} (\pi_t P_t^E + \mu_t^- I_t^- - \mu_t^+ I_t^+) + \beta Z^t \tag{2.30}$$

s.t.

$$\text{Constraints} : (2.2) - (2.4), (2.11) - (2.14) \tag{2.31}$$

where β is a penalization factor.

For each specific SOC proposal generated by the metaheuristic, the corresponding fitness function is calculated by adding the results from (2.17) and (2.30):

$$fitness = w + z \tag{2.32}$$

where w is obtained after using the SDA and z after solving (2.1)-(2.14). In order to iteratively find an SOC that returns the minimum cost, swarm-based metaheuristics can be used. This is because of their ability to handle real variables and its convenience for integrating the two subproblems described in the previous paragraphs.

2.4.4 Competitive Swarm Optimizer

The CSO algorithm is a metaheuristic optimization technique based on population behavior, first proposed in 2015 [90] and suitable for large optimization problems, following some of the principles of Particle Swarm Optimization. The algorithm assumes the existence of M particles. These particles move iteratively in an R-dimensional search space, where the i-th particle can be represented by a vector $x_i = (x_{i1}, ..., x_{iR})$. The velocity of each particle is denoted by $v_i = (V_{i1}, ..., V_{iR})$.

For this algorithm, $M/2$ pairs of particles are randomly formed, ensuring that each particle is selected only once. Each pair competes, and the particle with the best fitness function is designated as the winner ($x_m^w(k)$) and promoted into the next iteration. The loser ($x_m^l(k)$) has to update its position and velocity by learning from the winner.

For the m-th competition ($m \in [0, M/2]$), the loser's particle velocity and its position for iteration $k+1$ are updated according to (2.33) and (2.34):

$$\begin{aligned} V_m^l(k+1) &= r_1 V_m^l(k) + r_2(x_m^w(k) - x_m^l(k)) \\ &\quad + \psi r_3(\bar{x}_m(k) - x_m^l(k)) \end{aligned} \tag{2.33}$$

$$x_m^l(k+1) = x_m^l(k) + V_m^l(k+1) \tag{2.34}$$

where $\bar{x}_m(k)$ is the mean position of the particles in iteration k; and r_1, r_2 and r_3 are three random vectors with uniform distribution in the range (0,1). Finally, ψ is a parameter that controls the influence of $\bar{x}_m(k)$.

The algorithm ends when at least one of the following criteria is met: 1) a maximum number of iterations is achieved, or 2) a maximum number of iterations without improving the fitness function is achieved.

To adapt the optimization problem described in the previous subsections to be solved by the CSO, the codification of the particles must be determined. In this case, each particle refers to an aggregated SOC for the batteries, which is composed of T continous values, associated with the time steps in each scenario for the day-ahead dispatch. Each particle must be assigned with a fitness function according to equation (2.32). This means that for each particle in the swarm, the cycling and thermal subproblems described in subsections 2.4.2 and 2.4.3 need to be solved.

The initialization of the swarm is performed by randomly assigning SOC values to each specific time frame and scenario, to avoid homogenization of the swarm and avoid premature convergence to local optima. The stop criterion used in this work is related to consecutive cycles without improving the fitness function. The complete outline of the proposed algorithm is shown in figure 2.10.

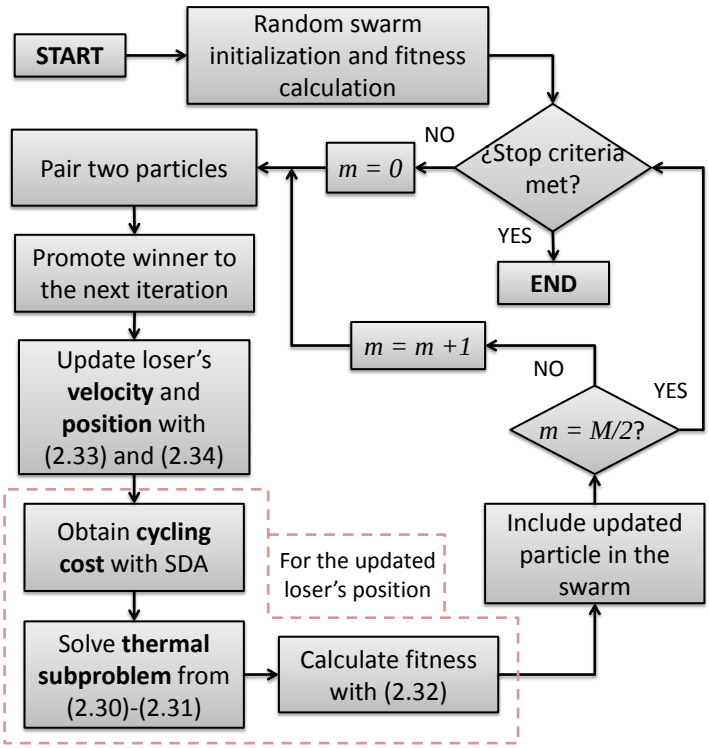


Figure 2.10: Flowchart of the CSO algorithm used

2.4.5 Performance of the SDA

Some tests are performed to analyze the adequacy of the algorithm proposed in section 2.4.2 to optimally allocate the individual SOC for each battery. Two initial

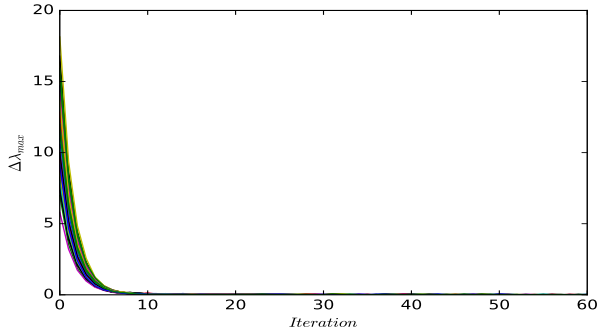


Figure 2.11: Convergence evolution the disaggregation algorithm under 100 random cases

tests are performed: first, 100 randomly generated aggregated SOC patterns are subject to the disaggregation process with random initialization, in order to determine the convergence capabilities by analyzing the evolution of $\Delta\lambda_{max}$; second, a specific SOC is selected and subject to 100 different random initialization tests to prove that the algorithm converges to close values, by measuring the evolution of the total cycling cost. Note that the first test is analyzed from the standpoint of $\Delta\lambda_{max}$, given that each of the 100 SOCs to be dissagregated are different, and the intention is to test the convergence capabilities despite the final cycling value (convergence test). The second test, verifies that the same SOC generates similar degradation equivalent cost in spite of the initialization of the algorithm (optimality test).

The converge criterion is set at $|\Delta\lambda_{max}| \leq 0.001$. As seen in figure 2.11, for all the cases run, the algorithm reaches low values of $|\Delta\lambda_{max}|$ after a few iterations. In addition, the convergence is achieved in 32 iterations on average for the 100 cases.

When one particular aggregated SOC is selected to be analyzed multiple times under different initial conditions, it is expected that the minimum total cycling cost obtained is the same or at least close for each simulation, given the non-linear characteristic of the cycling function. Figure 2.12 shows the evolution of the total cycling cost for one particular aggregated SOC under 100 different initial conditions. The minimum and maximum obtained cycling costs are 0.96 € and 1.02 €, respectively; and the mean is 0.98. This shows that the algorithm is robust towards different initialization values and that, for the specific case of monetary units, only one decimal place is enough to express currency in real-life applications, without losing sensitive information for DA electrical markets.

2.4.6 Results of the decomposition technique

To analyze the impacts on the battery operation when different sources of flexibility are taken into account, the model is run using forecasted values for PV and load, during the complete month of November 2015, given the availability of the data. All presented values correspond to a daily average resulting from running the 30 independent DA models for each day. Considering only PV injection and no battery or thermal storage, results in an average cost of 1.0 p.u., which is defined as the base case for comparison purposes. Different cases are tested to assess how each

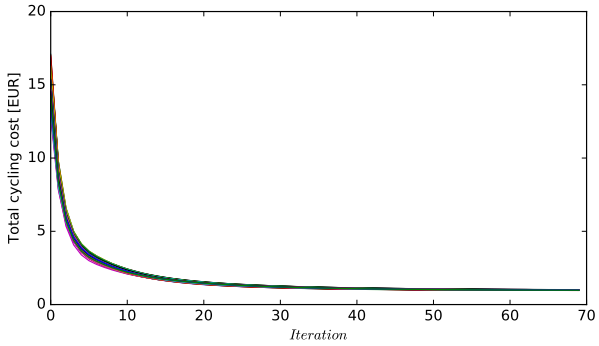


Figure 2.12: Cost evolution evolution of the disaggregation algorithm for 100 random initialization values

technology contributes in reducing costs, as shown in table 2.1.

Table 2.1: Cost of resource management for the deterministic scheme. Average daily costs. *Includes cycling effects in the optimization. **Calculated after the optimization

Case	Used flexibility BESS	Used flexibility TES	Equiv. cost cycling [€]	Total operation cost [p.u.]	Improvement with respect to base case
Base	No	No	N.A.	1.00	N.A.
1*	Yes	No	0.1	0.97	2.15%
2*	Yes	Yes	0.1	0.81	18.7%
3	Yes	No	3.8**	1.23	-22.7%
4	Yes	Yes	3.7**	1.21	-20.9%

Cases 1 and 2 in table 2.1 correspond to the problem detailed in equations (2.1)-(2.14), which considers the cycling equivalent cost within the optimization model. This approach allows to determine device settings and energy exchanges such that the total operation cost (energy purchases + equivalent cycling aging) is minimized at once. Specifically, case 1 disregards the possibility of thermal storage and only considers electrochemical storage. When thermal storage is not allowed, a 2.15% cost reduction is achieved by using only the battery to minimize the cost. When thermal and power storage are permitted (case 2), a greater cost reduction is obtained, showing that including thermal storage as another flexibility leads to a decrease in the cost. Case 2 shows a reduction of 18.7 % with respect to the base case.

The cost evolution for the complete month for all of the proposed cases can be found in figure 2.13. The cost evolution in the figure shows that not only are the average values (in table 2.1) for case 2 lower, but that improvements are achieved for each of the analyzed days. The costs savings compared to the base case, range from 14.0% to 32.5% with a median of 18.5%.

In order to demonstrate the value of taking into account the cycling cost embedded in the model, (as done for cases 1 and 2), two more cases are proposed, in which the optimization model only attempts to minimize the energy purchased and the battery cycling cost is disregarded and only calculated afterwards with the obtained SOC. This analysis corresponds to cases 3 and 4. Once again, it is shown that

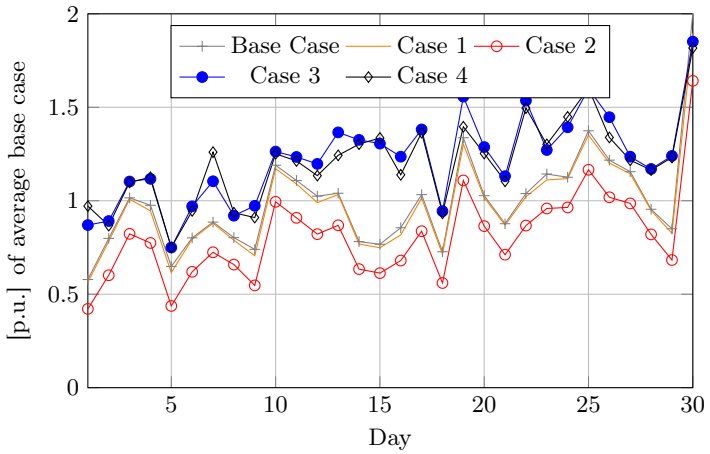


Figure 2.13: Evolution of daily cost for the deterministic model under the analyzed cases and for the whole month of November

including EWH adds flexibility to the model and allows cost reduction. However, these cases show that when cycling is not explicitly considered in the optimization model, the batteries are subject to deeper cycling, resulting in higher cycling aging and leading to higher total costs when compared to cases 1 and 2. The most critical case corresponds to an operation cost of 1.23 p.u. (case 3). It can be concluded that if cycling cost is ignored in the optimization model, batteries can cycle without any constraint of frequency or depth, which results in suboptimal operating points for the aggregator.

Analysis for one single day For the sake of example, one typical day is analyzed by selecting the aggregated SOC pattern for the four cases, shown in figure 2.14. As stated before, cases 3 (—◇—) and 4 (—□—) present deeper and more frequent cycling of batteries than cases 1 (—●—) and 2 (—■—). The coordinated scheduling of BESS and EWH with the complete optimization model (case 2) represents the best improvement with respect to the base case given the efficient scheduling of batteries and the full exploitation of BESS and EWH capabilities. The energy purchase for this deterministic case is shown in figure 2.16 (—●—) and it can be seen that around noon the energy requirements are minimized due to PV availability; on the other hand, purchases increase during late night and morning hours.

As explained before, the PV and load forecast used for these four cases correspond to the median (quantile 50%). When the deterministic scheduling described for case 2, is subject to all the combinations of quantiles 10% to 90% ($9 \times 9 = 81$ scenarios) of both load and PV forecasts, the aggregator must face penalties associated to imbalances, given that the committed energy and device settings do not meet the realization of the uncertainties condensed in the 81 scenarios for both PV and load, i.e., constraint 2.2 must be met by adjusting the quantities I^-/I^+, which results in extracosts in the operation. The minimum levels of penalty, as shown in figure 2.15, are associated with high PV quantiles and low load quantiles, given that excess of solar energy reduces the need of offsetting imbalances and maintains feasible operation of the system. On the other hand, when load quantiles increase and

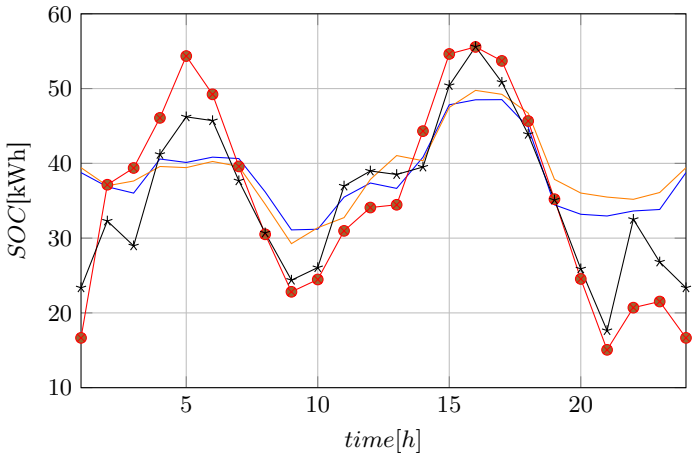


Figure 2.14: Aggregated SOC for deterministic cases 1 (—●—), 2 (—■—), 3 (—◇—) and 4 (—□—)

PV quantiles decrease, the scarcity of renewable generation leads to imbalances and consequent penalty. From the set of the 81 combined quantiles, 53 (65%) present penalties different from zero, ranging up to 6.1 € for the case of load quantile 90% and PV quantile 10%.

Computational performance of the CSO for the 25-household testbed
To test the performance of the CSO, several runs were carried out for a single day in order to determine the quality and consistency of the obtained solutions. Tests consist in running the algorithm 20 times for a 30-particle swarm, setting the stop criteria to 30 iterations without improving the best solution. In addition, the maximum number of iterations is set to 300. In these conditions, the CSO is run, and after each simulation the information saved is: best solution, computational time in achieving the best solution and iterations in achieving best solution.

Table 2.2 shows that the CSO presents feasible computational times for day-ahead, achieving good quality and stable solutions in the range of 729-1999s.

Table 2.2: Computational performance of the CSO for one typical day in November

Characteristic	CSO ($\psi = 0.3$)
Best solution [€]	19.00
Best solution range [€]	19.00 - 19.06
Best solution average [€]	19.03
Best solution SD [€]	0.02
Average time [s]	1433
Time range [s]	729-1999
Time SD [s]	391
Average iterations for achieving best solution	209

The previous methodology is one of the proposals to model cycling aging of batteries. The second alternative which is based on explicit modelling of cycling constraints is shown in the next section.

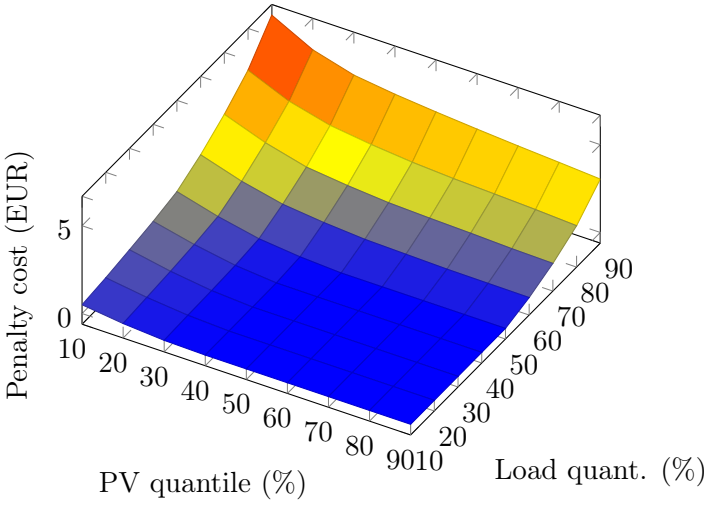


Figure 2.15: Negative imbalance (I^-) costs for deterministic case when all combined PV and load quantiles are analized

2.5 Solution approach 2: Explicit modeling of BESS degradation costs to solve (2.1)-(2.14)

The second alternative to capture the non-linear relation of life cycles vs. DoD, is a piecewise linearization approach.

The motivation for linearizing the cost characteristic lies in the fact that if the DoDs at which each cycle occurs can be identified by means of a set of equations, then an equivalent cycling cost can be determined in such a way that these equations can be explicitly modelled and fed into a commercial optimization solver. In the decomposition approach developed in the previous section, the difficulty of expressing RCA based degradation equations in closed form, impedes feeding the complete optimization problem into optimization solvers. This section presents an option to introduce a set of equations that capture and identify charging cycles by means of auxiliary variables and constraints, also known as special ordered sets. This way, the use of a meta-heuristic is avoided and instead a MILP problem is obtained and solved with off-the-self optimization software.

This explicit modelling consists in identifying the beginning of each charging cycle by means of constraint (2.35). This constraint detects the transition between an idle or charging state in $t-1$ to a charging state in t. In this situation, variable $x_{t-1,h}$ takes the value of 1, capturing the immediate time step before charging occurs. This transition detection is possible given that binary variable $u_{t,h}$ identifies when the battery is in charging mode. $y_{t-1,h}$ is a binary auxiliary variable that takes the value of 0 when no change in state occurs, or -1 when the battery stops charging. Constraint (2.37) ensures a mutually exclusive unitary value for the special ordered sets.

In general, equation (2.35) can take three possible values, i.e. 0, -1 or 1. The zero value means that $u_{t,h} = u_{t-1,h}$, which can also have four interpretations: a) the battery is in charging mode for both $t-1$ and t; b) the battery is in idle mode

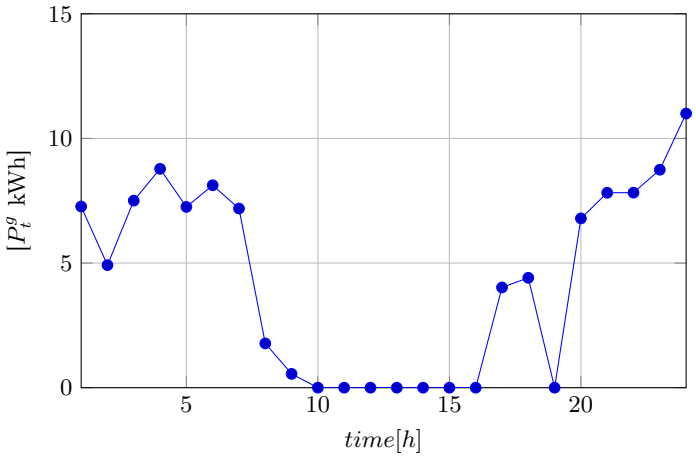


Figure 2.16: Energy purchased on the energy market for the deterministic (—●—) case

in both time-steps; c) the battery is going from idle to discharging; or d) battery is going from discharging to idle. Second, if constraint (2.35) equals -1, this means that $u_{t,h} = 0$ and $u_{t-1,h} = 1$, which means that the battery is charging in $t-1$ and is going to discharging or idle mode. Third, if equation (2.35) takes the value of 1, this is interpreted as a change from idle/discharging to charging mode. This latter situation is the one of interest, given that the proposed approach intends to identify only the beginning of charging cycles.

$$x_{t-1,h} - y_{t-1,h} = u_{t,h} - u_{t-1,h}, \forall t, t \neq 1, \forall h \tag{2.35}$$

$$x_{T,h} - y_{T,h} = u_{0,h} - u_{T,h}, \forall h \tag{2.36}$$

$$x_{t,h} + y_{t,h} \leq 1, x_{t,h}, y_{t,h} \in \{0,1\}, \forall t, \forall h \tag{2.37}$$

Following the identification of the beginning of a charging cycle, the DoD at which this cycle occurs can be extracted. Constraint (2.39) allows a value different from zero to be stored in X^D, right before the beginning of a charging cycle. To assign the proper value of depth of discharge, constraint (2.38) is used. The right-hand side of this constraint calculates the DoD in per unit of the rated battery energy. X^{Df} is a dummy variable to balance the equation each time a charging cycle is not identified ($x_{t,h} = 0$) and activated through constraint (2.40). Note that when $x_{t,h} = 0$, no DoD needs to be identified because no beginning of charging cycle has taken place, hence per equation (2.39), $X^D = 0$. and additionally, X^{Df} takes the value of the current DoD, but this DoD has no impacts on cycling cost calculation, as expected, given that is does not correspond to the beginning of a charging cycle.

$$X_{t,h}^D + X_{t,h}^{Df} = 1 - X_{t,h}/E_h^{rated}, \forall t, \forall h \tag{2.38}$$

$$X_{t,h}^D \leq x_{t,h}, \forall t, \forall h \tag{2.39}$$

$$X_{t,h}^{Df} \leq 1 - x_{t,h}, \forall t, \forall h \tag{2.40}$$

Note that conflicting definitions of DoD exist in the literature. The present study takes the definition of DoD as the energy discharged compared to 100 % SOC; in addition, the aging model is based on the assumption that each full charging cycle is accompanied by another full discharging event. Constraint (2.6) ensures that all charging events must equal the discharging level in order to reach the same initial and final SOC each day.

With constraints (2.35)-(2.40), the DoD at which each charging cycle occurs is identified as X^D. To extract the appropriate piece-wise cost function, the corresponding segment of the cost curve must be active. This is achieved by means of constraints (2.41)-(2.43). Constraint (2.42) forces the identified DoD to fall within the corresponding linearization segment and also leads to activation of a binary variable $l_{t,h,s}$ for the related active segment s.

$$\sum_{s=1}^{S} X^{Ds}_{t,h,s} = X^{D}_{t,h}, \forall t, \forall h \tag{2.41}$$

$$l^{min}_{s} l_{t,h,s} \leq X^{Ds}_{t,h,s} \leq l^{max}_{s} l_{t,h,s}, l_{t,h,s} \in \{0,1\}\, \forall t, \forall h \tag{2.42}$$

$$\sum_{s=1}^{S} l_{t,h,s} = x_{t,h}, \forall t, \forall h \tag{2.43}$$

Note that one difference between this approach and other previous explicit cycling models [64, 65], is that $l_{t,h,s}$ is efficiently used in the objective function (2.44) to include the parameter $b_{h,s}$ when needed. In a similar manner, $X^{Ds}_{t,h,s}$ is used as the independent variable of the aging cost function.

Quantities $a_{h,s}$ and $b_{h,s}$ in (2.44), correspond to the piece-wise approximation parameters of the cycling aging cost.

With this reformulated calculation of the aging cost, the objective function (2.1) can be re-written as:

$$\text{minimize} \sum_{t=1}^{T} \left\{ \pi_t P^E_t + \mu^-_t I^-_t - \mu^+_t I^+_t + \sum_{h=1}^{N} \sum_{s=1}^{S} (a_{h,s} X^{Ds}_{t,h,s} + b_{h,s} l_{t,h,s}) \right\} \tag{2.44}$$

The equivalent cost due to the battery's aging process for an specific value of DoD, should be added to the total dispatch cost. The accumulated cycling cost of aging for the identified DoDs is shown in the fourth term of equation (2.44), and the parameters $a_{h,s}$, $b_{h,s}$ are obtained by linearizing equation (2.16) in segments. An example for a 3 kW / 3.3 kWh li-ion battery is shown in figure 2.17. In this case, a 5-segment linearization is performed for the referred BESS with the mentioned parameters. First, six equally spaced points are evaluated with equation (2.16). Next, curve fitting is performed within each segment and parameters $a_{h,s}$ and $b_{h,s}$ are obtained.

2.5.1 Results for piecewise linearization approach

In order to determine the impact of the number of segments on the optimization problem, different values are tested. Figure 2.18, shows the evolution of the objective

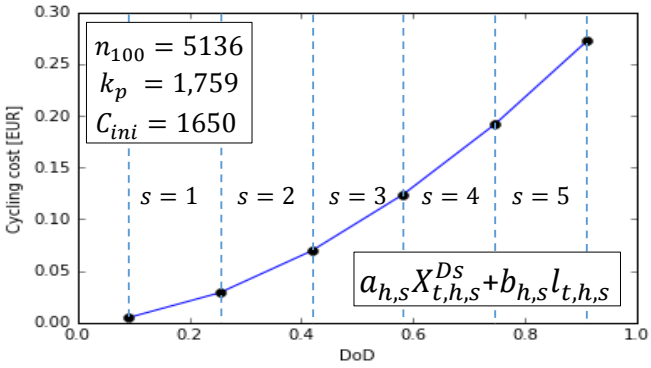


Figure 2.17: Example of piecewise linearization. Cycling Cost Vs. DoD for a selected li-ion battery

function 2.44 when subject to values of S (number of segments) that range from 2 to 40. It can be seen that after a few segments the value stabilizes and variations with respect to the final value (40 segments) are minimum.

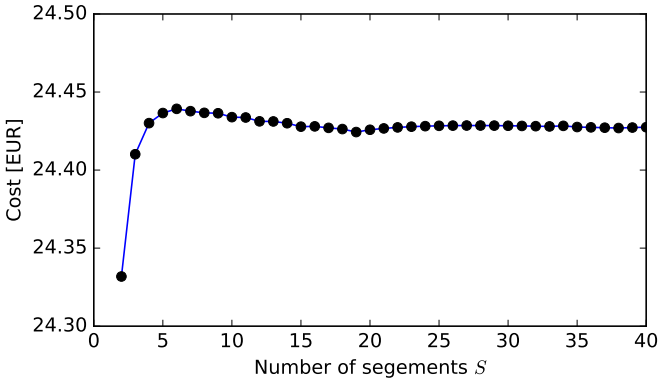


Figure 2.18: Impact of number of segments on the value of the objective function

When the error of each solution is calculated, taking the value for 40 segments as the reference value, it can be seen from figure 2.19 that error drops significantly after a few segments, and that this error is never higher than 0.05% after 6 segments. This is a positive outcome, given that fewer segments are desired in the formulation to avoid a large number of binary variables, which can lead to convergence issues and prohibitive computational times.

2.5.2 Results for piecewise linearization: impacts of cycling aging

When the optimization problem is solved by selecting 6 segments for the piecewise linearization and the same selected day for the CSO simulations in table 2.2 , the obtained total cost is 18.56€, from which 0.11 € correspond to equivalent cycling aging. The accumulated SOC for all batteries in the system can be seen in figure 2.20 (—●—). If the cycling cost is neglected from the model, i.e., assuming zero cost for degradation, the obtained day-ahead operation cost is 18.24 €, in appearance lower

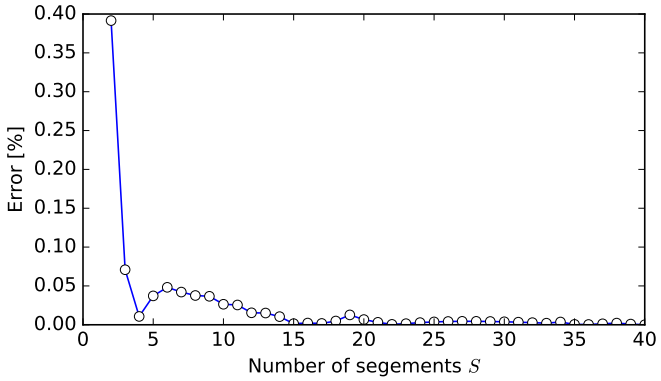


Figure 2.19: Error of the objective function as a function of the number of segments

than the cost of 18.56€. However, ignoring degradation leads to deeper and more frequent cycling, as shown in the SOC (-⊖-). In this case, this cycling pattern has an hidden associated cost of 5.29€, leading to a real total operation cost of 18.24€ + 5.29€ = 23.53€, which in turn represents an increase of 26.7% with respect to the complete formulation when piecewise linearization is included. This shows the importance of taking into account degradation factors into the day-ahead scheduling of storage devices.

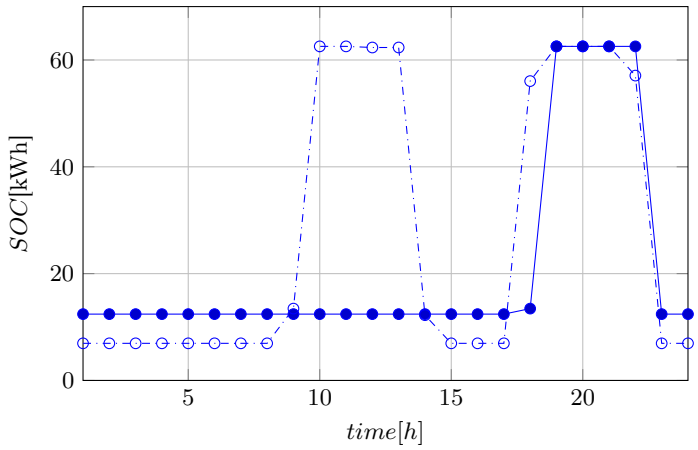


Figure 2.20: Accumulated SOC when cycling cost is included (—●—). Accumulated SOC when cycling cost is neglected (-⊖-)

2.5.3 Comparative remarks of the decomposition and explicit modelling approaches

If the optimal solutions of the decomposition approach in subsection 2.4 and the explicit modelling in subsection 2.5 are compared for the same day of simulation (November 15th), the summarized costs are the ones in table 2.3. This result evidence a difference in both the equivalent cycling aging cost and the cost of the day-ahead committed energy in the wholesale market. Despite the fact that the

simulations were carried out for the same test system and the same day of schedule, differences are expected for the following reasons.

First, the logic used for the calculation of equivalent battery cycling is different in both cases. For the decomposition approach, the direct calculation of the cycling aging is based on the RCA, which calculates equivalent charging or discharging half- (or full-) cycles and identifies the DoD range at which this cycles occur. This methodology differs from the one proposed in the explicit modelling, given that the latter identifies only full charging cycles, based on the assumption that discharging will always occur at a latter (or earlier) hour given that SOC has to be the same for the first and last time-frames. Hence, it comes natural that both approaches result in a different value of battery equivalent degradation even for a rare event in which SOC are the same.

Table 2.3: Cost comparison for the optimal solution obtained with the decomposition and explicit cycling aging approaches

Case	Equiv. cost cycling [€]	Energy purchases [€]	Total operation cost [€]
Decomposition approach	0.016	18.98	19.00
Explicit cycling	0.11	18.45	18.56

Second, given that there exists an underlying difference in cycling calculation, the optimal solution will also remain different not only for the resulting SOC, but also for the rest of the optimization variables, given the inherent correlation. So, day-ahead energy purchase will be different in order to attain minimum cost solution. This fact makes that the two approaches cannot be directly compared to conclude that one of them dominates the other, but what can be concluded, is that each approach separately presents better performance when compared to the case in which cycling aging is neglected. Despite the approach that is used, savings will be obtained in terms of overall operational costs and batteries will have less equivalent degradation.

To demonstrate that both approaches lead to different optimal solutions, aggregated SOC is shown in figure 2.21. This figure shows that each algorithm has different search spaces and hence the optimization process travels towards different points in this search space. In addition, it can be seen that the decomposition method (RCA based) presents higher variability in therms of the values taken by the SOC. This means that more control signals have to be sent to batteries in this approach. On the other hand, explicit modeling has lower charging and discharging values different from zero. For instance, charging only occurs during time frames 18h-19h and discharging only during time frame 22h. On the contrary, for the decomposition approach, all time frames have associated charging or discharging, even if those have low associated values. In addition, the cycling is shallower, which is also evidenced in the equivalent cycling aging cost (0.016 €).

2.6 Conclusions

Regarding aggregation of flexibility and device interaction This chapter presents the models of the devices that provide flexibility at the residential level for aggregation and participation in the day-ahead energy market. The optimization

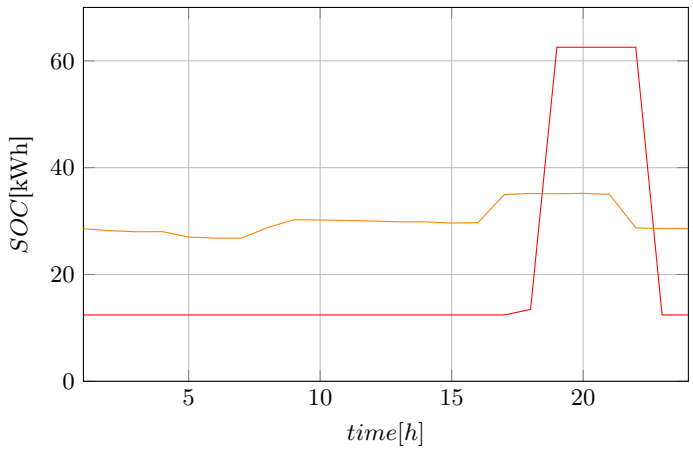


Figure 2.21: Accumulated SOC when for the explicit modeling of cycling (——). Accumulated SOC for cycling cost modelled with the decomposition approach (——)

model aims to minimize energy purchase while complying with the electrical and thermal demand in each household. The alternatives presented in this chapter allow to capture approximate cost of battery cycling. In this way, the philosophy of the proposal is in line with very recent research that intends to present models such that battery owners, operators, aggregators are able to reflect operating costs and recover at least equivalent battery loss of life during the operation and market participation [37, 38].

The presented deterministic model joins the flexibility related to the BESS and EWH with the objective of presenting a framework to optimally manage HEMS resources by integrating several aspects such as: Electric/Thermal load and storage, battery degradation costs and home/building level management. These aspects, analyzed from the stand point of an aggregator participating in DA and imbalance market.

For the particular test case, when BESS are included in the model, a reduction of 2.15% is achieved, with respect to a base case in which no storage technology is included. In addition, the inclusion EWHs with storage capabilities, shows a reduction of 18.7%. The EWHs in this case, act as a flexible load, given that hot water can be stored for later use given certain price of opportunity.

In addition, inclusion of thermal storage flexibility indirectly descreases battery cycling given that in this case, BESS are subject to shallower and less frequent cycling leading to lower equivalent degradation costs.

Regarding BESS cycling Two approaches were used to account for battery degradation effects. In general, the model includes cycling equivalent aging as a function of the number of the equivalent cycles during a day and the proportion of loss of life based on the initial cost of the battery. The number of equivalent cycles is affected by the non-linear relation of total cycles and DoD.

The first approach proposed for battery aging is a decomposition method. This decomposition attempts to solve two subproblems, i.e. 1) a cycling aging subproblem and 2) a thermal subproblem. The input for the aging subproblem is an aggregated

SOC (all batteries) that comes from a metaheuristic, in this case CSO was used. Once an aggregated SOC is proposed by the CSO, the individual SOC for each battery has to be determined in such a way that minimum aging cost is achieved. This is done by using an algorithm called SDA. The SDA is a Lagrangian based technique that uses numerical differentiation and the RCA to iteratively find optimal disaggregated SOCs. Afterwards, the setpoints of the EWH and the day-ahead purchase commitment are found by the thermal subproblem. With this decomposition approach, the cycling of the batteries is less deep, hence equivalent cycling and overall operation cost are reduced.

The same decomposition presented in this thesis can be used not only in residential level storage management, but in any level of storage facilities to be integrated for market participation. For instance, storage and resources at the commercial building level, often have higher rated power/energy and thus higher possibilities of complying with minimum bid levels. Additionally, this framework can also fit into models in which other agents with batteries at the DSO/TSO levels are willing to participate in energy and ancillary markets. In all cases, despite the agent, the ownership or the battery size, the decomposition approach will still be valid. Most certainly with low computational burden given that grid scale storage is not usually installed (and owned) in large numbers.

The second proposed alternative to include cycling was explicit modeling. For this approach, special ordered sets were used to detect charging cycles and the DoD at which this charging cycles occur. With the identification of this DoD, an equivalent cost can be found by means of piecewise linearization. With this scheme, a 21.12% decrease in operation costs was found, when compared to a model that disregards cycling aging. For the explicit modeling, 6 segments were used to model cycling cost non-linearities.

With explicit cycling there is also minimization of partial cycling. This is due to the identification charging cycles when previous state is idle or discharging. This makes that charging-idle-charging sequence results in costly operation from the degradation standpoint. In this case, this state sequence impacts on the objective function, given that when passing from idle/discharging to charging, DoDs are again captured and additional costs are activated. A consequence of this particularity is the minimization of control signals that the aggregator needs to send to the BESS controller.

All optimization models run in this chapter used deterministic information for PV, electrical base load, thermal load and energy prices. The next chapter will introduce the changes in the model when uncertainty is taken into account.

Chapter 3

Residential flexibility aggregation under uncertainty

This chapter presents a literature review about uncertainty issues in smart grid applications. In addition, it presents a two-stage stochastic alternative to model prosumer's flexibility by using an extension of the decomposition algorithm presented in the previous chapter. After that, an adjustable robust optimization approach is also developed and performance analysis is presented to show the advantages over deterministic and hybrid stochastic/robust formulations.

The models and results presented in this chapter led to publications [CF-1,CF-2,CF-4,CF-5].

3.1 Literature review

In the smart grid context, uncertainty plays an important role in the process of decision making. One common practice to facilitate these optimization processes is Stochastic Optimization (SO), which typically aims to optimize over the expectation of a number of predefined scenarios [13]. However, factors such as the requirements for probabilistic information of uncertain variables, the implementation of specialized scenario generation/reduction techniques and the computational burden related to large number of scenarios, are some of the drawbacks of SP. Several research has addressed the problem of uncertainty in optimization models in a smart grid context. For instance, authors in [91] propose a scheme for joint PV and ESS grid connected management. The ESS has to be managed accordingly to face deviations of the forecasted PV injection. This way, penalizations are minimized (for commited energy deviations), while considering predicted PV production and future energy prices uncertainty. This model takes into account reduced ESS capacity due to saturation resulting from cycling. Market participation for the commitment of energy is based on an intraday (ID) scheme that allows rescheduling of resources for six sessions during the operation day. This way, the management of the resources can be adjusted when new forecast information is available and costs minimization avoids potential imbalance operation. The ID optimization problem is solved by a MPC defined as a Linear Programmming (LP) problem. PV is continously adjusted

according to real time methereological conditions and estimated by the help of a parameter called Cloudiness Coefficient.

The work presented in [92], deals with DA and ID decisions by means of a two-stage model for scheduling of ESS and DR in the context of transmission networks. The wind uncertainty is treated by dividing the power output into several intervals with a given probability. Afer this, there is a scenario reduction methodology based on Kantorovich distance, in order to delete scenarios that are close to each other based on computed probability. For the DA, a unit commitment problem is solved to schedule the thermal plants to face potential shortage of wind power. After this, adjustments are made for hour-ahead scheduling when the latest forecasts of wind generation are known. This way, storage SOC and DR are revised to minimize costs. The implemented methodology to solve this two-stage optimization problem is a chaotic binary particle swarm optimization algorithm for different test cases combining inclusion/exclusion of ESS and DR.

A DA strategy is proposed in [49], considering several PV, wind turbines, battteries and HVAC systems to maintainin the indoor temperature within certain confort ranges. In this case, the MG aggregator controls the HVAC systems and the other resources to maximize profit, and minimize RES spillage and load curtailment while maintaining systems operational constraints. The considered uncertainties in this study are independent and correspond to wind speed, electricity prices, temperature, solar radiation and demand. Monte Carlo, Latin hypercube and scenario reduction are performed to build a two-stage optimization model.

Following a similar logic, [93] proposes a two-stage stochastic model for optimizing operation costs of a microgrid in the DA market. The first stage defines the commitment of DGs and the energy to be purchased/sold from/to the main distribution grid, then, a second stage includes wind and PV scenarios for modelling uncertainty. The model includes also electric vehicles, ESS and power flow constraints.

The work presented in [94] proposes daily operation of pumped hydro storage to compesate uncertainty of wind injection and maximize profits. The mathematical model includes asociated costs for pumping and generating, as well as penalization for output deviations. The technical constraints of the pumped storage are also taken into account and the source of uncertainty is solely the wind power output, with the forecast error represented by a normal distribution. Two solution methods are proposed to solve the stochastic optimization problem: chance constrained and scenario-based optimization; and these are compared with a deterministic approach. When the different approaches are subject to analysis under randomly generated scenarios, the stochastic optimization is able to better withstand the fluctuations in the wind output and guarantee higher levels of profit.

The approach in [34] presents a methodology for ID management of PV and EWH in a LV network. The EWH act as flexible load to achieve minimum operation cost for a 24h horizon. The uncertainty of PV is considered, and an MPC is used for dispatching the flexible load while minimizing also PV shedding and switching of EWH. The MPC allows the adjustment of the hourly dispatch for the EWH to cope with the uncertainties introduced by PV forecasts. This work also investigates the grouped and distributed control signals sent by the MPC and the impact on energy shedding and total costs.

3.1.1 Robust optimization for uncertainty treatment

An approach which has gained substantial attention in the recent years is Robust Optimization (RO) [14], which is an interval based optimization method. RO does not require knowledge of the Probability Density Function (PDF) of the uncertain variables, and instead it requires moderate information, i.e. an uncertainty set for each uncertain variable. RO will provide a robust optimal solution that is feasible (immunized) within the confidence interval.

RO has been successfully used to tackle uncertainty mainly in large scale power systems problems with a variety of objectives. For instance, it has been used to capture load and wind uncertainty in Unit Commitment [95]. In the case of large-size battery participation in energy and ancillary markets, RO was used in [96] to capture uncertainty in prices. In transmission expansion planning, this methodology has been used to cope with demand and renewable generation uncertainty [97]. In [98], strategic bidding for a wind farm and battery was achieved by inclusion of price and wind power uncertainty. Stand alone wind systems for market participation have also included RO analysis [99].

Although most of the applications of RO are related to large power systems applications, the increasing interest towards decentralized and distributed energy has pushed research community to explore this approach.

Although there is still little research for exploiting RO capabilities in residential storage based energy systems, some work has began be published in the recent years, specifically related to medium size DG/microgrid management. For instance, [17] presents a model for strategic bidding in energy and ancillary markets for a microgrid consisting of RES, a microturbine and a battery, in which RO is used to include RES uncertainty and SO is used to tackle price uncertainty. For bidding purposes in day-ahead and real time markets, reference [15] proposes a hybrid stochastic/robust approach, in which RO captures uncertainty in real time prices, while stochastic optimization is used to include wind and PV scenarios. Both approaches ([15, 17]) assume deterministic demand.

Robust resource scheduling of MG components is analyzed in [18, 19] with uncertainty in load and RES, but neglecting uncertainty in price information. In [20], a DR program for industrial customers is presented. Uncertainties with RO are considered in load and PV, and a multi-objective algorithm is used for minimizing cost and emissions. In [21], robust energy management is achieved for a MG consisting on a train station and a district. The model features complete uncertainty inclusion for PV, wind, load and energy prices. Although this model includes robustness for all uncertain parameters, it does not analyze different levels of uncertainty budget, immunizing the solution against any uncertainty realization but leading to over-conservative solutions.

Reference [22] proposes energy and reserve market participation using RO for wind uncertainty and considers PV and dispatchable units at MV level. Also in MV level, reference [16] includes uncertainty in net load and heat demand with chance constrained optimization and price uncertainty with RO.

Some of the previous work consider full uncertainty budget, i.e. worst case realization of uncertain variables to protect against realization [18, 21]. However, these solutions could lead to over-conservatism, given that it is very unlikely that

all uncertainties take extreme values at the same time, hence, robust parameter analysis can be introduced to achieve less expensive solutions [100]. This logic is used in [15, 16, 22] to present a sensitivity analysis for different values of the robust parameters, given that only one source of uncertainty is considered. When several sources of uncertainty are included, the interaction of different robust parameters can lead to find promising solutions. However, in [17, 19, 20], these interactions are neglected, and instead, all robust parameters are forced to assume the same arbitrary values.

Although some of the previous MG management approaches include at least one battery in their respective test systems, none of them includes the non-linear relation of DoD to account for impacts on degradation and cycling aging. At most, a simplified linear cost (function of power charge and discharge) is included in [15, 18, 19], and references [17, 20, 21] neglect cycling aging impacts. In this thesis, when using RO approaches, explicit modeling of BESS degradation is proposed, by means of piecewise linearization of the curve that describes the non linear relation of DoD and equivalent life cycles.

Very little work has been pusblished reagarding home level storage management using RO. Robust management for home appliances is presented in [23] to miminize electricity bill in a single house and including uncertainty in comfort variables. Regarding robust aggregation of storage at the residential level, reference [24] proposes a scheme for real-time decision making considering batteries and price uncertainty. Reference [25] does not include battery aggregation, but instead considers exploitation of thermal storage at the residential level in a 20-household testbed, using RO to account only for thermal demand uncertainty. Although this research does not include price or electrical load uncertainty, nor RES integration, is does present an interesting insight on scalability of the proposed model. Reference [26] presents a community energy managent system disregarding batteries, but including PV and wind power. RO is used to include uncertainty in RES and prices.

Despite its valuable contribution on participation in multiple markets, [26] lacks of an insight for budget of uncertainty analysis regarding the three considered robust parameters. Similarly, predefines parameters for both outdoor temperature and hot water use, and then presents a sensibility analysis by adjusting a parameter that influences both uncertain variables in the same amount. In addition, reference [25] does not consider adjustable parameters and only presents the worst case solution.

A more common practice in the specialized literature to account for aggregation of residential/building storage under uncertainty, is by using MPC and/or stochastic optimization. For instance, stochstic optimization and chance constrained methods are used in [28] for energy and reserve market participation by aggregating residential batteries and heating. This work presents inclusion of uncertainty in prices, weather and realized frequency. MPC based models for aggregation of distributed storage devices (at DSO level) is presented in [101] to provide local and frequency services; in [29] an aggregation of appartment buildings with multiple EWHs, EVs and a single battery is presented; and MPC is also used in [102] for the case of regulation services by aggregation of industrial thermal loads.

3.1.2 Discussion

Given the multiple sources of uncertainty in scheduling of flexibility resources, new optimization methods have to be used. For the treatment and modeling of uncertainty within an optimization problem, three main directions are identified.

First, if no information regarding the probability density functions of the uncertain variables is available, one possible approach is to use robust optimization (RO) theory. If uncertain variables remain within known boundaries, RO defines an uncertainty budget and a new optimization problem that has to be feasible for all realizations of uncertainty is defined, leading to a very conservative solution, as shown in [15, 66, 103]. For the flexibility management, a robust solution should be able to withstand any load scenario and RES realization, while maintaining feasible operation of all devices.

A second group is related to stochastic optimization. In this group, a selection of scenarios with a certain probability must be predefined and embedded into the optimization formulation. To define the scenarios, multiple methods can be used, such as point estimation methods, Taguchi orthogonal arrays, Kantorovich distance or clustering methods in general. This approach is not as robust as RO, given that the optimal solution is feasible for a finite number of uncertainty realizations, but at the same time leads to less expensive and less conservative solutions. In this group of proposals, two-stage optimization problems can be found [31, 49, 92, 93] for finding an expected operation value. The idea is to define a first stage (or here an now decision) with variables and decisions that usually correspond to the committed energy purchases in the DA market and the generation commitment for the conventional generation. After this, a set of second (or recourse) decisions is made, according to the realizations of the uncertain variables. This approach also has the advantage of simplicity in its modeling, with the trade-off of increasing the number of variables depending in the scenarios to be analyzed in the second stage.

A third group is associated to MPC theory. This appears to be suitable for rolling horizon decisions, such as the ones that have to be taken in ID and real-time (RT) markets, where the latest information of forecast might change some device settings for the remaining operation schedule.

RO approaches use a confidence interval for each uncertain variable. In this thesis, probabilistic forecasts for PV and demand are used as input to creating these intervals. An index to classify each simulation day depending on the characteristics of these invervals is defined in the next subsection. This information helps classifying days to develop specific simulations.

3.2 Characterization of uncertainty

To measure the amplitude of the net load in each day, an index is defined. This index is obtained by calculating the mean neat load interval (MI) for a 24-h period. First, the maximum/minimum net load is calculated by using (3.2)/(3.3). Then,

the MI for each day m is calculated by:

$$\mathrm{MI}_m = \frac{1}{T}\sum_{t=1}^{T}\frac{\bar{D}^{net}_{t,m} - \underline{D}^{net}_{t,m}}{\bar{D}^{net}_{t,m}} \times 100\% \tag{3.1}$$

where,

$$\bar{D}^{net}_{t} = \sum_{h=1}^{N}(D^{q90\%}_{t,h} - P^{pv10\%}_{t,h}) \tag{3.2}$$

$$\underline{D}^{net}_{t} = \sum_{h=1}^{N}(D^{q10\%}_{t,h} - P^{pv90\%}_{t,h}) \tag{3.3}$$

The index MI gives an idea of how wide the uncertainty set is, from the net load stand point, and it is used to classify each day according to the level of MI. For example, figure 3.1 depicts the MI for each day in November 2015. This information to run simulations on three representative days of high (Nov. 5th), medium (Nov. 15th) and low (Nov. 27th) MI and avoid arbitrary selection of days for Day-ahead simulations. In addition, figure 3.2 shows an example of net load confidence intervals for two selected days: November 5th and 27th.

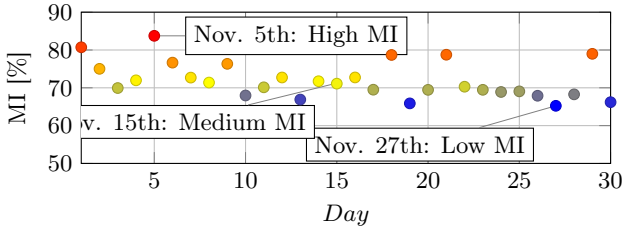


Figure 3.1: Average net load intervals calculated with equation (3.1)

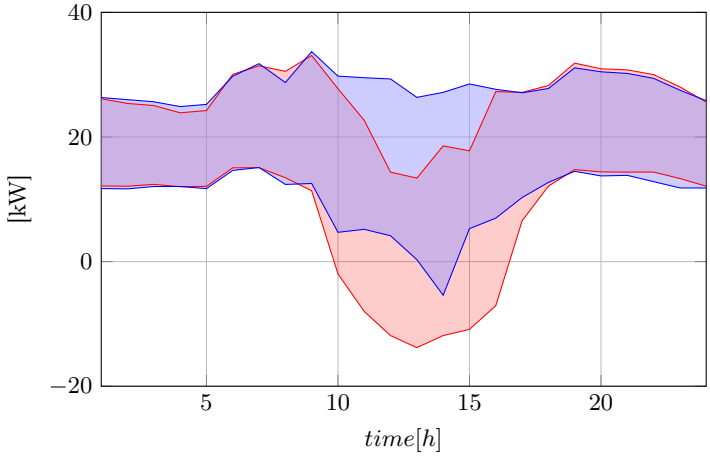


Figure 3.2: Net load interval for two days. November 5th (——) and November 27th (——)

3.3 Quantile-based two-stage stochastic optimization with SDA

This section presents an alternative for including PV and demand uncertainty into the optimization model described in chapter 2. This alternative is based on stochastic optimization in which PV and demand scenarios are created according to the information provided by the available probabilistic forecast.

The proposed two-stage stochastic optimization model minimizes the expected HEMS day-ahead operation cost by scheduling the batteries' power charge and discharge, and the power injected into the EWHs, the TES pattern, and exchanges with the energy market.

Objective function

As shown in Eq. (3.4), the two-stage stochastic optimization model minimizes the expected DA operation cost, in which the first-stage decision is associated with the DA purchase commitment (P_t^E), and second-stage (recourse) expected costs are related to the import/exports ($I_{t,e}^-/I_{t,e}^+$) imbalance and the expected cycling cost ($f_h^{cyc}(\cdot)$) for the batteries installed in each house h, which is a function of the SOC vector ($\mathbf{X}_{h,e}$). Subscript e index scenarios and p_e is the probability of scenario e.

$$\min \sum_{t=1}^{T} \pi_t P_t^E + \sum_{e=1}^{ES} p_e \left\{ \sum_{t=1}^{T} (\mu_t^- I_{t,e}^- - \mu_t^+ I_{t,e}^+) + \sum_{h=1}^{N} f_h^{cyc}(\mathbf{X}_{h,e}) \right\} \tag{3.4}$$

All of the terms in the objective function are linear, except the one related to the cycling. The decomposition method explained in section 2.4 is used to solve this two-stage stochastic problem.

The decomposition approach iteratively solves two subproblems: cycling subproblem and thermal subproblem.

Cycling subproblem

The main difference with the SDA already explained in subsection 2.4, is the fact that in this case a number of scenarios has to be included. Hence the complete algorithm has to be adjusted for stochastic formulations. The details of the generalized SDA for scenario-based optimization are shown in annex B and the outline of the decomposition approach to solve the cost minimization problem when considering scenarios, is shown in figure 3.3.

The outcome of the SDA is the SOC for each battery in the system in each scenario. With this information, the thermal subproblem can be solved for the two-stage stochastic proposed alternative.

Thermal subproblem

When a certain SOC is generated with the CSO and then disaggregated by means of the SDA the remaining set points that need to be determined in each household are those associated with the EWH.

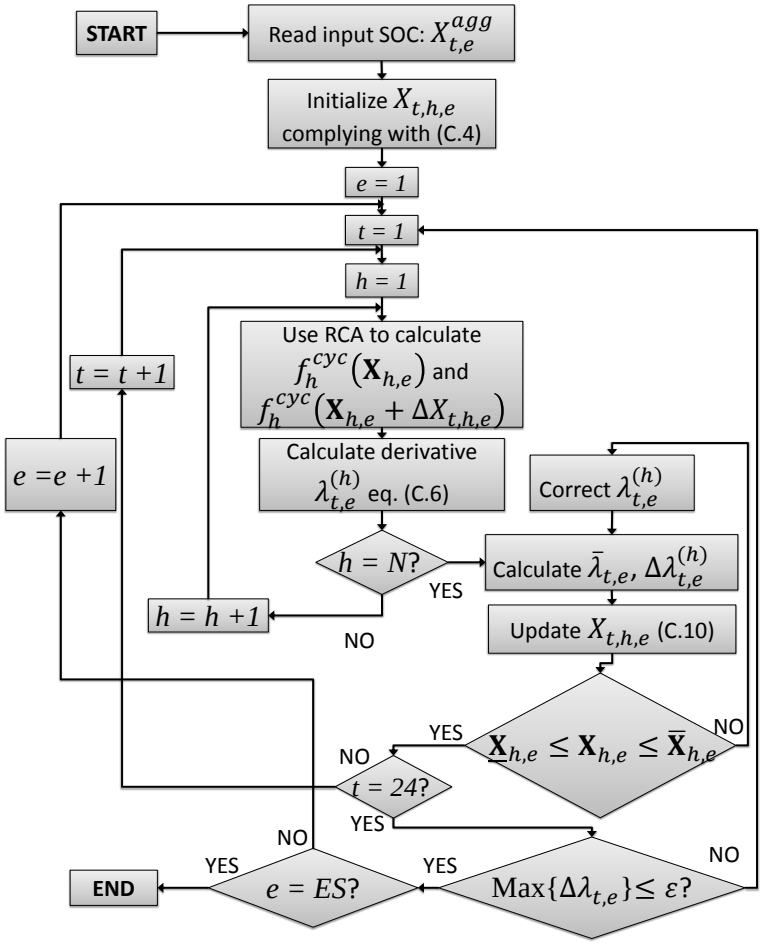


Figure 3.3: Flowchart of the SDA to two-stage stochastic approaches

First, $P_{t,h,e}^{c}$ and $P_{t,h,e}^{d}$ can be easily determined by applying the following rule:

$$P_{t-1,h,e}^{c} = \begin{cases} (X_{t,h,e} - X_{t-1,h,e})/(\eta^{c}\Delta t), & \text{if } X_{t,h,e} - X_{t-1,h,e} > 0 \\ 0, & \text{otherwise} \end{cases} \tag{3.5}$$

$$P_{t-1,h,e}^{d} = \begin{cases} (X_{t-1,h,e} - X_{t,h,e})\eta^{d}/\Delta t, & \text{if } X_{t-1,h,e} - X_{t,h,e} \geq 0 \\ 0, & \text{otherwise} \end{cases} \tag{3.6}$$

To maintain continuity of the BESS, both $P_{t,h,e}^{c}$ and $P_{t,h,e}^{d}$ have to be zero for the last time frame ($t = T$) in order to match the SOC for the first time frame of the following day. Thus, equations (3.5) and (3.6) are valid for $t : \{2, ..., T\}$.

Once $P_{t,h,s}^{c}$ and $P_{t,h,s}^{d}$ have been ascertained, a verification of these values is needed to determine if they are higher than the nominal power. If so, the analyzed SOC is infeasible and a penalization of this proposal is required. This penalization

is calculated as follows:

$$Z = \sum_{e=1}^{ES} \sum_{h=1}^{N} \sum_{t=1}^{T} [(P^c_{t,h,e} - \bar{P}^c_h) \cdot H(P^c_{t,h,e} - \bar{P}^c_h) - (P^d_{t,h,e} - \bar{P}^d_h) \cdot H(P^d_{t,h,e} - \bar{P}^d_h)] \tag{3.7}$$

From (3.7), whenever $P^c_{t,h,e}$ or $P^d_{t,h,e}$ are outside the boundaries, Z measures the proportion of the limit violation; and if feasible operation is achieved, then $Z = 0$.

Once the values of $X_{t,h,e}$, $P^c_{t,h,e}$, $P^d_{t,h,e}$ and Z are known, the model can be rewritten in the following way as a linear programming problem:

$$\min z = \sum_{t=1}^{T} \pi_t P^E_t + \sum_{e=1}^{ES} p_e \Big\{ \sum_{t=1}^{T} (\mu^-_t I^-_{t,e} - \mu^+_t I^+_{t,e}) \Big\} + \beta Z^t \tag{3.8}$$

Subject to:

$$P^E_t + I^-_{t,e} - I^+_{t,e} + \Delta t \sum_{h=1}^{H} P^{net}_{t,h,e} = 0, \forall t, \forall s \tag{3.9}$$

$$P^{net}_{t,h,e} = P^{PV}_{t,h,e} - P^c_{t,h,e} + P^d_{t,h,e} - D_{t,h,e} - H_{t,h,e}, \forall t, \forall h, \forall e \tag{3.10}$$

$$0 \leq P^{PV}_{t,h,e} \leq P^{PV_{max}}_{t,h,e}, \forall t, \forall e, \forall h \tag{3.11}$$

$$\begin{aligned} &Y_{t,h,e} = Y_{t-1,h,e} + \Delta t H_{t-1,h,e} \\ &-Y_{t-1,h,e}/R_h C_h - \Delta t Q_{t-1,h,e}, \forall t, t \neq 1, \forall e, \forall h \end{aligned} \tag{3.12}$$

$$Y_{1,h,e} = Y_{T,h,e}, \forall e, \forall h \tag{3.13}$$

$$\underline{Y}_{t,h,e} \leq Y_{t,h,e} \leq \bar{Y}_{t,h,e} \tag{3.14}$$

$$0 \leq H_{t,h,e} \leq \bar{H}_{t,h,e} \tag{3.15}$$

where β is a penalization factor.

For each specific SOC proposal generated by the metaheuristic, the corresponding fitness function is calculated by adding the results of the cost obtained by the SDA and z.

It is worth noting that the two-stage characteristic is maintained in both subproblems, given that the aggregated SOC proposals created by the metaheuristic contain the SOC for each of the recourse decisions, and that the thermal subproblem is a two-stage linear problem containing the information for the remaining second stage variables.

3.3.1 Creation of scenarios

The results of the quantile forecast are used to select a central value for both PV and load, by specifically using the median (quantile 50%) as this central forecast. To avoid defining arbitrary values of deviations from the central forecast to create scenarios, quantiles 10% and 90% are taken as the lower and upper bounds of forecast values. In this way, all central and deviated values of PV and load are combined to form a set of nine scenarios, representative of all potential combinations of minimum, maximum and central values according to realistic information from measurements

and predictions and assuming uncorrelation between demand and PV forecasts. These nine scenarios (e1-e9), shown in table 3.1 are used as input data for the second stage formulation or recourse problem defined in the next section.

Table 3.1: Scenarios included in the stochastic scheme

Scenario	e1	e2	e3	e4	e5	e6	e7	e8	e9
Load quantile	10	10	10	50	50	50	90	90	90
PV quantile	10	50	90	10	50	90	10	50	90

An example for a typical day of the normalized aggregated values for PV and load, containing the central, upper and lower values is shown in figure 3.4.

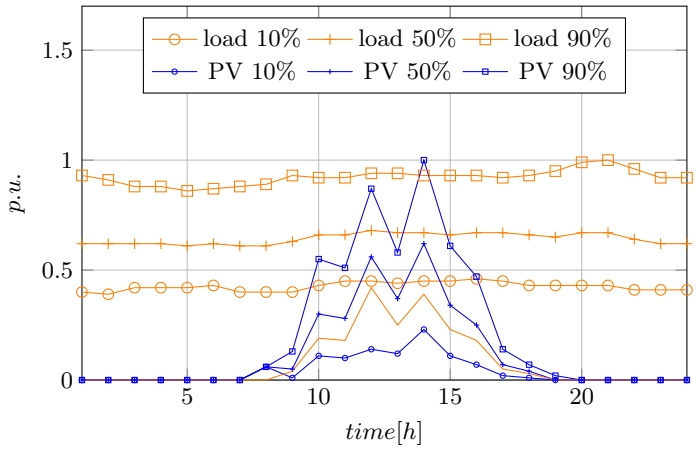


Figure 3.4: Normalized load and PV curves for each of the quantiles needed for scenario generation

It is important to emphasize that three groups can be identified from the nine scenarios described in table 3.1:

1. a conservative group: formed by the scenarios featuring high load and low PV quantiles (i.e. e4, e7 and e8);

2. an equilibrated group: formed by scenarios with similar quantiles for both load and PV (i.e. e1, e5 and e9);

3. and optimistic group: with scenarios featuring low demand and high PV quantiles (i.e. e2, e3 and e6).

The presence of these three groups of scenarios in the stochastic framework, allows a balance of optimality and robustness in the obtained solution, by combining the robustness introduced by the conservative group which generally leads to higher costs, but balanced by the potential low costs associated to optimistic scenarios, and complemented by the balance created resulting from the equilibrated scenarios. This set of nine scenarios, allow feasible and robust operation of the HEMS in the interval of extreme quantile realizations of demand and PV production, and allows exploitation of the probabilistic forecast methodology.

A visual representation of the aggregated net load (load minus PV) resulting from the nine scenarios for a typical day, can be seen in figure 3.5. The plot shows that curves e7 (——), e4 (——) and e8 (——) tend to have higher neat load during most of the 24 h horizon, which can be more clearly seen during the daytime when PV has values different from zero. In addition, e7 and e8 have also higher net load during nightime given that they are formed by using the 90% load quantile. This is a logical outcome, provided that these three scenarios (e4, e7 and e8) are indeed the ones classified in the conservative group. These scenarios will push the stochastic formulation to higher expected costs, in order to supply the required energy to be purchased in the market or injected from stored energy in the batteries.

Following the same logic, the optimistic scenarios can be identified as e2 (——), e6 (——) and e3 (——), with a clear tendency of low comparative values of net load, and even negative values for some time steps, meaning that available PV production is higher than the demand to be supplied. This situation could lead the stochastic formulation to take advantage of this available energy to store energy, supply load or sell back to the market.

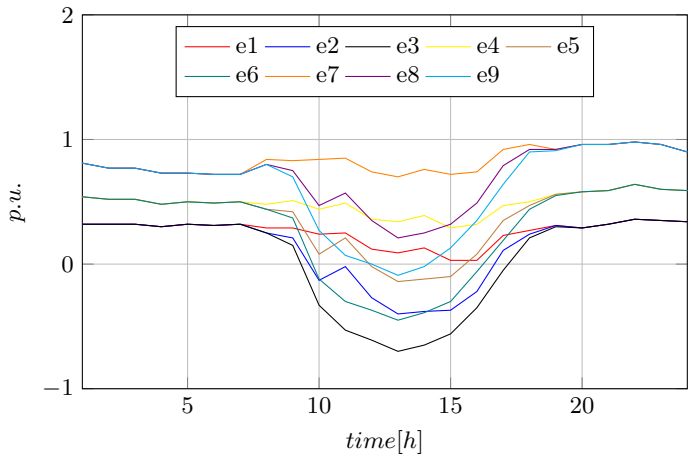


Figure 3.5: Normalized neat load per scenario

The proposed two-stage stochastic optimization model minimizes the expected prosumer's aggregation day-ahead operation cost by scheduling the batteries' power charge and discharge, and the power injected into the EWHs, the TES pattern, and exchanges with the energy market.

When the complete two-stage stochastic optimization model is solved for each of the 30 days, the first-stage variable obtained determines the day-ahead purchase commitment on the wholesale market. This two-stage model is run by defining the nine second-stage scenarios already explained.

The average expected daily cost of the stochastic solution (SS) is taken as the base value for comparison purposes (1 p.u.) and the associated cost for each of the 30 days is presented in figure 3.6 (——). This cost is the result of the DA commitment and the expected imbalance settling cost plus the expected battery cycling cost, for each of the nine scenarios, as per equation 3.4. To test the adequacy of the presented stochastic formulation, VSS (Value of Stochastic Solution) index is used [13].

To calculate the VSS, which measures the cost of ignoring uncertainty to make

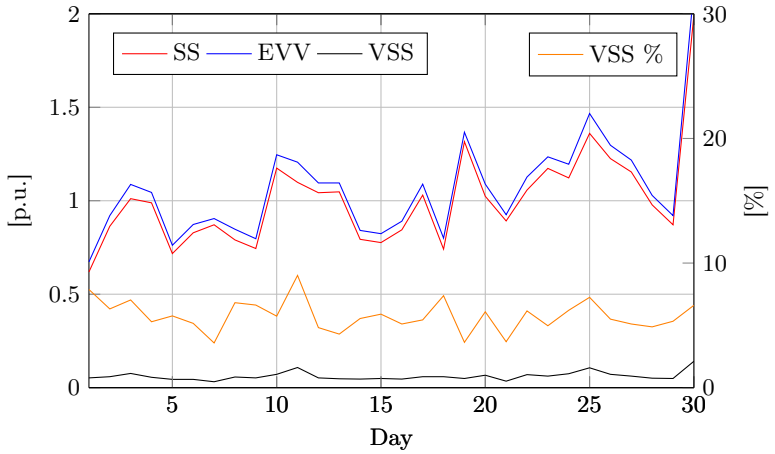


Figure 3.6: Evolution of daily cost for the deterministic case under the analyzed cases and for the whole month of November. Values in p.u. of mean SS

a decision, a quantity called the *expected value problem* (EVV) needs to be determined. The EVV consists in solving the stochastic problem using the second stage containing all the necessary scenario information, but fixing the first-stage variables with the result of the deterministic solution. This allows to find a second-stage optimal solution as a function of the first-stage variables obtained using the central forecast (quantile 50%). Then, the index is calculated by: $VSS = EVV - SS$. The value of EVV for the complete month is shown in figure 3.6 (——). The VSS is positive each day, as shown in curve (——). Average values VSS^{mean} and $VSS\%^{mean}$ are afterwards calculated using:

$$VSS^{mean} = 1/30 \sum_{1}^{30} (EVV_i - SS_i) \tag{3.16}$$

$$VSS\%^{mean} = 1/30 \sum_{1}^{30} \frac{EVV_i - SS_i}{EVV_i} \cdot 100\% \tag{3.17}$$

As a result, $VSS^{mean} = 0.06$ p.u.. By using equation (3.17), the stochastic approach allows a reduction of operating costs by $VSS\%^{mean} = 5.8\%$ on average through the analyzed month, which is also the mean value of the curve (——). The VSS gives an idea of how well the optimization under uncertainty performs. In this case, the two-stage stochastic optimization represents the best option, given that it allows a reduction of the expected average cost when compared to the deterministic approach for taking the DA purchase decisions (given by EVV).

The boxplot distribution created by the 30 day-ahead purchase commitments in each time frame, is shown in figure 3.7. From the figure it can be seen that interaction with the grid decreases in the time frames around noon, given the available PV. Concretely, the 12h and 13-15h time frames present respectively 22 and 23 days on which zero kW purchased on the wholesale market. In addition, time frames around midnight, such as the interval 23h-3h, indicate a low dispersion of purchased energy throughout the whole month.

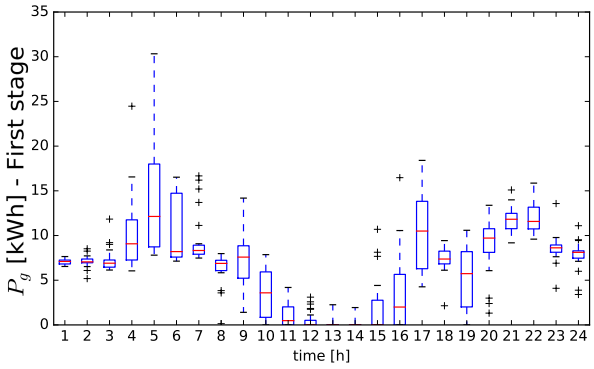


Figure 3.7: Power purchase boxplot for each DA timeframe

3.3.2 Analysis of a single day

Given that day-ahead purchase commitment variable is fixed for all scenarios (first-stage variable), second-stage imbalances allow feasible operation of the system in such a way that the expected cost is minimized. For this study case, imbalance is required at different time steps and for all of the second-stage scenarios, as shown in figure 3.8. The boxplots show that additional energy (negative imbalance) must be purchased in order to overcome shortages for the realizations of the different scenarios. In particular, scenarios 1, 4 and 7 present higher median and third quartile. These imbalance needs in fact, correspond to the scenarios with the lowest levels of PV production, so the aggregator has to purchase additional energy from the wholesale market to offset the energy imbalance.

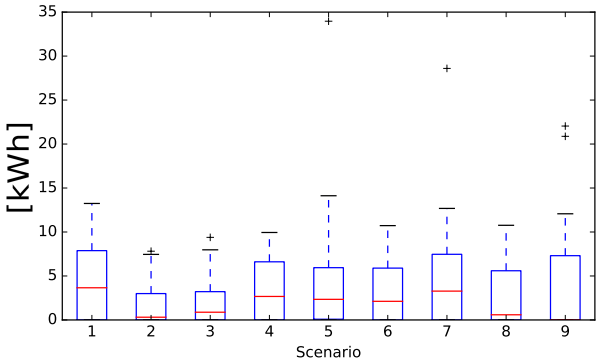


Figure 3.8: Imbalance boxplot for each scenario in the stochastic optimization

Regarding the accumulated SOC for all 16 batteries in the system, it can be seen from figure 3.9 that there is a pattern for all nine scenarios and that storage generally increases around 5h and 16h. It is interesting to point out that scenarios 4 —— and 7 —— tend to have higher SOC just before noon. This is explained by the fact that these scenarios feature low levels of PV, hence the energy discharge is treated in a more conservative way. The lowest degradation value is related to scenario 1 (——), which has minimum levels of both load and PV.

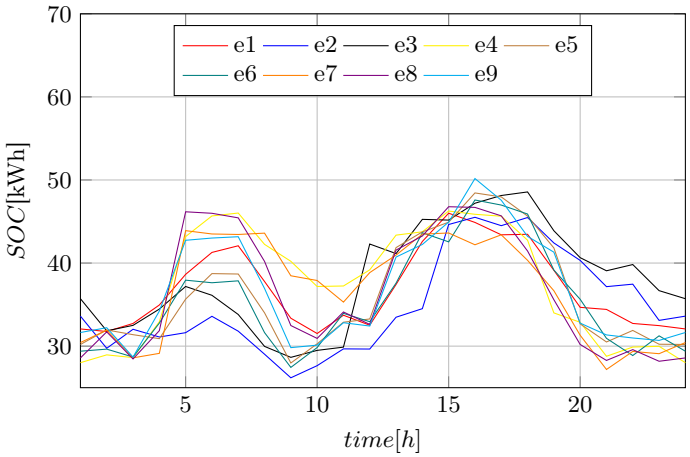


Figure 3.9: Aggregated SOC for each scenario in the stochastic approach

3.3.3 Computational performance of the CSO for the 25-household testbed

To test the performance of the CSO, several runs were carried out for a specific day in order to determine the quality and consistency of the obtained solutions. Tests consist in running the algorithm 20 times for different population sizes, setting the stop criteria to 30 iterations without improving the best solution. In addition, the maximum number of iterations is set to 300. In these conditions, the CSO is run, and after each simulation the information saved is: best solution and computational time in achieving the best solution. In addition, the performance of the implemented CSO is compared with the performance of a Particle Swarm Optimization (PSO) algorithm in order to have another swarm based metaheustic comparison. The values of the parameters used for the PSO are 0.9, 2.0 and 2.0, for inertia, cognitive and social parameters, respectively.

Table 3.6 shows the results for both CSO and PSO and the different population sizes. It can be observed that the CSO presents lower computational times for solutions close to those ones obtained with the PSO. Although the average best solutions obtained with the PSO are lower than those obtained with CSO, the computational times may be prohibitive for day-ahead decisions, given the need to run the algorithm for several hours. In contrast, the CSO achieves good quality and stable solutions in the range of 6500-12000s for population sizes of 30 and 50 particles.

The faster evolution of the CSO is explained by the constant update of the loser's velocity and the permanence in the swarm of the best paired particles, which allows good quality solutions to be maintained in each iteration and promoted into the next generational cycles.

3.3.4 Performance of the CSO for larger test systems

To test the performance of our algorithm for a larger number of households to be aggregated, four additional test cases with 50, 100, 150 and 226 households (referenced as A-50, A-100, A-150 and A-226 respectively) that belong to the same

Table 3.2: Computational performance of the CSO and PSO for one typical day in November

	CSO ($\psi = 0.3$)			PSO		
Population	30	50	80	30	50	80
Best solution [€]	5.29	5.27	5.26	5.24	5.24	5.22
Best sol. range [€]	5.29-5.37	5.27-5.31	5.26-5.34	5.24-5.31	5.24-5.27	5.22-5.26
Best sol. mean [€]	5.33	5.30	5.28	5.28	5.26	5.24
Best sol. SD [€]	0.02	0.02	0.02	0.02	0.01	0.01
Mean time [s]	6867	11103	17194	13455	25176	41351
Time range [s]	6571-7262	9750-12087	16121-18547	12750-14280	23574-26330	38687-43111
Time SD [s]	217	662	765	538	947	1624

neighbourhood in Evora, Portugal were included. All of the buildings are within a circle of 250 m radius, mainly residential, with some restaurants and stores.

Although PV, ESS and EWH in the real life are only installed in the 25 households of the original testbed, we mirrored the distribution of resources as outlined in figure 2.2 and we assigned a proportional number of resources in each case, based on the original 25-household HEMS.

For this performance analysis, the CSO was run 20 times for each test system with the following parameters: 30-particle population, $\psi = 0.3$ and stop criteria set to 30 iterations without improving the best solution and the maximum number of iterations is set to 300. The results are condensed in the following table:

Table 3.3: Computational Performance for different test systems

Test system	Best sol. mean (SD) [€]	Mean time (SD) [s]
A-50	-1.72 (0.05)	7811 (2053)
A-100	-3.36 (0.04)	9767 (2941)
A-150	-5.05 (0.05)	10372 (3809)
A-226	-7.62 (0.08)	11523 (2794)

As expected, the results show that the computational time increases when the number of households to aggregate is larger. However, the computational times for the larger test system (A-226 households) remains reasonable for day-ahead decision making with an average of 11523 s, and ranging from 5590 to 14632 s. This is an important result, provided that it demonstrates that the algorithm can deal with larger aggregation without leading to prohibitive computational burden. Negative results of the objective function indicate that management of larger number of resources leads to increased profits.

There are two main reasons to explain why the presented approach can withstand the proposed test systems within reasonable times: 1) the size of each particle is determined by the time step and the number of scenarios, but is independent of the number of batteries in the system. This allows to keep the search space of the CSO invariant and battery-independent; 2) the SDA returns the charging/discharging pattern for each battery; this information is used by the thermal subproblem, with the advantage that this subproblem is a linear programming problem, thus avoiding explosion of problem size and binary variables.

The presented stochastic model is a first approach to deal with the uncertainties introduced by PV and load. This model is fed by scenarios that come from the quantile-based forecast information in order to create different combinations of PV and demand levels. The next section will present a second alternative which is related to robust optimization, not only to model PV and demand uncertainty but also to include uncertain effects of prices.

3.4 Adjustable robust optimization approach

Robust optimization approaches aim to find optimal and feasible solutions over an interval of values that represent uncertainty. When inspecting the deterministic model in (2.1)-(2.14), four sources of uncertainty are identified: prices, PV production, electrical demand and thermal demand.

The robust counterpart of a deterministic problem can be found by maximizing the deviation of the uncertain parameters within each constraint. A tractable resulting problem is obtained with strong duality theorem. Interested readers can find detailed formulation in [100]. The details of the formulation of the robust counterpart and the relation with the model in this thesis is provided in the Appendix C

When applying strong duality due to energy price uncertainty in the objective function, the following equations are obtained:

$$\sum_{t=1}^{T}\sum_{h=1}^{N}\sum_{s=1}^{S}(a_{h,s}X_{t,h,s}^{Ds}+b_{h,s}l_{t,h,s})+\sum_{t=1}^{T}\hat{\pi}_t P_t^E+\sum_{t=1}^{T}q_t^c+\Gamma^c z^c \tag{3.18}$$

$$z^c+q_t^c\geq\frac{1}{2}(\bar{\pi}_t-\underline{\pi_t})y_t^c,\forall t \tag{3.19}$$

$$-y_t^c\leq P_t^E\leq y_t^c,\forall t \tag{3.20}$$

$$z^c,q_t^c,y_t^c\geq 0,\forall t,\forall h \tag{3.21}$$

Where z^c, q_t^c, y_t^c are dual variables of the robust counterpart. For price uncertainty, a robust parameter allows to control conservatism of the solution (Γ^c). This value can be adjusted in the range [0,T], given that T is the maximum number of uncertain parameters in the objective function (energy price). For instance, if $\Gamma^c = T$, means that the solution will remain optimal and feasible for T price deviations from the central value. Or in other words, the solution is capable of withstanding the worst case scenario.

Uncertainty in constraint (2.2) is introduced by PV and electrical load. Hence, a single uncertain right-hand parameter can be obtained by finding the net load in each time step (PV minus load). The robust counterpart of this constraint is given by equations (3.22)-(3.24).

$$P_t^E+\Delta t\sum_{h=1}^{N}P_{t,h}^d-P_{t,h}^c-H_{t,h}=D_t^{net}+q_t^D+\Gamma_t^D z_t^D,\forall t \tag{3.22}$$

$$z_t^D+q_t^D\geq\frac{1}{2}(\bar{D}_t^{net}-\underline{D}_h^{net})y_t^D,\forall t \tag{3.23}$$

$$z_t^D, q_t^D \geq 0, y_t^D \geq 1, \forall t \tag{3.24}$$

where,

$$D_t^{net} = \frac{1}{2}(\bar{D}_t^{net} + \underline{D}_h^{net}) \tag{3.25}$$

In this case, net load uncertainty indirectly captures electrical load and PV uncertainty. Robust parameter Γ_t^D controls the robustness in each constraint t. For simplicity, in the remainder of this document the subindex t is eliminated from this parameter and instead Γ^D is used to control net load robustness. Cardinality of Γ^D is [0,1], provided that there is maximum one uncertain parameter in each constraint.

Constraint (2.11), contains another uncertain parameter: thermal load. Application of strong duality results in the following constraints:

$$\begin{aligned} &Y_{t,s,h} = Y_{t-1,s,h} + \Delta t H_{t-1,s,h} - Y_{t-1,s,h}/R_h C_h \\ &-\Delta t(\hat{Q}_{t-1,s,h} + q_{t-1,h}^{th} + \Gamma_{t-1,h}^{th} z_{t-1,h}^{th}), \forall t, \forall h \end{aligned} \tag{3.26}$$

$$z_{t,h}^{th} + q_{t,h}^{th} \geq \frac{1}{2}(Q_{t,h}^{90\%} - Q_{t,h}^{10\%}) y_{t,h}^{th}, \forall t \tag{3.27}$$

$$z_{t,h}^{th}, q_{t,h}^{th} \geq 0, y_{t,h}^{th} \geq 1, \forall t, \forall h \tag{3.28}$$

For simplicity, we eliminate the subindex t, h from $\Gamma_{t,h}$ and instead we assume a general parameter to control robustness in thermal load: Γ^{th}. Note that $\Gamma^{th} \in [0, 1]$.

The complete adjustable robust MILP counterpart (ARO) is represented by the following equations:

$$\text{minimize } (3.18) \tag{3.29}$$

s.t.

$$\text{Constraints} : (2.5) - (2.10), (2.12) - (2.14), \tag{3.30}$$

$$(2.35) - (2.43), (3.19) - (3.24), (3.26) - (3.28) \tag{3.31}$$

where:

- (3.18): is the robust counterpart of the objective function.
- (2.5)-(2.10): are the BESS constraints.
- (2.12)-(2.14): are the EWH constraints
- (2.35)-(2.43): are the BESS cycling piece-wise linearization constraints.
- (3.19)-(3.24): are the robust counterpart constraints related to power balance and net demand uncertainty.
- (3.26)-(3.28): are the robust counterpart constraints related to thermal demand uncertainty.

This is a tractable MILP problem that can be solved with off-the-self commercial solvers. Three robust control parameters can be tuned to obtain different robust day-ahead bids: Γ^{DA}, Γ^{D} and Γ^{th}. Each one controls conservatism against uncertainty in energy prices, net load and thermal load, respectively.

For the simulations presented in the next section, electricity prices are taken from the EPEX-European Power Exchange database [104], and a persistence model is used to forecast the day-ahead and imbalance prices, consisting in assuming the last known data for the same weekday. This is done to consider a realistic case in which an aggregator, when defining day-ahead purchases, does not have the settled prices. Hence, by taking the prices for the same day in the previous week, we obtain available input data to make decisions. In line with [21, 24], price deviation from forecasted values are assumed to be $\pm 10\%$, in order to create confidence intervals for the ARO formulation.

The confidence intervals for the the net load and thermal demand are created by taking the 10% and 90 % quantiles of the probabilistic forecast.

3.4.1 Results for the robust approach

The following results present the behaviour of the main variables after solving the deterministic model presented in equations (2.1)-(2.14) and the adjustable robust optimization counterpart in (3.29)-(3.31), for a medium MI day (Nov. 15th). When solving the deterministic problem, the obtained day ahead operational cost is 14.93€. On the other hand, a cost of 29.88€ is found as the robust solution when $\Gamma^{DA} = 24$, $\Gamma^{D} = 1$ and $\Gamma^{th} = 1$, which corresponds to considering the full uncertainty budget for all the uncertain variables in the model. This robust DA operation cost, establishes an upper bound for the operation cost, while the deterministic solution is a lower bound. For the deterministic solution, this means that any uncertainty realization different from the central forecasts for prices, load and PV; would imply penalization due to imbalances. On the other hand, any realization of the uncertainty set within the budget, would never yield an operation cost higher than 29.88 €, acting as a guaranteed minimum.

Figure (3.10) shows the accumulated (all BESSs) SOC for both deterministic and ARO cases.

The deterministic (–●–) SOC shows, in general, a similar evolution when compared to the ARO. However, a particular difference is evident in timeframes 12h-16h, which coincides with PV production hours. In the ARO, there is a discharging pattern of the batteries during these time frames provided that a highly conservative scenario is implicitly assumed within the model when Γ^{D}=1 and Γ^{th}=1: minimum PV production and maximum demand. This situation leads the optimal solution to set BESS in discharging mode to compensate low levels of available PV. The ARO indicates a more conservative discharging-charging, given that stored energy during these time frames avoids a setting point close the boundaries, in order to cope with potential uncertainty realizations in a more cost-efficient way. For instance, if during time frames 12h-15h, uncertainty realizations were those of higher than forecasted PV values, the ARO solution would allow more room for power injection into the grid. On the contrary, the deterministic solution would be more limited to exploit this potential situation, given that the settings of BESSs would not allow

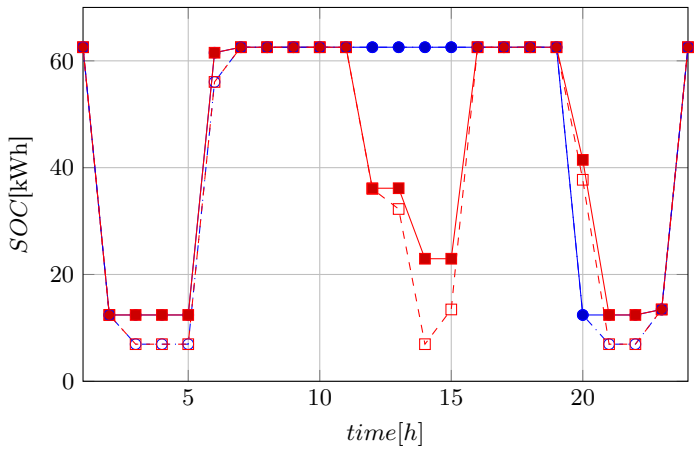


Figure 3.10: Accumulated SOC when cycling cost is included: Deterministic (—●—), ARO (—■—). Accumulated SOC when cycling cost is neglected: Deterministic (- ⊖ -), ARO (- ⊡ -).

additional storage. However, next subsection will analyze potential savings and cost advantages of the ARO versus the deterministic approach in more detail.

In addition, a simulation was carried out neglecting cycling aging cost (second term in equation (2.44) also for the deterministic (- ⊖ -) and ARO (- ⊡ -) cases. This simulation shows that deeper cycling is found for time frames: 3h-5h, 14h-16h and 20h-22h. This is an expected result provided that the omission of aging in the model, will cause the battery to cycle without degradation constraints and present deeper and more frequent cycling.

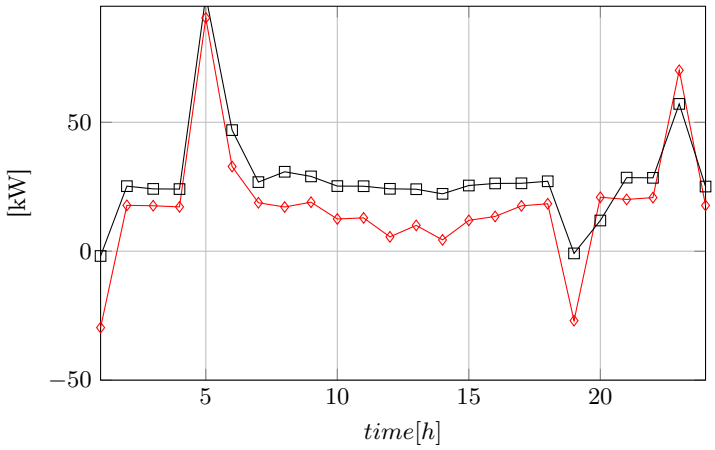


Figure 3.11: Day-ahead energy purchase: deterministic (—◇—), ARO (—□—)

The energy purchase commitment for both cases is shown in figure 3.11. Excepting two time frames (20h and 23h), purchase commitment for the ARO (—□—) is always higher than the deterministic approach (—◇—). This is an expected result given that, as explained before, the robust solution is conservative and represents a cost upper bound to withstand different uncertainty realizations while maintaining

final operation under this maximum assured cost.

When the aggregator bids in the day-energy energy market and determines the operation of its devices for each hour, there might be imbalances due to deviations, as explained in subsection 3.4.4. In this case, energy shortage/excess should be purchased/sold at the imbalance price, increasing final operational costs.

Robustness can be visualized by analyzing imbalances due to deviations when DA purchase commitment is subject to multiple random realizations of prices, PV production and demand. To generate boxplots of imbalance for deterministic and ARO solutions, MC simulation is used by assuming uniform distribution for prices, and the inverse cumulative distribution function (ICDF) for PV and load resulting from the real probabilistic forecast. Figure 3.12 shows a comparison of the imbalances (same selected day: 15th Nov.) for each time frame. For this specific case, it can be seen that the robust solution ($\Gamma^{DA} = 24$, $\Gamma^{D} = 1$ and $\Gamma^{th} = 1$) does not incur in negative imbalances (additional purchases), but only in selling energy excess, (positive imbalance) during all time periods, with particular higher median values during 5h and 6h and around noon. This is explained by the fact that the ARO returns a solution that is feasible for the lowest realizations of PV production and the highest load scenarios, leading to energy excess when different realizations of this uncertainty are analyzed. The early hours positive imbalance coincide with the high energy purchase (see figure (3.11)) used for battery charging (see figure(3.10)), which becomes an energy excess and is sold back to the market. In opposition, when the deterministic solution is subject to uncertainty realizations, negative imbalance appears in all time steps, given its limitation for handling realizations of uncertainty which are different from the central forecasted values, specially when load is higher and PV production is lower.

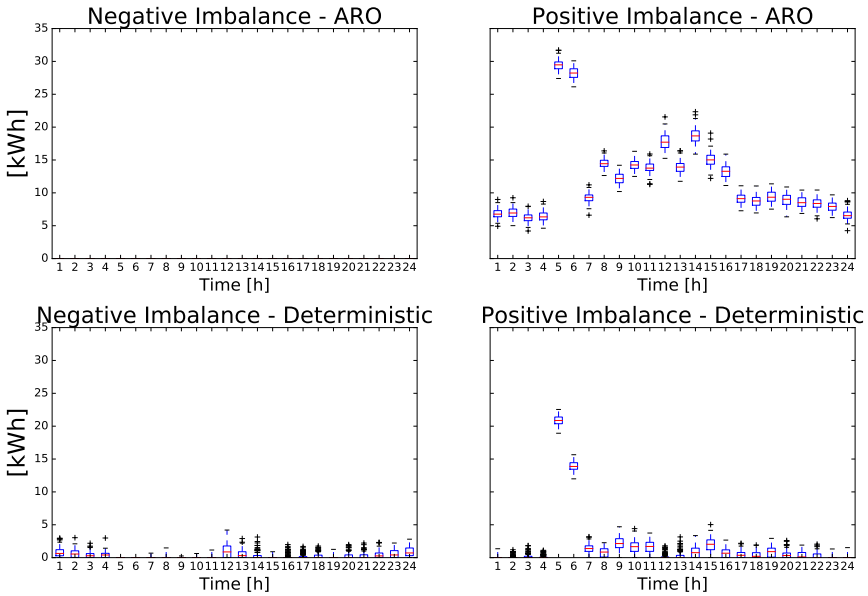


Figure 3.12: Comparison of imbalance needs for the deterministic and the robust approach when $\Gamma^{DA} = 24$, $\Gamma^{D} = 1$ and $\Gamma^{th} = 1$

3.4.2 Interaction of devices in the deterministic and robust approaches

Another simulation was carried out for the complete month of analysis. In this case, the interaction of different sources of flexibility was analyzed for the deterministic and ARO cases. The proposed test system has two technologies for storing energy: electrochemical batteries and EWHs. The possibility of using the EWHs to store thermal energy allows this device to act as a flexible load. Average costs were obtained for different cases as shown in table 3.4.

Table 3.4: Average daily costs of resource management

Case	Used flexibility		Equiv. cost	Total operation
	BESS	TES	cycling [€]	cost [€]
Deterministic	Yes	No	0.20	15.7
Deterministic	Yes	Yes	0.20	15.19
RO	Yes	No	0.19	28.89
RO	Yes	Yes	0.18	28.14

The table shows that for both cases (deterministic and ARO) better results are obtained when TES is allowed as a form of flexibility. In specific, when EWHs are used to store heat, deterministic and ARO approaches achieve 3.2% and 2.6% cost decrease respectively, when compared to cases in which only batteries are used to store energy. This shows the importance of allowing control of the EWHs' settings in order to store hot water to be used in later hours.

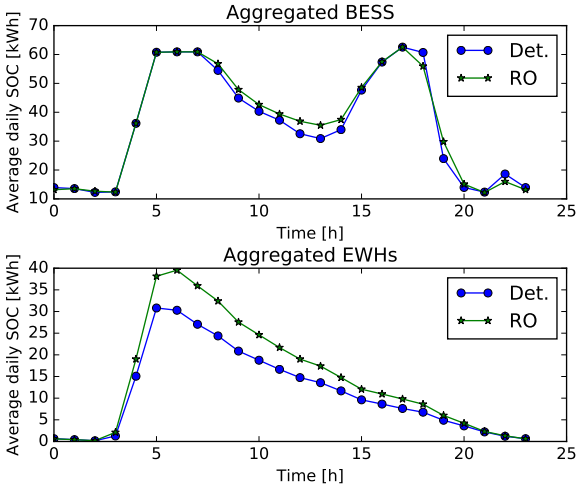


Figure 3.13: Daily average operation (state of charge) of BESS and EWHs

For instance, figure 3.13 shows the average stored heat of all EWHs in the test system. From the figure it can be concluded that the robust approach presents higher levels of stored heat versus the deterministic case. This is explained by the fact that the ARO is protected against potential variations of thermal load including the maximum values in the confidence interval. Hence the available hot water should be enough to face this extreme scenario in each time step.

The figure also shows aggregated average SOC for the BESS. In this case, stored energy for the ARO case differs from deterministic mainly around noon hours, presenting lower DoD, or similarly: available stored energy. This difference in stored energy also leads to lower average cycling aging in the robust case. For instance, 10% equivalent cycling average cost decrease is achieved in ARO versus the deterministic, due to the difference in the batteries' SOC.

3.4.3 Impacts of battery efficiency on cost

In this work, no information was available for the existing storage system in the test system regarding charging/discharging (or roundtrip) efficiency, hence we neglected inverter losses (as well as PV) and assumed the value of 95% for the batteries in line with previous research for residential applications [24,105–109] in which close or equal values were used. We are aware that efficiency of the system might certainly be lower than 95% and that this leads to changes in device settings and overall system profit/cost. However, provided that changes in η will affect both deterministic and ARO simulations, the philosophy of the general conclusions on advantages of ARO over deterministic will remain unchanged. Only specific numerical values of average costs / SD, etc., will suffer an offset according to the specific value of η.

To determine the impacts of charging and discharging efficiency on the total operation cost obtained by the deterministic and ARO approaches (with Γ^{DA}=24, Γ^{D}=1 and Γ^{th}=1), a sensitivity analysis is carried out.

This analysis consists on changing the value of $\eta = \eta^c = \eta^d$ in equation 2.5 and solving for each day during the analyzed month. Afterwards, the monthly average cost is calculated and associated to each η value. After this procedure is completed, the obtained values are depicted in figure 3.14.

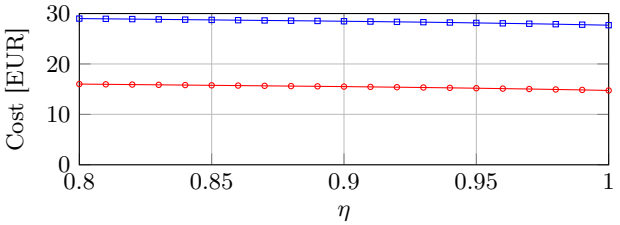


Figure 3.14: Sensitivity analysis for variations of charging and discharging efficiency. Average daily cost for November. Deterministic (—○—) and Robust case (—▫—)

This figure shows that lower values of efficiency lead to average cost increase for both cases: deterministic and ARO. For the case of the deterministic approach, when losses are neglected ($\eta = 1$) the cost is 14.74€, and increases up to 8.6% when an efficiency of 0.8 is considered for the storage system.

For the ARO case, an average cost of 27.69€ is obtained when losses are neglected, and cost increase reaches 8.3%. The direct comparison of the ARO and deterministic solutions shows that when losses are neglected, ARO presents an extracost of 87.85% when compared to the deterministic. Extracost of 81.1% is obtained for the case of $\eta = 0.8$, showing that despite large variations in η, the robust solutions present a higher guaranteed costs than the deterministic. This may lead

to different scheduling of devices and absolute costs for each methodology, but as expected, ARO solutions always present higher maximum guaranteed cost, as also explained in section 3.4.1.

3.4.4 Performance assessment of robust solutions

In order to analyze different levels of conservatism when bidding in the day-ahead energy market, different combinations of Γ^{DA}, Γ^{D} and Γ^{th} must be analyzed. When a solution is obtained for any combination, the energy purchase commitment (P_t^E) and the device settings are determined. The performance of this day-ahead plan is evaluated by calculating the imbalances I_t^-/I_t^+ in each time step due to energy mismatch. Negative/positive imbalance implies energy shortage/excess that has to be purchased/sold at higher/lower prices which leads to overcost in the operation. Each plan is subject to performance analysis under several realizations of energy price, PV, electrical and thermal load by means of Monte Carlo (MC) simulation.

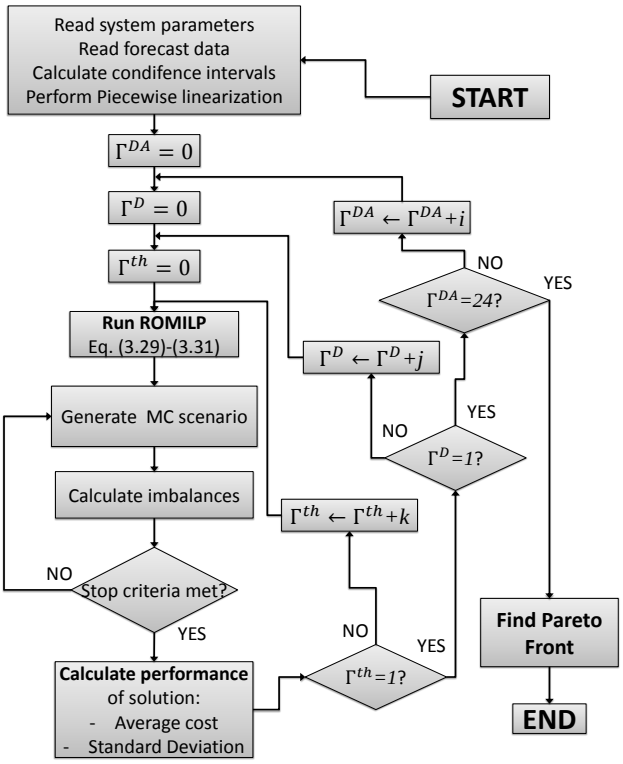


Figure 3.15: Flowchart of the algorithm to find best trade-off solutions

After several MC scenarios are generated and analyzed, the performance of the robust solution is assigned two attributes: average cost and standard deviation (SD). A decision maker is interested in minimizing both, to achieve low expectation of cost and minimize risk at the same time. Since a single day-ahead dispatch has as many average costs and SD as combinations of Γs, Pareto optimality theory is used to select the set of control parameters that yield better performance for both average cost and SD [110]. A complete outline of the methodology to find the Pareto front

for a specific day-ahead optimization, is shown in figure 3.15.

In the following subsection (3.4.5), to generate MC scenarios we consider the uniform distribution around a central persistence forecast for energy price [$0.9\hat{\pi}$,$1.1\hat{\pi}$], and for the case of PV and load, we consider the inverse cumulative distribution function (ICDF) resulting from the real forecast described in subsection 2.3.1. Since quantile information is discrete, interpolation to obtain proper values in-between quantiles is carried out. This is done to avoid arbitrary PDFs to generate data and to take advantage of available quantile forecast. Stop criteria for MC simulation is set to 1000 scenarios. Confidence levels of minimum 95% and margins of error less than 1%, were verified even below 1000 trials.

3.4.5 Results of the performance analysis

The selection of the budget of uncertainty influences the performance of obtained day ahead operation, hence the choice of using ARO approach in the presented thesis. In order to determine better choices of budget, the procedure explained in figure 3.15 is used. This allows to use MC for several combinations of Γ^{DA}, Γ^{D} and Γ^{th}, and determine average cost and SD. This way, a set of uncertainty budgets can be found such that the average cost and deviation are minimized. Two days are selected to develop this analysis: November 5th (High MI) and 27th (Low MI). The steps for Γ^{DA}, Γ^{D} and Γ^{th} are $i = 6$, $j = 0.2$ and $k = 0.2$ respectively, therefore, 180 combinations are generated to be analyzed under the performance evaluation methodology. After running MC simulation for each of the 180 budgets of uncertainty, the costs and deviations in figure 3.16 are obtained. Note that the values are normalized by using the deterministic values as the base (1 p.u.). The plot shows the performance for the deterministic solution as a blue square: (■).

This simulation shows that in both cases, the deterministic solution tends to have higher standard deviation when compared to the robust approach under different uncertainty budgets. This indicates that robust solutions tend to be more reliable and steady in terms of imbalances and the subsequent penalization, hence represent less risky operation for the aggregator.

In particular, the simulation for Nov. 5th shows that only 8 ARO have higher standard deviation than the deterministic solution, and the fourth largest for Nov. 27th. With the robust formulation, SD can be reduced in 27.3% and 36.4% for each day, respectively.

Regarding the performance costs obtained with ARO, and compared to the deterministic approach, costs can be reduced in average by 5.7% and 2.6% respectively for each day. In addition, the min-min Pareto front can be found by determining the non-dominated set of points according to Pareto optimality criteria [110]. This Pareto front (depicted by: •) represents the best set of solutions from the perspective of average performance cost and SD.

Table 3.5 shows the points that comply with the following two conditions: 1) form the Pareto front and 2) independently dominate the deterministic solution. The table also shows operation cost improvement with respect to the deterministic solution, obtaining cost improvements in the ranges of 5.2%-5.7% and 2.1%-2.6% for each day, respectively. In addition, the ranges of improvement for SD are 7.7%-27.2% and 17.5%-36.4%, respectively.

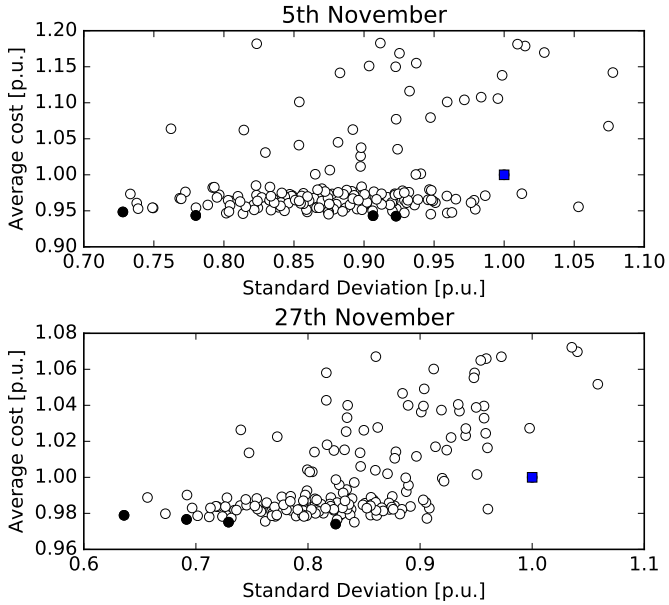


Figure 3.16: Average operation cost for two days under different budgets of uncertainty and Pareto front

Table 3.5: Details of the Pareto fronts values and improvement with respect to deterministic solution

Day	Γ^{DA} / Γ^{D} / Γ^{th}	Cost [p.u.]	SD [p.u.]
Nov. 5th	Γ_1^{D5}: 12 / 0 / 0.4	0.948	0.728
	Γ_2^{D5}: 12 / 0 / 0.8	0.944	0.780
	Γ_3^{D5}: 24 / 0 / 0	0.943	0.923
	Γ_4^{D5}: 24 / 0 / 0.8	0.943	0.906
Nov. 27th	Γ_1^{D27}: 18 / 0.2 / 0.2	0.974	0.825
	Γ_2^{D27}: 18 / 0.2 / 0.6	0.975	0.729
	Γ_3^{D27}: 24 / 0.4 / 0	0.979	0.636
	Γ_4^{D27}: 24 / 0 / 0.2	0.977	0.692

It should be noted that the Pareto front for Nov. 5th contains only zero values for Γ^D. This result shows that for high mean net load interval days, the methodology avoids using high values of this uncertainty budget, given the over-conservatism that this values yield. As for November 27th (low mean net load interval), ARO formulation performs in several cases even with values different from zero for all uncertainty budget parameters. This result is explained by the fact that the uncertainty realizations for load are contained in narrower intervals and close to central forecasts.

For further analysis, the ARO solutions in the Pareto front are selected to build Cumulative Density Functions (CDF) and compare performance versus the deterministic solution from the cost standpoint. As per figure 3.17, the ARO solutions for both days, independently, show similar behavior among themselves, and they all share a common feature in each day: the associated costs are lower than the ones obtained in the deterministic approach. This result shows again the robustness of

the proposed model to handle uncertain parameters and their potential realizations.

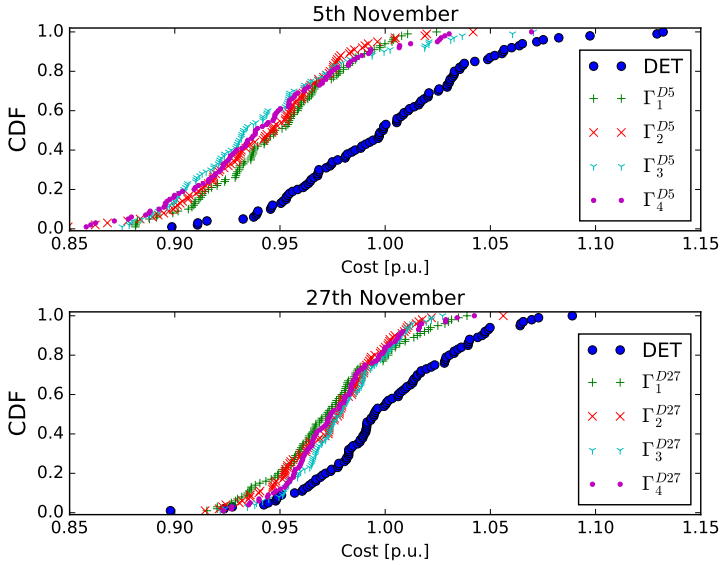


Figure 3.17: Performance Cumulative Density Functions for selected Robust Solutions

For instance, for November 5th the probability that the ARO solutions have lower cost than the deterministic average, lays in the range from 91.2% to 96.3%. For November 27th, there is a probability between 79.0% and 85.4%, for the ARO solutions to have better performance that the deterministic mean. These values can be simply found by intersecting the curves where cost equals 1 p.u. and determining the respective cumulative density. In general, the leftmost solutions represent better performance.

It can also be noted that the CDFs for November 27th are less scattered when compared to those of November 5th. This is again an expected solution, provided that this day presents a lower MI, so it is expected that robust and deterministic solutions will have a closer performance and behavior.

3.4.6 Effects of considering cycling aging in the model

To analyze this impact, the same day used in subsection 3.4.1 (Nov. 15th) and the following arbitrary values for the uncertainty budget are used: Γ^{DA}=12, Γ^{D}=0.5 and Γ^{th}=0.5. Three cases are run and their performances are calculated with MC:

Naive Solution (NS) Consists of neglecting the cycling aging cost described by equations (2.35)-(2.43) (cycling aging constraints) and the first term in objective function (3.18) (piece-wise degradation term). This solution allows unconstrained cycling of the batteries.

Real Cost of Naive Solution (RCNS) This solution is obtained by adding two terms: 1. obtained cost of NS, and 2. the equivalent cycling aging cost of this solution. This way, the real cost in which the NS incurs can be obtained.

Complete Robust Solution (ARO) This is the solution obtained by solving the complete formulation in equations (3.29)-(3.31).

After running the simulations and finding the respective performances, the following average costs are found: 14.43€, 22.04€ and 14.53€ for the NS, RCNS and ARO, respectively. These results show the importance of taking into account the degradation model within the optimization, so as to obtain an overall lower operation cost. The naive approach has a lower cost in appearance, but as the battery is allowed to cycle without constraints, there is a hidden cost that increases operation from 14.43€ to 22.04€. When the ARO complete formulation we propose is used, a 34.07% cost reduction is achieved when compared to the RCNS.

When the CDFs are analyzed, as depicted in figure 3.18 it can be seen that the NS could lead to think that lower costs are achieved as this curve presents more leftmost points. However, the real cost of ignoring the cycling model can be observed by the rightmost CDF.

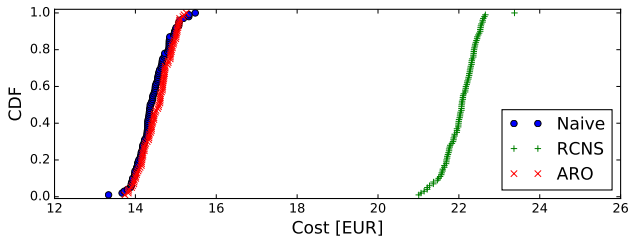


Figure 3.18: Cumulative Density Functions for the robust model when cycling is considered and neglected

3.4.7 Remarks about computational time

To give an insight on the solution time for each of the solution alternatives: ARO, NS and deterministic; additional simulations were carried out. These simulations consisted on running each alternative for each day in November and determining the computational time in seconds. Figure 3.19 shows the obtained simulation time in each day of the month. It can be seen that the NS presents lower computational times in each day and it is an expected outcome provided that this alternative does not include the additional constraints and binary variables used to calculate cycling aging of the battery.

In addition, the deterministic case presents higher computational times in average, compared to NS. This is explained by the fact that the deterministic alternative includes cycling aging, thus increasing the size of the problem and the number of binary variables.

Table 3.6 shows the behavior and comparison of the computational time for each alternative. As expected, the complete ARO formulation presents higher computational times given that it includes constraints and binary variables to calculate

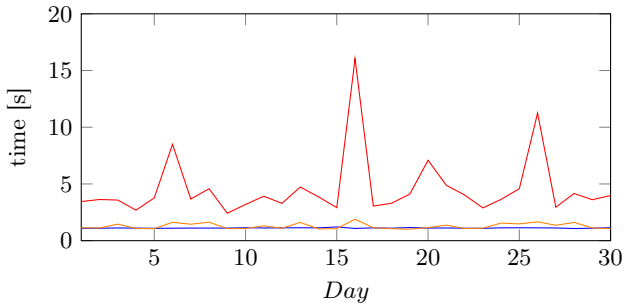


Figure 3.19: Solution time for ARO (—), NS (—) and deterministic (—) case

cycling aging, and also includes the additional constraints and dual variables that appear in the robust counterpart. This leads to higher average solution time and also higher SD. Average computational times of ARO solutions are 3.6 times higher than those of the deterministic approach.

Table 3.6: Daily average computational performance of the ARO, NS and deterministic approaches

	ARO	NS	Deterministic
Mean time [s]	4.59	1.11	1.28
Time range [s]	2.41-16.05	1.07-1.21	1.01-1.89
Time SD [s]	2.77	0.03	0.25

3.5 Comparative analysis of ARO modified models and hybrid formulations

Besides ARO for including price uncertainty, another option is to use the KDE sampling tool to create multiple price scenarios and use them for stochastic optimization. Given the nature of the available KDE sampling for price forecasts as explained in section 2.3.1, a set of scenarios can be obtained and included in the optimization model by means of stochastic programming. The information of the non-parametric KDE over the 90 days previous to the day of operation is used to create a number of price scenarios. At first, each scenario in the set is given the same probability. Given that a large number of scenarios may lead to long computational times, a scenario reduction technique is implemented. In this thesis, when scenarios are considered to model price uncertainty, a backward reduction algorithm based on Kantorovich Distance (KD) [111] is used to obtain a reduced representative set, consisting on the following steps:

1. Create a number of initial samples using KDE, and define a target number of scenarios.

2. Calculate KD for each pair of scenarios in the current set. This calculation leads to a Kantorovich Distance Matrix (KDM).

3. For each scenario, identify its closest neighbour j. This can be done by identifying the lowest value in each row i of the KDM.

4. For each closest neighbour j in each row i, calculate $KD_{i,j} \times p_e(i)$, where $p_e(i)$ is the probability of scenario i.

5. From the i-position vector containing of all values of $KD_{i,j} \times p_e(i)$, select the lowest value. Identify scenario i.

6. Eliminate scenario i and assign probability of i to $p_e(j)$. Update matrix KDM.

7. Repeat steps 3-6 until the target number of scenarios is obtained.

An graphical example of the application of this reduction technique is shown in figure 3.20. In this case, a total of 100 initial price scenarios were generated (dashed lines), and the reduction technique is applied until 10 representative scenarios (continuous lines) are obtained. For this specific example case, final probabilities of each scenario are: 0.166, 0.096, 0.16 , 0.085, 0.089, 0.088, 0.071, 0.091, 0.087, 0.067.

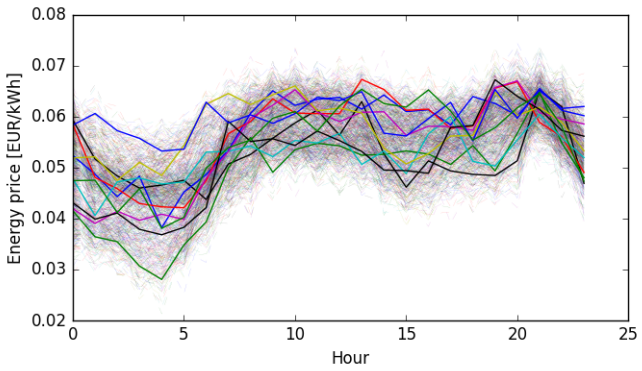


Figure 3.20: Example of KDE sampling and scenarios obtained after backward reduction technique for energy prices

In the remainder of this thesis, KDE is also used to create the confidence intervals of energy and imbalance prices. This is done by sampling multiple price trajectories and afterwards calculating the 10% and 90% quantiles. This information is used as the uncertainty intervals for ARO formulations in order to generate the confidence intervals needed to the robust optimization approach [112].

3.5.1 Alternatives of the ARO formulation

Modifications regarding objective function

Following robust optimization to account for uncertainty of energy prices, and after obtaining the reduced scenarios and corresponding probabilities with the methodology explained in the previous subsection, a stochastic optimization problem can be formulated. In this case, objective function 2.1 and constraint 2.2 have to be reformulated as follows:

$$\text{minimize} \sum_{e=1}^{N_e} p_e \sum_{t=1}^{T} (\pi_{t,e} P_t^E + \mu_{t,e}^- I_{t,e}^- - \mu_{t,e}^+ I_{t,e}^+) + \sum_{h=1}^{N} f_h^{cyc}(\mathbf{X}_h) \tag{3.32}$$

$$P_t^g + I_{t,e}^- - I_{t,e}^+ + \Delta t \sum_{h=1}^{H} P_{t,h}^{net} = 0, \forall t, \forall e \tag{3.33}$$

This stochastic formulation, represents an alternative to include price uncertainty in the day-ahead dispatch formulation and can be combined either with a deterministic formulation for load and PV production, or with robust formulation for load and PV uncertainty. If price uncertainty is accounted for with these scenarios and PV/demand uncertainty is treated with ARO, the remaining problem is a: **Hybrid stochastic/robust** (HSR) optimization problem. If only ARO is used to model uncertainties, this formulation will be referred to from now on as: **Complete ARO**.

The motivation of including also hybrid stochastic/robust schemes for comparison purposes, lies on the fact that in real-life applications it may not feasible to create high quality scenarios for all forecasted variables needed by the stochastic optimisation approach. To generate such scenarios one should take into account spatio-temporal correlations among the variables. For instance, creating PV and demand correlated scenarios for stochastic optimization can be a complex task and remains as an open research field, whereas defining an uncertainty interval for robust optimization is a more straightforward task, which does not necessarily need correlation analysis. In addition, suitable scenarios to model price uncertainty, independently of the available PV and demand information, can be practically created and used in stochastic optimization. The hybrid approach permits flexibility to consider probabilistic forecasts that may be provided in practical cases in different formats (i.e. in the form of scenarios or ensembles and in the form of prediction intervals).

Modifications regarding PV and demand uncertainty

The formulation presented in (3.22)-(3.24) to model uncertainty in PV and load, considers a unified uncertain parameter per constraint t: D_t^{net}. This leads to a single Γ parameter to control net load in which both PV and load uncertainty behaviour are condensed. Another option to model PV and demand uncertainty is to treat both uncertain parameters separately in such a way that separate robust parameters and dual variables are obtained, as follows:

$$P_t^E + I_{t,e}^- - {}_{t,e}^+ + \Delta t \sum_{h=1}^{N} P_{t,h}^{pv} + P_{t,h}^d - P_{t,h}^c - H_{t,h} = \hat{D}_t + q_t^D + \Gamma_t^D z_t^D, \forall t, \forall e \tag{3.34}$$

$$z_t^D + q_t^D \geq \frac{1}{2}(D_t^{90\%} - D_t^{10\%}) y_t^D, \forall t \tag{3.35}$$

$$\sum_{h=1}^{N} P_{t,h}^{pv} = \hat{P}_t^{pv} - q_t^{pv} - \Gamma_t^{pv} z_t^{pv}, \forall t \tag{3.36}$$

$$z_t^{pv} + q_t^{pv} \geq \frac{1}{2}(P_t^{90\%} - P_t^{10\%})y_t^D, \forall t \tag{3.37}$$

$$z_t^D, q_t^D, z_t^{pv}, q_t^{pv} \geq 0, y_t^D, y_t^{pv} \geq 1, \forall t \tag{3.38}$$

The alternative ARO formulation presented in (3.34)-(3.38) to model PV and electrical demand uncertainty is called: **separated approach**, to reflect that two robust parameters, Γ_t^D and Γ_t^{pv} result to control respectively demand and PV production. In the separated approach, it is assumed that $\Gamma^D = \Gamma^{th}$ The initial formulation in (3.22)-(3.24), in which net demand is used to compact load and PV, is called **unified approach**.

Modifications regarding control parameter Γ

Another simple modification is introduced in parameter Γ for controlling conservatism of the robust solutions, by using $\mathbf{\Gamma^2}$ values instead of **traditional $\mathbf{\Gamma}$**. The effect of this alternative is a more intensive search for solutions for values of Γ closer to zero for the same steps predefined for the robust parameter. Closer values to zero in the robust model avoid over-conservative solutions, provided that household level uncertainties tend to offset in the presence of aggregation.

3.5.2 Comparison of ARO alternatives

The input for the alternatives was composed of the information of the devices, the forecasts, and the uncertainty budget $\Gamma : \{\Gamma^{DA}, \Gamma^{D/PV}, \Gamma^{th}\}$. For unified ARO schemes, Γ^D was used, and Γ^{PV} was used for separated approaches. The outcome of each uncertainty budget analyzed was an energy schedule to be purchased or sold in the wholesale market P^E. This solution was then tested with the performance scheme such that an average cost and an SD deviation were obtained. These two results describe the performance of each robust solution.

There were four main robust optimization problems according to the alternatives defined in the previous paragraphs, which corresponded to solving the following problems:

- Unified Complete ARO (UCARO):

$$\text{minimize } (3.18) \tag{3.39}$$

s.t.

$$\text{constraints} : (2.5)\text{–}(2.10), (2.12)\text{–}(2.14), (2.35)\text{–}(2.43), \tag{3.40}$$

$$(3.19)\text{–}(3.24), (3.26)\text{–}(3.28) \tag{3.41}$$

  which corresponds to the robust counterpart when all sources of uncertainty are treated with ARO and PV and demand uncertainty are compacted in the form of net load. The resulting single parameter Γ^D was employed to model these two sources of uncertainty.

- Separated Complete ARO (SCARO):

$$\text{minimize } (3.18) \tag{3.42}$$

s.t.

$$\text{constraints} : (2.5)\text{–}(2.10), (2.12)\text{–}(2.14), (2.35)\text{–}(2.43), \tag{3.43}$$

$$(3.19)\text{–}(3.21), (3.34)\text{–}(3.38), (3.26)\text{–}(3.28) \tag{3.44}$$

which is the robust counterpart when all sources of uncertainty are treated with ARO and PV and demand uncertainty are treated in separate forms, resulting in two different uncertainty budgets, i.e., Γ^{PV} and Γ^{D}. In this case, it was assumed that $\Gamma^{th} = \Gamma^{D}$, to reflect equal uncertainty budget values for both electrical and thermal demand.

- Unified Hybrid Stochastic Robust Optimization (UHSRO):

$$\text{minimize } (3.32) \tag{3.45}$$

s.t.

$$\text{constraints} : (2.5)\text{–}(2.10), (2.12)\text{–}(2.14), (2.35)\text{–}(2.43), \tag{3.46}$$

$$(3.22)\text{–}(3.24), (3.26)\text{–}(3.28) \tag{3.47}$$

This problem corresponds to the robust counterpart when stochastic optimization is used to model price uncertainty and ARO is used to model thermal consumption, PV, and electrical demand uncertainty, with the latter two treated in a unified form.

- Separated Hybrid Stochastic Robust Optimization (SHSRO):

$$\text{minimize } (3.32) \tag{3.48}$$

s.t.

$$\text{constraints} : (2.5)\text{–}(2.10), (2.12)\text{–}(2.14), (2.35)\text{–}(2.43), \tag{3.49}$$

$$(3.34)\text{–}(3.38), (3.26)\text{–}(3.28) \tag{3.50}$$

This is the robust counterpart when stochastic optimization is used to model price uncertainty and ARO is used to model thermal consumption, PV, and electrical demand uncertainty, with the latter two treated in a separate form.

Comparisons are performed as a result of considering several combinations of aspects according to the different formulations, i.e. complete ARO versus hybrid stochastic/robust approaches, traditional Γ versus Γ^2, and unified robust parameter versus separated PV-load robust parameter. All of the combinations result in eight alternatives to be evaluated, which are detailed as follows:

- Alternative 1: UCARO scheme with traditional Γ.
- Alternative 2: SCARO scheme with traditional Γ.
- Alternative 3:UCARO scheme with Γ^2.

- Alternative 4: SCARO scheme with Γ^2.
- Alternative 5: UHSRO scheme with traditional Γ.
- Alternative 6: SHSRO scheme with traditional Γ.
- Alternative 7: UHSRO scheme with Γ^2.
- Alternative 8: SHSRO scheme with Γ^2.

A sensitivity analysis of the impact of scenarios was carried out to analyze the behavior of the stochastic formulation. A number of samples were first created by using the KDE, and afterwards, the scenario reduction technique was used to run several stochastic optimization problems ranging from 3–50 scenarios. In this case, uncertainty in PV and demand was neglected to isolate price scenarios' impact and visualize stabilization of the solution. The solution for 50 scenarios was taken as the base value to calculate the error of each stochastic problem. The result is shown in Figure 3.21.

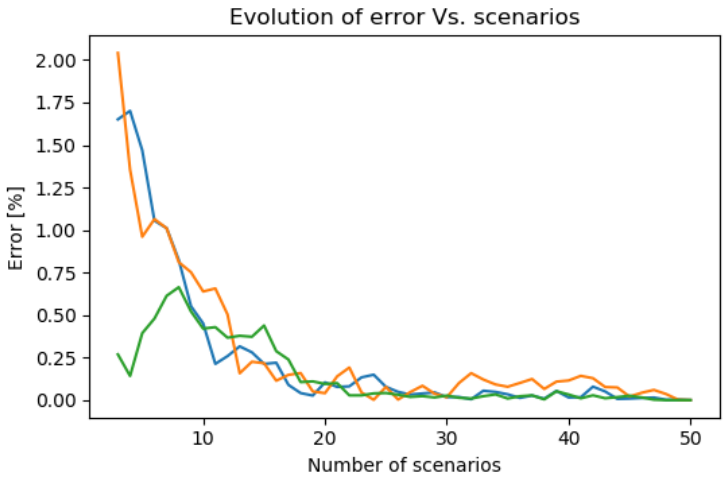


Figure 3.21: Error evolution as a function of price scenarios for the stochastic solution for three independent trials.

The error showed a decreasing behavior as the number of scenarios increased. For the simulations run, the range of 10–20 scenarios ensured, for the most part, errors below 0.5%. In the case of the present paper, we used 12 scenarios to solve the hybrid stochastic/robust formulations (Alternatives 5–8). With this selection, low values of error were achieved while avoiding an increase in the problem size and the consequent increase in computational effort.

The eight alternatives are evaluated with several combinations of budgets of uncertainty to calculate average cost and SD. The solutions with the best trade-off between cost and SD from the Pareto optimality standpoint are selected as the best solutions, hence eight Pareto fronts can be found and depicted, each belonging to each alternative.

The performance of the alternatives is calculated based on the algorithm presented in subsection 3.4.4. To define the uncertainty budgets to be evaluated, a

step of 6 is defined for Γ^{DA}, resulting in the following values: 0, 6, 12, 18 and 24, provided that cardinality is 24, i.e. the maximum number of parameters that can deviate from central values. For the remaining Γs, a step of 0.2 is used, resulting in the set of values: 0, 0.2, 0.4, 0.6, 0.8 and 1. All of these values are combined in order to map and analyse different levels of robustness and determine which combinations are the best from cost and SD standpoint. For complete ARO schemes (Atlernatives 1-4), there are $5 \times 6 \times 6 = 180$ possible combinations of budgets. For the hybrid, there are $6 \times 6 = 36$ combinations provided that there is no uncertainty budget for prices.

Figure 3.22 shows the eight Pareto fronts (black dots •) for the proposed alternatives. The green dots (•) represent dominated solutions (from the Pareto-optimality perspective) associated with different combinations uncertainty budget, but that, in all cases, turn out to be less attractive from the cost or SD point of view. The deterministic solution is depicted as a blue square (■).

In all cases, solutions always exist that result in more attractive cost and SD at the time, compared to the deterministic solution. This means that certain combinations of Γ^{DA}, $\Gamma^{D/PV}$ and Γ^{th} exist that outperform deterministic and some other conservative robust solutions. These solutions are of particular interest to define an appropriate day-ahead energy commitment plan in the wholesale market, as they can guarantee lower operational cost and risk when facing uncertainty during real-time operation. The selection of a particular solution, corresponding to a particular uncertainty budget, will depend upon the aggregator and its strategy to prioritize expected cost or decrease risk. In general, complete robust approaches (alternatives 1-4) present lower associated costs than hybrid schemes (alternatives 5-8). In addition, Pareto fronts are formed, in general, by a higher number of points, also for alternatives 1-4.

Table 3.7 shows the values of Γ that lead to the points of each Pareto. Each of the Γ configurations present in the Pareto front can be read in the following form: $\Gamma_{(m,n)}$ represents the m-th point in the n-th Pareto front, or in alternative n. For instance, for Pareto front 1 in table 3.7 there are 8 points, denoted by super-index 1. The points in this Pareto front are the best obtained with the complete robust approach (UCARO - alternative 1).

When inspecting each of the found Pareto fronts it can be seen that Complete ARO formulations (alternatives 1-4) outperform HSR approaches (alternatives 5-8). The best obtained solution from the perspective of average cost is $\Gamma_{(4,8)}$, which belongs to alternative 4: SCARO formulation with Γ^2. This solution improves the cost performance of the deterministic solution in 6.5%. The best obtained solution from the perspective of SD is $\Gamma(3, 2)$, which belongs to alternative 3: UCARO formulation with Γ^2. This solution improves the SD of the deterministic solution in 40.9%.

It is also found that the number of iterations in the Monte Carlo simulation to achieve performance convergence is related to the chosen alternative for Γ. For instance, the number of Monte Carlo iterations before convergence for each of the alternatives 1 to 8, is respectively: 766, 762, 389, 394, 920, 872, 403, 402. By inspecting this result, the lower number of iterations is associated with alternatives 3, 4, 7, 8, which are those related to Γ^2.

Other descriptors used to assess the performance of each individual alternative

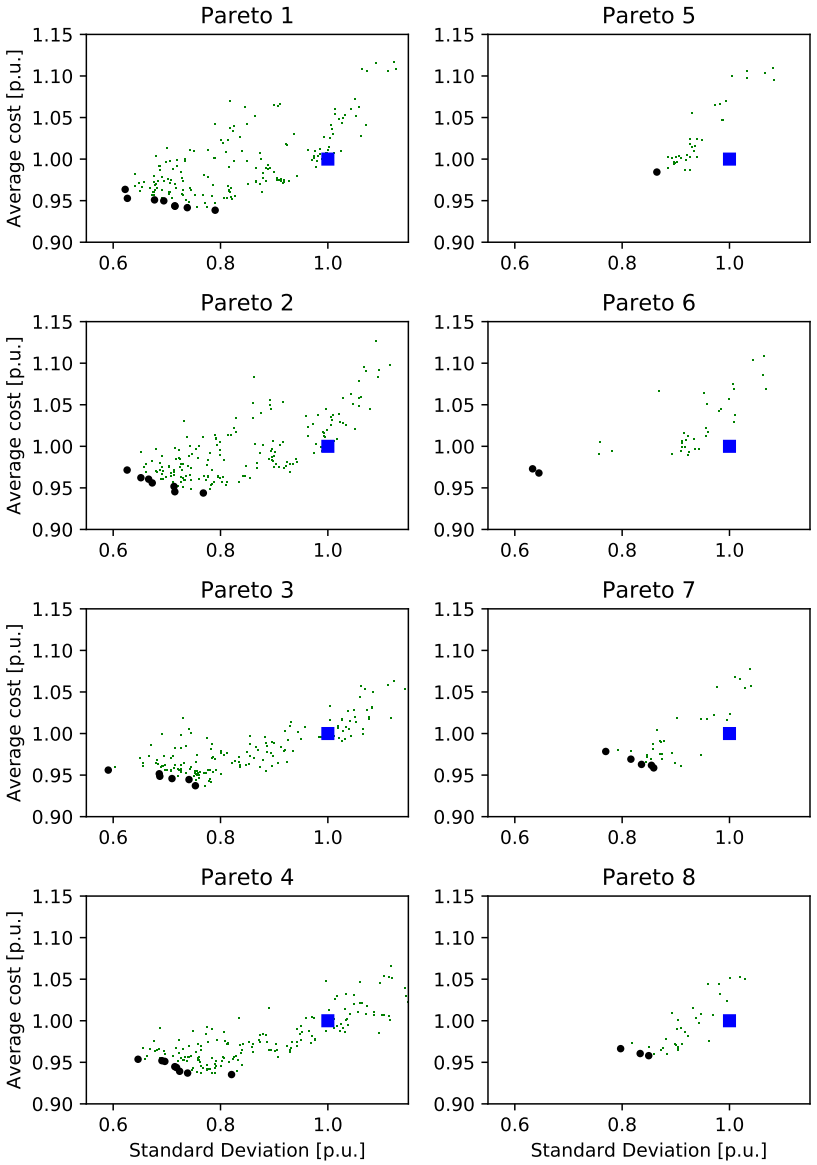


Figure 3.22: Performance points (green dots) and Pareto fronts (•) for each alternative 1 to 8. Deterministic solution in blue squares

are shown in table 3.8. In this case, there are nine descriptors based on the results shown in 3.22, which are described as follows:

- Descriptor 1 - Average cost of all points: Average value of the y-axis points belonging to each alternative.
- Descriptor 2 - Average cost of Pareto points: Average value of the y-axis Pareto points belonging to each alternative.
- Descriptor 3 - Median cost of all points: Median of the y-axis points belonging to each alternative.

Table 3.7: Details of the Pareto front values and improvements with respect to the deterministic solution. $^*\Gamma^D$ is valid for the unified approach and Γ^{PV} is valid for the separated approach

Pareto Front	Γ^{DA} / $\Gamma^{D/PV*}$ / Γ^{th}	Cost [p.u.]	SD [p.u.]
Pareto 1	$\Gamma_{(1,1)}$: 12 / 0 / 0.6	0.941	0.738
	$\Gamma_{(1,2)}$: 12 / 0.2 / 0.2	0.938	0.790
	$\Gamma_{(1,3)}$: 12 / 0.2 / 0.8	0.949	0.694
	$\Gamma_{(1,4)}$: 12 / 0.2 / 1	0.950	0.677
	$\Gamma_{(1,5)}$: 12 / 0.4 / 0	0.943	0.714
	$\Gamma_{(1,6)}$: 12 / 0.4 / 0.6	0.943	0.715
	$\Gamma_{(1,7)}$: 12 / 0.4 / 0.8	0.952	0.626
	$\Gamma_{(1,8)}$: 12 / 0.6 / 0.6	0.964	0.622
Pareto 2	$\Gamma_{(2,1)}$: 12 / 0 / 0.4	0.952	0.713
	$\Gamma_{(2,2)}$: 12 / 0 / 0.6	0.962	0.651
	$\Gamma_{(2,3)}$: 12 / 0.2 / 0.2	0.944	0.768
	$\Gamma_{(2,4)}$: 12 / 0.2 / 0.4	0.945	0.715
	$\Gamma_{(2,5)}$: 12 / 0.4 / 0.6	0.972	0.626
	$\Gamma_{(2,6)}$: 12 / 0.6 / 0	0.956	0.673
	$\Gamma_{(2,7)}$: 12 / 0.8 / 0.2	0.961	0.666
Pareto 3	$\Gamma_{(3,1)}$: 12 / 0 / 0.4	0.937	0.753
	$\Gamma_{(3,2)}$: 12 / 0 / 1	0.956	0.591
	$\Gamma_{(3,3)}$: 12 / 0.2 / 0	0.945	0.741
	$\Gamma_{(3,4)}$: 12 / 0.2 / 0.2	0.949	0.710
	$\Gamma_{(3,5)}$: 12 / 0.2 / 0.6	0.949	0.687
	$\Gamma_{(3,6)}$: 12 / 0.2 / 1	0.952	0.686
Pareto 4	$\Gamma_{(4,1)}$: 12 / 0 / 0	0.945	0.715
	$\Gamma_{(4,2)}$: 12 / 0.2 / 0.2	0.937	0.739
	$\Gamma_{(4,3)}$: 12 / 0.8 / 0	0.951	0.696
	$\Gamma_{(4,4)}$: 18 / 0 / 0.2	0.943	0.718
	$\Gamma_{(4,5)}$: 18 / 0 / 0.4	0.952	0.691
	$\Gamma_{(4,6)}$: 18 / 0.2 / 0.4	0.954	0.646
	$\Gamma_{(4,7)}$: 18 / 0.6 / 0	0.939	0.724
	$\Gamma_{(4,8)}$: 18 / 0.6 / 0.2	0.935	0.821
Pareto 5	$\Gamma_{(5,1)}$: Stochastic / 0.2 / 0.2	0.984	0.864
Pareto 6	$\Gamma_{(6,1)}$: Stochastic / 0.0 / 0.4	0.968	0.645
	$\Gamma_{(6,2)}$: Stochastic / 0.2 / 0	0.973	0.633
Pareto 7	$\Gamma_{(7,1)}$: Stochastic / 0.0 / 0.8	0.959	0.859
	$\Gamma_{(7,2)}$: Stochastic / 0.2 / 0	0.963	0.836
	$\Gamma_{(7,3)}$: Stochastic / 0.2 / 0.4	0.969	0.816
	$\Gamma_{(7,4)}$: Stochastic / 0.2 / 0.6	0.962	0.855
	$\Gamma_{(7,5)}$: Stochastic / 0.4 / 0.2	0.978	0.769
Pareto 8	$\Gamma_{(8,1)}$: Stochastic / 0.0 / 0.2	0.958	0.850
	$\Gamma_{(8,2)}$: Stochastic / 0.2 / 0	0.966	0.797
	$\Gamma_{(8,3)}$: Stochastic / 0.4 / 0	0.961	0.834

- Descriptor 4 - Average SD of all points: Average value of the x-axis points belonging to each alternative.
- Descriptor 5 - Average SD of Pareto points: Average value of the x-axis Pareto points belonging to each alternative.
- Descriptor 6 - Median SD of all points: Median of the x-axis points belonging to each alternative.
- Descriptor 7 - Number of points in the global Pareto: When all points of the

Table 3.8: Descriptors (Desc.) and assessment of each alternative.

Alt.	Desc. 1	Desc. 2	Desc. 3	Desc. 4	Desc. 5	Desc. 6	Desc. 7	Desc. 8	Desc. 9
1	0.994	0.948	0.985	**0.8355**	0.697	0.817	**4**	No	No
2	0.995	0.956	0.985	0.8426	0.688	**0.810**	0	No	No
3	0.986	0.947	0.976	0.870	0.695	0.834	3	No	**Yes**
4	**0.982**	**0.945**	**0.972**	0.890	0.719	0.855	**4**	**Yes**	No
5	1.029	0.984	1.012	0.946	0.865	0.928	0	No	No
6	1.025	0.970	1.012	0.925	**0.639**	0.934	0	No	No
7	0.997	0.966	0.980	0.902	0.827	0.874	0	No	No
8	0.991	0.962	0.979	0.913	0.827	0.904	0	No	No

performance of each alternative are combined, the number of points present in the global Pareto from each alternative.

- Descriptor 8 - Best Cost: Identifies if the alternative was able to find the best global cost.
- Descriptor 9 - Best SD: Identifies if the alternative was able to find the best global SD.

Table 3.8 shows the results of the descriptors calculated for each individual alternative. The results show that alternative 4 tends to perform better than the rest for the cost-related descriptors. In addition, this alternative presents 4 points in the final global Pareto front after combining all of the alternatives. Moreover, only one descriptor associated with hybrid approaches performs better, which is the case for alternative 6.

When we analyse the results in table 3.8 from the perspective of the proposed modifications to the model, i.e. complete ARO or hybrid ARO, separated or unified budget, Γ or Γ^2, the following results are obtained. Complete ARO schemes are present in 8/9 of the best ranked descriptors' values. In addition, separate alternatives are present in 7/9 of the best values obtained for the descriptors. Finally, Γ^2 modifications participate in 6/9 best values. Additionally, as mentioned before, better convergence capabilities in the performance evaluation are shown by option Γ^2. The results demonstrate the tendency of advantage when using complete ARO schemes versus hybrid, show that separate formulations perform better than unified approaches, and that Γ^2 outperforms Γ. These three performing features identified are all present together in alternative 4, which is in fact the most interesting alternative from the perspective of cost-related descriptors.

If the information contained in Pareto 4 and 8 are analysed, the different solutions obtained for alternatives 4 and 8 can be detailed. Figure 3.23 shows this information. It can be seen that the dominant points from the standpoint of average cost and SD are associated with the ARO formulation (blue dots). Although some solutions for the HSR approach (red crosses) outperform the deterministic solution and some ARO solutions, alternative 4 always features better solutions.

Figure 3.25 shows the eight obtained Pareto fronts combined in the same axis. This figure allows to visualize the descriptor "Global Pareto", which helps to determine the best global solutions from cost and SD standpoints. For instance, the best

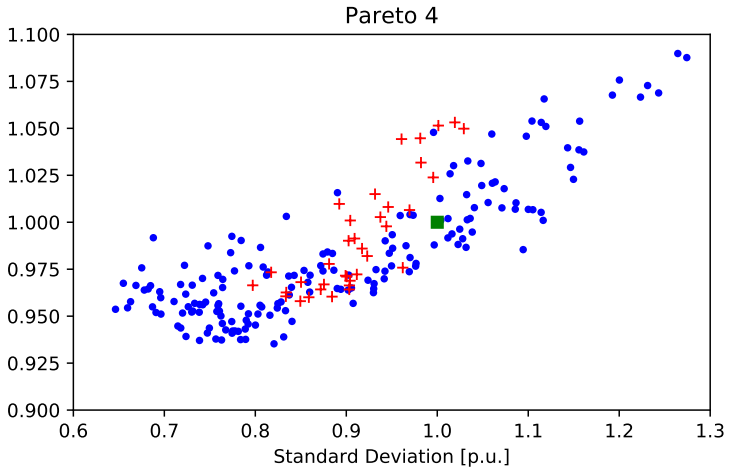


Figure 3.23: Performance points for alternative 4 (blue dots) and alternative 8 (red crosses). Deterministic solution in green square.

trade-off set of solutions is formed by 11 points, four belonging to alternative 1 (blue circles), three to alternative 3 (green X) and four to alternative 4 (red stars). These 11 solutions contain the best combinations of both measured quantities after the performance evaluation. The remaining points represent dominated solutions, i.e. one can always find at least one point among the 11 trade-off solutions, that is better in both objectives at the same time. It can also be visualized that hybrid solutions (alternatives 5-8) tend to be less attractive when compared to robust approaches.

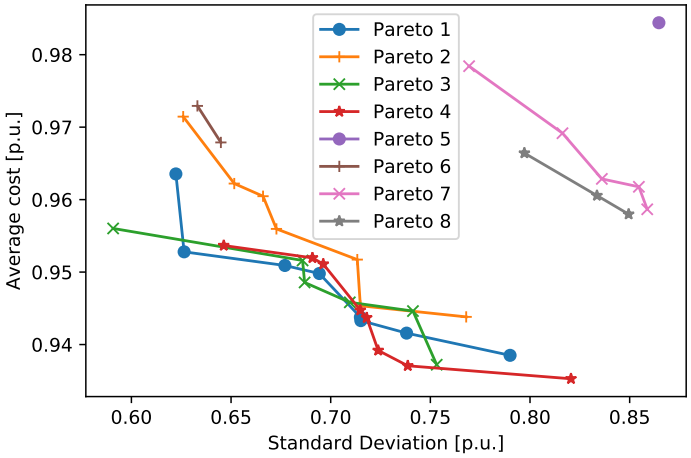


Figure 3.24: Comparison of all Pareto points.

Figure 3.25 presents the boxplots of computational times for the eight alternatives presented in the previous subsection. In general, Alternatives 1–4 presented higher dispersion of data in several cases with computational times ranging from 1–3 min. These solutions are related to the combinations of robust parameters mainly for Γ^{DA} different from zero. Hybrid stochastic/robust (Alternatives 5–8) solutions had

more consistent computational times even if the median was in some cases higher than those obtained for complete ARO cases (Alternatives 1–4). Due to the combinations of control parameters, 180 robust optimization problems had to be solved for Alternatives 1–4, and 36 hybrid problems had to be solved for Alternatives 5–8, leading to more intensive overall times for complete robust approaches.

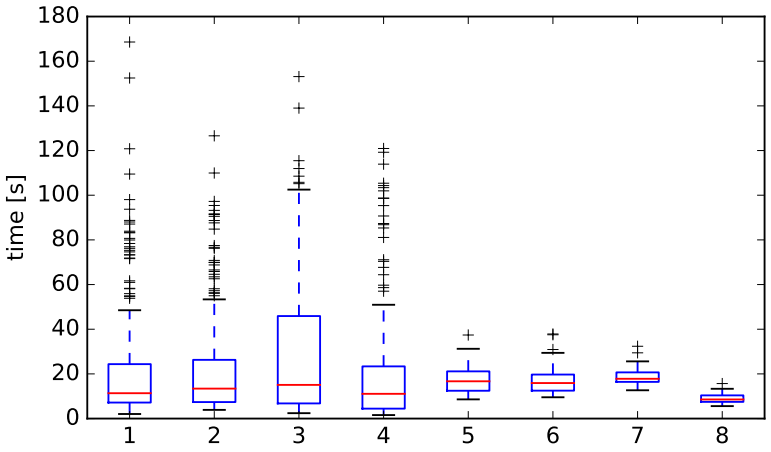


Figure 3.25: Computational time boxplots for each optimization alternative. Each datum corresponds to the optimization time for a given combination of control parameters.

Table 3.9 shows a summary of different obtained values for each alternative.

Higher overall times for Alternatives 1–4 are explained by the fact that more individual optimization problems had to be solved to cope with the combinations of budgets of uncertainty. Moreover, lower median values were obtained for complete robust alternatives. However, average times were higher when compared to hybrid schemes. This is explained by the presence of high-value outliers for Alternatives 1–4. Although the hybrid schemes had more attractive overall computational times, the quality of the solutions obtained remained a drawback when compared to complete robust approaches, as explained in detail in the previous subsection.

Table 3.9: Details of computational time for each alternative.

Alternative	**1**	**2**	**3**	**4**	**5**	**6**	**7**	**8**
Overall computational time (s)	4274	4323	5717	4004	631	631	686	321
Median (s)	11	13	15	11	16	15	17	8
Average (s)	23	24	31	22	17	17	19	9

3.6 Conclusions

Three sources of uncertainty were included in the optimization model for simulations: energy prices, electrical load, thermal load and PV production.

Regarding two-stage quantile-based stochastic approach The decomposition logic is applied to a two-stage approach in which PV and demand scenarios are created by combining extreme scenarios based on quantile forecasts. This formulation is assessed by using the Values of Stochastic Solution (VSS) as a measure of performance. For the analyzed cases, the VSS shows better performance that the deterministic case.

The two-stage stochastic approach, shows the importance of taking into account uncertainties arising from PV and load, in order to avoid higher expected operation costs in comparison to deterministic approaches. In our case, the benefit of using a stochastic approach is demonstrated by means of the VSS. The average monthly reduction in operation cost measured by the VSS is 5.8%, and the interval of reduction ranges from 3.6% to 9.0%. These results show that considering a stochastic model with battery cycling leads to savings when compared to deterministic approaches.

The computational times for larger test systems remain adequate for day-ahead decision-making. The characteristic of the aggregated virtual battery by means of the SDA, makes that the increase of batteries in the test system does not impact proportionally time effort even in the case of stochastic approaches. However, given that the structure proposed in the literature to evaluate stochastic solutions (VSS) is based on the universe of scenarios created, the defined second stage variables (imbalances, devices's settings) and their performance, are evaluated (and valid) only for the combined proposed scenarios.

Regarding robust apporaches For the case of uncertainty in price, two approaches were considered: stochastic programming and robust optimization. For uncertainty handling in load and PV production, robust optimization was considered.

The model shows that including the explicit degradation cost into the optimization model leads to cost savings due to less cycling of the battery. In the concrete case of the presented results, a 34.07% reduction was achieved.

The proposed approach, which can also be applied by aggregators of medium and large size equipment, shows that by using ARO for load and PV, and analyzing interactions of robust parameters, different levels of cost reduction versus the deterministic approach can be achieved. For the performed simulations, up to 5.7% cost savings were obtained. For the case of SD, the best result reduced in 36.4% the performance of the deterministic solution. This shows that not only expected costs can be reduced but also lower risk is associated with decision-making under this approach. The results prove that using ARO, also increases the probability of having lower expected costs. When compared to the deterministic scheme, probabilities of up to 96.33% are obtained by analyzing CDFs.

In addition, the robust optimization approach shows better performance than deterministic solution despite the net load confidence intervals, measured by means of the MI.

For the case of HSR, price scenarios were created by using KDE. A backward reduction technique based on Kantorovich Distance is used to obtain a reduced set of scenarios. For the run simulations, The hybrid approach shows to have better performance than the deterministic approach and some of the ARO solutions. However, there are ARO solutions that present better performance than the HSR from

both the average cost and SD standpoints.

In particular, alternative 4: separated complete ARO with Γ^2 presents better performance that the rest of alternatives in several of the measured descriptors. In also presents the lower average operational cost from all run simulations. In this case, separate treatment of uncertainty for load and PV allows finding a dual equivalent (robust counterpart) and hence two separate robust parameters to adjust and achieve lower costs and SDs.

Chapter 4

Aggregation of flexibility for participation in multiple markets

This chapter presents the mathematical model for robust bidding in energy markets and local flexibility markets. At first, an hybrid stochastic/robust approach is presented to analyze changes in net exchanged energy power at the point of common coupling. Afterwards, a complete robust framework is presented to bid in both energy and local markets. The models are preceded by a detailed literature review on home level aggregation for the provision of services.

The models and results presented in this chapter led to publications [CF-3,CF-5,CF-8].

4.1 Literature review

4.1.1 Traditional grid scale approach

Several research has addressed the problem of provision of ancillary service through the use of grid scale ESS. For example, the analysis presented in [113] gives an insight on the possibilities of ESS for the provision of different services. Authors claim that only considering storage for arbitrage leads to underuse and limited exploitation of the resources. This case shows how ESS can be used for energy (day-ahead and real time) and ancillary services (regulation), and the sources of revenue come from the effective payment due to the participation in these markets. The model returns the amount of energy to be offered in the regulation market, as well as the energy that should be exchanged in DA and RT markets. It is shown that revenue is increased but the authors also point the importance of exploring the provision of other grid functions. Inclusion of uncertainties of different nature is an identified opportunity of improvement for this work.

Following this research line, [114], presents a methodology for spinning reserve and frequency regulation, in which multiple grid ESS are considered, while system reliability is evaluated. Authors in [115] also analyse the benefits of using ESS to provide ancillary services in the context of the Nordic Power Market. In concrete, provision of services such as reactive power, reserve, regulation and restoration is

analysed. In general, frequency regulation services show to be an important part of the revenue in wholesale power markets, as demonstrated in [116].

4.1.2 Provision of services in the presence of RES

Inclusion of RES calls for special attention regarding provision of services in this new context and tackle the inherent fluctuations. A framework for provision of ancillary services is presented in [117]. The analysis include day-ahead and real-time unit commitment, economic dispatch and frequency support. The control scheme is able to respond to different time scales and to control signals corresponding to AGC and Primary Frequency Control (PFC). Authors show that the control strategy allows to bid and provide primary and secondary frequency response and that the inclusion of the BESS allows a wind power plant to effectively commit to the DA market while achieving better performance.

A comparison of different storage technologies for regulation services is presented in [118]. The analysis includes flywheels, superconductive magnetic energy storage; pumped hydrostorage, compressed air energy storage (CAES), super capacitors, electrochemical battery types and demand-side control. Different aspects to provide fast regulation services were analyzed, such as power output change, ramping rates, life time, costs, among others.

An optimal ESS sitting and sizing problem is developed in [119] to reduce system cost with consideration of energy and reserve markets. The mathematical formulation consists on an upper level problem that returns ESS investment decisions and a lower level that minimizes operation costs. One interesting feature of this study is the fact that the methodology is tested on the 240-bus Western Electricity Coordinating Council real life power system and also considers two types of storage technologies: CAES and li-ion BESS. Although CAES results in lower total system costs, the authors warn that this technology is still at the pilot stage.

Reference [120] also presents a model for including ESS in energy and reserve markets in systems with wind penetration. A particularity of this work is the fact that it is assumed that the ESS is owned by an independent actor, and considers that the market treats this ESS as any other energy and reserve resource present in the system. The bidding scheme allows the independent ESS maximize its profit in spite of wind farm penetration into the grid. This is achieved by scheduling the ESS in the DA and hour-ahead markets by means of stochastic programming.

Paper [121] presents a method for handling imbalances due to increasing wind penetration. It considers ESS and conventional generation. The mathematical model includes spinning reserve and minimizes fuel costs for a power system containing an open cycle gas turbine and wind generation. Other research has also addressed the importance of ESS to offset power imbalance due to wind production [122, 123].

Authors in [124] present a coordinnated dispatch model to reduce the impacts of wind power fluctuations. The scheme determines the power capacity of the BESS and improves wind dispatchability even in the case of wind forecast error, finding that not only imbalances can be mitigated but also BESS lifetime can be extended. ESS services with reneable integration can also include peak absorbing, valley supression and charging/discharging during fast ramping [125, 126].

4.1.3 Home/building aggregation for flexibility services

Besides optimal management of building resources, it is interesting to determine the impacts that the resource management at this level have on the system. Locally, the building/home resources should not jeopardize grid constraints and could also provide local services to DSO. The flexibility can also be used to participate in the wholesale market to offer different types of services and increase revenue.

In order to provide frequency regulation services, the authors of [127] aggregate commercial buildings to determine the robust bids while achieving minimum operation costs by adjusting HVAC systems. Although storage is not considered in this research, the proposed framework gives an insight on the potential of buildings to offer secondary frequency services while maintaining occupant comfort under perfect predictions of weather and occupancy, which means that uncertainties in this study are not present. MPC is used here to determine HVAC setting each 30 minutes, and the feedback control readjusts settings in real time. The authors developed an improved version of this paper in [128] by including a combination of robust and stochastic optimization. In the same line of frequency regulation services, [129] proposed thermodynamic storage in commercial buildings to adjust power consumption in the intra-day market based on the Swiss regulatory framework.

Another work that considers participation in regulating and day ahead market is developed by Kilkki et al. in [130]. An electricity aggregator is the proposed actor for taking decisions on customers' storage, while minimizing costs of purchasing energy from the spot market, and scheduling flexibility to maximize profit from the reserve market, by using a weighted sum multi-objective method. An interesting remark of this model consists on the scaled simulation for 5000 households. However, potential improvements are inclusion of uncertainty and extension to other ESS devices, given that the authors only consider electric storage space heating.

A methodology for minimizing data sharing between a building aggregator and a DSO is presented in [131]. One interesting remark of this proposal is that DSO does not need to deal with demand uncertainty, and that task is left to the aggregator to locally offset imbalances. The method deals with congestion alleviation in the distribution network by means of the flexibility provided by buildings, provided by an HVAC fan based system. Distribution locational marginal prices (DLMP) are calculated by means of robust optimization theory, in which the uncertainty set is formed by solar irradiation, electronic device disturbances and building occupancy. After this, another calculation for DLMP is performed in real time in order to reduce the conservatism of the robust optimization step. In addition, authors use a dual decomposition approach to minimize the need for data sharing between the actors. The authors also recommend that future studies should take into account market mechanisms and coordination between TSO and DSO and faster power flow methods for improving computational times. Although this paper has a thorough mathematical background, it should be noted that the service provided by the building aggregation is only circumscribed to congestion alleviation by power flow constraints, which leads to think that more complex flexibility products and services could be an improvement of the proposed model. Another potential improvement is the inclusion of other storage technologies to increase the flexibility capabilities of the building aggregator.

A deterministic model for medium and large consumers aggregation is presented in [132]. This model attempts to minimize the total energy cost for a portfolio of energy consumers. In this deterministic scheme, the aggregator participates in the wholesale energy market to purchase energy and also in the reserve market to offer capacity services. The authors aggregate 9 medium size commercial consumers and the flexibility is associated to heating loads, oil/gas substitution, air conditioning, lighting; in addition, the aggregator manages a lead-acid ESS which is another source of flexibility. This is an interesting and straightforward model, however, an important drawback is the lack of uncertainty in the optimization, which is a potential improvement for a study of similar characteristics.

Other research has also attempted to calculate the available flexibility given by home aggregation. For example, in [133] a generic battery model is used to represent thermostatically controlled loads (TCL) as providers of regulation service provision; in [134], residential aggregation of thermal energy storage is carried out in the Californian system to provide ancillary services showing potential earning for loads participating in this market; authors in [135] also use demand side flexibility provided by TCL to participate in the Portuguese tertiary DA reserve market; in [136] reserve services are offered by using flexibility coming from domestic thermal loads.

When it comes to the aggregation of multiple customers, there is still a lack of detail in the modelling of available flexibility options that could appear in this context. For example, the previous literature, although it presents a thorough insight on the possibilities of services to be provided, doesn't account for inclusion of multi-energy systems (MES), which are an opportunity to increase the flexibility options in home/building levels [4, 137]. MES include other devices such as CHP plants, heat pumps, boilers, heat storage, etc., and the coordination possibilities with active demand, ESS and RES become an interesting opportunity not only to minimize operation costs, but also to offer local and energy/reserve services by reaching minimum bid quantities. This integration for the provision of flexibility services does not appear to be yet very explored in the specialized literature. In addition, the interaction of smart homes/building with the local grid must also be taken into account as another possibility of revenue, even if market rules for these exchanges are not widely develop.

4.1.4 Local flexibility of prosumers and decentralized storage

Given that prosumers are physically connected to the distribution grid, market environment and products must be geographically defined to allow local trading [5]. In addition, communication and coordination of DSO and new local energy agents is necessary to avoid upstream operative problems.

Research that articulates local flexibility and prosumers has emerged in recent years. One common practice is to directly include local flexibility scheduling in distribution power flow calculations to solve voltage and congestion issues [39–43]. This approach assumes that the DSO and aggregator form a unique entity and decisions about flexibility exploitation are driven by grid state analysis through power flows. However, these schemes might not be applicable in all real-life cases, due to the inherent separation of agents' activities, ownership of the resources connected to

the grid and privacy-related constraints. For instance, the authors in [131] discuss about these privacy issues for solving the problem of locational marginal pricing of building aggregators for alleviating grid congestion problems.

In contrast with the reference above, [44] presents an optimization model that receives external signals from the DSO and schedules resources to provide the required flexibility service. This service is provided in the form of upward or downward regulation with respect to a baseline scenario. Moreover, it proposes a local market platform in which energy cooperatives and prosumers offer flexibility and DSO purchases this product.

Authors in [45] present a mathematical optimization model to analyze the participation of an energy community controlled by an aggregator, in wholesale and local markets. This work is centered on the market modelling and clearing process in a transactive environment in which multiple aggregators interact among themselves and the wholesale market. However, in this paper, local market prices are assumed as a percentage of wholesale energy prices.

The research presented in [46] analyzes a microgrid that schedules devices taking into account distribution net ramping into the model. These constraints act as a service required by the utility. In addition, this study integrates inter-hour and intra-hour interactions, grid connected and islanded operation, however, disregards uncertainty and considers resources and load from a broad perspective without detailing building or home level integration. Other studies have also addressed the importance of managing ramping at the distribution level by smoothing net exchanges [17, 47]. In the case of [17] ramping capabilities are not traded locally but in traditional wholesale and ancillary markets.

Reference [48] proposes a local energy system in which an aggregator acts as an intermediate of multi-energy resources and the wholesale market. Although the aggregation is local, the market interaction is only with the wholesale market, and supposes that local flexibility is traded in this centralized market. Similarly [15, 49], propose bidding schemes in traditional wholesale markets.

When it comes to residential/building aggregation with storage technologies, MPC and/or SO are typically used to include uncertainty. For instance, stochastic optimization and chance constrained methods are used in [28] for energy and reserve market participation by aggregating residential batteries and heating. This work presents inclusion of uncertainty in prices, weather and realized frequency. MPC based models for aggregation of distributed storage devices (at DSO level) is presented in [101] to provide local and frequency services; and MPC is also used in [102] for the case of regulation services by aggregation of industrial thermal loads.

Although most efforts to model uncertainties with robust optimization have been directed at large power systems applications, some work related to medium size DG/microgrids has begun to be published, as developed with more level of detail in subsection 3.1.1. For instance, [17] presents a model for strategic bidding in energy and ancillary markets for a microgrid consisting on RES, a microturbine and a battery, in which RO is used to include RES uncertainty and SO is used to tackle price uncertainty. For bidding purposes in day-ahead and real-time markets, reference [15] proposes a hybrid stochastic/robust approach, in which RO captures uncertainty in real time prices, while stochastic optimization is used to include wind and PV scenarios. Both approaches ([15, 17]) assume deterministic demand.

References [22,26] also include robust participation in multiple markets, specifically in energy and ancillary markets.

Robust models for home-level aggregation are still very scarce in the literature. Some proposals aim to minimize electricity bills [23], while others propose real-time decision-making for batteries [24] or the management of thermal storage systems [25].

In contrast with [15, 17, 22, 26, 28, 29, 48, 49, 101], and in line with [44–46], this thesis proposes a bidding strategy that establishes a difference between wholesale and local energy markets for flexibility bidding purposes; considering that local flexibility markets (LFM) constitute an independent trading space/platform with specific bidding rules, following the recommendations of [5, 7, 138]. Unlike [44], which presents a thorough model for DG participation in LFM, this thesis presents a bidding strategy that takes into account uncertainty of multiple sources and includes bidding in the traditional wholesale market, in addition to the local market. This chapter shows a model from the stand-point of a residential aggregator, unlike [45], which solves the problem from the market operator perspective in a transactive environment. In addition, the approach presented here differs from [46], in that: 1) we include uncertainty effects, storage systems, 2) we solve the problem from the perspective of residential storage aggregation and not from an MV-level DG standpoint, and 3) in the sense that we include a local flexibility trading strategy, in addition to the local constraint support. The latter being a valuable contribution of the authors in the mentioned reference. Finally, in contrast to [39–43] we do not consider power flow calculations to be part of the flexibility aggregator's tasks.

This chapter aims to fill an existing gap in the literature, related to bidding strategies of smart-home aggregators for coordinated participation in both wholesale energy markets and emerging local flexibility markets, also considering uncertainties in prices, PV production and demand. To the author's knowledge, these combined aspects have never been addressed holistically from the standpoint of an aggregator that controls residential flexibilities, in this case, provided by PV panels and thermal and electro-chemical storage.

4.2 A first hybrid approach: impacts of local flexibility provision in day-ahead scheduling

To demonstrate the impacts of local flexibility provision on the aggregation of resources and the day-ahead committed energy, a simplified model neglecting battery cycling will be used at first. This model uses a scenario-based modelling of prices and robust optimization for PV and demand uncertainty.

The flexibility aggregator participates in the day-ahead and imbalance markets to optimize its portfolio, while complying with physical microgrid limitations and the signals sent from the local DSO regarding flexibility products for load management. Bidirectional power flows can occur at the PCC with the local DSO grid. The DSO flexibility requirements in the PCC are of two types: a) power flexibility, which imposes limits or certain power exchange patterns according to grid needs at specific times; b) ramping flexibility, which limits the net load ramping seen by the local DSO (see upper part of figure 4.1).

The DSO and the aggregator establish communication to send/receive informa-

tion, while only the aggregator has communication and control capabilities with devices at home level. It is supposed the existence of the necessary IT and communication platform, so that the aggregator controls devices at the home level and decides over their set-points.

Decisions regarding DSO flexibility requirements and products at the PCC correspond to grid analysis concerning voltage limits, congestion management, equipment degradation, and scheduled maintenance, among others. The definition of these requirements and the market design of the payment of this service are out of the scope of this thesis.

4.2.1 Mathematical model

The proposed hybrid stochastic/robust optimization model minimizes the DA expected operation cost, in which the cost is associated with the day-ahead net exchange (P_t^E) expected costs and the import/exports ($I_{t,s}^-/I_{t,e}^+$) imbalance as expressed in equation (4.1), where subscripts t, e and h index time step, scenario and household, respectively. Parameters $\pi_{t,e}$, $\mu_{t,e}^-$, -$\mu_{t,e}^+$, represent respectively spot price, negative imbalance cost, and positive imbalance cost. In addition, p_e is the probability of scenario e.

$$\text{minimize} \sum_{e=1}^{ES} p_e \left\{ \sum_{t=1}^{T} \left[\pi_{t,e} P_t^E + \mu_{t,e}^- I_{t,e}^- - \mu_{t,e}^+ I_{t,e}^+ \right] \right\} \tag{4.1}$$

Next, the operational constraints describe the behavior of the devices and balance the load of the proposed system. Constraint (4.2) represents the power balance and includes the robust counterpart for including electrical demand and PV uncertainty in terms of net load (demand minus PV). This constraint includes the robust parameter Γ_t^D for controlling conservatism of net demand uncertainty. Constraints (4.3)-(4.4) are additional constraints of the robust counterpart that result from strong duality theorem.

$$\begin{gathered} P_t^E + I_{t,e}^- - I_{t,e}^+ + \Delta t \sum_{h=1}^{N} P_{t,h}^d - P_{t,h}^c - H_{t,h} = \\ D_t^{net} + q_t^D + \Gamma_t^D z_t^D, \forall t, \forall e \end{gathered} \tag{4.2}$$

$$z_t^D + q_t^D \geq \frac{1}{2}(\bar{D}_t^{net} - \underline{D}_h^{net}) y_t^D, \forall t \tag{4.3}$$

$$z_t^D, q_t^D \geq 0, y_t^D \geq 1, \forall t \tag{4.4}$$

Constraints (4.5) and (4.10) describe the energy state for batteries and the TES, respectively, and $X_{t,h}$, $Y_{t,h}$ represent the stored energy of these devices. Constraints (4.10)-(4.12) are the resulting robust counterpart of considering uncertainty in thermal load, with Γ_t^{th} controlling thermal load conservatism.

$$X_{t,h} = X_{t-1,h} + \eta^c P_{t-1,h}^c - P_{t-1,h}^d / \eta^d, \forall t, t \neq 1, \forall h \tag{4.5}$$

$$X_{1,h} = X_{T,h}, \forall h \tag{4.6}$$

$$0 \leq P_{t,h}^c \leq \bar{P}_h^c \cdot u_{t,h}, u_{t,h} \in \{0,1\}, \forall t, t \neq 1, \forall h \tag{4.7}$$

$$0 \leq P^d_{t,h} \leq \bar{P}^d_h \cdot (1 - u_{t,h}), \forall t, \forall h \tag{4.8}$$

$$\underline{X}_h \leq X_{t,h} \leq \bar{X}_h, \forall t, \forall h \tag{4.9}$$

$$\begin{aligned} Y_{t,h} = Y_{t-1,h} + \Delta t H_{t-1,h} - Y_{t-1,h}/R_h C_h - \\ \Delta t(\hat{Q}_{t-1,h} + q^{th}_{t-1,h} + \Gamma^{th}_{t-1,h} z^{th}_{t-1,h}), \forall t, \forall h \end{aligned} \tag{4.10}$$

$$z^{th}_{t,h} + q^{th}_{t,h} \geq \frac{1}{2}(Q^{90\%}_{t,h} - Q^{10\%}_{t,h}) y^{th}_{t,h}, \forall t, \forall h \tag{4.11}$$

$$z^{th}_{t,h}, q^{th}_{t,h} \geq 0, y^{th}_{t,h} \geq 1, \forall t, \forall h \tag{4.12}$$

$$Y_{1,h} = Y_{T,h}, \forall h \tag{4.13}$$

$$\underline{Y}_{t,h} \leq Y_{t,h} \leq \bar{Y}_{t,h}, \forall t, \forall h \tag{4.14}$$

$$0 \leq H_{t,h} \leq \bar{H}_{t,h}, \forall t, \forall h \tag{4.15}$$

The grid flexibility constraints describe the requirements or signals sent by the utility grid, in terms of net ramping (R_t) and net allowed power exchanges. Constraints (4.16)-(4.19) model the ramping flexibility, which represents the maximum allowed net power change in consecutive time steps. Constraint (4.16) ensures that the day-ahead commitment respects maximum ramping, and in the same way, constraint (4.18) also includes negative and positive imbalance exchanges in each scenario. Constraints (4.17), (4.19) ensure continuity between the last and first time steps of the operation day. Constraints (4.20)-(4.21) model the maximum allowed power flexibility. Parameters $P^{PCC_{min}}_t / P^{PCC_{max}}_t$ are the min/max net power in the PCC.

These last two constraints are general enough to represent any DSO signal in terms of net power exchange, as shown in figure 4.1 (powercap, power requirement, load trajectory).

$$|P^E_t - P^E_{t-1}| \leq R_t, \forall t, t \neq 1 \tag{4.16}$$

$$|P^E_1 - P^E_T| \leq R_t \tag{4.17}$$

$$|P^E_t + I^-_{t,e} - I^+_{t,e} - (P^E_{t-1} + I^-_{t-1,e} - I^+_{t-1,e})| \leq R_t, \forall t, t \neq 1, \forall e \tag{4.18}$$

$$|P^E_1 + I^-_{1,e} - I^+_{1,e} - (P^E_T + I^-_{T,e} - I^+_{T,e})| \leq R_t, \forall e \tag{4.19}$$

$$P^{PCC_{min}}_t \leq P^E_t \leq P^{PCC_{max}}_t, \forall t \tag{4.20}$$

$$P^{PCC_{min}}_t \leq P^E_t + I^-_{t,e} - I^+_{t,e} \leq P^{PCC_{max}}_t, \forall t, \forall e \tag{4.21}$$

The previous model is the complete hybrid stochastic/robust problem. When only one scenario for price is considered and $\Gamma^D_t = \Gamma^{th}_t = 0$, the model is the deterministic equivalent.

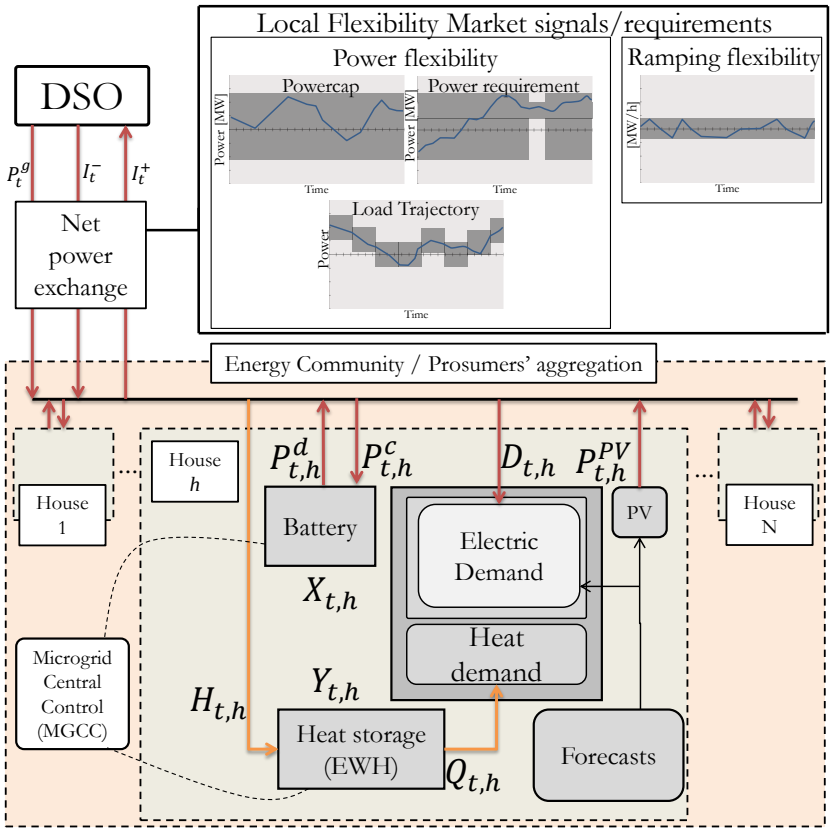


Figure 4.1: Schematic diagram of the proposed framework

4.2.2 Results for the Hybrid stochastic/robust model with DSO flexibility requirements

The hybrid stochastic-robust optimization model described in (4.1)-(4.21) is considering all flexibilities provided by the microgrid and also including different values for grid flexibility requirements ($P_t^{PCC_{max}}$ and R_t). When DSO flexibility requirements are present in the model, the energy committed and the devices' scheduling must adjust to comply with maximum net power and ramping constraints. In this hybrid case, the operation cost without considering flexibility constraints is €24.92 (unconstrained case). Table 4.1 shows the costs obtained for different combinations of $P_t^{PCC_{max}}$ and R_t. For instance, when ramping is limited to 0.01 MW/h and maximum power to 0.03 MW, the operation cost of the aggregator is €25.49, which represents a 2.3% increase with respect to the unconstrained case. This means that if the DSO sends this signal, the HEMS aggregator would have to adjust its settings and incur extra costs to satisfy the DSO's needs.

The different operation points lead to different committed energy on the day-ahead market. For example, if R_t is kept constant at 0.03 MW/h and $P_t^{PCC_{max}}$ assumes different values, the energy that should be exchanged in the wholesale market is shown in figure 4.2. While the changes in the operation cost range between €24.97 and €25.40, the changes in committed energy are more evident so as to comply with the different values of maximum power.

Table 4.1: Operation costs for different values of flexibility requirements

R_t	$P_t^{PCC_{max}}$ 0.03 MW	0.05 MW	0.07 MW
0.01 MW/h	25.49	25.20	25.20
0.03 MW/h	25.40	24.99	24.97
0.06 MW/h	25.39	24.98	24.94

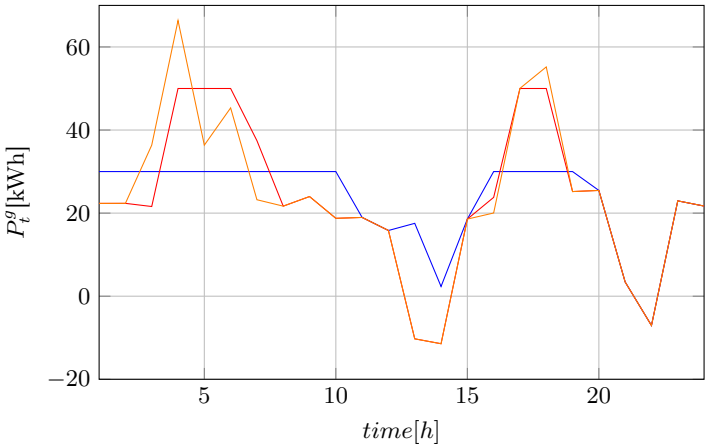


Figure 4.2: Day-ahead committed energy for $P_t^{PCC_{max}} = 0.03$ MW (——), $P_t^{PCC_{max}} = 0.05$ MW (——), $P_t^{PCC_{max}} = 0.07$ MW (——) when constant $R_t = 0.03$ MW/h

The day-ahead energy commitment for different allowed ramping values and fixed $P_t^{PCC_{max}} = 0.05MW$ is shown in figure 4.3. In this case, it can be seen that peaks are shaved at the level of 50 kW, and that $R_t = 0.06MW$ (—●—) allows more unconstrained ramping, as is the case for time frames 13h-14h-15h and 21h-22h-23h. In general, each case leads to a different operation point and the operation cost ranges from €24.98 to €25.20. It can be seen that operational costs for the flexibility aggregator increase when flexibility needs from utilities narrow their margins, which in turn signals the remuneration that an aggregator should receive for providing flexibility services to the grid.

In addition, the signals from the utility force a reshaping of the net load at the PCC, hence leading to an adjustment of the devices' settings.

4.2.3 A first proposal for bidding in the local market

Demand bidding curves

Figure 4.4 shows the demand bidding curves for two different hours. These piecewise curves show the hourly bids made by the aggregator for economical operation when only wholesale market participation is allowed and no other local flexibility market exists. The curves are built using the hybrid stochastic/robust approach by varying the day-ahead energy price at the specific hour. The variations range from the 10% to the 90% percentile of the price predicted by the KDE. It is important to note that bids for hour 21 have higher associated prices given the history of prices

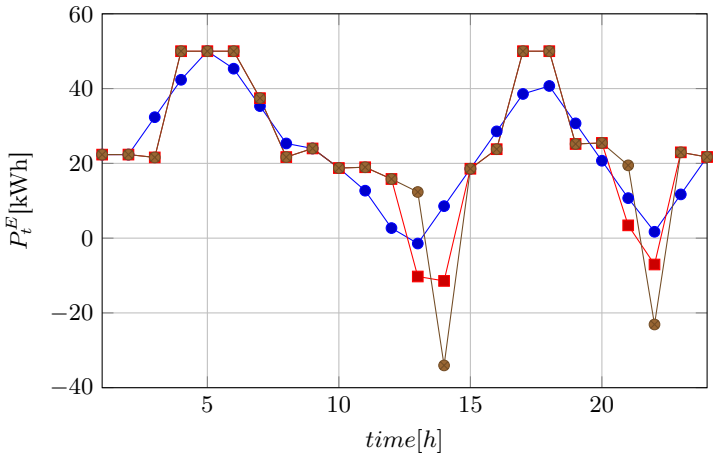


Figure 4.3: Day-ahead committed energy for $R_t = 0.01$ MW/h (—●—), $R_t = 0.03$ MW/h (—■—), $R_t = 0.06$ MW/h (—●—) when constant $P_t^{PCC_{max}} = 0.05$ MW

for these night-time frames.

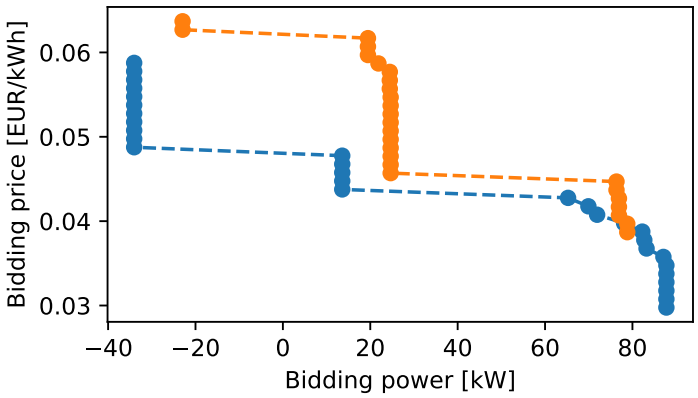


Figure 4.4: Demand bidding curves for t = 14h (green), t = 21h (orange)

Local flexibility supplying curves

If a local market is established to define the appropriate flexibility prices to be provided by the aggregator at the PCC, then the construction of supplying bidding curves could give an idea of the appropriate remuneration that the aggregator should receive for modifying the net power exchange coming from a DSO signal. This option is shown in figure 4.5. These curves measure the extra cost of the aggregator's operation when deviating from the committed day-ahead energy. Hence, this price is the minimum that should be paid to the aggregator if the DSO requires flexibility.

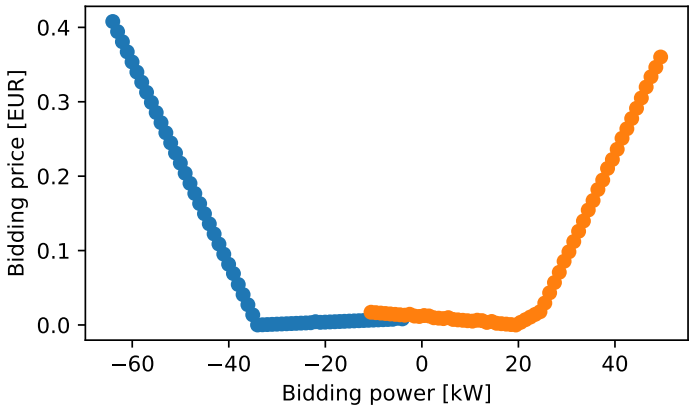


Figure 4.5: flexibility supply bidding curves for t = 14h (green), t = 21h (orange)

4.3 Complete robust framework for local flexibility provision

4.3.1 Description of the aggregators' interactions

The present approach proposes a bidding strategy for an aggregator of smart-homes, which are present in an energy community that is connected to the main distribution grid. Some of the households have solar panels, li-ion batteries and heat storage devices. This strategy is composed by interactions of the aggregator with three entities: wholesale market, DSO and local flexibility market. The interaction with the wholesale market is established in a traditional manner, in which the aggregator commits certain amount of energy in the day-ahead market, and during the operation day, deviations are settled in the form of negative and positive imbalances.

The interaction with the DSO, as previously explained for the hybrid case, is given in terms of operational constraint support at the PCC. In concrete, two types of constraints/products that might be activated by the DSO, if needed, are considered in this work: 1) ramping constraints (R_t [MW/h]) and 2) Power-Max, in which the aggregator ensures that its local portfolio will not exceed $P_t^{PCC_{max}}$ [kW]. Ramping products are motivated by the need to offset variability of the increasing renewable penetration in distribution grids; and Power-Max allows peak modulation to control overloads or to promote investment deferral [139, 140]. Given the difficulty of creating a tuple to describe the temporality/quantity of these products so they can fit into traditional auction architectures, bilateral contracts are considered between the two agents [138, 139] to remunerate the service. Gaming opportunities are reduced for the aggregator provided that highly-priced offers won't be attractive for the DSO and standard grid-control actions might be preferred. Also because artificial/forced congestion will lead the aggregator to sub-optimal scheduling and bidding plans.

The aggregator and the Local Market Operator (LMO) interact in such a way that when flexibility is needed by the DSO (or other third party. i.e. BRP), the LMO communicates with the aggregator in order to request a flexibility bid. If the

flexibility is awarded to the aggregator, it will receive the bid price (pay-as-bid) for providing the service, as it is commonly used for ancillary and service markets [5], and also to avoid price increase of the local flexibility services. The specifics of the market design concept and architecture, the flexibility clearing algorithm, which is a task performed by the LMO, are not part of this thesis's scope and objectives.

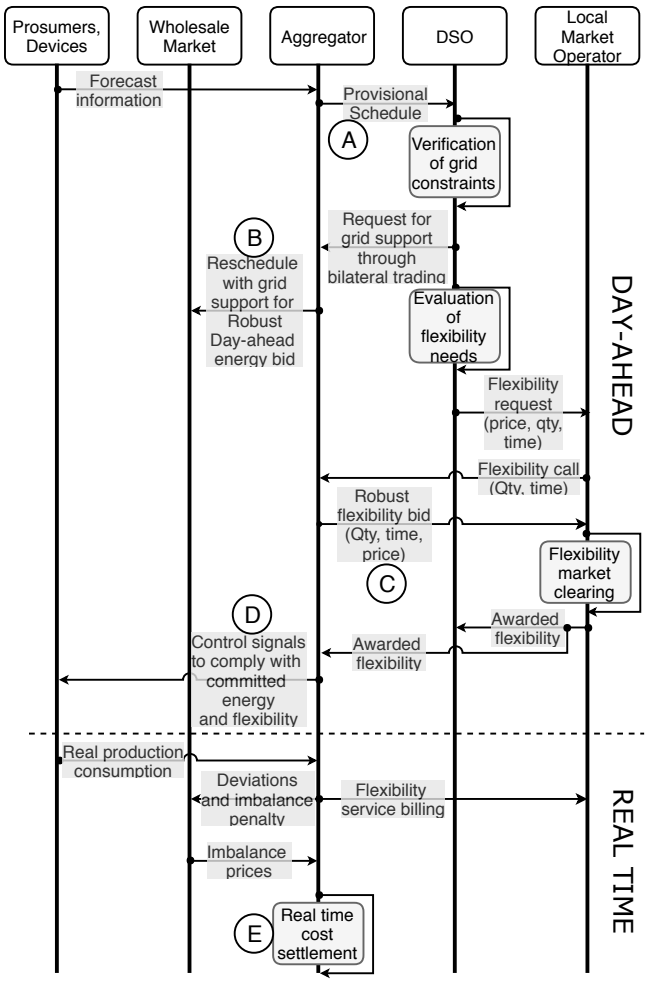


Figure 4.6: Sequence of actions

4.3.2 Main steps of the proposed framework

The main steps and timeline of the process that involves the participation of the aggregator, are described in the sequence depicted in figure 4.6 and detailed as follows:

First, the aggregator gathers the information related to PV forecasts, device availability, consumption forecasts and energy price forecast. With this information, the aggregator determines a baseline (unconstrained) or provisional schedule (in figure 4.6, referenced as action Ⓐ) that minimizes total operation costs supposing no operational constraints imposed by the DSO at the PCC. The DSO proceeds

to determine the expected operation state of the grid and sends ramping or power-limit constraints to the aggregator (and/or all distributed resources connected to the distribution grid) if needed, as detailed in subsection 4.3.3. If no constraint support is required by the DSO, there are no changes in the provisional schedule. On the other hand, if constraint support is needed, a bilateral transaction takes place between the DSO and the aggregator, in which the aggregator has to be paid the incurred extra-cost of rescheduling its devices to provide the adjustments needed by the DSO. After this, with or without constraint support, the aggregator sends its definitive day-ahead energy commitment to the wholesale market (action Ⓑ).

Next, the local flexibility market opens and receives requests from the DSO or other parties (i.e. BRP) specifying a tuple with location, time-frame (t^{fl}) and quantity (P^{fl}) of the required flexibility. With this information, the LFO calls flexibility bids from all potential flexibility providers, amongst which, the aggregator. If the aggregator has available flexibility to offer, a bid containing quantity and price for the required time frame is sent to the LMO (action Ⓒ). This bid, has to be robust enough to withstand: energy- and imbalance-price uncertainties, PV production and demand uncertainties, and additionally, has to be robust towards acceptance or not of the flexibility bid. After this, the LMO clears all flexibility bids and informs the aggregator if its bid is accepted.

The aggregator's schedule (action Ⓓ) is such that takes into account the mentioned sources of uncertainty, the awarded flexibility and the constraint support, while minimizing total operational costs.

Next, during the operation day, given the fluctuations of PV production and demand, deviations have to be met by additional purchase/sell of energy. This leads to negative/positive imbalances settled by the wholesale market. The total real time operation cost (action Ⓔ) will be given by the combination of the day-ahead energy commitment, the imbalance penalizations, the bilateral trading with the DSO (if called upon) and the flexibility service provided through the LFM (if called upon). Given the uncertain nature of the imbalance prices, the aggregator bidding strategy in all markets has to be robust in the sense of predicting potential deviations, and in consonance, value accordingly the services to offer.

4.3.3 Mathematical model for local provision of flexibilities

Deterministic model

Objective function The day-ahead operation of the aggregation of houses aims to minimize costs given by energy purchase in the wholesale market, imbalance penalization and cycling equivalent cost of the batteries. This objective function is shown in equation (4.22).

$$\text{minimize} \sum_{t=1}^{T}[\hat{\pi}_t^+ P_t^E + \hat{\mu}_t^- I_t^- - \hat{\mu}_t^+ I_t^+ + \sum_{h=1}^{N}\sum_{s=1}^{S}(a_{h,s}X_{t,h,s}^{Ds} + b_{h,s}l_{t,h,s})] \qquad (4.22)$$

The second term in the objective function corresponds to the piece-wise linearization of the battery degradation equivalent cost, in line with [51] and supported on constraints (4.30)-(4.38). The presence of this term in the objective function allows

to capture the interdependence of cycling patterns with energy prices and more accurately value the opportunity cost during the day-ahead operation.

Operational constraints Equation (4.23) describes the energy balance of the physical system and the net exchange at the PCC with the distribution grid. The negative and positive imbalance guarantee equilibrium in the case of deviations but its activation implies a monetary penalization as already expressed in objective function (4.22).

$$P_t^E + I_t^- - I_t^+ + \Delta t \sum_{h=1}^{N} (P_{t,h}^{pv} - P_{t,h}^c + P_{t,h}^d - \hat{D}_{t,h} - H_{t,h}) = 0, \forall t \tag{4.23}$$

Devices' constraints PV production is limited to the forecasted values as expressed in constraint (4.24). In this case, the total forecasted power of all panels in each time frame is compacted in $\hat{P}_t^{pv}$.

$$\sum_{h=1}^{N} P_{t,h}^{pv} \leq \hat{P}_t^{pv}, \forall t \tag{4.24}$$

Equations (4.25)-(4.29) describe the behaviour of the BESS in terms of the intertemporal charging/discharging pattern and the energy/power limits of each device. Equations (4.27) and (4.28), and binary variable $u_{t,h}$ ensure that charging and discharging of the battery are mutually exclusive.

$$X_{t,h} = X_{t-1,h} + \eta^c \Delta t P_{t-1,h}^c - \Delta t P_{t-1,h}^d / \eta^d, \forall t, t \neq 1, \forall h \tag{4.25}$$

$$X_{1,h} = X_{T,h}, \forall h \tag{4.26}$$

$$0 \leq P_{t,h}^c \leq \bar{P}_h^c \cdot u_{t,h}, u_{t,h} \in \{0,1\}, \forall t, t \neq 1, \forall h \tag{4.27}$$

$$0 \leq P_{t,h}^d \leq \bar{P}_h^d \cdot (1 - u_{t,h}) \tag{4.28}$$

$$\underline{X}_h \leq X_{t,h} \leq \bar{X}_h \tag{4.29}$$

The model to identify the adequate cost segment of the batteries' degradation linearized cost function, is expressed by equations (4.30)-(4.38). Special ordered sets and auxiliary constraints/variables are used to identify the beginning of charging cycles, expressed by binary variable $x_{t-1,h}$.

$$x_{t-1,h} - y_{t-1,h} = u_{t,h} - u_{t-1,h}, \forall t, t \neq 1, \forall h \tag{4.30}$$

$$x_{T,h} - y_{T,h} = u_{0,h} - u_{T,h}, \forall h \tag{4.31}$$

$$x_{t,h} + y_{t,h} \leq 1, x_{t,h}, y_{t,h} \in \{0,1\}, \forall t, \forall h \tag{4.32}$$

$$X_{t,h}^D + X_{t,h}^{Df} = 1 - X_{t,h} / E_h^{rated}, \forall t, \forall h \tag{4.33}$$

$$X_{t,h}^D \leq x_{t,h}, \forall t, \forall h \tag{4.34}$$

$$X_{t,h}^{Df} \leq 1 - x_{t,h}, \forall t, \forall h \tag{4.35}$$

$$\sum_{s=1}^{S} X_{t,h,s}^{Ds} = X_{t,h}^{D}, \forall t, \forall h \tag{4.36}$$

$$l_s^{min} l_{t,h,s} \leq X_{t,h,s}^{Ds} \leq l_s^{max} l_{t,h,s}, l_{t,h,s} \in \{0,1\} \, \forall t, \forall h \tag{4.37}$$

$$\sum_{s=1}^{S} l_{t,h,s} = x_{t,h}, \forall t, \forall h \tag{4.38}$$

After the beginning of a charging cycle is identified by constraints (4.30)-(4.32), the appropriate value of Depth of Discharge (DoD) ($X_{t,h}^{D}$) at which this charging cycle occurs, is extracted by constraints (4.33)-(4.35). Finally, the appropriate parameters of the linearized cost segment s ($a_{h,s}$ and $b_{h,s}$ in equation (4.22)) are activated when $X_{t,h,s}^{Ds}$ and $l_{t,h,s}$ take values different from zero. A more detailed description of the methodology for including equivalent degradation battery costs can be found in [51] and also explained in section 2.5.

The presence of the BESS binary variables in the model increases complexity and turns it into a Mixed-Integer Linear Programming (MILP) problem.

The TES capabilities provided by the EWHs that are present in the energy community are modeled by constraints (4.39)-(4.42), in which inter-temporal energy storage behaviour, energy losses and variable limits are described.

$$Y_{t,s,h} = Y_{t-1,s,h} + \Delta t H_{t-1,s,h} - Y_{t-1,s,h}/R_h C_h - \Delta t \hat{Q}_{t-1,s,h}, \forall t, t \neq 1, \forall s, \forall h \tag{4.39}$$

$$Y_{1,s,h} = Y_{T,s,h}, \forall s, \forall h \tag{4.40}$$

$$\underline{Y}_{t,h,s} \leq Y_{t,h,s} \leq \bar{Y}_{t,h,s} \tag{4.41}$$

$$0 \leq H_{t,h,s} \leq \bar{H}_{t,h,s} \tag{4.42}$$

Grid operational requirements

When the DSO directly requests grid support to the aggregator in the form of maximum power exchanges ($P_t^{PCC_{max}}$) or ramping constraint (R_t) at the PCC, additional equations must be included in the day-ahead scheduling problem for the aggregator in order to capture extra-costs and determine new schedules. Constraints (4.43)-(4.46) model the allowed ramping, which represent the maximum allowed net power change in consecutive time steps. Constraint (4.43) ensures that the day-ahead commitment respects maximum ramping, and in the same way, constraint (4.45) includes also negative and positive imbalance exchanges. Constraints (4.44), (4.46) ensure continuity between the last and first time steps of the operation day. Constraints (4.47)-(4.48) model the maximum allowed power exchange. Parameters $P_t^{PCC_{min}}/P_t^{PCC_{max}}$ are the min/max net power at the PCC.

These last two constraints are general enough to represent any DSO signal in terms of net power exchange, even for more complex power flexibility products [44, 140].

$$|P_t^E - P_{t-1}^E|/\Delta t \leq R_t \Delta t, \forall t, t \neq 1 \tag{4.43}$$

$$|P_1^E - P_T^g|/\Delta t \leq R_t \Delta t \tag{4.44}$$

$$|P_t^E + I_t^- - I_t^+ - (P_{t-1}^E + I_{t-1}^- - I_{t-1}^+)|/\Delta t \leq R_t \Delta t, \forall t, t \neq 1 \tag{4.45}$$

$$|P_1^E + I_1^- - I_1^+ - (P_T^E + I_T^- - I_T^+)|/\Delta t \leq R_t \Delta t \tag{4.46}$$

$$P_t^{PCC_{min}} \leq P_t^E \leq P_t^{PCC_{max}}, \forall t \tag{4.47}$$

$$P_t^{PCC_{min}} \leq P_t^E + I_t^- - I_t^+ \leq P_t^{PCC_{max}}, \forall t \tag{4.48}$$

As explained before, if these constraints were to be activated to support grid operation, their inclusion will likely lead to a different schedule and operation point for the aggregator, when compared to the provisional schedule. Hence, any extra-cost due to these constraints will determine the minimum fixed cost that the DSO has to pay the aggregator for providing this service, and settled through a bilateral contract between these two parties, as explained in subsection 4.3.3.

Robust counterpart

The previous deterministic model has multiple sources of uncertainty, namely, energy and imbalance prices, PV production and electrical and thermal demand. Strong duality theorem is used to find an adjustable robust optimization (ARO) counterpart [27] and rewrite all constraints with uncertain parameters and coefficients.

For the case of the objective function (4.22), the cost coefficients of P_t^E, I_t^- and I_t^+ present uncertainty and the equivalent dual robust counterpart is represented by constraints (4.49)-(4.56).

$$\begin{aligned}\sum_{t=1}^{T}\sum_{h=1}^{N}\sum_{s=1}^{S}(a_{h,s}X_{t,h,s}^{Ds} + b_{h,s}l_{t,h,s}) + \sum_{t=1}^{T}(\hat{\pi}_t P_t^E + \hat{\mu}_t^- I_t^- - \hat{\mu}_t^+ I_t^+) \\ + \sum_{t=1}^{T}(q_t^c + q_t^- + q_t^+) + \Gamma^c z^c + \Gamma^- z^- + \Gamma^+ z^+\end{aligned} \tag{4.49}$$

$$z^c + q_t^c \geq \frac{1}{2}(\bar{\pi}_t - \underline{\pi_t})y_t^c, \forall t \tag{4.50}$$

$$-y_t^c \leq P_t^E \leq y_t^c, \forall t \tag{4.51}$$

$$z^- + q_t^- \geq \frac{1}{2}(\bar{\mu}_t^- - \underline{\mu_t}^-)y_t^-, \forall t \tag{4.52}$$

$$-y_t^- \leq I_t^- \leq y_t^-, \forall t \tag{4.53}$$

$$z^+ + q_t^+ \geq \frac{1}{2}(\bar{\mu}_t^+ - \underline{\mu_t}^+)y_t^+, \forall t \tag{4.54}$$

$$-y_t^+ \leq I_t^+ \leq y_t^+, \forall t \tag{4.55}$$

$$z^c, q_t^c, y_t^c, z^-, q_t^-, y_t^-, z^+, q_t^+, y_t^+ \geq 0, \forall t, \forall h \tag{4.56}$$

To control conservatism for the uncertainty in energy, negative and positive imbalance prices, three parameters appear: Γ^c, Γ^- and Γ^+, respectively. Each of these parameters can take values from zero (deterministic case) to T, in correspondence with the maximum number of coefficients that can deviate from the central forecast.

Constraints (4.23) and (4.24) include additional uncertain parameters: electrical demand and PV production, respectively. The robust counterpart includes the robust parameters Γ_t^D and Γ_t^{pv} for controlling conservatism of demand and PV uncertainty. Constraints (4.57)-(4.61) represent the robust counterpart that results from strong duality theorem. The adjustable robust counterpart alternative is the

separated version explained in the previous chapter for the treatment of PV and demand uncertainty. In addition, the alternative of using Γ^2 is selected.

$$P_t^E + I_{t,s}^- - {}_{t,s}^+ + \Delta t \sum_{h=1}^{N} P_{t,h}^{pv} + P_{t,h}^d - P_{t,h}^c - H_{t,h} = \hat{D}_t + q_t^D + (\Gamma_t^D)^2 z_t^D, \forall t, \forall s \quad (4.57)$$

$$z_t^D + q_t^D \geq \frac{1}{2}(D_t^{90\%} - D_t^{10\%}) y_t^D, \forall t \quad (4.58)$$

$$\sum_{h=1}^{N} P_{t,h}^{pv} = \hat{P}_t^{pv} - q_t^{pv} - \Gamma_t^{pv} z_t^{pv}, \forall t \quad (4.59)$$

$$z_t^{pv} + q_t^{pv} \geq \frac{1}{2}(P_t^{90\%} - P_t^{10\%}) y_t^D, \forall t \quad (4.60)$$

$$z_t^D, q_t^D, z_t^{pv}, q_t^{pv} \geq 0, y_t^D, y_t^{pv} \geq 1, \forall t \quad (4.61)$$

Constraints (4.62)-(4.64) are the resulting robust counterpart of considering uncertainty in thermal load, with Γ_t^{th} controlling thermal load conservatism and cardinality [0,1].

$$\begin{aligned} Y_{t,h} &= Y_{t-1,h} + \Delta t H_{t-1,h} - Y_{t-1,h}/R_h C_h \\ &-\Delta t(\hat{Q}_{t-1,h} + q_{t-1,h}^{th} + (\Gamma_{t-1,h}^{th})^2 z_{t-1,h}^{th}), \forall t, \forall h \end{aligned} \quad (4.62)$$

$$z_{t,h}^{th} + q_{t,h}^{th} \geq \frac{1}{2}(Q_{t,h}^{90\%} - Q_{t,h}^{10\%}) y_{t,h}^{th}, \forall t, \forall h \quad (4.63)$$

$$z_{t,h}^{th}, q_{t,h}^{th} \geq 0, y_{t,h}^{th} \geq 1, \forall t, \forall h \quad (4.64)$$

The previous equations are the building block to optimally manage the resources of the aggregator in multiple markets and taking into account uncertainty. The relation of this mathematical model with the actions Ⓐ-Ⓔ depicted in figure 4.6, will be explained in the following subsections.

Provisional and robust reschedule with grid support

The provisional schedule (action Ⓐ) corresponds to the robust optimization problem when no grid constraint support is considered and minimization of the operation cost is pursued. Action Ⓐ is achieved by solving the following adjustable robust counterpart MILP:

$$\text{minimize } C^A = (4.49) \quad (4.65)$$

s.t.

$$\text{Constraints} : (4.25) - (4.38), \quad (4.66)$$

$$(4.40) - (4.42), (4.50) - (4.64) \quad (4.67)$$

where:

- (4.49): is the robust counterpart of the objective function.
- (4.25)-(4.38): are the BESS constraints.

- (4.40)-(4.42): are the EWH constraints.
- (4.50)-(4.64): are the remaining robust counterpart constraints.

When this unconstrained baseline robust schedule is determined, the net power exchange is communicated to the DSO to check if constraint support is needed: action Ⓑ. If this is the case, R_t and $P_t^{PCC_{max/min}}$ values are received and the following ROMILP is solved:

$$\text{minimize } C^B = (4.49) \tag{4.68}$$

s.t.

$$\text{Constraints} : (4.43) - (4.48), \tag{4.69}$$

$$(4.66), (4.67) \tag{4.70}$$

Where (4.43)-(4.48) are the local flexibility constraints.

The minimum remuneration for the aggregator in the bilateral transaction for providing the service of ramping and max. power, is given by the difference: $\pi^{dso} = C^B - C^A$.

Algorithm for bidding local flexibility

If the LMO asks the aggregator for a flexibility bid, the robust flexibility bidding process, action Ⓒ, followed by the aggregator is the following:

Step 1 Find the cost of the baseline (constrained) case, C^B, by solving (4.68)-(4.70).

Step 2 Flexibility request sent by the LMO is received by the aggregator in terms of: time-step of required flexibility, t^{fl}; required power flexibility, P^{fl}.

Step 3 The aggregator determines its robust cost to provide the required flexibility (C^{fl}) by solving (4.68)-(4.70) and including constraint:

$$\Delta t \sum_{h=1}^{N} P^{pv}_{t^{fl},h} + P^{d}_{t^{fl},h} - P^{c}_{t^{fl},h} - H_{t^{fl},h} - \hat{D}_{t^{fl}} - q^{D}_{t^{fl}} - \Gamma^{D}_{t^{fl}} z^{D}_{t^{fl}} = P^{fl} \tag{4.71}$$

Step 4 Compute the flexibility bid: $\pi^{fl} = C^{fl} - C^B$, and send bid to LMO.

The minimum price that should be paid to the aggregator for providing the required flexibility is given by π^{fl}. Constraint (4.71) allows to ensure that flexibility will be met by adjusting device settings of smart-homes. This set of control signals, settings and expected penalties is called action Ⓓ in the timeline of figure 4.6. Additionally, the robust characteristic of the formulation permits the inclusion of potential imbalances, and the corresponding penalties paid to the wholesale market which are assumed by the aggregator. In this approach, these costs are accounted for in the bidding process to protect the aggregator against uncertainties. Note that when no local constraint support is needed by the DSO, calculated C^B in step 1, becomes the same C^A.

This bidding methodology is general enough to bid in local market schemes that accept no only single point bids, but also bidding curves. The characteristic of the robust bid will depend upon the capabilities of the clearing algorithm used by the LMO. To construct a flexibility bidding curve for an specific time-frame t^{fl}, steps 1-4 need to be repeated for a range of values of $P^{fl} = [P^{fl}_{min}, P^{fl}_{max}]$, given by the LMO or determined by the technical flexibility capabilities of the aggregator for the specific period of time.

Real time performance evaluation

The performance aims to evaluate the ability of the aggregator to comply with: 1) the committed day-ahead energy; 2) the constraint support; and 3) the local awarded flexibility, while minimizing total operation cost when facing the multiple sources of uncertainty. Montecarlo simulation is used to test the robustness of the proposed approach for several patterns of random generated prices, consumption and PV production during the operation day. The total cost calculation when these random values are generated and used as input, is given by the day-ahead energy payments, the equivalent cycling cost of the batteries, the revenues for providing constraint support to the DSO, the revenues for providing local flexibility and the penalization due to imbalances produced by real time production/consumption in each household. Montecarlo simulation returns a measure of the performance in terms of average cost and standard deviation (SD), as a measure of the risk related to a particular robust bidding strategy.

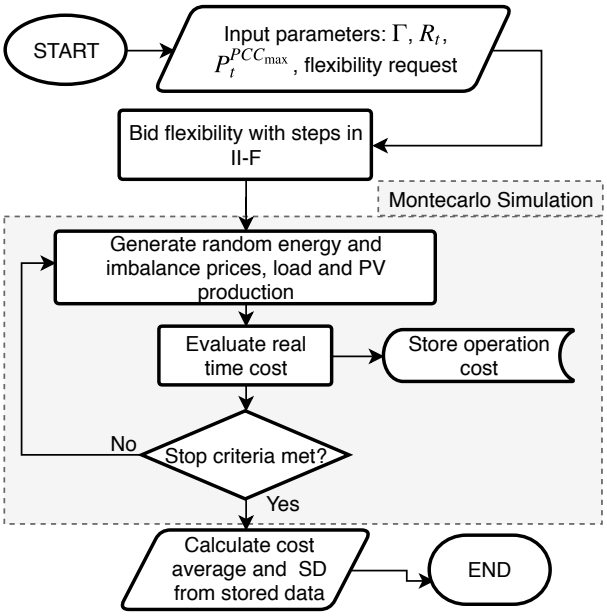


Figure 4.7: Real time performance evaluation: action E

The outline of the performance methodology is presented in figure 4.7. The number of simulations (stop criteria) is limited to the maximum between a) 1000 trials, and b) the number of trials in achieving a margin of error of maximum 1%

with a confidence interval of 95%.

The cost of each trial is given the following expression:

$$C^{trial} = C^{ws} - \pi^{dso} - \pi^{fl} + C^{cyc} \tag{4.72}$$

Where C^{ws} is the result of solving the following optimization problem:

$$\text{minimize } C^{ws} = (4.22) \tag{4.73}$$

s.t.

$$\text{Constraints} : (4.23) - (4.48), (4.71) \tag{4.74}$$

Given that each trial corresponds to a deterministic optimization problem, cycling constraints (4.30)-(4.38) are included in model, but equivalent degradation cost (C^{cyc}) is calculated after the optimization process with the last term of equation (4.22). This helps to reduce computational time while taking into account the equivalent degradation costs into the performance evaluation.

4.3.4 Results of robust participation in the wholesale market

Local constraints unactivated

If the provisional schedule (action Ⓐ) does not jeopardize grid operation, this schedule will remain as the robust day-ahead bid (action Ⓑ). Figure 4.8 shows the demand bidding curves for t=14, when energy prices are varied in the range 10%-90% percentile of the predicted priced by the KDE. These piece-wise curves show the hourly bids of the aggregator for economical operation when only wholesale market participation is allowed and no other local flexibility market exists. Hence, these curves show the interaction of local net power with the price variations in the wholesale market. They can also be interpreted as the bids if flexibility could be traded in the centralized wholesale market, as proposed in [15, 48, 49].

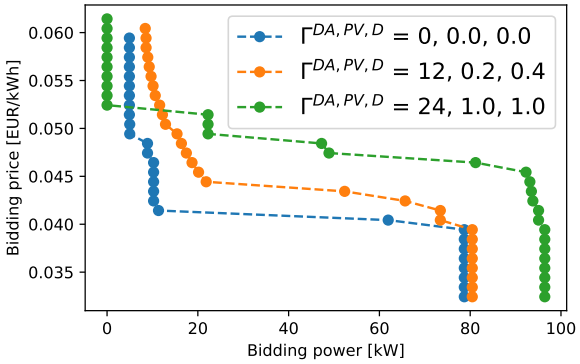


Figure 4.8: Demand bidding curves in the wholesale market for t = 14h and different levels of robustness without local constraint support (Action A = Action B).

The results show that increasing robustness (higher values of Γ) results in bids that can withstand higher purchase energy prices for similar values of bidding power, and for most part of the bidding range. It can be seen that the green curve (full robustness) tends to be the right-most.

Impact of local constraints

If ramping and $P_t^{PCC_{max}}$ constraints are locally activated during the day-ahead scheduling, the committed power in the wholesale market and the devices' settings, change in order to comply with the ramping and power requirements. Figure 4.9 shows the day-ahead energy commitment for different allowed ramping values and fixed $P_t^{PCC_{max}} = 0.07MW$. In this case, it can be seen that peaks are shaved at the level of maximum 70 kW, and that $R_t = 0.06MW$ (—●—) allows more unconstrained ramping as the case for time frame sequences 5h-10h and 17h-19h.

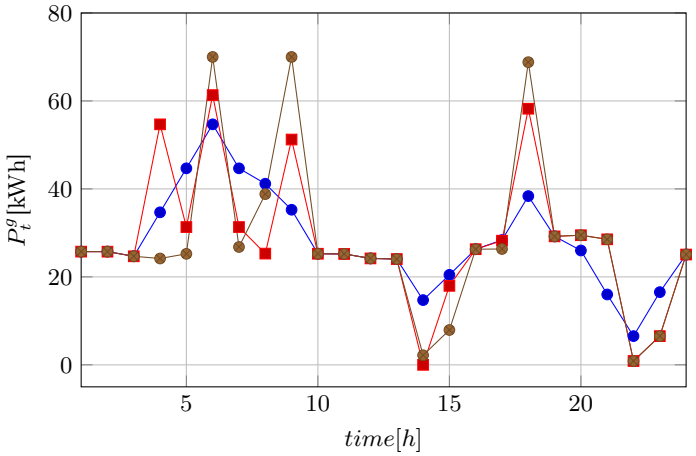


Figure 4.9: Day-ahead committed energy for R_t = 0.01 MW/h (—●—), R_t = 0.03 MW/h (—■—), $R_t = 0.06$ MW/h (—●—) when constant $P_t^{PCC_{max}} = 0.05$ MW

In general, each case leads to a different operation point and the robust operation cost ranges from €33.90 when no local constraints are considered, to €35.03 when ramping and power-max values are activated. For instance, when ramping is limited to 0.01 MW/h and maximum power to 0.04 MW, the operation cost of the HEMS is €35.03, which represents a 3.3% increase with respect to the unconstrained case. This means that if the DSO sends these signals, the HEMS aggregator would have to adjust its settings and incur in extracosts to satisfy DSO needs. This fixed remuneration (π^{dso}) component is shown in table 4.2 for different values of $P_t^{PCC_{max}}$ and R_t and for the case in which full robustness is considered ($\Gamma^{DA} = \Gamma^{PV} = \Gamma^{D} = \Gamma^{th} = 1$).

Table 4.2: Remuneration π^{dso} for the aggregator for different values of allowed ramping and maximum power

	$P_t^{PCC_{max}}$		
R_t	0.04 MW	0.05 MW	0.07 MW
0.01 MW/h	1.13	1.10	1.10
0.03 MW/h	1.04	1.00	0.99
0.06 MW/h	1.04	1.00	0.97

4.3.5 Robust bidding in the local flexibility market

If a local market is set in place to define appropriate prices for flexibility to be provided by the aggregator at the PCC, construction of supplying bidding curves could give an idea of the proper remuneration that the aggregator should receive for modification of the net power exchange coming from flexibility requests. This option is shown in figure 4.3.5. These curves measure the extracost of the aggregator's operation when deviating from the committed day-ahead energy. Hence, this price is the minimum that should be paid to the aggregator if DSO requires flexibility.

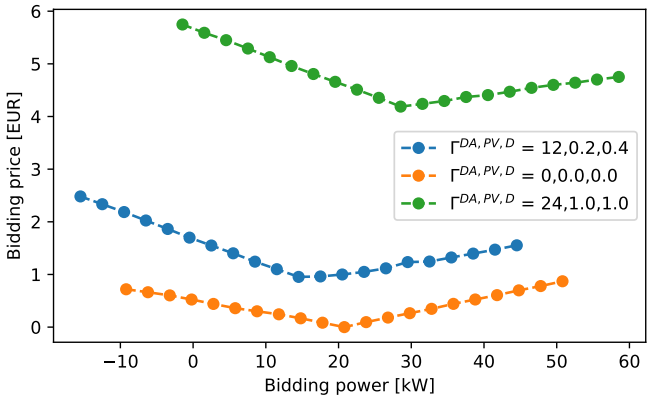


Figure 4.10: Local flexibility bidding curves for t = 21h

When the local flexibility bidding algorithm described in subsection 4.3.3 (action Ⓒ) is ran for a range of flexibility requested values, the bidding curves in figure are obtained. From these figures it can be seen that when flexibility is requested at the PCC, the remuneration increases as the requested deviation from he original day-ahead schedule increases. For instance, original day-ahead schedule for the aggregator when Γ^{DA}=12, Γ^{PV}=0.2, Γ^{D}=0.4 (blue dotted curve) in hour 21h is 29.2 kW, which is the point with the lowest flexibility bidding price and maintaining this power will be less costly for the aggregator. When other values of flexibility are requested, the remuneration starts increasing due to the activation of home flexibility and the potential imbalance costs that should be settled in the wholesale market and foreseen by the aggregator.

Given that the aggregator has to manage residential resources to supply the offered flexibility and also foresee PV and demand deviations, imbalances might occur and have to be accounted for in the flexibility bids. For instance, due to the fact that the aggregator bids also in the energy market, the flexibility offered in figure 4.3.5 (blue dotted curve), includes the expected robust imbalances shown in figure 4.11 to be capable of adjusting device's settings and also supply local electrical and thermal demand. The aggregator is responsible for negotiating these quantities in the wholesale market which act as a form of penalization or deviation from the original day-ahead committed energy. In this approach, the formulation allows also to account for imbalance price uncertainty when determining bidding quantities and prices. This protects the aggregator from the inherent uncertainty of demand, PV production, electricity prices and the subsequent penalizations due to deviations.

The levels of protection against uncertainty explain the difference in the bidding prices in figure 4.3.5. When full robustness is considered (green dotted curve), the aggregator is protected against all deviations in forecasted imbalance prices, PV production and load. The trade-off being that flexibility bids are higher and might not be awarded by the LMO in the clearing process. It is important to mention that the imbalances boxplot is associated to the imbalance pattern resulting from each point in figure 4.3.5 and is not associated to the real time expected deviations after uncertainty realization. The analysis related to the performance when the aggregator is facing multiple random realizations of the uncertainties in real time, is developed in subsection 4.3.6.

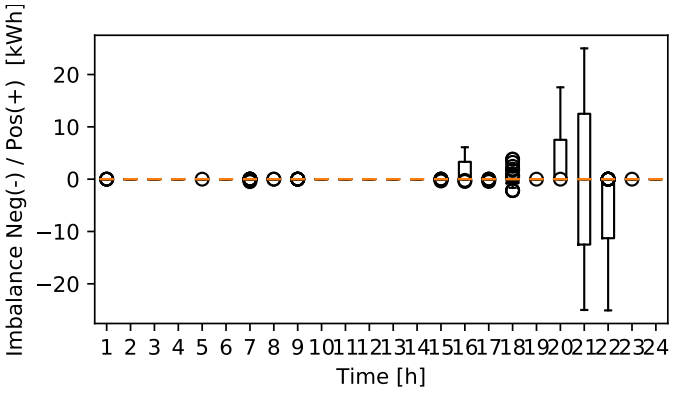


Figure 4.11: Boxplots of expected negative and positive imbalances to comply with robust flexibility bids in figure 4.3.5, for t=21h

In order to bid different quantities in the local market in the presence of uncertainty, not only imbalances occur, but also changes in the devices' settings. The average behavior of the storage devices (all HEMS batteries aggregated) resulting from the points of the bidding curve, is shown in figure 4.12. For instance, the energy stored in the batteries changes slightly during most of the time frames, but changes more actively during time-frames 21h and 22h to provide the necessary flexibility. Similarly, the stored energy in the EWHs presents higher variation during time-frames prior to t=21h, to adjust the operation for provision of flexibility and supply local thermal residential load.

4.3.6 Assessing the performance when facing uncertainties

To measure the performance, a first test is developed by comparing deterministic and robust approaches when the aggregator participates in both wholesale energy and local flexibility markets. This test is based on the methodology explained in figure 4.7 and considering an arbitrary flexibility request of -10 kW by the LMO for demonstration purposes. After running the performance algorithm by setting margin of error to maximum 1% with a confidence interval of 95%, the expected real time operation costs are 26.15€ for the deterministic solution and 22.05€, 22.42€, 22.48€ for ARO1 ($\Gamma^{DA,PV,D} = 12, 0.2, 0.4$), ARO2 ($\Gamma^{DA,PV,D} = 18, 0.2, 0.2$) and ARO3 ($\Gamma^{DA,PV,D} = 12, 0.4, 0.6$) respectively. Improvement of the proposed robust approach in expected operation cost ranges from 14.0% to 15.7% when compared

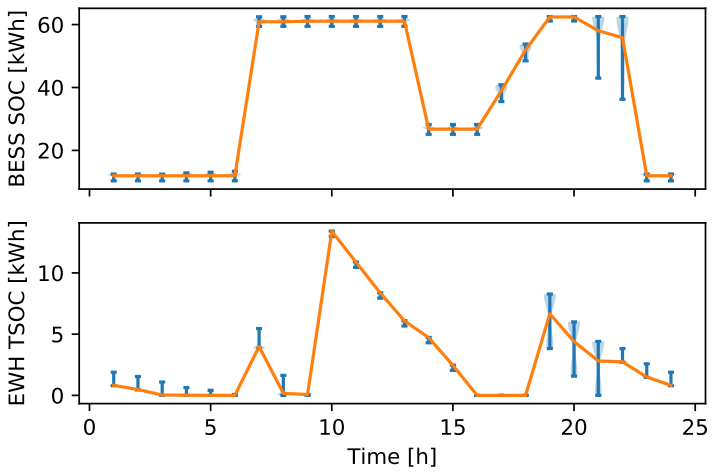


Figure 4.12: Average (orange) state of charge and boxplots (blue) of batteries and EWHs for the bidding quantities in t=21h

to the deterministic case, showing the ability of the robust formulation to optimize participation in the wholesale market and comply with the local flexibility despite the uncertainty in prices, PV and load.

The CDF (cumulative density function) of the performance is depicted in figure 4.13. This CDF shows that the leftmost curves are the ones related to the proposed ARO approach, which shows that probabilities of having lower associated costs are higher for the ARO cases. For instance, the ARO cases have between 91% to 96% probability of presenting an operation cost lower than the deterministic mean (1.0 p.u.). The standard deviation is also measured to determine related risk of decision-making. The obtained SD values are 3.47€, 2.15€, 2.91€, 2.49€ for the deterministic, ARO1, ARO2 and ARO3 cases respectively. In all cases, robust solutions improve the deterministic SD in the ranges from 16.1% to 38.0%.

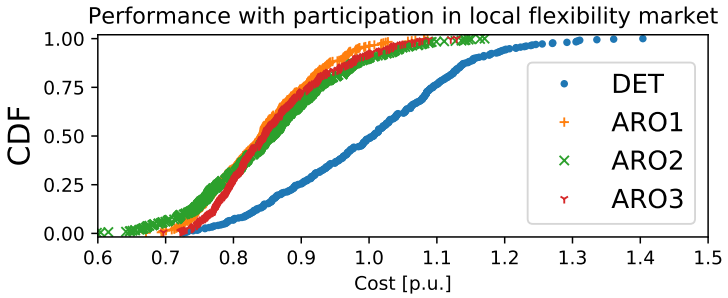


Figure 4.13: Performance CDF of different bidding strategies : deterministic, ARO1: $\Gamma^{DA,PV,D} = 12, 0.2, 0.4$, ARO2: $\Gamma^{DA,PV,D} = 18, 0.2, 0.2$ ARO3: $\Gamma^{DA,PV,D} = 12, 0.4, 0.6$, for november 15th and flexibility activated of -10 kW (up regulation).

In addition to the analysis of participation in energy and local markets (case 1) in table 4.3) performance was evaluated for local constraint activation (case 2) and

for the case in which flexibility bid is not accepted by the local market (case 3). For case 3, performance is not jeopardized by the rejection of the flexibility offer, given that ARO bidding strategy outperforms the deterministic solution in the range of 9.1%-9.7%.

However, if the local flexibility offer is accepted, dispatched and remunerated, there are improvements in the operation. For the ARO-1 case, for example, acceptance of the local flexibility offer (case 1) implies a cost reduction when compared to the case of offer rejection (case 3). This reduction represents a 6.4% improvement in real time expected cost.

ARO approaches also show better behavior when local constraint support (case 2) is included, and improvement is achieved in comparison to participation in only-energy market.

Cost reduction exist in all cases when ARO approaches are compared to the deterministic solution. Additionally, when each robust case is analyzed separately, improvements persist for the cases in which local flexibility market participation is included. This shows the ability of the proposed approach to optimally bid in multiple market platforms even with different settlement schemes. Cases 1 and 2 imply a probability of acceptance of the flexibility bid of 100%, whereas case 3 implies 0% acceptance probability.

Table 4.3: Performance for participation in different markets with different robust bidding strategies. $^*R_t = 30kW/h$, $P_t^{PCC_{max}} = 50kW$

Case	Market	Det.	ARO1	ARO2	ARO3
1	Energy + Local Market accepted bid	26.15	22.05	22.42	22.48
2	Energy + Local Market accepted bid + Local Constraint Support*	26.21	22.25	22.43	22.81
3	Only Energy (local market rejected bid)	26.13	23.57	22.69	23.74

4.3.7 Analysis of the probability of bid acceptance

The expected operation cost is also dependant on the acceptance or not of the bid by the LMO. The acceptance of the bid depends on many factors, such as the bidding price, which depends also on the desired level of robustness, the hour, the quantity, etc.. The higher the robustness, the higher the bidding prices (as seen in figure 4.3.5). The trade-off is that the lower the price is, the more probabilities that the flexibility will be awarded and dispatched. However, the remuneration is lower.

For the sake of example, this fact can be seen in figure 4.14. Two cases are shown: average cost for the deterministic case and an arbitrary ARO case with $\Gamma^{DA,PV,D} = 12, 0.5, 0.5$. The simulation consists in generating bids for hour $t = 21$ and for -10 kw of required flexibility by the LMO. When analyzing performance of each alternative, not only Montecarlo simulation is used for price, PV and demand values, but also uniform random values are generated to be compared with different bid acceptance probabilities. If the random value is lower than the predefined probability, then the bid is accepted and dispatched. The obtained results show that the robust bidding strategy becomes more appealing than the deterministic only if the probability of

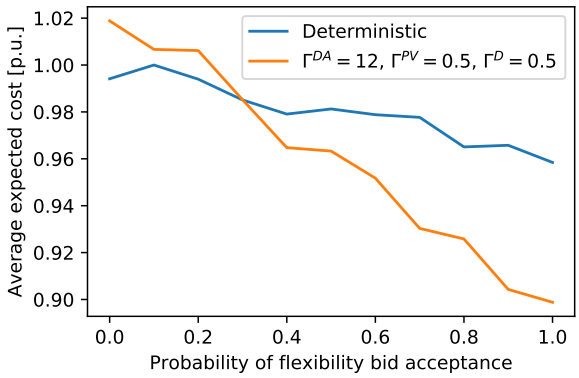


Figure 4.14: Average expected costs for different levels of flexibility bid accetpance. Simulation for november 15th and flexibility activated of -10 kW (up regulation).

the acceptance of the bid is higher than 27%.

Another case is shown in figure 4.15, in which the deterministic and the full robust case are compared. In this case, it can be analyzed that the probability of acceptance has to be higher in order for the robust approach to be more attractive than the deterministic. In addition, the cost for the robust case has a steeper slope. This is explained by the fact that higher robustness means higher cost for providing the flexibility, hence a higher remuneration when flexibility is awarded.

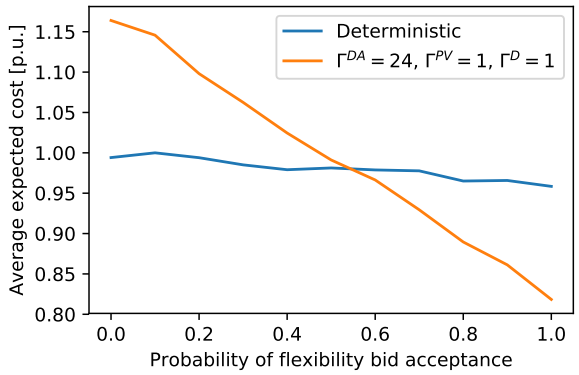


Figure 4.15: Comparison of average expected costs for different levels of flexibility bid acceptance. Simulation for november 15th and flexibility activated of -10 kW (up regulation).

The combination of the three preceding cases is depicted in figure 4.16. This figure shows that the complete robust approach becomes the most interesting alternative only for high acceptance probabilities (>70%). However, as stated before, the bids of the robust approach are more expensive and hence have lower probabilities of being accepted. Moreover, for these three case, the deterministic approach results more attractive for lower bid acceptance probabilities. The figure also evidences the difference in the slope of both proposed robust bidding strategies, showing that

case $\Gamma^{DA,PV,D} = 12, 0.5, 0.5$ has a descending behavior due to the remuneration of flexibility, but not as steep as the complete robust scheme.

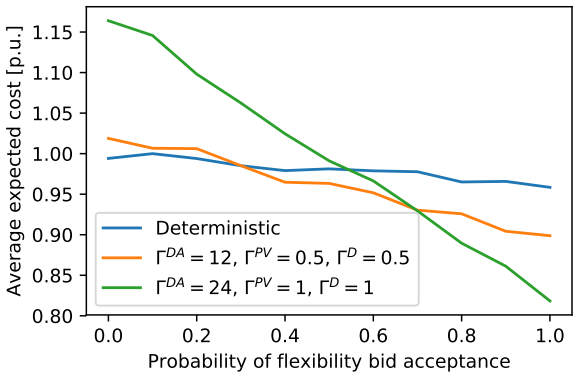


Figure 4.16: Average expected costs for different levels of flexibility bid acceptance. Simulation For november 15th and flexibility activated of -10 kW (up regulation).

When the robust strategy ARO1: $\Gamma^{DA,PV,D} = 12, 0.2, 0.4$ already analyzed in table 4.3 is subject to the same analysis taking into account probability of bid acceptance, the obtained evolution of average costs is obtained in figure 4.17. In this case, this strategic bidding has lower average costs when compared to the deterministic, despite the probability of bid accetpance. This is a very important result given that full certainty of bid acceptance cannot be foreseen when sending the bid to the LMO. This means that the proposed strategy is robust enough to withstand uncertainties not only coming from demand, prices and PV, but also performs towards bid acceptance uncertainty.

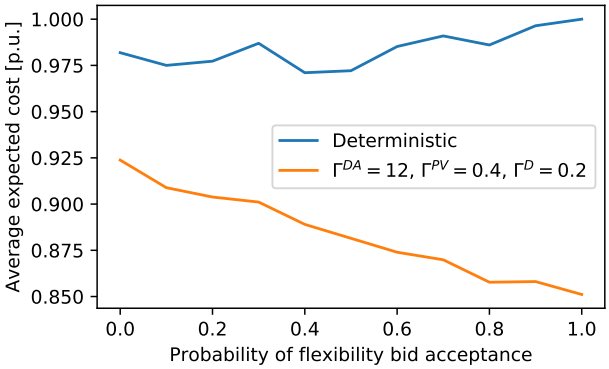


Figure 4.17: Average expected costs for different levels of flexibility bid acceptance. Simulation For november 15th and flexibility activated of -10 kW (up regulation).

4.4 Conclusions

The proposed approach presents a mathematical model to include local flexibility in the form of 1) maximum allowed net power exchange and ramping at the PCC and 2) participation in local flexibility markets. The simulations analyzed different cases in which the aggregator participates in wholesale and flexibility markets and determines the changes in the devices' schedule to achieve minimum operation cost while complying with DSO's flexibility constraints, flexibility requests and energy committed in the day-ahead market. These adjustments in the operation of HEMS allow an aggregator to participate in the electricity market while cooperating with the local DSO to enhance network operation and promote decentralization of the electrical system.

When no limits are imposed, that net power exchange may yield values that jeopardize upstream operation, such as violation of voltage limits, congestion in distribution lines, among others. This makes it necessary to take into account DSO signals and enhance cooperation between agents in order to minimize potential risks.

For the stochastic/robust case and flexibility values analyzed, the operation cost for the aggregator increases up to 2.3% with respect to a base case in which no DSO flexibility signals are considered. This information is useful to determine potential remuneration for the aggregator for providing local flexibility services, given that scheduling of resources has to change to provide the needed flexibility.

For proper remuneration of provision of flexibility needs, the variations of operational cost of the microgrid must be taken into account, to achieve benefitial market environment for all participants. For instance, if a local market is set in place, bidding curves can be submitted in order to correctly price and remunerate the service provided by the microgrid.

For the analyzed complete robust framework, the expected cost outperforms the deterministic case up to 15.7% when participation in multiple markets is allowed. In addition, participation in LFM allows to decrease operational costs due to remuneration of providing flexibility service. The robust approach allows to place bids in all markets and schedule devices in such a way that cost is minimized while facing uncertainties produced by energy prices, PV production and load.

The remuneration of the flexibility is related to the level of robustness. If robust parameters are set to high values, the cost for providing flexibility also increases provided that the aggregator includes the expected cost for potential deviations of prices, demand and PV production. In addition, there is a trade-off between level of robustness and possibilities of being awarded the flexibility service, given that higher cost for providing the service will have less possibility of being dispatched by the LMO. However, for the analyzed case, there exist combination of robust parameters that yield better costs than the deterministic scheme despite the probability of bid acceptance.

Chapter 5

Concluding remarks

5.1 General conclusions

In this section we synthesize the overall conclusions that have been separately presented in detail at the end of each chapter. The partial conclusions in each preceding chapter focus also on covering quantitative results. However, here we emphasize mainly on the general contributions.

Aggregation of resources at the residential level is drawing increasing attention in the energy transition context given its importance to integrate energy consumers into the smart grids paradigm. This thesis presented a literature review in which the current trends for treating uncertainty in the smart grid context were identified, and the opportunities of using robust optimization for prosumers' aggregation was detected, specifically for the case of the adjustable version. In addition, cycling aging cost calculation alternatives were analyzed and the adequate options for short-term electrical markets were identified. The literature review also presented the current opportunities for proposing comprehensive models including uncertainty, battery degradation and exploitation of prosumers' flexibility in multiple markets, with special emphasis on local flexibility markets.

The main contributions of this thesis are related to the modeling of uncertainty into the optimization model for participation of an aggregator in short-term energy markets. Energy prices, demand and PV production are included as sources of uncertainty through ARO. In this context, battery cycling models are also included and participation and bidding in traditional day-ahead energy markets and new local flexibility markets are proposed.

This thesis was developed in three main parts: chapter 2, presented the generalities of the deterministic mathematical model and two alternatives for inclusion of battery aging. Chapter 3 developed the model in the presence of uncertainties and finally chapter 4 presented a strategy for robust bidding in local flexibility markets.

Aggregation and interaction of different sources of flexibility lead to operation cost decrease for a market agent in charge of controlling several devices at the residential level. In the case of the present work, and specifically in chapter 2, interactions of PV, electric water heaters and batteries are analyzed. The best behavior from the standpoint of operational costs for day-ahead market participation

is obtained when all sources of flexibility are included. In the case of EWHs, which act as thermal storage, the behavior is similar to that of a flexible load, given that the pattern of consumption varies depending on the cost of opportunity and the thermal load needs.

Aggregators usually have multiple assets to manage and get profit from. This would help to overcome potential market barriers regarding minimum installed capacities or minimum bid quantities (power/energy) for bidding in energy and/or ancillary markets. An aggregator can also have a portfolio mix of resources such as medium/large size storage, pumped hydro plants, wind turbines, heat-ventilating systems, other building aggregations, electrical vehicles, etc. In this context, the proposed HEMS would be a part of the resources to manage.

The first part of chapter 2 was also dedicated to present a decomposition technique to include degradation of batteries into the aggregator's model. When the SDA is used to disaggregate a SOC value sent by a metaheuristic algorithm, a particule with only T positions is needed, despite the number of batteries in the test system. This is important, provided that any metaheuristic will require higher computational effort if the dimension of the decision variable increases. Hence, the SDA allows to keep solutions' size constant.

If the SDA is to be used in a stochastic optimization framework, the size of the solution will depend on the definition of the first and second stage variables and the corresponding number of scenarios (N_e). The decomposition method avoids the complexity of dealing with a MINLP problem and can be used and adjusted in other applications in which battery degradation costs need to be accounted for to bid in energy markets.

The presented explicit modeling alternative in the last part of chapter 2 for including degradation directly into the optimization model, is based on piecewise linearization of the equivalent cost function. This cost is represented as a function of the DoD at which each charging cycle occurs. It is important to mention that the degradation cost obtained with this alternative is different from a cost obtained with an expost calculation with the RCA, given that the cycle counting differs from one method to another, hence direct comparison of the two methods is not adequate. The explicit modeling efficiently uses the binary auxiliary variables introduced to detect state transitions and beginning of charging cycles. This variables are present also in the objective function to activate the corresponding independent term of the linearized cost function.

Explicit modeling achieves accurate approximations for a moderate number of segments. For instance, in this work, 6 segments are enough to guarantee errors lower than 0.05% in the final day-ahead operation cost. Errors in the isolated degradation function are higher and were not used to select the number of segments. This is explained by the fact that the cycling cost function is more sensitive to changes in the number of segments, provided that each option may lead to a different final setpoint of batteries, thus changing the equivalent value of degradation. Therefore, it is more logical to analyze the error of the total day-ahead operation objective function.

In chapter 3, uncertainties of the following types were considered in the mathematical formulation with either SO or ARO: energy prices, electrical load, thermal load and PV production.

When using strong duality to obtain the robust counterpart of the deterministic model, and for the specific case of PV and electrical load, an additional calculation was established to obtain net load in each time step. This results in one unified budget of uncertainty to control conservatism of net load. In addition, $3 \times T$ dual variables and $2 \times T$ new constraints are introduced. An alternative was also explored, by maintaining separate budgets and dual variables for electrical load and PV. Although this formulation results in a larger optimization problem, separate handling of both sources of uncertainty lead to impacts on the performance of the solutions and better mitigation of over-conservatism. An additional modification was made to the model by using Γ^2 budget of uncertainty. This allows to better exploit lower values of the budget in closer intervals and also counter over-conservatism of the solutions. In general, ARO ensures a guaranteed minimum cost and lower imbalances. Depending on the market design for aggregators and imbalance prices to settle deviations, overall performance and absolute values of cost and SD decrease can vary.

The proposed performance analysis consisted of detecting the combination of robust parameters that yielded in the set of Pareto optimal solutions from the standpoint of cost and standard deviation, when the obtained solution is subject to random realizations of the uncertain variables. Hybrid stochastic/robust and complete robust alternatives were compared. For some combinations of robust parameters, the deterministic solution outperforms some HSR and complete ARO solutions. Nonetheless, HSR and complete ARO solutions can always be found in such a way that both cost and SD outperform the deterministic approach. The proposed descriptors to evaluate the modified models allow to conclude that alternative 4 outperforms the remaining complete ARO models, the hybrid models and the deterministic solution from the standpoint of risk and cost.

Local provision of flexibilites was explored in chapter 4. In this case, a framework that allows participation in three different market places was proposed. First, day-ahead energy and imbalance market participation; second, bilateral transaction of local flexibility with DSO; and third, participation in a local flexibility market to sell flexibility to the DSO or other third parties.

Coordination between residential aggregators and DSOs is necessary and leads to an natural inherent transaction for both agents. This is explained by the fact that unrestricted scheduling of devices at the residential level might lead to operational problems in the upstream network. This thesis proposes two types of flexibility products to be traded directly with the DSO: maximum allowed power at the PCC and net ramping rate. The activation of these products lead to change in the operation of the devices and hence a different sub-optimal setpoint that increases operational costs. This cost increase acts as a price signal to remunerate the provision of flexibility. Given that uncertainties are taken into account, the deviations to respect flexibility commitment are minimum while maintaining minimum operational cost for the aggregator.

When flexibility is traded in a local flexibility market, the proposed framework assumes that there exists a local market operator to clear the market. If flexibility is needed, the aggregator can submit bids if required. The flexibility bids explored in chapter 4 have different levels of robustness depending on the predefined budget

of uncertainty. The obtained flexibility bidding curves show that the price of the flexibility tends to be higher if robust parameters have also higher values. This is explained by the fact that the robust model is protected against uncertainty measured by the deviations and the consequent penalization (imbalance). Hence, the optimal robust solution takes into account the changes in devices' settings and potential needs of the aggregator for incurring in extracosts in the case of deviations of the uncertain parameters. This information is traduced in price of flexibility and the bids sent to the LMO.

For the simulations ran, a combination of robust parameters can be found to obtain a solution that has better performance than deterministic approaches, despite the probability of bid acceptance. This is carried out by analyzing only performance of participation in the energy market, given that this is the more conservative scenario, and taking into account that bid acceptance leads to remuneration, in the case it is accepted. Hence it is not necessary to run an exhaustive performance analysis for all bid acceptance scenarios. The proposed robust approach is capable of finding robust optimal solutions even in absence of knowledge of the probabilities of bid acceptance.

However, if probability of acceptance was to be incorpored into the model, historical data would be necessary for building an appropriate model. This shows the importance of the robust approach for local emerging flexibility markets, provided that there is still a lack of sufficient historical information to create proper scenario based models and stochastic optimization approaches.

5.2 Perspectives and future work

The study carried out during this thesis has also led to identification of potential improvements and future work, which are condensed in the following lines.

On prosumers and aggregators:

- Inclusion of multi-energy systems/hubs, as identified in the literature review. MES include other devices such as CHP plants, heat pumps, boilers, heat storage, etc., and the coordination possibilities with active demand, ESS and RES become an interesting opportunity not only to minimize operation costs, but also to offer local and energy/reserve services and by reaching minimum bid quantities.

- Comparison of remuneration schemes for aggregation approaches versus peer-to-peer (transactive) frameworks.

- Determination of billing mechanism and contract framework between aggregators and end-users to enhance active citizen participation.

- Management/operation and market frameworks for energy communities and energy democracy related tendencies through cooperatives. Multi-objective approaches for aggregators/communities can arise as an option to include several "hard-to-monetize" objectives: environmental, social and other externalities.

On specifics of mathematical models:

- Combined sizing and operation optimization models for decision making regarding resource planning for energy communities and aggregators.
- Extension of the proposed decomposition approach in this thesis in the cases of DSO/TSO ownership of batteries. This case will require iterative calculation of battery aging and optimal power flow methods to achieve pursued objective (minimize losses, economic dispatch, reliable operation, congestion management, etc.).
- Hybrid Robust/MPC models can be developed to account for uncertainties with rolling horizon in the context of intra-day market participation.
- Analyze scalability of ARO schemes for aggregation or large number of customers. Machine learing methods appear as an option to decrease computational burden of performance evaluation by predicting attractive ranges of uncertainty budget.

On market participation and architectures:

- Extension of aggregator's bidding mechanisms and capabilities for day-ahead, intra-day and real-time markets. In addition to models for participation in energy, local flexibility and traditional ancillary markets (i.e. tertiary regulation).
- Local flexibility service characterization. For instance, inclusion of reactive power products for congestion management and voltage support. Additionally, and given the unbalanced nature of the distribution grids, "unbalanced flexibility products" can also be explored.
- Architectures and clearing schemes for local flexibility markets from the local market operator perspective in order to develop a complete test-case and create historical synthetic data for the research community. There is a lack of historical information for local flexibility markets: activation probabilities, required flexibility, actual dispatched flexibility, prices, etc.
- Decentralized and coordinated request for flexibility should be possible for DSOs and TSOs. A discussion on the hierarchy between DSO and TSO must be addressed to avoid potential conflicts (or to promote cooperation) in the provision of flexibility in different levels.

Appendix A

SDA correction algorithm

When performing the SDA and after updating the variables by using (2.26), some of the variables may exceed the boundaries. If this happens, a correction procedure involves each multiplier $\lambda^{(j)}$ associated to each violating variable x_j. Let Λ_Y be the set that contains the violating variables, Λ_N the set of the non-violating variables, and x_j^* indicates the minimum or the maximum allowed value for x_j. For each variable in Λ_Y, a correction that complies with the following equation needs to be carried out:

$$x_j + \phi \cdot \Delta\lambda^{(j)} = x_j^* \tag{A.1}$$

Reorganizing the terms we obtain the following:

$$\begin{aligned} x_j^* - x_j &= \phi\Big(\frac{1}{N}\sum_{i\in\Lambda_N}\lambda^{(i)} + \frac{1}{N}\sum_{i\in\Lambda_Y}\lambda^{(i)} - \lambda^{(j)}\Big) \\ &= \frac{\phi}{N}\sum_{\substack{i\in\Lambda_Y \\ i\neq j}}\lambda^{(i)} + \frac{\phi}{N}\sum_{i\in\Lambda_N}\lambda^{(i)} + (\frac{\phi}{N} - 1)\lambda^{(j)} \end{aligned}$$

If all of the equations in Λ_Y are written, a linear system of the type $A \cdot \lambda^{new} = b$ is generated, where A is a square matrix, b is a column vector and λ^{new} is the vector with the multipliers in Λ_Y that have to be corrected. To solve this system, the elements of A are calculated as follows:

$$A_{jj} = \frac{\phi}{N} - 1 \tag{A.2}$$

and,

$$A_{ji} = \frac{\phi}{N} \tag{A.3}$$

where A_{jj} are the elements in the diagonal and A_{ji} the elements outside the main diagonal. Elements of b, are calculated with the following expression:

$$b_j = x_j^* - x_j - \frac{\phi}{N}\sum_{i\in\Lambda_N}\lambda^{(i)} \tag{A.4}$$

After the linear system is solved, a set of multipliers is obtained such that the update of x_j, $\forall j \in \Lambda_Y$ is in the bounds.

Appendix B

Generalized SDA for scenario-based stochastic approaches

When a certain SOC ($X_{t,e}^{agg}$) is determined by the CSO logic, where e corresponds to a scenario, it has to be optimally allocated/dissagregated in each battery. This depends on each battery's cycling aging characteristics and the associated SOC. This subproblem can be mathematically formulated as follows:

$$\min w = \sum_{e=1}^{N_e} \sum_{h=1}^{N} f_h^{cyc}(\mathbf{X}_{h,e}) \tag{B.1}$$

s.t.

$$X_{t,e}^{agg} = \sum_{h} X_{t,h,e}, \forall t, \forall e \tag{B.2}$$

When applying Lagrangian relaxation to this optimization problem, one multiplier appears for each time step in each scenario ($\lambda_{t,e}$), as shown in the function:

$$\mathcal{L} = \sum_{e=1}^{N_e} \sum_{h=1}^{N} f_h^{cyc}(\mathbf{X}_{h,e}) + \sum_{e=1}^{N_e} \sum_{t=1}^{T} \lambda_{t,e}(X_{t,e}^{agg} - \sum_{h} X_{t,h,e}) \tag{B.3}$$

After applying optimality conditions to the langrangian function (B.3) (i.e., derivative with respect to $X_{t,h,e}$ and $\lambda_{t,e}$), the equations obtained are:

$$\frac{\partial \mathcal{L}}{\partial X_{t,h,e}} = \frac{\partial f_h^{cyc}(\mathbf{X}_{h,e})}{\partial X_{t,h,e}} + \lambda_{t,e} = 0, \forall t, \forall h, \forall e \tag{B.4}$$

$$\frac{\partial \mathcal{L}}{\partial \lambda_{t,e}} = X_{t,e}^{agg} - \sum_{h} X_{t,h,e} = 0, \forall t, \forall e \tag{B.5}$$

From equation (B.4) it is concluded that the derivative for each time step and scenario is battery invariant. This is a very important condition given that, in other words, the derivative of each battery should be the same for any given t and e:

$$\frac{\partial f_1^{cyc}(\mathbf{X}_{1,e})}{\partial X_{t,1,e}} = \cdots = \frac{\partial f_h^{cyc}(\mathbf{X}_{h,e})}{\partial X_{t,h,e}} = \cdots$$
$$\cdots = \frac{\partial f_N^{cyc}(\mathbf{X}_{N,e})}{\partial X_{t,N,e}} = -\lambda_{t,e}, \forall t, \forall e \tag{B.6}$$

To calculate the derivative adn given that there is no analytic function to express f_h^{cyc}, numerical differentiation is used in order to iteratively find the $X_{t,h,e}$ that leads to (B.6) while satisfying (B.5):

$$\lambda_{t,e}^{(h)} \approx \frac{f_h^{cyc}(\mathbf{X}_{h,e}) - f_h^{cyc}(\mathbf{X}_{h,e} + \Delta X_{t,h,e})}{\Delta X_{t,h,e}} \tag{B.7}$$

Superindex (h) is introduced to denote that a multiplier $\lambda_{t,e}^{(h)}$ should be calculated for each battery h, and the iterative process should correct the values $X_{t,h,e}$ until the multiplier is the same for all batteries (until $\lambda_{t,e}^{(1)} = ... = \lambda_{t,e}^{(N)} = \lambda_{t,e}$).

This disaggregation algorithm is initialized by selecting a $X_{t,h,e}$ in such a way that eq. (B.2) (same as eq. B.5) is met. After this, $\lambda_{t,e}^{(h)}$ are calculated by using (B.7). Given that $X_{t,h,e}$, in each t and e, needs to be updated to achieve equal $\lambda_{t,e}^{(h)}$ for all batteries, a deviation for each (h) is calculated by:

$$\Delta\lambda_{t,e}^{(h)} = \lambda_{t,e}^{(h)} - \bar{\lambda}_{t,e} \tag{B.8}$$

where,

$$\bar{\lambda}_{t,e} = \sum_h \lambda_{t,e}^{(h)}/N \tag{B.9}$$

Equation (B.8) measures the deviation of each battery's derivative with respect to the mean, hence, a simple heuristic rule is used to update SOC values according to:

$$X_{t,h,e}^{new} = X_{t,h,e}^{old} + \phi \cdot \Delta\lambda_{t,e}^{(h)} \tag{B.10}$$

where ϕ is a tuning parameter. Once the SOC is updated for each battery, eq. (B.7) is used again and the process is repeated until all deviations for each t and e are lower than a tolerance threshold. One very important feature of the presented method is that in this iterative process, optimality condition (B.5) (equivalent to constraint (B.2)) is always ensured, given that $\sum \Delta\lambda_{t,e}^{(h)} = 0$. This allows the aggregation of all batteries to equal the aggregated SOC at any time and scenario.

The outline of the proposed disaggregation algorithm is shown in figure 3.3.

Appendix C

Obtention of the robust counterpart

To introduce uncertainty in the decision making process through RO, the following canonical optimization problem is defined:

$$\text{minimize } \mathbf{c}'\mathbf{x} \tag{C.1}$$

s.t.

$$\mathbf{A}\mathbf{x} \leq \mathbf{b} \tag{C.2}$$

$$\mathbf{x} \geq \mathbf{0} \tag{C.3}$$

If uncertainty in cost coefficients ($\mathbf{c}$) is present in the model in such a way that maximum deviation for a given coefficient j is given by $(c_j + c_j^{max})$, an optimal solution ($\mathbf{x}^*$) must satisfy the worst case scenario (robust solution):

$$\text{minimize } \mathbf{c}'\mathbf{x} + \max \left\{ \sum_{j \in J_0} c_j^{max} |x_j| \right\} \tag{C.4}$$

s.t.

$$\mathbf{A}\mathbf{x} \leq \mathbf{b} \tag{C.5}$$

$$\mathbf{x} \geq \mathbf{0} \tag{C.6}$$

A quantity $\Gamma \in [0, |J_0|]$ is introduced such that $|J_0|$ is the maximum number of uncertain coefficients. For a vector ($\mathbf{x}^*$), the following problem is defined:

$$\text{maximize } \sum_{j \in J_0} c_j^{max} |x_j^*| w_i \tag{C.7}$$

s.t.

$$\sum_{j \in J_0} w_j \leq \Gamma \tag{C.8}$$

$$0 \leq w_j \leq 1,\ j \in J_0 \tag{C.9}$$

In the previous problem, Γ aims to measure the level of protection of an optimal solution ($\mathbf{x}^*$) in the original problem, against Γ deviations of (c). Auxiliary variable w_j takes values between 0 and 1 in order to impact cost coefficients and maximize deviation for a given Γ.

Next, by strong duality, if problem (C.7)-(C.9) is feasible and bounded, the dual problem is also feasible and bounded, and their objective function values are the same. The equivalent dual problem is then:

$$\text{minimize} \sum_{j \in J_0} q_j + \Gamma z \tag{C.10}$$

s.t.

$$q_j + \Gamma z \geq c_j^{max} |x_j^*|,\ j \in J_0 \tag{C.11}$$

$$z, q_j \geq 0,\ j \in J_0 \tag{C.12}$$

If the previous dual problem is substituted in (C.4)-(C.6), and auxiliary variable y_i is introduced, the following equivalent problem is obtained:

$$\text{minimize } \mathbf{c}'\mathbf{x} + \sum_{j \in J_0} q_j + \Gamma z \tag{C.13}$$

s.t.

$$\mathbf{A}\mathbf{x} \leq \mathbf{b} \tag{C.14}$$

$$q_j + \Gamma z \geq c_j^{max} y_i,\ j \in J_0 \tag{C.15}$$

$$-y_i \leq x_j \leq y_i,\ j \in J_0 \tag{C.16}$$

$$z, q_j, y_i \geq 0,\ j \in J_0 \tag{C.17}$$

$$\mathbf{x} \geq 0 \tag{C.18}$$

where z, q_j are dual variables. The problem in (C.13)-(C.18) is the robust counterpart when cost coefficients present uncertainty. The robust control parameter Γ controls conservatism of the solution. If $\Gamma = 0$, the resulting problem is the deterministic one in (C.1)-(C.3). This procedure is applied to the objective function (2.44) to reflect uncertainty in coefficients π_t, μ_t^- and μ_t^+.

When the uncertainty is related to the right-hand side (RHS) ($\mathbf{b}$) of the optimization problem (i.e. uncertainty in PV and load), the equivalent optimization problem that has to be solved to satisfy the worst case scenario is the following:

$$\text{minimize } \mathbf{c}'\mathbf{x} \tag{C.19}$$

s.t.

$$\sum_j a_{ij} x_j - \max\ \{b_i^{max}\} \leq b_i,\ \forall i \tag{C.20}$$

$$x_j \geq 0,\ \forall j \tag{C.21}$$

After defining the maximization problem for the deviation of the RHS, the equivalent dual problem associated with each constraint i, is the following:

$$\text{minimize } q_i + \Gamma z_i \tag{C.22}$$

s.t.

$$q_i + \Gamma z_i \geq b_i^{max} y_i \tag{C.23}$$

$$z_i, q_i \geq 0 \tag{C.24}$$

$$y_i \geq 1 \tag{C.25}$$

After substitution of the previous robust counterpart in each constraint i of (C.19)-(C.21), the equivalent takes the following form:

$$\text{minimize } \mathbf{c}'\mathbf{x} \tag{C.26}$$

s.t.

$$\sum_j a_{ij}x_j \leq b_i + q_i + \Gamma z_i,\ \forall i \tag{C.27}$$

$$q_i + \Gamma z_i \geq b_i^{max} y_i,\ \forall i \tag{C.28}$$

$$z_i, q_i \geq 0,\ \forall i \tag{C.29}$$

$$y_i \geq 1,\ \forall i \tag{C.30}$$

$$x_j \geq 0,\ \forall j \tag{C.31}$$

In the formulation of this thesis, the following RHS quantities present uncertain behavior: electrical demand $\hat{D}_{t,h}$, PV production $\hat{P}_t^{pv}$ and thermal demand $\hat{Q}_{t-1,s,h}$.

Appendix D

General outline of "Home Analytics" tool for project SENSIBLE

The presented work is within the scope of the project SENSIBLE (Storage Enabled Sustainable Energy for Buildings and Communities) which is a Horizon 2020 funded initiative. According to the SENSIBLE use case "Flexibility and demand side management in the market participation", the proposed model is focused specifically on the day-ahead time frame with the purpose of optimizing clients energy through the management of flexibilities at the building level, where it is assumed that clients are equipped with management tools and flexible loads, which is the case in Evora's Demostrator in Portugal. In the framework of this project, the "Home Analytics" tools aimed to provide a calculation of the individual (per household) and aggregated available flexibility coming from the devices installed in the test system. In addition to the availability, the tool returns an estimation of the cost of using this flexibility.

The Home Analytics tools is composed by two algorithms: 1) Flexibility forecast and 2) flexibility dispatch. Each algorithm takes into account the topology of the HEMS in which certain points of aggregation (or buses) have a number of households and devices to be controlled down-stream. For instance, as it can be seen in figure D.1, the bus 676 has 16 houses downstream with a total of 16 PV panels, 11 batteries and 11 electric water heaters. The calculation of the flexibility capabilities will depend on the analysed point of aggregation (a bus or a house) and the downstream associated devices that can inject or withdraw power. Each aggregation point/device is classified as parent or child depending on the topology. For instance, bus 676 acts as a parent node for 16 houses that are classified as children, and house 3 is classified as parent of three children devices (one EWH, one PV and one battery). All of this information is contained in a topology input file.

D.0.1 Flexibility forecast

The Flexibility Forecast algorithm was developed in Python environment with the purpose of calculating the equivalent cost of injecting/absorbing power in different nodes of the system. The cost calculation takes into account the topology to deter-

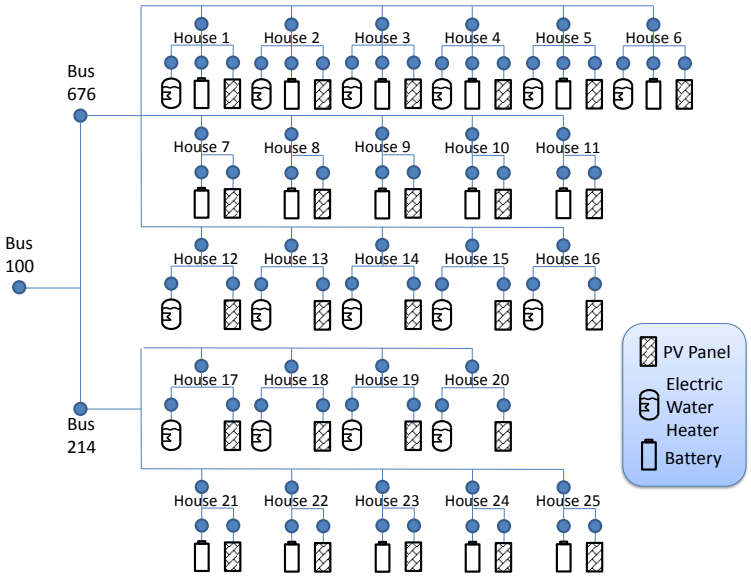


Figure D.1: Topology of the test system.

mine the downstream devices to be aggregated for cost calculation. For the case of batteries, an equivalent cost of operation is calculated by determining the associated DoD (Depth of Discharge) for full charging/discharging at each time step, and then calculating the equivalent cost from the DoD-cycling curve. For the case of the EWH, an operation cost was integrated by using the equivalent cycling for each time step and the cost information provided by the utility in Portugal. The algorithm returns a file for each aggregation point and each time step. The information in this file contains also the minimum and maximum values of energy and power that can be used for flexibility purposes. The main steps of the flexibility forecast algorithm are the following:

1. Read the topology and devices static information file.
2. List and loop over each parent in the topology file.
3. For the parent under analysis, list and loop over the downstream children.
4. Depending on the characteristic of the children,
   - if children is a battery, compute charging/discharging cycling cost,
   - if children is a PV, compute discharging cost,
   - if children is an EWH, compute charging cycling cost,
   - if children is not a device, look for downstream devices and repeat this step.

   Repeat this step until all children are analysed.
5. For the aggregated results in 4, calculate the maximum charging/ discharging power, the maximum energy storage capacity and the equivalent average

charging/discharging cost per kW associated to the parent, and then go to step 2.

6. Write the file with the results after repeating steps 2-5 for each time step.

D.0.2 Flexibility dispatch

The Flexibility Dispatch algorithm receives a file containing flexibility requirements to be disaggregated and assigned to the devices. The allocation and disaggregation is carried out by assigning power injection/absorption to the most economic devices, and giving priority to the ones with more energy availability for the case of same cost. This allows minimization of control actions on the entire system. The algorithm returns a set-point plan for each device and time step. The main steps of the flexibility dispatch algorithm are the following:

1. Read the flexibility request file.
2. Loop over each time step.
3. Identify the aggregation points (buses) with flexibility needs to be dispatched. Loop over those points.
4. For the downstream children of the point with flexibility needs, adjust device settings according to the following rule:
    - If the flexibility need is positive (power from network to devices):
        - List the batteries downstream the aggregation point in descending order of equivalent cycling cost and start filling flexibility request by setting the batteries in charging mode. If more flexibility is needed to complete the request,
        - list the EWHs downstream the aggregation point in descending order of available storage and start filling flexibility request by charging EWHs. If more flexibility is needed to complete the request,
        - list the PV downstream the aggregation point in descending order of forecasted PV production and start decreasing filling flexibility request by decreasing the PV production.
    - If the flexibility need is negative (injection from devices to network):
        - List the batteries downstream the aggregation point in descending order of equivalent cycling cost and start filling flexibility request by setting the batteries in discharging mode.
5. Update the state of all devices and go to step 2 if more time steps need to be analysed, otherwise go to 6.
6. Write the file with the power stetting for each device as calculated in 4.

Appendix E

Extended abstract in French

E.1 Résumé du chapitre: Introduction

Les systèmes de stockage d'énergie (ESS) et la gestion de la demande (DSM) jouent un rôle important pour soutenir les décisions prises par les multiples acteurs présents dans le système. Dans le cas des ressources énergétiques distribuées (DER), la gestion des appareils est également importante pour compenser localement les variations de charge ou de sources d'énergie renouvelables, ainsi que pour atteindre un coût d'exploitation minimal. En ce qui concerne les opportunités potentielles des opérateurs de réseau de distribution, nous pouvons énumérer de nombreux avantages techniques tels que le support de tension, la compensation de puissance réactive, la gestion de la congestion, le report de l'investissement, le suivi de la charge, la réduction des pertes, entre autres. En outre, la présence de microgrids (MG) dans les couches inférieures du réseau de distribution sous la forme de aggrégateurs bâtiments/domiciles intelligents ou de communautés énergétiques positionne des dispositifs de gestion active de la charge et de stockage afin de faciliter les décisions opérationnelles et d'augmenter/réduire les bénéfices / coûts lorsque les règles du marché permettent de négocier des services de flexibilité sur les marchés de gros, locaux ou de services auxiliaires. Différents acteurs peuvent être impliqués dans la propriété et le fonctionnement du DER. Par conséquent, les modèles et le potentiel des multiples services que ces ressources peuvent fournir doivent être explorés.

Review [4] souligne l'absence d'un cadre commun permettant de définir et de classifier la flexibilité dans les nouveaux contextes des systèmes d'alimentation. En outre, une distinction claire des impacts de la fiabilité et de la flexibilité sur les systèmes électriques doit également être développée, en tenant compte également de l'inclusion de mesures de flexibilité probabilistes. Ces derniers, considérant que les sources d'intermittence et de perturbation sont régies par un comportement incertain, et que cette incertitude pourrait entraîner des problèmes techniques et économiques.

Les barrières existantes sont logiques, étant donné que les marchés ont été conçus avant la pénétration massive des énergies renouvelables et de la production décentralisée. Par conséquent, la redéfinition des responsabilités et des rôles des agrégateurs, des centrales électriques virtuelles (VPP), des MG et d'autres acteurs doit être alignée sur les besoins actuels et les lacunes de la réglementation. En outre, une demande de flexibilité décentralisée et coordonnée devrait être possible pour

les gestionnaires du réseau de distribution (DSO) et les gestionnaires du réseau de distribution (TSO).

Dans l'article [5] une différence est établie entre la flexibilité technique et celle du marché pour conclure que la flexibilité peut être utilisée pour équilibrer le système et résoudre les contraintes, tandis que la flexibilité disponible peut être utilisée par différents acteurs du marché afin de maximiser les portefeuilles individuels . Les auteurs soutiennent que ce scénario peut générer des conflits d'intérêts non seulement entre les propriétaires de réseaux à différents niveaux, mais également entre les acteurs participants. Dans le cas concret des échanges de flexibilité locaux, les auteurs soulignent trois directions principales: 1) tirer parti des marchés actuels (journalier, intra-journalier, équilibrage); 2) créer des marchés nouveaux et distincts; et 3) la flexibilité des contrats en tant que réserve système. Avec le développement récent des possibilités de production et de contrôle des énergies renouvelables décentralisées, les modèles, les règles du marché et le cadre permettant la flexibilité dans les couches inférieures du réseau font toujours défaut. Au niveau MT et BT, non seulement ESS est appelé à jouer un rôle important dans le fonctionnement du réseau flexible, mais l'agrégation des ressources au niveau des bâtiments et des logements doit également jouer un rôle important dans l'optimisation du portefeuille des différents acteurs tout en offrant de la flexibilité [6].

Les autorités européennes ont souligné qu'il importait de promouvoir la participation des consommateurs aux marchés de l'énergie en créant les marchés nécessaires ou en supprimant les barrières commerciales pour permettre la participation des communautés locales de l'énergie [7]. Cette stimulation des consommateurs à les placer au centre du marché de l'énergie peut être réalisée à partir de points de vue individuels ou par des mécanismes agrégés. Dans ce contexte, les DSO sont également encouragés à gérer les défis posés par la production d'énergie renouvelable en utilisant des stratégies locales, ce qui est également conforme à la promotion des cadres de coordination des consommateurs et des DSO. Ce changement de paradigme permet aux consommateurs d'intégrer davantage la production locale aux fins d'autoconsommation et de participation au marché, leur permettant ainsi de devenir des consommateurs potentiels.

Dans cette thèse, la définition de «prosommateur» correspond au rapport de la Commission européenne, qui définit les consommateurs résidentiels comme des consommateurs capables de produire leur propre énergie, l'accent étant mis sur la production sur site au moyen de systèmes photovoltaïques solaires à petite échelle [8]. Il convient de mentionner que l'énergie solaire photovoltaïque est l'une des technologies de production les plus répandues dans le secteur résidentiel [9]. Les recommandations actuelles visant à permettre aux utilisateurs potentiels d'agir comme acteurs clés du processus de transition énergétique mettent l'accent sur la promotion des technologies de stockage, l'engagement des consommateurs auprès des agrégateurs, leur permettant de participer au marché de l'électricité avec une rémunération adéquate de la flexibilité. Afin de contribuer aux orientations mentionnées et aux priorités établies par l'industrie et le gouvernement, de nouveaux modèles mathématiques permettant de gérer de manière optimale les ressources des futurs consommateurs et d'exploiter la flexibilité doivent être développés. Étant donné que la participation directe des prosommateurs rencontre encore des obstacles, les agrégateurs apparaissent comme une option permettant de combler le fossé. Cependant,

outre les barrières de marché bien connues dépendant de l'évolution des différents cadres réglementaires, les nouveaux modèles d'optimisation mathématique doivent tenir compte de l'incertitude et imposer une complexité supplémentaire au processus de prise de décision. L'objectif de cette recherche est d'évaluer les avantages et les limites des modèles mathématiques sous incertitude pour les agrégateurs de la flexibilité du client potentiel participant au marché énergétique journalière et aux marchés de la flexibilité locaux. L'agrégateur gère les dispositifs de stockage résidentiels et les sources d'énergie renouvelables en tant que sources de flexibilité, participant directement au marché de l'énergie libéralisé et offrant plusieurs services afin de minimiser les coûts opérationnels.

À partir de l'objectif général précédent, trois objectifs spécifiques sont détaillés:

- Inclure la flexibilité basée sur le stockage au niveau résidentiel du point de vue d'un agrégateur, en tenant compte des modèles de vieillissement et de dégradation pour le stockage électrochimique. Le stockage résidentiel est composé des capacités de stockage thermique et électrochimique installées au niveau de la maison.

- Inclure l'incertitude de différentes sources (prix d'electricité, production renouvelable, consommation) dans la formulation mathématique afin de tester la performance des solutions pour une participation adéquate aux marchés de l'énergie.

- Déterminer les calendriers optimaux pour le lendemain, qui se traduisent par une minimisation des coûts pour l'agrégateur de flexibilité, y compris le marché de l'énergie traditionnel et de nouveaux systèmes d'offre de flexibilité locale.

Les principales contributions de cette thèse sont énumérées ci-dessous:

- Les interactions entre le stockage agrégé électrique et thermique sont analysées dans le contexte de la flexibilité résidentielle dans des conditions d'incertitude, et les avantages du fonctionnement coordonné sont détaillés.

- Deux alternatives pour inclure le coût de vieillissement de la batterie sont présentées. Tout d'abord, une approche originale appelée algorithme de désagrégation de stockage (SDA) basée sur la relaxation lagrangienne et l'algorithme de comptage Rainflow (RCA) est présentée. Cette méthode est présentée pour la première fois dans la littérature et permet de gérer le comportement cyclique complexe et de réduire l'espace de recherche d'optimisation. Deuxièmement, la modélisation explicite du coût du cycle de la batterie est présentée au moyen d'ensembles ordonnés spéciaux. Cette modélisation de la dégradation permet de saisir la relation non linéaire entre le DoD et le cycle de vie total afin de proposer des quantités suffisantes sur les marchés à un jour.

- Une stratégie de décomposition complétée par un optimiseur d'essaim concurrentiel est proposée. Cette approche permet de résoudre séparément le problème de cyclage de la batterie résolu par le SDA et la planification des ressources pour le lendemain. Cette logique de séparation des problèmes pour les ressources de planification d'un agrégateur n'a encore jamais été utilisée par des recherches afin de résoudre le problème de planification résultant, notamment le vieillissement cyclique de BESS.

- Les sources d'incertitude suivantes sont prises en compte: demande d'électricité et de chaleur, production photovoltaïque et prix de l'énergie. Ces incertitudes sont incluses dans le modèle mathématique au moyen de la théorie ARO.

- Une méthodologie est proposée pour détecter les meilleures solutions robustes pour la participation au jour le jour sur les marchés de l'énergie, basée sur la théorie de Pareto-optimality. Cette approche permet d'analyser la performance de plusieurs décisions robustes prises au jour le jour et de sélectionner le front de Pareto contenant des solutions offrant le meilleur compromis entre coût et risque. Dans ce cas, le risque est mesuré par l'écart type après l'exécution de la simulation de Monte Carlo.

- Une nouvelle stratégie de gestion de la flexibilité locale est proposée, qui repose sur deux produits: 1) des offres de flexibilité sur un marché local; et 2) prise en charge de contraintes locales pour le DSO sous la forme de la puissance nette et du taux nette du rampe autorisés.

- Un modèle ARO est proposé pour la gestion coordonnée des ressources de la communauté énergétique et les enchères sur les marchés de gros et de flexibilité locaux. La contrepartie robuste comprend l'incertitude des prix de l'énergie / déséquilibre, la production photovoltaïque, la demande en électricité et la consommation thermique.

- Les résultats numériques démontrent que le cadre d'enchères stratégique est suffisamment robuste pour permettre une participation coordonnée sur trois marchés différents (énergie, flexibilité locale et échanges bilatéraux avec DSO) avec divers mécanismes de règlement.

E.2 Résumé du chapitre: Modélisation mathématique de la flexibilité pour l'agrégation résidentielle

Le système de gestion énergétique des maisons intelligentes (HEMS) proposé à des fins de modélisation est composé de panneaux solaires, de batteries Li-ion, de batteries de stockage en ligne dotées de capacités de stockage, d'une connexion au réseau principal et d'un certain nombre de foyers. Chaque ménage comprend une charge de base électrique totale à fournir et une charge thermique qui doit être satisfaite par un EWH, qui stocke également de l'énergie sous forme de chaleur, jouant ainsi le rôle de charge flexible. L'interaction de tous les appareils permet un fonctionnement flexible du système pour atteindre un coût minimum.

En général, l'entrée EWH et la charge électrique pendant la période de 24h peuvent être satisfaites par le réseau principal, les panneaux solaires et la puissance injectée par les batteries. L'idée est d'obtenir un coût d'exploitation minimal en ajustant les paramètres des appareils afin de gérer les ressources de manière optimale.

Une des caractéristiques du système HEMS proposé est la possibilité de contrôler indépendamment le BESS et le EWH lorsque ce dernier dispose de capacités de stockage et de contrôle. Cela signifie que le réseau BT n'alimente pas directement la charge thermique. En d'autres termes, cette charge est alimentée par l'énergie stockée disponible dans le TES et l'entrée pour l'EWH est considérée comme une

charge du réseau BT. Ceci peut être vu comme une charge flexible qui réagit en fonction du prix d'opportunité saisi par le modèle d'optimisation en stockant de l'eau chaude même si elle n'est pas utilisée immédiatement par les occupants.

Le modèle actuel suppose un agrégateur de flexibilité résidentielle qui participe au marché de l'énergie journalière en contrôlant les points de réglage sur un horizon prédéfini de pas de temps de 24 heures (T). La fonction objectif vise à minimiser les achats d'énergie sur le marché de gros et les coûts opérationnels globaux. Ce modèle prend en compte les prix de l'énergie et la possibilité d'acheter ou de vendre de l'énergie au point de couplage commun (PCC). De plus, l'agrégateur compense les écarts d'achat journaliers avec les niveaux de production et de demande réels en participant au marché des déséquilibres.

Le problème déterministe présente trois types de flexibilités à gérer par un agrégateur: production photovoltaïque, stockage électrochimique et stockage thermique . Le résultat de cette optimisation renvoie les consignes de tous les appareils et l'énergie échangée avec le marché de gros afin d'obtenir un coût d'exploitation minimal pour l'ensemble du portefeuille, tout en respectant la demande électrique et thermique de chaque maison.

Les 25 maisons d'étude de cas sont situées dans un réseau LV-rural à Evora, au Portugal, comprenant la répartition des ressources indiquée dans la figure. Au total, il y a 25 panneaux photovoltaïques, 16 systèmes de stockage d'énergie par batterie (BESS) et 15 chauffe-eau électriques (EWH) pouvant agir en tant que stockage d'énergie thermique (TES). Le cas de test est composé du HEMS et des capacités de contrôle d'un agrégateur sur les paramètres du périphérique. L'exploitation et le contrôle des réseaux de distribution MT et BT sont effectués par le DSO et ne font pas partie des capacités ou des responsabilités de l'agrégateur.

Compte tenu de la difficulté d'incorporer mathématiquement le comptage des transitions / cycles des batteries dans le modèle d'optimisation, le problème peut être reformulé de manière à ce qu'un algorithme propose, de manière itérative, d'analyser des état de charge (SOC) à partir de deux perspectives: 1) le coût de vieillissement équivalent produit par ce SOC; et 2) le nombre minimal d'opérations journalières atteintes par l'agrégateur compte tenu du SOC proposé.

Si un algorithme est utilisé pour générer des SOC, le Rainflow Copunting Algorithm (RCA) peut être appliqué pour calculer un coût de dégradation équivalent dans la fonction objectif, et réaliser de manière itérative une solution de coût minimum. Dans ce travail, le Competitive Swarm Optimizer (CSO) est proposé comme métaheuristique.

Le problème d'optimisation complet peut être décomposé en deux sous-problèmes: l'un d'eux analyse les propositions SOC des batteries et calcule le coût équivalent en vieillissement cyclique correspondant; le deuxième sous-problème prend ce SOC comme une valeur fixe et calcule le coût journalier dû à l'achat d'énergie sur le marché de gros et aux paramètres des ressources restantes liées à la HEMS. Une fois les deux sous-problèmes résolus, on peut obtenir le coût total en additionnant simplement les deux résultats (achat d'énergie et coût du vieillissement).

Chaque solution (également appelée individu ou particule) proposée par le CSO devrait contenir les informations de SOC dans chaque pas de temps et chaque batterie, ce qui donnerait un espace de recherche dimensionnel $T \times N$. Etant donné que a) l'ensemble des prosommateurs a généralement plusieurs batteries à exploiter;

et b) les métaheuristiques étant sensibles à la taille de la zone de recherche, il devient important de réduire la taille des particules pour éviter des temps de calcul prohibitifs.

Cette thèse propose une agrégation virtuelle des batteries du système afin de réduire l'espace de recherche de $T \times N$ à T. Avec cette approche, la dimension sera la même, même si le système contient un nombre élevé de batteries. Etant donné qu'il existe un nombre infini de possibilités d'attribution de SOC individuels, lorsqu'un SOC agrégé est proposé, il devrait exister une désagrégation / attribution de charge économique pour chacune des batteries, et ceci est effectué en appliquant un algorithme de désagrégation de stockage (SDA) Lorsqu'un certain SOC est généré avec une métaheuristique, puis désagrégé au moyen de la SDA, le problème complet doit être reformulé. Ce sous-problème s'appelle le sous-problème thermique, puisqu'une fois qu'un SOC est connu, les points de consigne restants à déterminer dans chaque ménage sont ceux associés à l'EWH.

Notez que lorsque le SDA est appliqué, le SOC de chaque batterie est connu. Par conséquent, tous les paramètres de batteries peuvent être calculés et deviennent des paramètres connus pouvant être introduits dans le modèle. De plus, les contraintes binaires du BESS ne sont plus nécessaires.

La seconde alternative permettant de capturer la relation non linéaire des cycles de vie par rapport au DoD est une approche de linéarisation par morceaux.

La motivation de la linéarisation de la caractéristique de coût réside dans le fait que si les définitions auxquelles chaque cycle se produit peuvent être identifiées à l'aide d'un ensemble d'équations, un coût cyclique équivalent peut alors être déterminé de manière à ce que ces équations puissent être explicitement modélisées. et alimenté à un résolveur d'optimisation commerciale. Dans l'approche de décomposition développée dans la section précédente, la difficulté d'exprimer les équations de dégradation basées sur RCA sous forme fermée empêche de traiter le problème d'optimisation complet dans les résolveurs d'optimisation. On présente une option pour introduire un ensemble d'équations permettant de capturer et d'identifier les cycles à l'aide de variables auxiliaires et de contraintes, également appelées ensembles ordonnés spéciaux. De cette façon, l'utilisation d'une méta-heuristique est évitée et un problème MILP est obtenu et résolu avec un logiciel d'optimisation autonome. Si les solutions optimales de l'approche de décomposition et de la modélisation explicite sont comparées pour le même jour de simulation (15 novembre), ce résultat met en évidence une différence entre le coût de vieillissement cyclique équivalent et le coût de l'énergie journalière engagée sur le marché de gros. Bien que les simulations aient été effectuées pour le même système de test et le même jour du calendrier, des différences sont attendues pour les raisons suivantes.

Premièrement, la logique utilisée pour le calcul du nombre équivalent de cycles de batterie est différente dans les deux cas. Pour l'approche de décomposition, le calcul direct du vieillissement cyclique est basé sur la RCA, qui calcule des cycles de charge ou de décharge équivalents demi (ou complet) et identifie la plage de DoD à laquelle ces cycles se produisent. Cette méthodologie diffère de celle proposée dans la modélisation explicite, dans la mesure où cette dernière identifie uniquement les cycles de charge complets, en partant de l'hypothèse que la décharge aura toujours lieu à une heure plus tardive (ou plus tôt), étant donné que SOC doit être identique pour le premier et le dernière pas du temps. Il est donc naturel que les deux

approches entraînent une valeur différente de la dégradation équivalente à la batterie, même pour un événement rare dans lequel les SOC sont identiques.

Deuxièmement, étant donné qu'il existe une différence sous-jacente dans le calcul du cycle, la solution optimale restera également différente non seulement pour le SOC résultant, mais également pour le reste des variables d'optimisation, compte tenu de la corrélation inhérente. Ainsi, l'achat d'énergie le lendemain sera différent afin d'atteindre une solution de coût minimum. Ce fait explique pourquoi les deux approches ne peuvent pas être directement comparées pour conclure que l'une d'elles domine l'autre, mais on peut en conclure que chacune d'elles offre séparément de meilleures performances que dans le cas où le vieillissement cyclique est négligé. Malgré l'approche utilisée, des économies seront réalisées sur les coûts opérationnels globaux et la dégradation des batteries sera moins équivalente. Le modèle déterministe présenté associe la flexibilité liée aux systèmes BESS et EWH dans le but de présenter un cadre permettant de gérer de manière optimale les ressources HEMS en intégrant plusieurs aspects tels que: la charge et le stockage électriques/thermiques, les coûts de dégradation de la batterie et la gestion au niveau de la maison/bâtiment. Ces aspects, analysés du point de vue d'un agrégateur participant au marché journalièr et des déséquilibres. Pour le scénario de test particulier, lorsque BESS est inclus dans le modèle, une réduction de 2,15% est atteinte, par rapport à un scénario de base dans lequel aucune technologie de stockage n'est incluse. De plus, l'inclusion des EWH avec des capacités de stockage montre une réduction de 18,7%. Dans ce cas, les EWH agissent comme une charge flexible, étant donné que l'eau chaude peut être stockée pour une utilisation ultérieure, moyennant un certain prix.

De plus, l'inclusion de la flexibilité de stockage thermique diminue indirectement le cycle de la batterie, dans la mesure où, dans ce cas, les BESS sont soumis à des cycles moins profonds et moins fréquents, ce qui entraîne des coûts de dégradation équivalents moins élevés.

La même décomposition présentée dans cette thèse peut être utilisée non seulement dans la gestion de stockage de niveau résidentiel, mais dans n'importe quel niveau d'installations de stockage à intégrer pour une participation au marché. Par exemple, le stockage et les ressources au niveau des bâtiments commerciaux ont souvent une puissance/énergie nominale supérieure et, par conséquent, de meilleures possibilités de respecter les niveaux de soumission minimaux. En outre, ce cadre peut également s'intégrer dans des modèles dans lesquels d'autres agents disposant de batteries au niveau DSO/TSO sont disposés à participer aux marchés de l'énergie et des produits auxiliaires. Dans tous les cas, malgré l'agent, la propriété ou la taille de la batterie, la méthode de décomposition sera toujours valable. Très certainement avec une charge de calcul réduite étant donné que le stockage à l'échelle du réseau n'est généralement pas installé (et possédé) en grand nombre.

La deuxième alternative proposée pour inclure le cyclage était la modélisation explicite. Pour cette approche, des ensembles ordonnés spéciaux ont été utilisés pour détecter les cycles de charge et les DoDs auxquels ces cycles de charge ont lieu. Avec l'identification de ce DoD, un coût équivalent peut être trouvé au moyen d'une linéarisation par morceaux. Avec ce schéma, une réduction de 21,12% des coûts d'exploitation a été constatée par rapport à un modèle qui tient compte du vieillissement cyclique. Pour la modélisation explicite, 6 segments ont été utilisés pour modéliser les non-linéarités des coûts de cycle.

E.3 Résumé du chapitre: Agrégation de flexibilité résidentielle sous incertitude

Étant donné les multiples sources d'incertitude dans la planification des ressources de flexibilité, de nouvelles méthodes d'optimisation doivent être utilisées. Pour le traitement et la modélisation de l'incertitude dans un problème d'optimisation, trois directions principales sont identifiées.

Premièrement, si aucune information concernant les fonctions de densité de probabilité des variables incertaines n'est disponible, une approche possible consiste à utiliser la théorie de l'optimisation robuste (RO). Si des variables incertaines restent dans des limites connues, RO définit un budget d'incertitude et définit un nouveau problème d'optimisation devant être réalisable pour toutes les réalisations d'incertitude, ce qui conduit à une solution très conservatrice, comme indiqué dans [15, 66, 103]. Pour la gestion de la flexibilité, une solution robuste doit pouvoir résister à tout scénario de charge et à toute réalisation de système RES, tout en maintenant le fonctionnement possible de tous les appareils.

Un deuxième groupe concerne l'optimisation stochastique. Dans ce groupe, une sélection de scénarios avec une certaine probabilité doit être prédéfinie et intégrée à la formulation d'optimisation. Pour définir les scénarios, plusieurs méthodes peuvent être utilisées, telles que les méthodes d'estimation de points, les matrices orthogonales de Taguchi, les méthodes de distance de Kantorovich ou d'aggroupation en général. Cette approche n'est pas aussi robuste que RO, étant donné que la solution optimale est réalisable pour un nombre fini de réalisations d'incertitude, tout en aboutissant à des solutions moins coûteuses et moins conservatrices. Dans ce groupe de propositions, des problèmes d'optimisation en deux étapes peuvent être trouvés [31, 49, 92, 93] pour trouver une valeur de fonctionnement attendue. L'idée est de définir une première étape (ou ici une décision maintenant) avec des variables et des décisions qui correspondent généralement aux achats d'énergie engagés sur le marché journalièr et à l'engagement de production pour la production conventionnelle. Après cela, un ensemble de décisions secondaires (ou de recours) sont prises, en fonction des réalisations des variables incertaines. Pour les cas analysés, les décisions de la deuxième étape sont liées aux paramètres des dispositifs contrôlables, tels que les batteries, le stockage de chaleur, les installations de cogénération et la demande active. Cette approche présente également l'avantage de la simplicité de sa modélisation, avec le compromis d'augmenter le nombre de variables en fonction des scénarios à analyser dans la seconde étape.

Un troisième groupe est associé à la théorie des MPC. Cela semble convenir aux décisions à horizon glissant, telles que celles devant être prises sur les marchés intra-journalièr et en temps réel, où les dernières informations de prévision peuvent modifier certains paramètres de périphérique pour le programme d'opérations restant.

Les approches d'optimisation robustes visent à trouver des solutions optimales et réalisables sur un intervalle de valeurs représentant l'incertitude. Pour trouver une contrepartie robuste du problème déterministe, chaque contrainte contenant des paramètres avec incertitude doit être transformée au moyen d'une théorie de la dualité forte. Lors de l'inspection du modèle déterministe, quatre sources d'incertitude ont été identifiées: prix, production photovoltaïque, demande électrique et demande

thermique.

Une approche stochastique est mise en place en utilisant la méthode de décomposition et le SDA. L'approche stochastique en deux étapes montre l'importance de prendre en compte les incertitudes liées à la charge et au PV, afin d'éviter des coûts d'exploitation plus élevés par rapport aux approches déterministes. Dans notre cas, l'avantage de l'utilisation d'une approche stochastique est démontré au moyen du VSS. La réduction mensuelle moyenne des coûts d'exploitation mesurée par le VSS est de 5,8% et l'intervalle de réduction varie de 3,6% à 9,0%. Ces résultats montrent que considérer un modèle stochastique avec cycle de batterie conduit à des économies par rapport aux approches déterministes.

Les temps de calcul pour des systèmes de test plus grands restent adéquats pour la prise de décision d'un jour à l'autre. La caractéristique de la batterie virtuelle agrégée au moyen du SDA fait que l'augmentation du nombre de batteries dans le système de test n'impacte pas proportionnellement l'effort en temps, même dans le cas d'approches stochastiques. Cependant, étant donné que la structure proposée dans la littérature pour évaluer les solutions stochastiques (VSS) est basée sur l'univers des scénarios créés, les variables définies de deuxième étape (déséquilibres, paramètres des appareils) et leurs performances ne sont évaluées (et valides) que pour les scénarios proposés.

La contrepartie robuste d'un problème déterministe peut être trouvée en maximisant l'écart des paramètres incertains au sein de chaque contrainte. Un problème résultant est obtenu avec le théorème fort de la dualité.

Le résultat est un problème MILP qui peut être résolu avec des solveurs commerciaux standard. Trois paramètres de contrôle robustes peuvent être ajustés pour obtenir différentes enchères robustes à un jour. Chacun contrôle le conservatisme contre l'incertitude des prix de l'énergie, de la charge nette et de la charge thermique.

Afin d'analyser différents niveaux de conservatisme lors d'une enchère sur le marché de l'énergie à un jour, différentes combinaisons de paramètres doivent être analysées (ARO, version ajustable d'optimisation robuste). Lorsqu'une solution est obtenue pour une combinaison quelconque, l'engagement d'achat d'énergie et les paramètres de l'appareil sont déterminés. La performance de ce plan journalier est évaluée en calculant les déséquilibres de chaque pas de temps dus au déséquilibre énergétique. Un déséquilibre négatif/positif implique une manque/un excès d'énergie qui doit être acheté/vendu à des prix plus élevés/plus bas, ce qui entraîne des coûts supplémentaires pour l'opération. Chaque plan est soumis à une analyse de performance pour plusieurs réalisations de prix de l'énergie, de PV et de charge électrique et thermique au moyen d'une simulation de Monte Carlo (MC).

Outre ARO pour la modélisation de l'incertitude des prix, une autre option consiste à utiliser l'échantillonnage KDE pour créer plusieurs scénarios de prix et les utiliser pour une optimisation stochastique. Compte tenu de la nature de l'échantillonnage KDE disponible pour les prévisions de prix, comme expliqué dans la section 2.3.1, un ensemble de scénarios peut être obtenu et inclus dans le modèle d'optimisation au moyen d'une programmation stochastique. Les informations du KDE non paramétrique des 90 derniers jours précédant le jour de fonctionnement sont utilisées pour créer un certain nombre de scénarios de prix. Au début, chaque scénario de l'ensemble a la même probabilité. Étant donné qu'un grand nombre de scénarios peut entraîner des temps de calcul élevés, une technique de réduction de

scénario est mise en œuvre. Dans cette thèse, lorsque des scénarios sont envisagés pour modéliser l'incertitude de prix, un algorithme de réduction arrière basé sur la distance de Kantorovich (KD) [111] est utilisé pour obtenir un ensemble représentatif réduit. Trois modèles d'incertitude ont été inclus dans le modèle d'optimisation pour les simulations: prix de l'énergie, charge électrique, charge thermique et production photovoltaïque. La logique de décomposition est appliquée à une approche en deux étapes dans laquelle des scénarios PV et de demande sont créés en combinant des scénarios extrêmes basés sur des prévisions quantiles. Cette formulation est évaluée en utilisant les valeurs de la solution stochastique (VSS) comme mesure de performance. pour les cas analysés, le VSS montre de meilleures performances que le cas déterministe.

En cas d'incertitude de prix, deux approches ont été envisagées: la programmation stochastique et l'optimisation robuste. Pour la gestion des incertitudes dans la production de charge et PV, une optimisation robuste a été envisagée. Le modèle montre que l'inclusion du coût de dégradation explicite dans le modèle d'optimisation permet de réaliser des économies de coûts grâce à un cycle moins long de la batterie. Dans le cas concret des résultats présentés, une réduction de 34,07% a été réalisée. L'approche proposée, qui peut également être appliquée par des agrégateurs d'équipements de moyenne et grande taille, montre qu'en utilisant l'ARO pour la charge et le PV, et en analysant les interactions de paramètres robustes, différents niveaux de réduction des coûts par rapport à l'approche déterministe peuvent être atteints. Pour les simulations effectuées, des économies de coûts pouvant atteindre 5,7% ont été réalisées. Dans le cas de l'écart type (SD), le meilleur résultat a réduit de 36,4% les performances de la solution déterministe. Cela montre que non seulement les coûts escomptés peuvent être réduits, mais qu'un risque moins élevé est également associé à la prise de décision dans le cadre de cette approche.

Les résultats prouvent que l'utilisation de ARO augmente également la probabilité d'avoir des coûts prévus plus bas. En comparant le schéma déterministe, des probabilités allant jusqu'à 96,33 % sont obtenues en analysant les CDF. En outre, l'approche d'optimisation robuste affiche de meilleures performances que la solution déterministe malgré les intervalles de confiance de la charge nette. Dans le cas de l'approache hybride (HSR), des scénarios de prix ont été créés à l'aide de KDE. Une technique de réduction en arrière basée sur la distance de Kantorovich est utilisée pour obtenir un ensemble réduit de scénarios. Pour les simulations d'exécution, l'approche hybride montre avoir de meilleures performances que l'approche déterministe et certaines des solutions ARO. Cependant, certaines solutions ARO offrent de meilleures performances que le système grande vitesse, tant du point de vue du coût moyen que de celui du développement durable. En particulier, l'option 4: un ARO complet séparé avec Γ^2 présente de meilleures performances que le reste des alternatives dans plusieurs des descripteurs mesurés. Il présente également le coût opérationnel moyen inférieur de toutes les simulations effectuées. Dans ce cas, un traitement séparé de l'incertitude pour la charge et la PV permet de trouver une contrepartie robuste et, partant, deux paramètres robustes distincts permettant d'ajuster et d'obtenir des coûts et des SD plus bas.

E.4 Résumé du chapitre: Agrégation de flexibilité pour la participation à plusieurs marchés

Ce chapitre vise à combler une lacune dans la littérature concernant les stratégies d'appel d'offres des agrégateurs de maisons intelligentes pour une participation coordonnée aux marchés de gros de l'énergie et aux marchés locaux de la flexibilité émergents, en tenant compte également des incertitudes sur les prix, la production et la demande de systèmes photovoltaïques. À la connaissance des auteurs, ces aspects combinés n'ont jamais été abordés du point de vue d'un agrégateur contrôlant les marges de manœuvre résidentielles, données en l'occurrence par les panneaux photovoltaïques et le stockage thermique et électrochimique.

Pour démontrer les effets de la flexibilité locale sur l'agrégation des ressources et l'énergie engagée au lendemain, un modèle simplifié, qui néglige le cycle de la batterie, sera utilisé dans un premier temps. Ce modèle utilise une modélisation des prix basée sur des scénarios et une optimisation robuste pour l'incertitude de la PV et de la demande.

L'agrégateur de flexibilité participe à l'optimisation de son portefeuille sur les marchés du jour et du déséquilibre, tout en respectant les limites physiques des micro-réseaux et les signaux envoyés par le DSO local concernant les produits de flexibilité pour la gestion de la charge. Des flux d'énergie bidirectionnels peuvent se produire au niveau du CCP avec le réseau DSO local. Les exigences de flexibilité du DSO dans le PCC sont de deux types: a) la flexibilité de l'énergie, qui impose des limites ou certains modèles d'échange d'énergie en fonction des besoins du réseau à des moments spécifiques; b) la flexibilité en rampe, qui limite la rampe de charge nette vue par le DSO local.

Le DSO et l'agrégateur établissent la communication pour envoyer / recevoir des informations, tandis que seul l'agrégateur dispose de capacités de communication et de contrôle avec des appareils situés au niveau local. Il est supposé l'existence de la plate-forme informatique et de communication nécessaire, de sorte que l'agrégateur contrôle les appareils au niveau du domicile et décide de leurs points de consigne.

Les décisions concernant les exigences de flexibilité des DSO et les produits au niveau du CCP correspondent, entre autres, à une analyse du réseau concernant les limites de tension, la gestion de la congestion, la dégradation des équipements et la maintenance planifiée. La définition de ces exigences et la conception du marché du paiement de ce service sont hors du champ de cette thèse. L'approche actuelle propose une stratégie d'appel d'offres pour un agrégateur de maisons intelligentes, présentes dans une communauté énergétique connectée au réseau de distribution principal. Certains ménages disposent de panneaux solaires, de batteries li-ion et de dispositifs de stockage de chaleur. Cette stratégie est composée d'interactions de l'agrégateur avec trois entités: marché de gros, DSO et marché de la flexibilité locale. L'interaction avec le marché de gros s'établit de manière traditionnelle, l'agrégateur engageant une certaine quantité d'énergie sur le marché journalièr, et le jour de l'exploitation, les écarts sont réglés sous forme de déséquilibres négatifs et positifs.

L'interaction avec le DSO, comme expliqué précédemment pour le cas hybride, est donnée en termes de prise en charge de la contrainte opérationnelle au niveau du CCP. Concrètement, deux types de contraintes / produits pouvant être activés par le DSO sont pris en compte dans ce travail: 1) les contraintes de rampe (R_t [MW/h])

et 2) Power-Max, dans lequel agrégateur veille à ce que son portefeuille local ne dépasse pas $P_t^{PCC_{max}}$ [kW]. Les produits de rampe sont motivés par la nécessité de compenser la variabilité de la pénétration croissante des énergies renouvelables dans les réseaux de distribution; et Power-Max permet une modulation de crête pour contrôler les surcharges ou promouvoir le report d'investissement [139,140]. Compte tenu de la difficulté de créer un tuple pour décrire la temporalité / la quantité de ces produits afin qu'ils s'intègrent aux architectures traditionnelles d'enchères, des contrats bilatéraux sont envisagés entre les deux agents [138, 139] pour rémunérer le service. Les possibilités de jeu sont réduites pour l'agrégateur, à condition que les offres à prix élevé ne soient pas attractives pour le gestionnaire de réseau de distribution et que des actions de contrôle de réseau standard puissent être préférées. De plus, parce que la congestion artificielle / forcée conduira l'agrégateur à une planification et à des plans d'enchères sous-optimaux.

L'agrégateur et l'opérateur de marché local (LMO) interagissent de manière à ce que, lorsque le DSO (ou un autre tiers) ait besoin de flexibilité, le LMO communique avec l'agrégateur afin de demander une offre de flexibilité. Si la flexibilité est accordée à l'agrégateur, il recevra le prix de l'offre (paiement en tant qu'offre) pour la fourniture du service, comme c'est le cas pour les marchés des services auxiliaires et des services, et pour éviter une augmentation du prix des services de flexibilité locaux. Les spécificités du concept de conception du marché et de l'architecture, l'algorithme de compensation de la flexibilité, qui est une tâche exécutée par le LMO, ne font pas partie du cadre et des objectifs de cette thèse.

Les principales étapes et la chronologie du processus impliquant la participation de l'agrégateur sont décrites comme suit. Tout d'abord, l'agrégateur rassemble les informations relatives aux prévisions PV, à la disponibilité des appareils, aux prévisions de consommation et aux prévisions de prix de l'énergie. Avec ces informations, l'agrégateur détermine une planification de base (sans contrainte) ou provisoire (dans la figure 4.6, référencée sous le nom action Ⓐ) qui minimise les coûts totaux d'exploitation, en supposant que les contraintes opérationnelles imposées par le DSO ne soient pas respectées. PCC. Le DSO détermine ensuite l'état de fonctionnement attendu du réseau et envoie des contraintes de montée en puissance ou de limite de puissance à l'agrégateur (et / ou à toutes les ressources distribuées connectées au réseau de distribution) si nécessaire, comme indiqué dans la sous-section 4.3.3. Si aucune prise en charge de contrainte n'est requise par le DSO, il n'y a aucun changement dans la planification prévisionnelle. D'autre part, si une prise en charge de contraintes est nécessaire, une transaction bilatérale a lieu entre le gestionnaire de réseau de distribution et l'agrégateur, dans laquelle l'agrégateur doit payer le surcoût encouru pour le rééchelonnement de ses appareils afin de fournir les ajustements requis par le gestionnaire de réseau de distribution. Après cela, avec ou sans support de contrainte, l'agrégateur envoie son engagement énergétique journalier définitif au marché de gros (action Ⓑ).

Ensuite, le marché local de la flexibilité s'ouvre et reçoit des demandes du DSO ou d'autres parties (par exemple, BRP) spécifiant un tuple avec lieu, durée (t^{fl}) et quantité (P^{fl}) de la flexibilité requise. Avec ces informations, le LFO appelle les offres de flexibilité de tous les fournisseurs de flexibilité potentiels, parmi lesquels l'agrégateur. Si l'agrégateur dispose de la flexibilité nécessaire pour offrir, une offre contenant la quantité et le prix pour la période requise est envoyée à le LMO (action

Ⓒ). Cette offre doit être suffisamment robuste pour supporter les incertitudes liées aux prix de l'énergie et aux déséquilibres, à la production photovoltaïque et à la demande, et doit en outre être solide face à l'acceptation ou non de l'offre de flexibilité. Après cela, le LMO équilibre toutes les offres de flexibilité et informe l'agrégateur si son offre est acceptée.

Le planning de l'agrégateur (action Ⓓ) est tel qu'il prend en compte les sources d'incertitude mentionnées, la flexibilité attribuée et le support de contrainte, tout en minimisant les coûts opérationnels totaux.

Ensuite, pendant la journée d'opération, compte tenu des fluctuations de la production et de la demande de systèmes photovoltaïques, les écarts doivent être compensés par des achats/ventes d'énergie supplémentaires. Cela conduit à des déséquilibres négatifs/positifs réglés par le marché de gros. Le coût total de l'opération en temps réel (action Ⓔ) sera donné par la combinaison de l'engagement énergétique journalier, des pénalisations pour déséquilibre, des échanges bilatéraux avec le DSO (s'il est demandé) et du service de flexibilité fourni par LFM (si demandé). Compte tenu de la nature incertaine des prix de déséquilibre, la stratégie d'enchères des agrégateurs sur tous les marchés doit être solide dans le sens où elle permet de prévoir les déviations potentielles et, en conséquence, d'évaluer les services à offrir.

Le prix minimum qui devrait être payé à l'agrégateur pour fournir la flexibilité requise est donné par π^{fl}. Le modèle permet de garantir la flexibilité en ajustant les paramètres de périphérique des maisons intelligentes. Cet ensemble de signaux de contrôle, de paramètres et de pénalités prévues est appelé action Ⓓ. De plus, la caractéristique robuste de la formulation permet l'inclusion des déséquilibres potentiels et des pénalités correspondantes payées sur le marché de gros qui sont assumées par l'agrégateur. Dans cette approche, ces coûts sont pris en compte dans le processus d'appel d'offres afin de protéger l'agrégateur contre les incertitudes.

Cette méthode d'appel d'offres est suffisamment générale pour pouvoir soumissionner sur des systèmes du marché local qui acceptent non seulement des offres ponctuelles, mais également des courbes d'enchères. Les caractéristiques de la solide offre dépendront des capacités de l'algorithme de compensation utilisé par le LMO.

La performance vise à évaluer la capacité de l'agrégateur à respecter: 1) l'énergie journalière engagée; 2) le support de contrainte; et 3) la flexibilité allouée par le local, tout en minimisant le coût total d'exploitation face aux multiples sources d'incertitude. La simulation de Montecarlo est utilisée pour tester la robustesse de l'approche proposée pour plusieurs modèles de prix, de consommation et de production de PV générés de manière aléatoire au cours de la journée d'opération. Le calcul du coût total lorsque ces valeurs aléatoires sont générées et utilisées en tant qu'input est donné par les paiements d'énergie journaliers, le coût cyclique équivalent des batteries, les revenus générés par le support sous contrainte du DSO, les revenus générés par la flexibilité locale et la pénalisation due aux déséquilibres produits par la production / consommation en temps réel dans chaque ménage. La simulation de Montecarlo renvoie une mesure de la performance en termes de coût moyen et d'écart-type (SD), en tant que mesure du risque lié à une stratégie d'enchères robuste.

L'approche proposée présente un modèle mathématique incluant la flexibilité locale sous la forme 1) d'échange d'énergie net maximum autorisé et d'une rampe de montée en puissance au niveau du PCC et 2) d'une participation aux marchés de la

flexibilité locale. Les simulations ont analysé différents cas dans lesquels l'agrégateur participait à des marchés de gros et de flexibilité et déterminait les modifications à apporter au calendrier des dispositifs afin d'obtenir un coût d'exploitation minimal tout en respectant les contraintes de flexibilité, les demandes de flexibilité et l'énergie investies par DSO sur le marché day-ahead. Ces ajustements dans le fonctionnement de HEMS permettent à un agrégateur de participer au marché de l'électricité tout en coopérant avec le DSO local pour améliorer le fonctionnement du réseau et promouvoir la décentralisation du système électrique.

Lorsqu'aucune limite n'est imposée, cet échange d'énergie peut générer des valeurs compromettant le fonctionnement en amont, telles que le non-respect des limites de tension, la congestion des lignes de distribution, entre autres. Cela nécessite de prendre en compte les signaux DSO et de renforcer la coopération entre les agents afin de minimiser les risques potentiels.

Pour le cas stochastique / robuste et les valeurs de flexibilité analysées, le coût de fonctionnement de l'agrégateur augmente jusqu'à 2,3% par rapport à un scénario de base dans lequel aucun signal de flexibilité DSO n'est pris en compte. Ces informations sont utiles pour déterminer la rémunération potentielle de l'agrégateur pour la fourniture de services de flexibilité locaux, étant donné que la planification des ressources doit être modifiée pour offrir la flexibilité nécessaire.

Pour bien rémunérer les besoins de flexibilité, il faut tenir compte des variations des coûts opérationnels du microréseau afin de créer un environnement de marché avantageux pour tous les participants. Par exemple, si un marché local a été mis en place, des courbes d'enchères peuvent être soumises afin de tarifier et de rémunérer correctement le service fourni par le microréseau.

Pour le cadre robuste complet analysé, le coût escompté est supérieur au cas déterministe jusqu'à 15,7% lorsque la participation à de multiples marchés est autorisée. De plus, la participation à LFM permet de réduire les coûts opérationnels grâce à la rémunération fournie pour la fourniture du service de flexibilité. Cette approche robuste permet de placer des offres sur tous les marchés et de programmer des appareils de manière à minimiser les coûts tout en faisant face aux incertitudes générées par les prix de l'énergie, la production photovoltaïque et la charge.

La rémunération de la flexibilité est liée au niveau de robustesse. Si des paramètres robustes sont définis sur des valeurs élevées, le coût associé à la flexibilité augmente également, à condition que l'agrégateur inclut le coût prévu des éventuels écarts de prix, de la demande et de la production photovoltaïque. En outre, il existe un compromis entre le niveau de robustesse et les possibilités d'obtenir le service de flexibilité, étant donné que des coûts plus élevés pour la fourniture du service auront moins de chances d'être acheminés par le LMO. Cependant, dans le cas analysé, il existe une combinaison de paramètres robustes générant de meilleurs coûts que le schéma déterministe malgré la probabilité d'acceptation des offres.

E.5 Résumé du chapitre: Conclusions

L'agrégation de ressources au niveau résidentiel attire de plus en plus l'attention dans le contexte de la transition énergétique, compte tenu de son importance pour l'intégration des utilisateurs finaux dans le paradigme des réseaux intelligents. Cette thèse a présenté une revue de la littérature dans laquelle les tendances actuelles en

matière de traitement de l'incertitude dans le contexte du réseau intelligent ont été identifiées, et les opportunités d'utilisation d'une optimisation robuste pour l'agrégation de clients potentiels ont été détectées, en particulier dans le cas de la version ajustable. En outre, les alternatives de calcul du coût de vieillissement lié au cycle ont été analysées et les options adéquates pour les marchés de l'électricité à court terme ont été identifiées. La revue de littérature a également présenté les options actuelles pour exploiter la flexibilité des consommateurs potentiels sur plusieurs marchés, en mettant un accent particulier sur les marchés de flexibilité locaux. Les principales contributions de cette thèse sont liées à la modélisation de l'incertitude dans le modèle d'optimisation de la participation d'un agrégateur à des marchés de l'énergie à court terme. Les prix de l'énergie, la demande et la production photovoltaïque sont inclus comme sources d'incertitude via ARO. Dans ce contexte, des modèles de cycle de batterie sont également inclus et une participation et des offres sur les marchés de l'énergie traditionnels ainsi que sur les nouveaux marchés de la flexibilité locale sont proposées.

Cette thèse a été développée en trois parties principales: chapitre 2, a présenté les généralités du modèle mathématique déterministe et deux alternatives pour l'inclusion du vieillissement de la batterie. Le chapitre 3 a développé le modèle en présence d'incertitudes et enfin le chapitre 4 a présenté une stratégie d'appel d'offres robuste sur les marchés locaux de la flexibilité.

L'agrégation et l'interaction de différentes sources de flexibilité entraînent une réduction des coûts d'exploitation pour un agent du marché en charge du contrôle de plusieurs appareils au niveau résidentiel. Dans le cas du présent travail, et plus particulièrement dans le chapitre 2, les interactions des systèmes photovoltaïques, des chauffe-eau électriques et des batteries sont analysées. Le meilleur comportement du point de vue des coûts opérationnels pour une participation au marché journalière est obtenu lorsque toutes les sources de flexibilité sont incluses. Dans le cas des EWH, qui agissent en tant que stockage thermique, le comportement est similaire à une charge flexible, étant donné que le modèle de consommation varie en fonction du coût de l'opportunité et des besoins en charge thermique.

Les agrégateurs ont généralement plusieurs actifs à gérer et à en tirer profit. Cela aiderait à surmonter les obstacles potentiels du marché en ce qui concerne les capacités installées minimales ou les quantités de soumission minimales (puissance/énergie) pour les appels d'offres sur les marchés de l'énergie et / ou des marchés auxiliaires. Un agrégateur peut aussi avoir un portefeuille combinaison de ressources telles que stockage de taille moyenne/grande, centrales hydroélectriques pompées, éoliennes, systèmes de ventilation, autres aggrégations de bâtiments, véhicules électriques, etc. Dans ce contexte, la HEMS proposée ferait partie des ressources à gérer. La première partie du chapitre 2 était également destinée à présenter une technique de décomposition permettant d'inclure la dégradation des batteries dans le modèle de l'agrégateur. Lorsque le SDA est utilisé pour désagréger une valeur SOC envoyée par un algorithme métaheuristique, une particule avec uniquement des positions T est nécessaire, malgré le nombre de batteries dans le système de test. Ceci est important, à condition que toute métaheuristique nécessite un effort de calcul plus important si la dimension de la variable de décision augmente. Par conséquent, le SDA permet de maintenir la taille des solutions constante.

Si le SDA doit être utilisé dans un cadre d'optimisation en deux étapes, la taille de la solution dépend de la définition des variables des première et deuxième étapes et du nombre correspondant de scénarios (N_e). La méthode de décomposition évite la complexité du traitement d'un problème MINLP et peut être utilisée et ajustée dans d'autres applications dans lesquelles les coûts de dégradation de la batterie doivent être pris en compte pour pouvoir soumissionner sur les marchés de l'énergie.

La variante de modélisation explicite présentée dans la dernière partie du chapitre 2 pour inclure la dégradation directement dans le modèle d'optimisation est basée sur la linéarisation par morceaux de la fonction de coût équivalente. Ce coût est représenté en fonction du DoD auquel chaque cycle de charge se produit. Il est important de mentionner que le coût de dégradation obtenu avec cette alternative est différent d'un coût obtenu avec un calcul expost avec le RCA, étant donné que le comptage de cycles diffère d'une méthode à l'autre, la comparaison directe des deux méthodes n'est donc pas adéquate. La modélisation explicite utilise efficacement les variables auxiliaires binaires introduites pour détecter les transitions d'état et le début des cycles de charge. Ces variables sont également présentes dans la fonction objectif pour activer le terme indépendant correspondant de la fonction de coût linéarisée. La modélisation explicite permet d'obtenir des approximations précises pour un nombre modéré de segments. Par exemple, dans ce travail, 6 segments suffisent pour garantir des erreurs inférieures à 0,05% dans le dernier coût d'opération. Les erreurs dans la fonction de dégradation isolée sont plus importantes et n'ont pas été utilisées pour sélectionner le nombre de segments. Cela s'explique par le fait que la fonction de coût de cycle est plus sensible aux changements du nombre de segments, à condition que chaque option puisse conduire à un point de consigne final différent pour les batteries, modifiant ainsi la valeur équivalente de dégradation. Par conséquent, il est plus logique d'analyser l'erreur de la fonction d'objectif d'opération journalière totale.

Dans le chapitre 3, les incertitudes des types suivants ont été prises en compte dans la formulation mathématique avec SO ou ARO: prix de l'énergie, consommation électrique, consommation thermique et production PV.

Lors de l'utilisation du théorème fort de la dualité pour obtenir la contrepartie robuste du modèle déterministe, et pour le cas spécifique de la PV et de la charge électrique, un calcul supplémentaire a été établi pour obtenir la charge nette à chaque pas de temps. Cette formulation permet d'avoir une équation de bilan énergétique plus compacte, à condition que deux sources d'incertitude soient converties en une. Il en résulte un budget unifié d'incertitude pour contrôler le conservatisme de la charge nette. De plus, de nouvelles contraintes $3 \times T$ dual et $2 \times T$ sont introduites. Une alternative a également été explorée, en maintenant des budgets séparés et des variables doubles pour la charge électrique et la PV. Bien que cette formulation entraîne un problème d'optimisation plus important, une gestion séparée des deux sources d'incertitude a des répercussions sur la performance des solutions et une meilleure atténuation du sur-conservatisme dans certains cas. Une modification supplémentaire a été apportée au modèle en utilisant le budget d'incertitude Γ^2. Cela permet de mieux exploiter les faibles valeurs du budget dans des intervalles plus rapprochés et de lutter contre le conservatisme excessif des solutions. En règle générale, ARO garantit un coût minimum garanti et réduit les déséquilibres. En

fonction de la conception du marché pour les agrégateurs et des prix de déséquilibre permettant de corriger les écarts, les performances globales et les valeurs absolues de réduction des coûts et du SD peuvent varier.

L'analyse des performances proposée a consisté à détecter la combinaison de paramètres robustes générés dans l'ensemble des solutions optimales de Pareto du point de vue du coût et de l'écart type, lorsque la solution obtenue est soumise à des réalisations aléatoires des variables incertaines. Des solutions hybrides stochastiques / robustes et complètes robustes ont été comparées. Pour certaines combinaisons de paramètres robustes, la solution déterministe surpasse certaines solutions HSR et ARO complètes. Néanmoins, HSR et les solutions complètes ARO peuvent toujours être trouvés de manière à ce que le coût et le SD surpassent l'approche déterministe.

La fourniture locale de flexibilites a été explorée au chapitre 4. Dans ce cas, un cadre permettant la participation à trois marchés différents a été proposé. Premièrement, participation journalière au marché de l'énergie et des déséquilibres; deuxièmement, transaction bilatérale de flexibilité locale avec DSO; et troisièmement, la participation à un marché local de flexibilité pour vendre de la flexibilité au DSO ou à d'autres tiers.

La coordination entre les agrégateurs résidentiels et les DSO est nécessaire et conduit à une transaction inhérente naturelle pour les deux agents. Cela s'explique par le fait qu'une programmation illimitée des appareils au niveau résidentiel peut entraîner des problèmes opérationnels dans le réseau en amont. Cette thèse propose deux types de produits de flexibilité à échanger directement avec le DSO: la puissance maximale autorisée au PCC et le taux rampe nette. L'activation de ces produits entraîne une modification du fonctionnement des appareils et donc un point de consigne sous-optimal différent, qui augmente les coûts opérationnels. Cette augmentation des coûts sert de signal de prix pour rémunérer la flexibilité fournie. Étant donné que les incertitudes sont prises en compte, les écarts pour respecter l'engagement de flexibilité sont minimes tout en maintenant un coût opérationnel minimal pour l'agrégateur.

Lorsque la flexibilité est échangée sur un marché de flexibilité local, le cadre proposé suppose qu'il existe un opérateur de marché local pour effacer le marché. Si la flexibilité est nécessaire, l'agrégateur peut soumettre des offres si nécessaire. Les offres de flexibilité explorées dans le chapitre 4 ont différents niveaux de robustesse en fonction du budget d'incertitude prédéfini. Les courbes d'enchères de flexibilité obtenues montrent que le prix de la flexibilité a tendance à être plus élevé si les paramètres robustes ont également des valeurs plus élevées. Cela s'explique par le fait que le modèle robuste est protégé contre l'incertitude mesurée par les déviations et la pénalisation qui en résulte (déséquilibre). Par conséquent, la solution robuste optimale prend en compte les modifications des paramètres des appareils et les besoins potentiels de l'agrégateur en termes de coûts supplémentaires en cas de déviations des paramètres incertains. Cette information est traduite en prix de flexibilité et les offres envoyées au marché local. Pour les simulations exécutées, une combinaison de paramètres robustes peut être trouvée pour obtenir une solution plus performante que les approches déterministes, malgré la probabilité d'acceptation des offres. Ceci est effectué en analysant uniquement les performances de la participation au marché de l'énergie, étant donné qu'il s'agit du scénario le plus conservateur, et

en tenant compte du fait que l'acceptation d'une offre conduit à une rémunération, le cas échéant. Il n'est donc pas nécessaire de procéder à une analyse exhaustive des performances pour tous les scénarios d'acceptation des offres. L'approche robuste proposée est capable de trouver des solutions optimales robustes même en l'absence de connaissance des probabilités d'acceptation des offres.

Cependant, si la probabilité d'acceptation devait être intégrée au modèle, des données historiques seraient nécessaires pour créer un modèle approprié. Cela montre l'importance d'une approche solide pour les marchés émergents de flexibilité locaux, à condition qu'il y ait toujours un manque d'informations historiques suffisantes pour créer des modèles appropriés basés sur des scénarios et une optimisation stochastique.

Bibliography

[1] International Energy Agency, *Energy Technology Perspectives 2017*. IEA, 2017. [Online]. Available: https://www.iea.org/etp2017/summary

[2] The European Commission, *Clean Energy for All Europeans*. The European Commission, 2016. [Online]. Available: https://ec.europa.eu/energy/en/topics/energy-strategy-and-energy-union/clean-energy-all-europeans

[3] The European Technology and Innovation Platform for Smart Networks for the Energy Transition, *Vision 2050: Integrating Smart Networks for the Energy Transition*. ETIP SNET, 2018. [Online]. Available: https://www.etip-snet.eu/etip_publ/etip-snet-vision-2050/

[4] M. Alizadeh, M. P. Moghaddam, N. Amjady, P. Siano, and M. Sheikh-El-Eslami, "Flexibility in future power systems with high renewable penetration: A review," *Renewable and Sustainable Energy Reviews*, vol. 57, pp. 1186 – 1193, 2016. [Online]. Available: http://www.sciencedirect.com/science/article/pii/S136403211501583X

[5] A. Ramos, C. D. Jonghe, V. Gómez, and R. Belmans, "Realizing the smart grid's potential: Defining local markets for flexibility," *Utilities Policy*, vol. 40, pp. 26 – 35, 2016. [Online]. Available: http://www.sciencedirect.com/science/article/pii/S0957178716300820

[6] A. M. Carreiro, H. M. Jorge, and C. H. Antunes, "Energy management systems aggregators: A literature survey," *Renewable and Sustainable Energy Reviews*, vol. 73, pp. 1160 – 1172, 2017. [Online]. Available: http://www.sciencedirect.com/science/article/pii/S1364032117301776

[7] European Commission, "Proposal for a REGULATION OF THE EUROPEAN PARLIAMENT AND OF THE COUNCIL on the internal market for electricity," Brussels, 2016.

[8] The European Commission, *Study on "Residential Prosumers in the European Energy Union"*. The European Commission, 2017. [Online]. Available: https://ec.europa.eu/commission/sites/beta-political/files/study-residential-prosumers-energy-union_en.pdf

[9] C. Eid, L. A. Bollinger, B. Koirala, D. Scholten, E. Facchinetti, J. Lilliestam, and R. Hakvoort, "Market integration of local energy systems: Is local energy management compatible with european regulation for retail

competition?" *Energy*, vol. 114, pp. 913 – 922, 2016. [Online]. Available: http://www.sciencedirect.com/science/article/pii/S0360544216311859

[10] R. Bessa, C. Moreira, B. Silva, and M. Matos, "Handling renewable energy variability and uncertainty in power systems operation," *Wiley Interdisciplinary Reviews: Energy and Environment*, vol. 3, no. 2, pp. 156–178. [Online]. Available: https://onlinelibrary.wiley.com/doi/abs/10.1002/wene.76

[11] S. Burger, J. P. Chaves-Ávila, C. Batlle, and I. J. Pérez-Arriaga, "A review of the value of aggregators in electricity systems," *Renewable and Sustainable Energy Reviews*, vol. 77, pp. 395 – 405, 2017. [Online]. Available: http://www.sciencedirect.com/science/article/pii/S1364032117305191

[12] H. Liang and W. Zhuang, "Stochastic modeling and optimization in a microgrid: A survey," *Energies*, vol. 7, no. 4, pp. 2027–2050, 2014. [Online]. Available: http://www.mdpi.com/1996-1073/7/4/2027

[13] J. R. Birge and F. Louveaux, *Introduction to Stochastic Programming*, 2nd ed. New York, NY, USA: Springer-Verlag, 2011.

[14] D. Bertsimas and M. Sim, "Robust discrete optimization and network flows," *Math. Program., Ser. B*, vol. 98, no. 1-3, pp. 49–71, 2003.

[15] G. Liu, Y. Xu, and K. Tomsovic, "Bidding strategy for microgrid in day-ahead market based on hybrid stochastic/robust optimization," *IEEE Transactions on Smart Grid*, vol. 7, no. 1, pp. 227–237, Jan 2016.

[16] R. Wang, P. Wang, and G. Xiao, "A robust optimization approach for energy generation scheduling in microgrids," *Energy Conversion and Management*, vol. 106, pp. 597 – 607, 2015. [Online]. Available: http://www.sciencedirect.com/science/article/pii/S0196890415009115

[17] J. Wang, H. Zhong, W. Tang, R. Rajagopal, Q. Xia, C. Kang, and Y. Wang, "Optimal bidding strategy for microgrids in joint energy and ancillary service markets considering flexible ramping products," *Applied Energy*, vol. 205, pp. 294 – 303, 2017. [Online]. Available: http://www.sciencedirect.com/science/article/pii/S0306261917309212

[18] W. Hu, P. Wang, and H. B. Gooi, "Toward optimal energy management of microgrids via robust two-stage optimization," *IEEE Transactions on Smart Grid*, vol. 9, no. 2, pp. 1161–1174, March 2018.

[19] G. Liu, M. Starke, B. Xiao, and K. Tomsovic, "Robust optimisation-based microgrid scheduling with islanding constraints," *IET Generation, Transmission Distribution*, vol. 11, no. 7, pp. 1820–1828, 2017.

[20] L. Wang, Q. Li, R. Ding, M. Sun, and G. Wang, "Integrated scheduling of energy supply and demand in microgrids under uncertainty: A robust multi-objective optimization approach," *Energy*, vol. 130, pp. 1 – 14, 2017. [Online]. Available: http://www.sciencedirect.com/science/article/pii/S0360544217306813

[21] E. Kuznetsova, Y.-F. Li, C. Ruiz, and E. Zio, "An integrated framework of agent-based modelling and robust optimization for microgrid energy management," *Applied Energy*, vol. 129, pp. 70 – 88, 2014. [Online]. Available: http://www.sciencedirect.com/science/article/pii/S0306261914003766

[22] R. Gupta and N. K. Gupta, "A robust optimization based approach for microgrid operation in deregulated environment," *Energy Conversion and Management*, vol. 93, pp. 121 – 131, 2015. [Online]. Available: http://www.sciencedirect.com/science/article/pii/S0196890415000126

[23] J. Wang, P. Li, K. Fang, and Y. Zhou, "Robust optimization for household load scheduling with uncertain parameters," *Applied Sciences*, vol. 8, no. 4, 2018. [Online]. Available: http://www.mdpi.com/2076-3417/8/4/575

[24] M. Ampatzis, P. H. Nguyen, I. G. . Kamphuis, and A. van Zwam, "Robust optimisation for deciding on real-time flexibility of storage-integrated photovoltaic units controlled by intelligent software agents," *IET Renewable Power Generation*, vol. 11, no. 12, pp. 1527–1533, 2017.

[25] M. Diekerhof, F. Peterssen, and A. Monti, "Hierarchical distributed robust optimization for demand response services," *IEEE Transactions on Smart Grid*, pp. 1–1, 2017.

[26] Y. Zhou, Z. Wei, G. Sun, K. W. Cheung, H. Zang, and S. Chen, "A robust optimization approach for integrated community energy system in energy and ancillary service markets," *Energy*, vol. 148, pp. 1 – 15, 2018. [Online]. Available: http://www.sciencedirect.com/science/article/pii/S0360544218300963

[27] D. Bertsimas, D. B. Brown, and C. Caramanis, "Theory and applications of robust optimization," *SIAM Review*, vol. 53, no. 3, pp. 464–501, 2011. [Online]. Available: https://doi.org/10.1137/080734510

[28] O. Kilkki, I. Seilonen, K. Zenger, and V. Vyatkin, "Optimizing residential heating and energy storage flexibility for frequency reserves," *International Journal of Electrical Power & Energy Systems*, vol. 100, pp. 540 – 549, 2018. [Online]. Available: http://www.sciencedirect.com/science/article/pii/S0142061517322615

[29] J. Li, Z. Wu, S. Zhou, H. Fu, and X. P. Zhang, "Aggregator service for pv and battery energy storage systems of residential building," *CSEE Journal of Power and Energy Systems*, vol. 1, no. 4, pp. 3–11, Dec 2015.

[30] G. Comodi, A. Giantomassi, M. Severini, S. Squartini, F. Ferracuti, A. Fonti, D. Nardi, M. Morodo, and F. Polonara, "Multi-apartment residential microgrid with electrical and thermal storage devices : Experimental analysis and simulation of energy management strategies," *Applied Energy*, vol. 137, pp. 854–866, 2015.

[31] N. Good, E. Karangelos, A. Navarro-Espinosa, and P. Mancarella, "Optimization under Uncertainty of Thermal Storage-Based Flexible Demand Response

with Quantification of Residential Users' Discomfort," *IEEE Transactions on Smart Grid*, vol. 6, no. 5, pp. 2333–2342, 2015.

[32] Z. Xu, X. Guan, Q. S. Jia, J. Wu, D. Wang, and S. Chen, "Performance analysis and comparison on energy storage devices for smart building energy management," *IEEE Transactions on Smart Grid*, vol. 3, no. 4, pp. 2136–2147, Dec 2012.

[33] A. Ouammi, "Optimal power scheduling for a cooperative network of smart residential buildings," *IEEE Transactions on Sustainable Energy*, vol. 7, no. 3, pp. 1317–1326, July 2016.

[34] X. Li, T. Borsche, and G. Andersson, "PV integration in Low-Voltage feeders with Demand Response," *2015 IEEE Eindhoven PowerTech, PowerTech 2015*, 2015.

[35] D. Dutt, "Life cycle analysis and recycling techniques of batteries used in renewable energy applications," in *2013 International Conference on New Concepts in Smart Cities: Fostering Public and Private Alliances (SmartMILE)*, Dec 2013, pp. 1–7.

[36] E. Sarasketa-Zabala, E. Martinez-Laserna, M. Berecibar, I. Gandiaga, L. Rodriguez-Martinez, and I. Villarreal, "Realistic lifetime prediction approach for li-ion batteries," *Applied Energy*, vol. 162, pp. 839 – 852, 2016. [Online]. Available: http://www.sciencedirect.com/science/article/pii/S0306261915013513

[37] B. Xu, J. Zhao, T. Zheng, E. Litvinov, and D. S. Kirschen, "Factoring the cycle aging cost of batteries participating in electricity markets," *IEEE Transactions on Power Systems*, vol. 33, no. 2, pp. 2248–2259, March 2018.

[38] B. Xu, Y. Shi, D. S. Kirschen, and B. Zhang, "Optimal regulation response of batteries under cycle aging mechanisms," in *2017 IEEE 56th Annual Conference on Decision and Control (CDC)*, Dec 2017, pp. 751–756.

[39] A. Esmat, J. Usaola, and M. Moreno, "Distribution-level flexibility market for congestion management," *Energies*, vol. 11, no. 5, 2018. [Online]. Available: http://www.mdpi.com/1996-1073/11/5/1056

[40] N. Holjevac, T. Capuder, N. Zhang, I. Kuzle, and C. Kang, "Corrective receding horizon scheduling of flexible distributed multi-energy microgrids," *Applied Energy*, 2017. [Online]. Available: http://www.sciencedirect.com/science/article/pii/S0306261917307973

[41] A. Esmat, J. Usaola, and M. Moreno, "A decentralized local flexibility market considering the uncertainty of demand," *Energies*, vol. 11, no. 8, 2018. [Online]. Available: http://www.mdpi.com/1996-1073/11/8/2078

[42] I. D. de Cerio Mendaza, I. G. Szczesny, J. R. Pillai, and B. Bak-Jensen, "Demand response control in low voltage grids for technical and commercial aggregation services," *IEEE Transactions on Smart Grid*, vol. 7, no. 6, pp. 2771–2780, Nov 2016.

[43] B. Morvaj, K. Knezović, R. Evins, and M. Marinelli, "Integrating multi-domain distributed energy systems with electric vehicle {PQ} flexibility: Optimal design and operation scheduling for sustainable low-voltage distribution grids," *Sustainable Energy, Grids and Networks*, vol. 8, pp. 51 – 61, 2016.

[44] P. Olivella-Rosell, E. Bullich-Massagué, M. Aragüés-Peñalba, A. Sumper, S. Ødegaard Ottesen, J.-A. Vidal-Clos, and R. Villafáfila-Robles, "Optimization problem for meeting distribution system operator requests in local flexibility markets with distributed energy resources," *Applied Energy*, vol. 210, pp. 881 – 895, 2018. [Online]. Available: http://www.sciencedirect.com/science/article/pii/S0306261917311522

[45] F. Lezama, J. Soares, P. Hernandez-Leal, M. Kaisers, T. Pinto, and Z. M. A. do Vale, "Local energy markets: Paving the path towards fully transactive energy systems," *IEEE Transactions on Power Systems*, pp. 1–1, 2018.

[46] A. Majzoobi and A. Khodaei, "Application of microgrids in supporting distribution grid flexibility," *IEEE Transactions on Power Systems*, vol. PP, no. 99, pp. 1–1, 2016.

[47] M. Ahmed and S. Kamalasadan, "An approach for local net-load ramp rate control using integrated energy storage based on least square error minimization technique," in *2018 IEEE Power and Energy Conference at Illinois (PECI)*, Feb 2018, pp. 1–6.

[48] G. Graditi, M. D. Somma, and P. Siano, "Optimal bidding strategy for a der aggregator in the day-ahead market in the presence of demand flexibility," *IEEE Transactions on Industrial Electronics*, pp. 1–1, 2018.

[49] D. T. Nguyen and L. B. Le, "Optimal bidding strategy for microgrids considering renewable energy and building thermal dynamics," *IEEE Transactions on Smart Grid*, vol. 5, no. 4, pp. 1608–1620, July 2014.

[50] C. A. Correa-Florez, A. Gerossier, A. Michiorri, and G. Kariniotakis, "Stochastic operation of home energy management systems including battery cycling," *Applied Energy*, vol. 225, pp. 1205 – 1218, 2018. [Online]. Available: http://www.sciencedirect.com/science/article/pii/S0306261918306597

[51] C. A. Correa-Florez, A. Michiorri, and G. Kariniotakis, "Robust optimization for day-ahead market participation of smart-home aggregators," *Applied Energy*, vol. 229, pp. 433 – 445, 2018. [Online]. Available: http://www.sciencedirect.com/science/article/pii/S0306261918311553

[52] C. A. Correa, A. Gerossier, A. Michiorri, and G. Kariniotakis, "Optimal scheduling of storage devices in smart buildings including battery cycling," in *2017 IEEE Manchester PowerTech*, June 2017, pp. 1–6.

[53] C. A. Correa-Florez, A. Gerossier, A. Michiorri, R. Girard, and G. Kariniotakis, "Residential electrical and thermal storage optimisation in a market environment," *CIRED - Open Access Proceedings Journal*, vol. 2017, no. 1, pp. 1967–1970, 2017.

[54] C. A. Correa-Florez, A. Michiorri, A. Gerossier, and G. Kariniotakis, "Day-Ahead Management of Smart Homes Considering Uncertainty and Grid Flexibilities," in *11th Mediterranean Conference on Power Generation, Transmission, Distribution and Energy Conversion, MEDPOWER 2018*, Dubrovnik (Cavtat), Croatia, Nov. 2018. [Online]. Available: https://hal.archives-ouvertes.fr/hal-01948634

[55] Project SENSIBLE. [Online]. Available: https://www.projectsensible.eu/

[56] H. I. Su and A. E. Gamal, "Modeling and analysis of the role of energy storage for renewable integration: Power balancing," *IEEE Transactions on Power Systems*, vol. 28, no. 4, pp. 4109–4117, Nov 2013.

[57] A. Ulbig and G. Andersson, "Analyzing operational flexibility of electric power systems," *International Journal of Electrical Power & Energy Systems*, vol. 72, pp. 155 – 164, 2015, the Special Issue for 18th Power Systems Computation Conference. [Online]. Available: http://www.sciencedirect.com/science/article/pii/S0142061515001118

[58] A. Mohd, E. Ortjohann, A. Schmelter, N. Hamsic, and D. Morton, "Challenges in integrating distributed energy storage systems into future smart grid," in *2008 IEEE International Symposium on Industrial Electronics*, June 2008, pp. 1627–1632.

[59] *The Role of energy storage with renewable electricity generation*, National Renewable Energy Laboratory, 2010.

[60] D. Linden and T. B. Reddy, *Handbook of batteries*. New York, NY: McGraw-Hill, 2002.

[61] M. Zheng, C. J. Meinrenken, and K. S. Lackner, "Smart households : Dispatch strategies and economic analysis of distributed energy storage for residential peak shaving," *Applied Energy*, vol. 147, pp. 246–257, 2015.

[62] R. Davies, M. Sumner, and E. Christopher, "Energy storage control for a small community microgrid," in *7th IET International Conference on Power Electronics, Machines and Drives (PEMD 2014)*, April 2014, pp. 1–6.

[63] C. Goebel, H. Hesse, M. Schimpe, A. Jossen, and H. A. Jacobsen, "Model-based dispatch strategies for lithium-ion battery energy storage applied to pay-as-bid markets for secondary reserve," *IEEE Transactions on Power Systems*, vol. 32, no. 4, pp. 2724–2734, July 2017.

[64] I. Duggal and B. Venkatesh, "Short-term scheduling of thermal generators and battery storage with depth of discharge-based cost model," *IEEE Transactions on Power Systems*, vol. 30, no. 4, pp. 2110–2118, July 2015.

[65] M. A. Ortega-Vazquez, "Optimal scheduling of electric vehicle charging and vehicle-to-grid services at household level including battery degradation and price uncertainty," *IET Generation, Transmission Distribution*, vol. 8, no. 6, pp. 1007–1016, June 2014.

[66] M. R. Sarker, H. Pandzic, and M. A. Ortega-Vazquez, "Optimal operation and services scheduling for an electric vehicle battery swapping station," *IEEE Transactions on Power Systems*, vol. 30, no. 2, pp. 901–910, March 2015.

[67] M. Koller, T. Borsche, A. Ulbig, and G. Andersson, "Defining a degradation cost function for optimal control of a battery energy storage system," in *2013 IEEE Grenoble Conference*, June 2013, pp. 1–6.

[68] D. Wang, X. Guan, J. Wu, P. Li, P. Zan, and H. Xu, "Integrated energy exchange scheduling for multimicrogrid system with electric vehicles," *IEEE Transactions on Smart Grid*, vol. 7, no. 4, pp. 1762–1774, July 2016.

[69] O. Mégel, J. L. Mathieu, and G. Andersson, "Scheduling distributed energy storage units to provide multiple services under forecast error," *International Journal of Electrical Power & Energy Systems*, vol. 72, no. Supplement C, pp. 48 – 57, 2015, the Special Issue for 18th Power Systems Computation Conference. [Online]. Available: http://www.sciencedirect.com/science/article/pii/S0142061515000939

[70] K. Darcovich, B. Kenney, D. MacNeil, and M. Armstrong, "Control strategies and cycling demands for li-ion storage batteries in residential micro-cogeneration systems," *Applied Energy*, vol. 141, no. Supplement C, pp. 32 – 41, 2015. [Online]. Available: http://www.sciencedirect.com/science/article/pii/S0306261914012495

[71] G. He, Q. Chen, C. Kang, P. Pinson, and Q. Xia, "Optimal bidding strategy of battery storage in power markets considering performance-based regulation and battery cycle life," *IEEE Transactions on Smart Grid*, vol. 7, no. 5, pp. 2359–2367, Sept 2016.

[72] M. Musallam and C. M. Johnson, "An efficient implementation of the rainflow counting algorithm for life consumption estimation," *IEEE Transactions on Reliability*, vol. 61, no. 4, pp. 978–986, Dec 2012.

[73] S. Downing and D. Socie, "Simple rainflow counting algorithms," *International Journal of Fatigue*, vol. 4, no. 1, pp. 31 – 40, 1982. [Online]. Available: http://www.sciencedirect.com/science/article/pii/0142112382900184

[74] Y. Niu and S. Santoso, "Sizing and coordinating fast- and slow-response energy storage systems to mitigate hourly wind power variations," *IEEE Transactions on Smart Grid*, vol. PP, no. 99, pp. 1–1, 2017.

[75] X. Ke, N. Lu, and C. Jin, "Control and size energy storage systems for managing energy imbalance of variable generation resources," *IEEE Transactions on Sustainable Energy*, vol. 6, no. 1, pp. 70–78, Jan 2015.

[76] "Saft batteries lithium ion battery life, may 2014," saftbatteries.com/force_download/li_ion_battery_life__TechnicalSheet_en_0514 _Protected.pdf.

[77] B. Zhou, W. Li, K. W. Chan, Y. Cao, Y. Kuang, X. Liu, and X. Wang, "Smart home energy management systems: Concept, configurations, and scheduling strategies," *Renewable and Sustainable Energy Reviews*, vol. 61, pp. 30 – 40, 2016. [Online]. Available: http://www.sciencedirect.com/science/article/pii/S1364032116002823

[78] R. Missaoui, H. Joumaa, S. Ploix, and S. Bacha, "Managing energy smart homes according to energy prices: Analysis of a building energy management system," *Energy and Buildings*, vol. 71, pp. 155 – 167, 2014. [Online]. Available: http://www.sciencedirect.com/science/article/pii/S0378778813008335

[79] A. Anvari-Moghaddam, H. Monsef, and A. Rahimi-Kian, "Optimal smart home energy management considering energy saving and a comfortable lifestyle," *IEEE Transactions on Smart Grid*, vol. 6, no. 1, pp. 324–332, Jan 2015.

[80] Z. Zhao, W. C. Lee, Y. Shin, and K. B. Song, "An optimal power scheduling method for demand response in home energy management system," *IEEE Transactions on Smart Grid*, vol. 4, no. 3, pp. 1391–1400, Sept 2013.

[81] S. Lee, B. Kwon, and S. Lee, "Joint energy management system of electric supply and demand in houses and buildings," *IEEE Transactions on Power Systems*, vol. 29, no. 6, pp. 2804–2812, Nov 2014.

[82] *Battery Storage for Renewables: Market Status and Technology Outlook*, IRENA International Renewable Energy Agency, 2015. [Online]. Available: http://www.irena.org/documentdownloads/publications/irena{_}battery{_}storage{_}report{_}2015.pdf

[83] A. Gerossier, R. Girard, G. Kariniotakis, and A. Michiorri, "Probabilistic day-ahead forecasting of household electricity demand," *CIRED - Open Access Proceedings Journal*, vol. 2017, pp. 2500–2504(4), October 2017. [Online]. Available: http://digital-library.theiet.org/content/journals/10.1049/oap-cired.2017.0625

[84] A. Bocquet, A. Michiorri, A. Bossavy, R. Girard, and G. Kariniotakis, "Assessment of probabilistic pv production forecasts performance in an operational context," in *6th Solar Integration Workshop - International Workshop on Integration of Solar Power into Power Systems, Vienna, Austria*, November 2016.

[85] "Entsoe transparency. central collection and publication of electricity generation, transportation and consumption data and information for the pan-european market, day-ahead prices," https://transparency.entsoe.eu/transmission-domain/r2/dayAheadPrices/show, accessed: 2018-01-25.

[86] F. Pedregosa, G. Varoquaux, A. Gramfort, V. Michel, B. Thirion, O. Grisel, M. Blondel, P. Prettenhofer, R. Weiss, V. Dubourg, J. Vanderplas, A. Passos, D. Cournapeau, M. Brucher, M. Perrot, and E. Duchesnay, "Scikit-learn: Machine learning in Python," *Journal of Machine Learning Research*, vol. 12, pp. 2825–2830, 2011.

[87] Nordic Council of Ministers, *Flexible demand for electricity and power: Barriers and opportunities*. Nordic Energy Research, 2017. [Online]. Available: http://www.nordicenergy.org/publications/flexible-demand-for-electricity-and-power-barriers-and-opportunities/

[88] C. Eid, P. Codani, Y. Chen, Y. Perez, and R. Hakvoort, "Aggregation of demand side flexibility in a smart grid: A review for european market design," in *2015 12th International Conference on the European Energy Market (EEM)*, May 2015, pp. 1–5.

[89] Federal Energy Regulatory Commission, Order N. 841, *Electric Storage Participation in Markets Operated by Regional Transmission Organizations and Independent System Operators*. United States of America, 2018. [Online]. Available: https://ferc.gov/whats-new/comm-meet/2018/021518/E-1.pdf

[90] R. Cheng and Y. Jin, "A competitive swarm optimizer for large scale optimization," *IEEE Transactions on Cybernetics*, vol. 45, no. 2, pp. 191–204, Feb 2015.

[91] E. Perez, H. Beltran, N. Aparicio, and P. Rodriguez, "Predictive power control for pv plants with energy storage," *IEEE Transactions on Sustainable Energy*, vol. 4, no. 2, pp. 482–490, April 2013.

[92] Z. fu Tan, L. wei Ju, H. huan Li, J. yu Li, and H. juan Zhang, "A two-stage scheduling optimization model and solution algorithm for wind power and energy storage system considering uncertainty and demand response," *International Journal of Electrical Power & Energy Systems*, vol. 63, pp. 1057 – 1069, 2014. [Online]. Available: http://www.sciencedirect.com/science/article/pii/S0142061514004190

[93] W. Su, J. Wang, and J. Roh, "Stochastic energy scheduling in microgrids with intermittent renewable energy resources," *IEEE Transactions on Smart Grid*, vol. 5, no. 4, pp. 1876–1883, July 2014.

[94] H. Ding, Z. Hu, and Y. Song, "Stochastic optimization of the daily operation of wind farm and pumped-hydro-storage plant," *Renewable Energy*, vol. 48, pp. 571 – 578, 2012. [Online]. Available: http://www.sciencedirect.com/science/article/pii/S0960148112003588

[95] D. Bertsimas, E. Litvinov, X. A. Sun, J. Zhao, and T. Zheng, "Adaptive robust optimization for the security constrained unit commitment problem," *IEEE Transactions on Power Systems*, vol. 28, no. 1, pp. 52–63, Feb 2013.

[96] M. Kazemi, H. Zareipour, N. Amjady, W. D. Rosehart, and M. Ehsan, "Operation scheduling of battery storage systems in joint energy and ancillary services markets," *IEEE Transactions on Sustainable Energy*, vol. 8, no. 4, pp. 1726–1735, Oct 2017.

[97] R. A. Jabr, "Robust transmission network expansion planning with uncertain renewable generation and loads," *IEEE Transactions on Power Systems*, vol. 28, no. 4, pp. 4558–4567, Nov 2013.

[98] A. A. Thatte, L. Xie, D. E. Viassolo, and S. Singh, "Risk measure based robust bidding strategy for arbitrage using a wind farm and energy storage," *IEEE Transactions on Smart Grid*, vol. 4, no. 4, pp. 2191–2199, Dec 2013.

[99] Z. Hu, M. Zhang, X. Wang, C. Li, and M. Hu, "Bi-level robust dynamic economic emission dispatch considering wind power uncertainty," *Electric Power Systems Research*, vol. 135, pp. 35 – 47, 2016. [Online]. Available: http://www.sciencedirect.com/science/article/pii/S0378779616300578

[100] D. Bertsimas and M. Sim, "The price of robustness," *Operations Research*, vol. 52, no. 1, pp. 35–53, 2004. [Online]. Available: https://doi.org/10.1287/opre.1030.0065

[101] O. Mégel, J. L. Mathieu, and G. Andersson, "Scheduling distributed energy storage units to provide multiple services," in *2014 Power Systems Computation Conference*, Aug 2014, pp. 1–7.

[102] S. Rahnama, J. D. Bendtsen, J. Stoustrup, and H. Rasmussen, "Robust aggregator design for industrial thermal energy storages in smart grid," *IEEE Transactions on Smart Grid*, vol. 8, no. 2, pp. 902–916, March 2017.

[103] T. Dragicevic, H. Pandzic, D. Skrlec, I. Kuzle, J. M. Guerrero, and D. S. Kirschen, "Capacity optimization of renewable energy sources and battery storage in an autonomous telecommunication facility," *IEEE Transactions on Sustainable Energy*, vol. 5, no. 4, pp. 1367–1378, Oct 2014.

[104] "Epex spot auction, day ahead price for french market, nov. 2nd 2015," https://www.epexspot.com/en/market-data/dayaheadauction/chart/auction-chart/2015-11-02/FR/1d/7d, accessed: 2016-10-13.

[105] G. C. Mouli, P. Bauer, and M. Zeman, "System design for a solar powered electric vehicle charging station for workplaces," *Applied Energy*, vol. 168, pp. 434 – 443, 2016. [Online]. Available: http://www.sciencedirect.com/science/article/pii/S0306261916300988

[106] I. Ranaweera, O.-M. Midtgård, and M. Korpås, "Distributed control scheme for residential battery energy storage units coupled with pv systems," *Renewable Energy*, vol. 113, pp. 1099 – 1110, 2017. [Online]. Available: http://www.sciencedirect.com/science/article/pii/S0960148117305888

[107] B. Yu, "Design and experimental results of battery charging system for microgrid system," *International Journal of Photoenergy*, vol. 2016, 2016. [Online]. Available: http://dx.doi.org/10.1155/2016/7134904

[108] F. Y. Melhem, O. Grunder, Z. Hammoudan, and N. Moubayed, "Optimization and energy management in smart home considering photovoltaic, wind, and battery storage system with integration of electric vehicles," *Canadian Journal of Electrical and Computer Engineering*, vol. 40, no. 2, pp. 128–138, Spring 2017.

[109] X. Jin, K. Baker, D. Christensen, and S. Isley, "Foresee: A user-centric home energy management system for energy efficiency and demand response," *Applied Energy*, vol. 205, pp. 1583 – 1595, 2017. [Online]. Available: http://www.sciencedirect.com/science/article/pii/S0306261917311856

[110] K. Deb, *Multi-objective Optimization using Evolutionary Algorithms*. John Wiley and sons, 2001.

[111] N. M. M. Razali and A. H. Hashim, "Backward reduction application for minimizing wind power scenarios in stochastic programming," in *2010 4th International Power Engineering and Optimization Conference (PEOCO)*, June 2010, pp. 430–434.

[112] R. Weron and A. Misiorek, "Forecasting spot electricity prices: A comparison of parametric and semiparametric time series models," *International Journal of Forecasting*, vol. 24, no. 4, pp. 744 – 763, 2008, energy Forecasting. [Online]. Available: http://www.sciencedirect.com/science/article/pii/S0169207008000952

[113] A. Berrada, K. Loudiyi, and I. Zorkani, "Valuation of energy storage in energy and regulation markets," *Energy*, vol. 115, pp. 1109 – 1118, 2016. [Online]. Available: http://www.sciencedirect.com/science/article/pii/S0360544216313639

[114] W. W. Kim, J. S. Shin, and J. O. Kim, "Operation strategy of multi-energy storage system for ancillary services," *IEEE Transactions on Power Systems*, vol. 32, no. 6, pp. 4409–4417, Nov 2017.

[115] B. Zakeri and S. Syri, "Value of energy storage in the nordic power market - benefits from price arbitrage and ancillary services," in *2016 13th International Conference on the European Energy Market (EEM)*, June 2016, pp. 1–5.

[116] N. Yu and B. Foggo, "Stochastic valuation of energy storage in wholesale power markets," *Energy Economics*, vol. 64, pp. 177 – 185, 2017. [Online]. Available: http://www.sciencedirect.com/science/article/pii/S0140988317300762

[117] J. Tan and Y. Zhang, "Coordinated control strategy of a battery energy storage system to support a wind power plant providing multi-timescale frequency ancillary services," *IEEE Transactions on Sustainable Energy*, vol. 8, no. 3, pp. 1140–1153, July 2017.

[118] B. Yang, Y. Makarov, J. Desteese, V. Viswanathan, P. Nyeng, B. McManus, and J. Pease, "On the use of energy storage technologies for regulation services in electric power systems with significant penetration of wind energy," in *2008 5th International Conference on the European Electricity Market*, May 2008, pp. 1–6.

[119] B. Xu, Y. Wang, Y. Dvorkin, R. Fernández-Blanco, C. A. Silva-Monroy, J. P. Watson, and D. S. Kirschen, "Scalable planning for energy storage in energy and reserve markets," *IEEE Transactions on Power Systems*, vol. 32, no. 6, pp. 4515–4527, Nov 2017.

[120] H. Akhavan-Hejazi and H. Mohsenian-Rad, "Optimal operation of independent storage systems in energy and reserve markets with high wind penetration," *IEEE Transactions on Smart Grid*, vol. 5, no. 2, pp. 1088–1097, March 2014.

[121] M. Black and G. Strbac, "Value of bulk energy storage for managing wind power fluctuations," *IEEE Transactions on Energy Conversion*, vol. 22, no. 1, pp. 197–205, March 2007.

[122] S. Teleke, M. E. Baran, A. Q. Huang, S. Bhattacharya, and L. Anderson, "Control strategies for battery energy storage for wind farm dispatching," *IEEE Transactions on Energy Conversion*, vol. 24, no. 3, pp. 725–732, Sept 2009.

[123] M. A. Abdullah, K. M. Muttaqi, D. Sutanto, and A. P. Agalgaonkar, "An effective power dispatch control strategy to improve generation schedulability and supply reliability of a wind farm using a battery energy storage system," *IEEE Transactions on Sustainable Energy*, vol. 6, no. 3, pp. 1093–1102, July 2015.

[124] F. Luo, K. Meng, Z. Y. Dong, Y. Zheng, Y. Chen, and K. P. Wong, "Coordinated operational planning for wind farm with battery energy storage system," *IEEE Transactions on Sustainable Energy*, vol. 6, no. 1, pp. 253–262, Jan 2015.

[125] J. M. Eyer and G. P. Corey, "Energy storage for the electricity grid : benefits and market potential assessment guide : a study for the doe energy storage systems program."

[126] J. Wood, "Integrating renewables into the grid: Applying ultrabattery x00ae; technology in mw scale energy storage solutions for continuous variability management," in *2012 IEEE International Conference on Power System Technology (POWERCON)*, Oct 2012, pp. 1–4.

[127] E. Vrettos, F. Oldewurtel, and G. Andersson, "Robust energy-constrained frequency reserves from aggregations of commercial buildings," *IEEE Transactions on Power Systems*, vol. 31, no. 6, pp. 4272–4285, Nov 2016.

[128] E. Vrettos and G. Andersson, "Scheduling and provision of secondary frequency reserves by aggregations of commercial buildings," *IEEE Transactions on Sustainable Energy*, vol. 7, no. 2, pp. 850–864, April 2016.

[129] T. T. Gorecki, L. Fabietti, F. A. Qureshi, and C. N. Jones, "Experimental demonstration of buildings providing frequency regulation services in the swiss market," *Energy and Buildings*, vol. 144, pp. 229 – 240, 2017. [Online]. Available: http://www.sciencedirect.com/science/article/pii/S0378778816311616

[130] O. Kilkki, C. Giovanelli, I. Seilonen, and V. Vyatkin, "Optimization of decentralized energy storage flexibility for frequency reserves," in *IECON 2015 - 41st Annual Conference of the IEEE Industrial Electronics Society*, Nov 2015, pp. 002 219–002 224.

[131] S. Hanif, H. B. Gooi, T. Massier, T. Hamacher, and T. Reindl, "Distributed congestion management of distribution grids under robust flexible buildings operations," *IEEE Transactions on Power Systems*, vol. 32, no. 6, pp. 4600–4613, Nov 2017.

[132] A. Roos, S. Ottesen, and T. F. Bolkesjø, "Modeling consumer flexibility of an aggregator participating in the wholesale power market and the regulation capacity market," *Energy Procedia*, vol. 58, pp. 79 – 86, 2014, renewable Energy Research Conference, RERC 2014. [Online]. Available: http://www.sciencedirect.com/science/article/pii/S1876610214017792

[133] H. Hao, B. M. Sanandaji, K. Poolla, and T. L. Vincent, "Aggregate flexibility of thermostatically controlled loads," *IEEE Transactions on Power Systems*, vol. 30, no. 1, pp. 189–198, Jan 2015.

[134] J. L. Mathieu, M. E. Dyson, and D. S. Callaway, "Resource and revenue potential of california residential load participation in ancillary services," *Energy Policy*, vol. 80, pp. 76 – 87, 2015. [Online]. Available: http://www.sciencedirect.com/science/article/pii/S0301421515000427

[135] M. Heleno, M. A. Matos, and J. P. Lopes, "A bottom-up approach to leverage the participation of residential aggregators in reserve services markets," *Electric Power Systems Research*, vol. 136, pp. 425 – 433, 2016. [Online]. Available: http://www.sciencedirect.com/science/article/pii/S0378779616300724

[136] M. Heleno, M. A. Matos, and J. A. P. Lopes, "Availability and flexibility of loads for the provision of reserve," *IEEE Transactions on Smart Grid*, vol. 6, no. 2, pp. 667–674, March 2015.

[137] P. Mancarella, "Mes (multi-energy systems): An overview of concepts and evaluation models," *Energy*, vol. 65, pp. 1 – 17, 2014. [Online]. Available: http://www.sciencedirect.com/science/article/pii/S0360544213008931

[138] J. Villar, R. Bessa, and M. Matos, "Flexibility products and markets: Literature review," *Electric Power Systems Research*, vol. 154, pp. 329 – 340, 2018. [Online]. Available: http://www.sciencedirect.com/science/article/pii/S0378779617303723

[139] C. Zhang, Y. Ding, J. Østergaard, H. W. Bindner, N. C. Nordentoft, L. H. Hansen, P. Brath, and P. D. Cajar, "A flex-market design for flexibility services through ders," in *IEEE PES ISGT Europe 2013*, Oct 2013, pp. 1–5.

[140] N. C. Nordentoft, "Development of a DSO-Market on flexibility services," Strategic platform for innovation and research in intelligent power (iPower), Tech. Rep., 04 2013.

RÉSUMÉ

Cette thèse présente un cadre d'optimisation avec incertitude dans le cas où un agrégateur gère des dispositifs de stockage résidentiels et des énergies renouvelables comme sources de flexibilité, participant directement au marché journalier de l'énergie et proposant des services visant à minimiser les coûts opérationnels. Les actifs de flexibilité résidentiels sont composés de batteries, de chauffe-eau électriques et de panneaux photovoltaïques, gérés et contrôlés de manière optimale par l'agrégateur. Le modèle d'optimisation prend également en compte le coût de vieillissement de la batterie, qui permet de capturer la relation non linéaire entre la profondeur de décharge et le cycle de vie total. Les sources d'incertitude sont: la demande électrique et thermique, la production photovoltaïque et le prix de l'énergie. Ces incertitudes sont incluses dans le modèle mathématique au moyen d'une optimisation robuste et une méthodologie est proposée pour détecter les solutions offrant le meilleur compromis entre coût et risque. De plus, cette thèse présente une stratégie de gestion de la flexibilité locale basée sur deux produits: 1) les offres sur un marché local; et 2) prise en charge de contraintes locales pour le gestionnaire du réseau de distribution (GRD) sous la forme de la puissance nette et de la rampe nette. Un modèle d'optimisation robuste ajustable est proposé pour la gestion coordonnée des ressources et permet de démontrer que le cadre d'appel d'offres stratégique est suffisamment robuste rendant possible une participation coordonnée sur trois marchés différents: l'énergie, la flexibilité locale et les échanges bilatéraux (GRD).

MOTS CLÉS

Aggregateurs, consommacteurs, marché d'electricité, stockage, réseaux intelligents, incertitude, optimisation robuste, maisons intelligentes

ABSTRACT

This thesis presents an optimization framework under uncertainty for the case in which an aggregator manages residential storage devices and renewable energy as sources of flexibility, participating directly in the day-ahead energy market and offering services to minimize operational costs. Residential flexibility assets are composed by batteries, electric water heaters and PV panels, which are optimally managed and controlled by an aggregator. The optimization model also considers battery's cycling aging cost which allows capturing the non-linear relation between depth of discharge and total life cycling. The following sources of uncertainty are considered: electrical and thermal demand, PV production and energy prices. These uncertainties are included in the mathematical model by means of robust optimization theory and a methodology based on Pareto-optimality is proposed to detect the solutions with the best trade-off between cost and risk. In addition, this thesis presents a local flexibility management strategy, which is based on two products: 1) flexibility bids into a local market; and 2) local constraint support for the Distribution System Operator (DSO) in the form of maximum allowed net power and net ramping rate. An adjustable robust optimization model is proposed for coordinated management of resources and allows to demonstrate that the strategic bidding framework is robust enough to enable coordinated participation in three different marketplaces: energy, local flexibility and bilateral trading with the DSO.

KEYWORDS

Aggregators, prosumers, electricity markets, storage, smart grids, uncertainty, robust optimization, smart homes